UNIVERSIDAD NACIONAL AUTÓNOMA DE MÉXICO

Maestría y Doctorado en Ciencias Bioquímicas

Estudio del papel de TFIIH durante la diferenciación de células germinales y la activación de la transcripción cigótica en *Drosophila melanogaster*

TESIS

QUE PARA OPTAR POR EL GRADO DE:

Doctora en Ciencias

PRESENTA:
M.C. GRISEL LIZANDRA CRUZ BECERRA

TUTOR PRINCIPAL
Dr. Mario Enrique Zurita Ortega. Instituto de Biotecnología, UNAM

MIEMBROS DEL COMITÉ TUTOR
Dra. Susana López Charretón. Instituto de Biotecnología, UNAM
Dr. Alfonso León del Río. Instituto de Investigaciones Biomédicas, UNAM

Ciudad de México. Marzo, 2017

AGRADECIMIENTOS

Al Dr. Mario Zurita por su apoyo y su confianza, y por brindarme innumerables oportunidades para crecer académicamente y formarme como científico.

A Saraí Valerio y Mandy Juárez, por enriquecer sustancialmente esta investigación con su trabajo, y por su admirable compromiso con el mismo.

Al Dr. Enrique Reynaud por compartirme su conocimiento y experiencia siempre que solicité su ayuda en el laboratorio.

A la Dra. Viviana Valadez y la Dra. Martha Vázquez por aportar valiosas críticas y sugerencias durante el curso de esta investigación.

A "las Zuritas" y "los Reynauds" con los que coincidí en tiempo y espacio, por el intercambio de conocimientos, consultas y consejos.

A la Dra. Susana López y al Dr. Alfonso León por contribuir en mi formación como Doctora en Ciencias, como miembros del comité tutor.

A la Dra. Claudia Treviño, a la Dra. Verónica Narváez, a la Dra. Leonor Pérez, al Dr. Mario Cruz y al Dr. José Luis Reyes por la revisión y discusión de este trabajo, y las observaciones que permitieron mejorar este escrito.

Al Colegio de Sinaloa por apoyar la conclusión de mis estudios de Doctorado a través de la beca de disertación doctoral Hugo Aréchiga Urtuzuástegui.

Al Programa de Apoyo para Estudiantes de Posgrado, por el financiamiento otorgado para presentar este trabajo en el congreso titulado: 53rd Annual *Drosophila* Research Conference.

Al Dr. Arturo Pimentel, al Dr. Chris Wood y al M.C. Andrés Saralegui por su apoyo durante el uso de las instalaciones y los equipos del Laboratorio Nacional de Microscopía Avanzada.

A Gloria y a Toño, por su excelente trabajo en la Unidad de Docencia del IBT.

A Carmen, por su apoyo técnico en el laboratorio.

A Adrián, por esperar "cinco minutos IBT" siempre que fue necesario para terminar un experimento.

A Daniel ,

por ser, por estar y por todo lo demás...!

"By the sword"

Saul Hudson /Andrew Stockdale

Este proyecto se desarrolló como tesis doctoral dentro del Programa de Maestría y Doctorado en Ciencias Bioquímicas de la Universidad Nacional Autónoma de México, bajo la dirección del Dr. Mario Enrique Zurita Ortega, en el departamento de Genética del Desarrollo y Fisiología Molecular del Instituto de Biotecnología.

ÍNDICE GENERAL

ÍNDICE DE FIGURAS

ÍNDICE DE TABLAS

ABSTRACT

Proliferation and cell differentiation in multicellular organisms during development are linked to cell cycle modulation, global gene expression and genome maintenance. Several factors are involved in proper crosstalk maintenance among these mechanisms; one of these is TFIIH, which is composed by p8, p34, p44, p52, p62, XPD, XPB, CDK7, MAT1 and Cyclin H. Because TFIIH subunits participate in transcription, DNA repair, chromosome segregation and cell cycle control, the importance of understanding how this complex operates becomes evident. This study provides an analysis of the role of TFIIH in cell differentiation and zygotic genome activation during the development of *Drosophila melanogaster*.

This analysis shows that TFIIH mutants cause a meiotic arrest phenotype that affects male germ cell differentiation. Global gene expression data from TFIIH mutant testes showed the misregulation of only a small fraction of the transcripts (<10%), suggesting differential TFIIH requirements for gene expression in the testis. Furthermore, TFIIH shows nuclear and perinucleolar localization in the primary spermatocyte stage during spermatogenesis. Interestingly, the absence of the p8 subunit causes the dissociation of the transcriptional repressor Polycomb (Pc) from the periphery of the nucleolus in these cells. On the other hand, Pc enrichment is not enhanced at the promoters of some repressed differentiation genes in the TFIIH mutant testes, which argues against the current model for Pc-mediated repression of these genes in some meiotic arrest mutants. Interestingly, the absence of p8 does not affect the levels of other TFIIH subunits or the recruitment of this complex to DNA promoter sequences in the *Drosophila* testis. Instead, we observed that the stability of TFIIH depends on the p52 subunit.

On the other hand, this work describes for the first time the *in vivo* dynamics of TFIIH at the onset of transcription in the early *Drosophila* embryo, in which, TFIIH shows a highly dynamic behavior during the fast mitotic divisions in the syncytial blastoderm embryo. Intriguingly, a fraction of TFIIH as well as TBP and RNA polymerase II remain bound to chromatin during mitosis, enriched at the promoters of histone genes, acting as possible bookmarks to achieve the fast activation of transcription after mitosis. Furthermore, several subunits of TFIIH are essential for proper mitosis in the syncytial blastoderm. This is due in part

to transcriptional deficiencies in maternal genes that operate during mitosis in the early embryo. However, a direct role of the holoTFIIH in mitosis cannot be discarded.

RESUMEN

TFIIH es un complejo formado por diez subunidades: p8, p34, p44, p52, p62, XPD, XPB, CDK7, MAT1 y Ciclina H. Los componentes de TFIIH participan en transcripción, reparación de daño en el ADN, segregación de los cromosomas y control del ciclo celular, por lo tanto, su importancia para la célula es evidente. El presente trabajo aborda el estudio del papel de algunas subunidades de TFIIH en la diferenciación celular y durante la activación de la transcripción cigótica en *Drosophila melanogaster*.

Este estudio muestra que mutaciones en las subunidades p8 y p52 de TFIIH causan un fenotipo de detención en meiosis durante la diferenciación de las células germinales en el testículo. Se observó que TFIIH se enriquece en los cromosomas bivalentes y la periferia del nucléolo en los espermatocitos primarios, la misma etapa de la espermatogénesis en la cual se detiene la diferenciación en las mutantes de *p8* y *p52*. Se encontró que la falta de p8 causa la deslocalización del represor transcripcional Polycomb (Pc) del nucléolo de estas células. Sin embargo, contrario a lo observado en estudios previos realizados en mutantes con fenotipo de detención en meiosis, Pc no se recluta a los promotores de los genes de diferenciación.

El análisis del transcriptoma de testículo de las mutantes de TFIIH reveló la desregulación de la transcripción de una proporción pequeña de genes (<10%), lo cual sugiere el requerimiento diferencial de TFIIH para la transcripción. Adicionalmente, este estudio muestra por primera vez que, en testículo, p52 es esencial en la estabilidad de otros componentes de TFIIH, mientras que la falta de p8 no afecta el nivel de otras subunidades o su unión a promotores en la cromatina.

Por otra parte, este trabajo muestra que TFIIH, TBP y la ARN polimerasa II tienen un patrón de localización semejante al de los cromosomas durante los ciclos de división nuclear en el blastodermo sincicial. De manera interesante, se encontró que estos componentes de la maquinaria basal de la transcripción se mantienen unidos a la cromatina durante la mitosis, sugiriendo que pueden actuar como "bookmarks" para posibilitar la activación rápida de la transcripción en cada ciclo de división nuclear en esta etapa de la embriogénesis. Adicionalmente, se encontró que mutaciones en distintas subunidades de TFIIH causan mitosis catastróficas durante el blastodermo sincicial. El transcriptoma de embriones que no tienen p8 sugiere que este fenotipo se debe, al menos en parte, a la disminución de transcritos involucrados

en la replicación del ADN y la mitosis depositados por herencia materna en el embrión. Sin embargo, en este estudio no puede descartarse el papel directo del holocomplejo en la mitosis.

1. INTRODUCCIÓN

El desarrollo de un organismo complejo depende de un conjunto de procesos celulares y mecanismos moleculares finamente regulados para coordinar los eventos requeridos desde la formación de una nueva célula hasta su diferenciación y organización en tejidos y órganos. Entre estos procesos destaca la expresión genética, cuya regulación determina qué genes se expresan en cada célula en un momento particular durante desarrollo.

La expresión de un gen inicia con la transcripción, un mecanismo fundamental a través del cual se sintetiza ARN a partir de un templado de ADN. En organismos eucariotas la ARN polimerasa II (ARNP II) se encarga de la transcripción de los genes que codifican proteínas y algunos ARNs no codificantes. Esta enzima se recluta a la región promotora del gen blanco durante el ensamblaje del complejo de preinicio (CPI) que también incluye a TFIIA, TFIIB, TFIID, TFIIE, TFIIF y TFIIH, denominados en conjunto factores basales de la transcripción (Figura 1). Durante la activación de la transcripción de un gen, el complejo TFIID se une a motivos específicos en la secuencia de ADN del promotor. Después de esto se reclutan secuencialmente TFIIA, TFIIB, la ARNP II, TFIIF, TFIIE y TFIIH. Una vez ensamblado el CPI, ocurre la apertura de la doble cadena de ADN e inicia la síntesis del primer enlace fosfodiéster del ARN. El escape de la ARNP II del promotor permite la elongación del transcrito y finalmente tiene lugar la etapa de terminación de la transcripción [1].

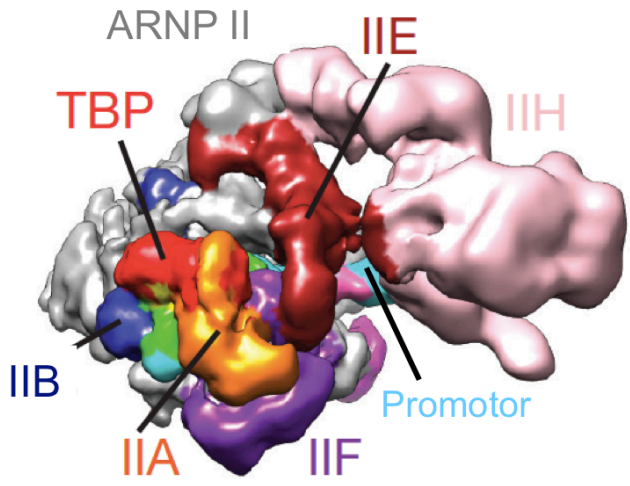

Figura 1. Complejo de preinicio (CPI) de la transcripción. Los factores basales de la transcripción IIA, IIB, IID (TBP), IIF, IIE y IIH forman el CPI en el promotor del gen blanco durante el inicio de la transcripción mediada por la ARNP II (Figura adaptada de [2]).

El factor de transcripción basal TFIIH cumple funciones esenciales durante los pasos iniciales de este proceso. Debido a que TFIIH es el objeto de estudio de este trabajo, la composición, estructura y función de este complejo durante la transcripción y otros procesos celulares se describen en las siguientes secciones.

1.1 TFIIH

TFIIH es un complejo proteico originalmente identificado como uno de los factores basales de la transcripción, sin embargo, tras más de 20 años de estudio se ha encontrado que sus componentes participan además de en transcripción, en reparación de daño en el ADN, en la segregación de los cromosomas y en la progresión del ciclo celular [3]. De esta forma TFIIH conecta procesos fundamentales para el desarrollo de un organismo como son la expresión genética, el mantenimiento de la estabilidad del genoma y la proliferación celular.

Composición y estructura

El holocomplejo TFIIH está constituido por diez proteínas que se dividen en dos subcomplejos: "core" y CAK. El "core" incluye las subunidades XPD, XPB, p8, p34, p44, p52 y p62. El CAK ("cyclin dependent kinase-activating kinase") está formado por las subunidades CDK7, Ciclina H y MAT1 (Figura 2) [4,5].

La organización estructural de TFIIH se ha modelado a partir de información generada mediante cristalografía, resonancia magnética nuclear, espectrometría de masas y crio-microscopía electrónica [6,7]. El modelo más reciente de la estructura de TFIIH muestra que las subunidades p34 y p44 forman un heterodímero a través de la interacción de sus dominios vWA (denominados así por la proteína fundadora de la familia de proteínas que lo poseen: von Willebrand factor A), a los cuales también se une la subunidad p62. Así mismo, las subunidades p8 y p52 forman un heterodímero y ambas interaccionan con XPB. Simultáneamente, p52 contacta al heterodímero p34/p44, lo que permite el anclaje de p52, p8 y XPB al "core". Además, la subunidad XPD une al CAK y al "core" a través de su interacción con un componente de cada subcomplejo: MAT1 y p62 respectivamente [6].

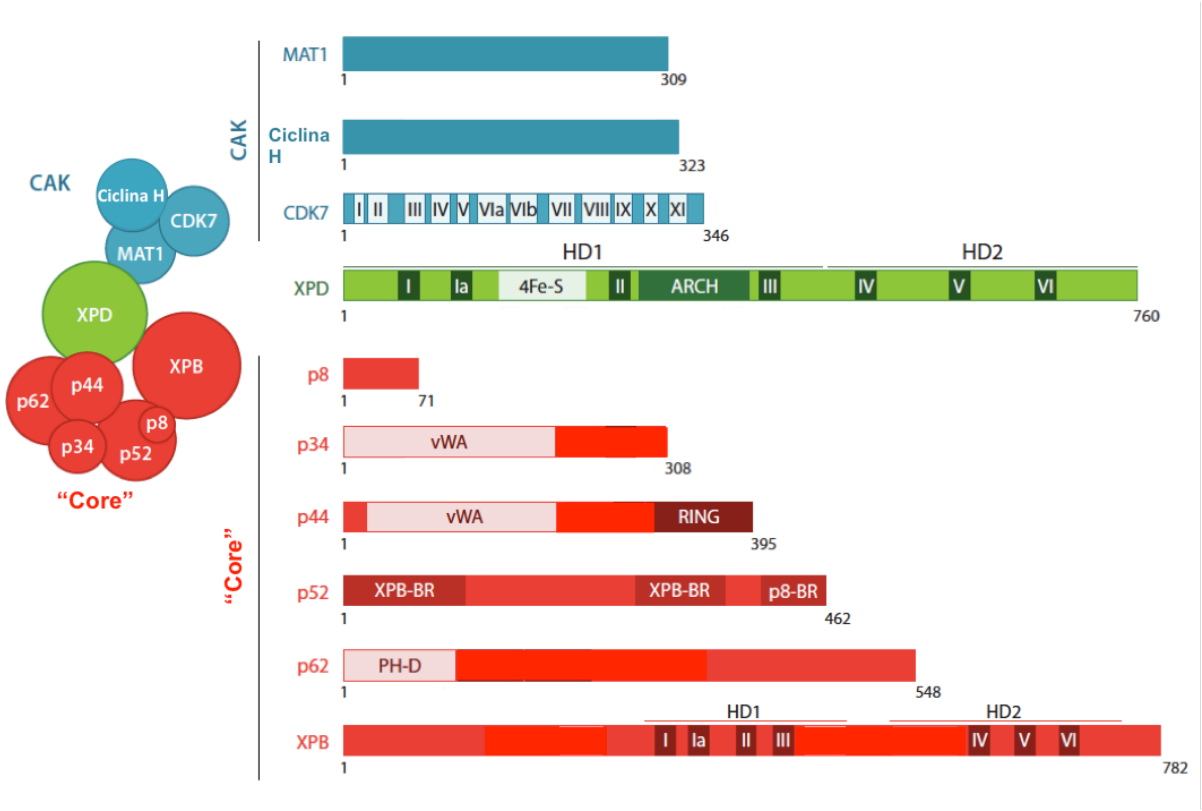

Figura 2. Composición de TFIIH. TFIIH está constituido por dos subcomplejos: "core" y CAK. Izquierda: el "core" incluye las subunidades XPD, XPB, p8, p34, p44, p52 y p62. El CAK está formado por las subunidades CDK7, Ciclina H y MAT1. La subunidad XPD interacciona con componentes de ambos subcomplejos para formar el holocomplejo. Derecha: se indican algunos de los dominios importantes en las subunidades de TFIIH. En CDK7, los motivos I y II poseen sitios de unión a ATP, el motivo III se requiere para la interacción con Ciclina H. XPD presenta siete motivos (I-VI) que forman dos dominios de helicasa de ADN (HD1 y HD2), además de un dominio 4Fe-S esencial para su actividad, mientras que su dominio ARCH es indispensable para su interacción con MAT1. p34 y p44 contienen dominios vWA que participan en la interacción entre ellas y su interacción con otras subunidades del complejo. p44 posee además un dominio tipo RING. En p52 se conocen dos regiones importantes para la interacción con XPB (XPB-BR) y una región indispensable para su interacción con p8 (p8-BR). p62 tiene un dominio tipo PH-D involucrado en la interacción de TFIIH con otros complejos. Al igual que XPD, XPB contiene siete motivos (I-VI) que forman dos dominios de helicasa de ADN (HD1 y HD2). Se indica el número de aminoácidos de las subunidades de TFIIH en humano (Figura adaptada de [3]).

La mayor parte de estas interacciones se incluyen en un modelo tridimensional que muestra una estructura de TFIIH en forma de anillo, con el "core" en la base y el CAK en la parte superior de éste (Figura 3) [6,7].

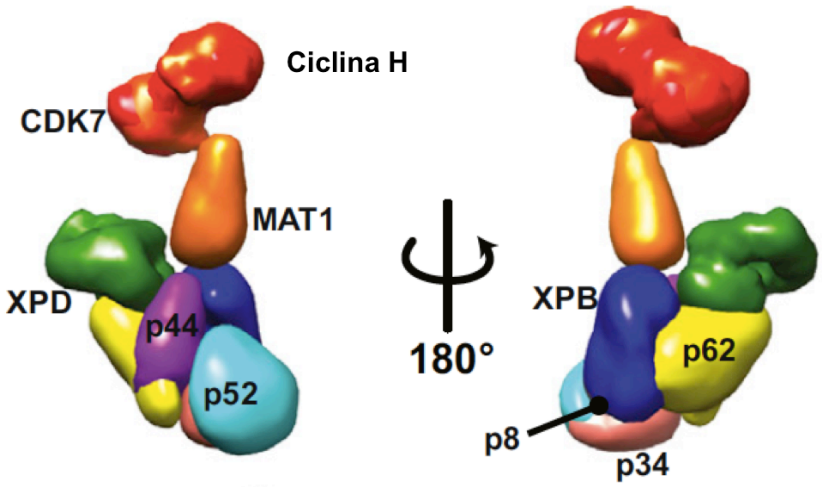

Figura 3. Estructura de TFIIH. El modelo de la arquitectura de TFIIH generado a partir de datos de espectrometría de masas y microscopía electrónica muestra la ubicación de las subunidades dentro del complejo. Las subunidades del "core" se observan en la base mientras que el CAK se posiciona en la parte superior de la estructura. Se muestran dos imágenes en diferente orientación (Figura adaptada de [6]).

Funciones

Las subunidades XPD, XPB y CDK7 poseen actividades enzimáticas que confieren multifuncionalidad a TFIIH. A su vez, la combinación de estas proteínas con el resto de las subunidades del complejo permite modular su actividad (Figura 4).

Dos de las subunidades con actividad enzimática forman parte del "core" de TFIIH, estas son XPB y XPD, helicasas/ATPasas de ADN de polaridad opuesta requeridas para la apertura del ADN en el promotor durante el inicio de la transcripción [8–10]. Adicionalmente, XPB posee actividad de translocasa de ADN, con la cual permite el posicionamiento de esta molécula en la región catalítica de la ARNP II para el inicio de la síntesis de ARN mensajero (ARNm) [11]. Así mismo, las actividades de XPB y XPD participan en la apertura de la doble cadena de ADN para formar la burbuja de reparación en el mecanismo de reparación por escisión de nucleótidos (REN), involucrado en la respuesta a daño al ADN causado por luz UV y algunos agentes químicos [9,10,12].

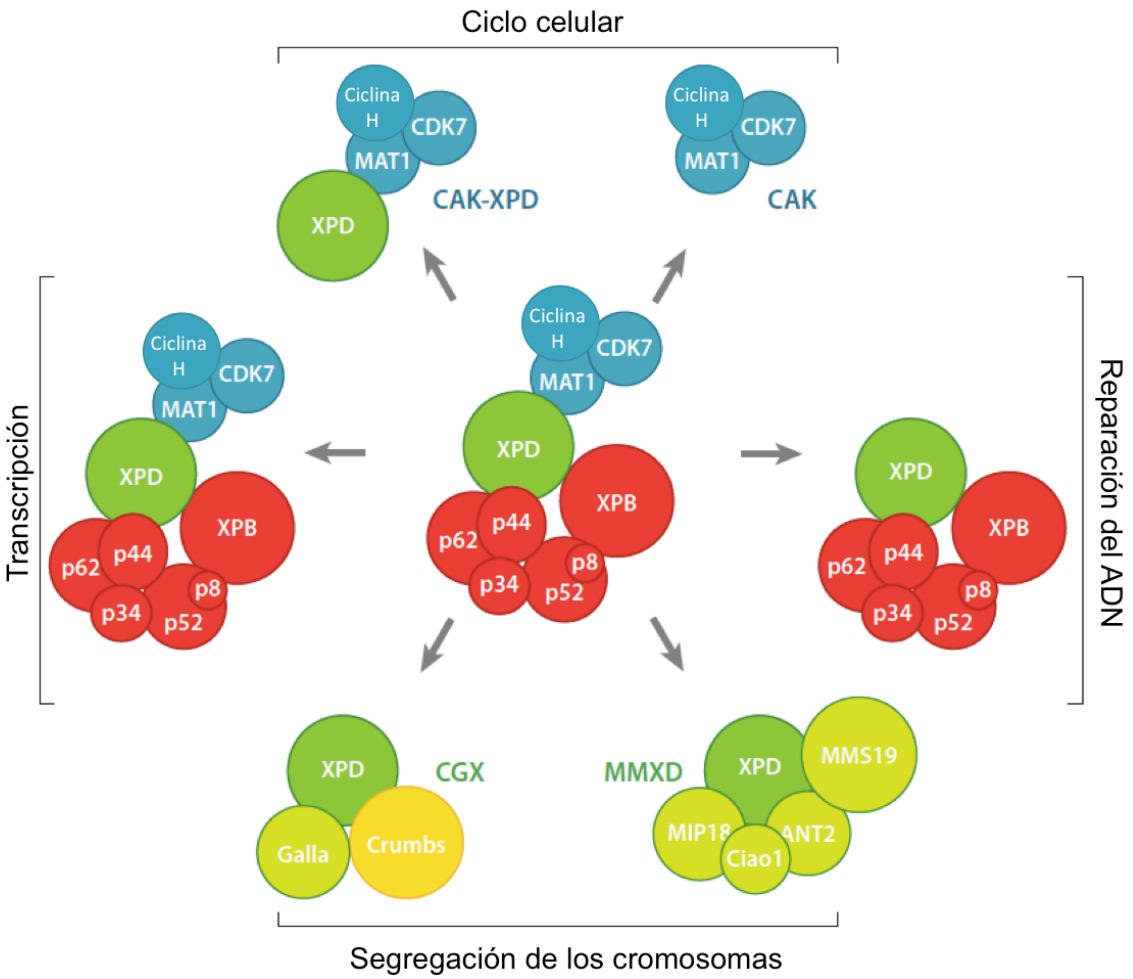

Figura 4. TFIIH es multifuncional. Las subunidades de TFIIH pueden formar el holocomplejo, complejos intermediarios o subcomplejos. El holocomplejo TFIIH participa en el inicio de la transcripción mediada por la ARNP II. El subcomplejo CAK y el complejo intermediario XPD-CAK están involucrados en el control del ciclo celular, mientras que el "core" participa en la reparación del ADN mediante el mecanismo de reparación por escisión de nucleótidos. Además, XPD es parte de los complejos CGX y MMXD, ambos involucrados en la segregación de los cromosomas e identificados en *Drosophila* y humano respectivamente (Figura adaptada de [3]).

Las actividades enzimáticas del "core" de TFIIH se modulan por componentes del mismo subcomplejo. Las subunidades p8 y p52 estimulan la actividad ATPasa de XPB [13,14], mientras que p44 regula la actividad helicasa de XPD [15].

La subunidad catalítica del CAK es CDK7, una cinasa que como parte del holocomplejo fosforila las serinas cinco y siete del dominio carboxilo terminal (“caboxi terminal domain”, CTD) de la subunidad mayor de la ARNP II y permite con ello el inicio de la elongación y el reclutamiento de factores que procesan el ARNm [10,16,17]. Adicionalmente, el subcomplejo CAK fosforila a CDK1, CDK2, CDK4 y CDK6, otras cinasas dependientes de ciclina que

participan en la progresión del ciclo celular [18,19]. Así mismo, la actividad cinasa y la especificidad de CDK7 están reguladas por las otras dos subunidades del CAK: Ciclina H y MAT1[20].

Adicionalmente, la subunidad p44 posee una secuencia consenso de ligasa de ubiquitina tipo E3, cuya actividad *in vitro* se estimula por p34 [21]. Por otra parte, XPD en conjunto con las proteínas MMS19 y MIP18 forma el complejo MMXD, involucrado en la segregación los cromosomas durante la mitosis. Sin embargo, se desconoce cuál es el papel de XPD dentro de este complejo [22].

1.2 Mutaciones en subunidades de TFIIH producen enfermedades en humanos.

Dada su multifuncionalidad, la importancia de TFIIH en la célula es evidente. Mutaciones en las subunidades XPB y XPD se asocian con tres síndromes en humano: xeroderma pigmentosum (XP), síndrome de Cockayne (SC) y tricotiodistrofia (TTD) [23–25]. Por otra parte, mutaciones en la subunidad p8 se han encontrado solo en pacientes con TTD [5].

Una característica común entre los enfermos afectados en cualquiera de estas proteínas es la fotosensibilidad, sin embargo, cada síndrome posee además características específicas (Figura 5). Por ejemplo, los pacientes con XP poseen elevada predisposición para desarrollar cáncer de piel, mientras que los enfermos de tricotiodistrofia se caracterizan por presentar cabello y uñas frágiles. El estudio del efecto en las funciones de TFIIH de las mutaciones en estas subunidades ha revelado que estos fenotipos son producto de deficiencias en la transcripción y la reparación del ADN en los pacientes afectados [13,25,26]. En todos los casos, se han identificado mutaciones puntuales en las secuencias codificantes de *XPB*, *XPD* o *p8* que generan cambios en la secuencia de aminoácidos o proteínas truncas que afectan principalmente los dominios de interacción con otros componentes del complejo [26].

Por otra parte, no existen reportes de casos de pacientes con mutaciones en el resto de las subunidades de TFIIH, lo cual sugiere que pueden tener un efecto tan deletéreo que impide la viabilidad de un organismo, o por el contrario no afectar la función de TFIIH a un nivel que permita observar un fenotipo mutante.

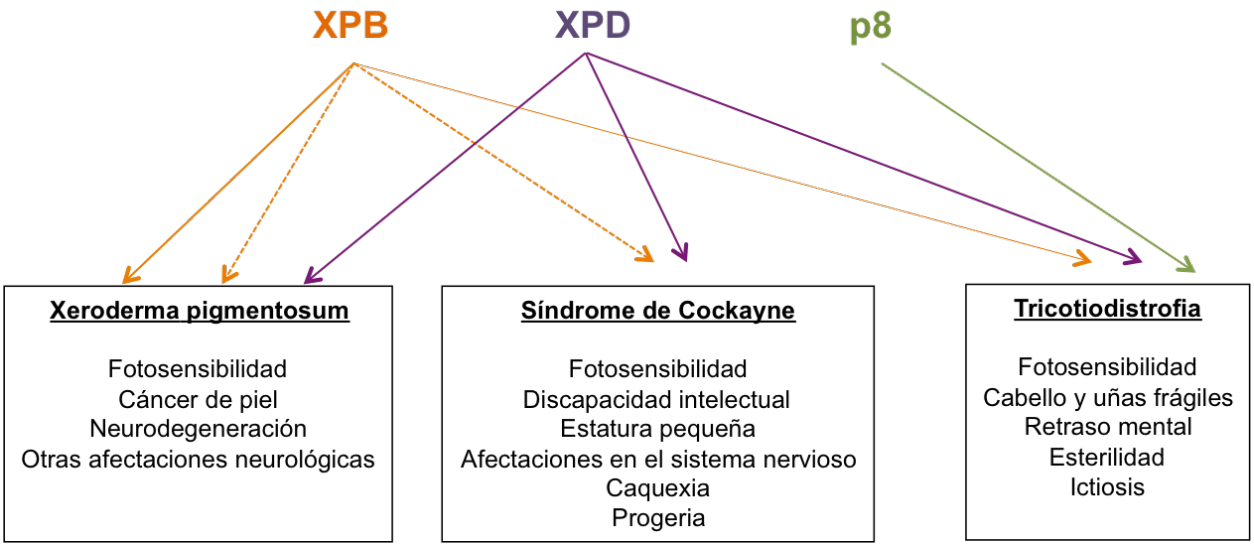

Figura 5. Mutaciones en subunidades de TFIIH causan enfermedades en humano. Mutaciones en la subunidad XPB causan tricotiodistrofia (TTD), xeroderma pigmentosum (XP), síndrome de Cockayne (SC) o una combinación de éstos últimos (XP/SC). Mutaciones en la subunidad XPD causan TTD, XP o SC. Mutaciones en la subunidad p8 se han encontrado solamente en pacientes con TTD. La fotosensibilidad es una característica común entre estos síndromes; otros síntomas se enlistan para cada caso (Figura adaptada de [27]).

El uso de organismos modelo ha permitido estudiar la función de algunas subunidades de TFIIH cuya mutación podría no ser compatible con el desarrollo humano. Por ejemplo, un estudio reciente mostró que la eliminación de diferentes dominios de Tfb1 (el ortólogo de p62) en levadura afectan la viabilidad y la sensibilidad a luz UV. De manera interesante, la severidad de estos fenotipos correlaciona con la disminución en la estabilidad de TFIIH en estos organismos [6].

2. ANTECEDENTES

En *Drosophila*, la afectación de diferentes subunidades de TFIIH resulta en fenotipos mutantes durante el desarrollo que mimetizan algunas de las características de los síndromes causados por las mutaciones en *XPB*, *XPD* y *p8* en humano. Las moscas con mutaciones en TFIIH presentan alta sensibilidad a luz UV, tamaño pequeño y defectos durante el desarrollo de la cutícula y las alas, quetas frágiles, tumores melanóticos e infertilidad [28–34].

Los estudios realizados en la mosca han contribuido a entender la relación genotipo-fenotipo de los organismos afectados en TFIIH que, al igual que las células provenientes de pacientes humanos, presentan defectos en la transcripción y la respuesta al daño en el ADN causado por luz UV. Por lo tanto, *Drosophila* resulta muy útil en el estudio de la función de las proteínas que forman el complejo TFIIH durante el desarrollo.

2.1 Fenotipos asociados a la falta de p8 o la disminución de p52 en *Drosophila melanogaster*

Con el objetivo de estudiar el papel de las subunidades p8 y p52 de TFIIH durante el desarrollo se obtuvieron organismos nulos de p8 o hipomorfos de p52. Se utilizó una línea de mosca que tiene insertado un elemento P en el segundo exón de *p8* y con ello, en condición homocigótica, impide por completo la síntesis de esta proteína [33]. Por otra parte, se emplearon alelos de mutaciones puntuales dentro de la secuencia codificante de *p52* que codifican versiones truncadas de la proteína (*mrn*^{3} y *mrn*^{5}) en combinación con una línea que tiene insertado un elemento P en la región 5' no traducida de *p52* (*EP3605*) [32] (Figura 6). En todos los casos, la proporción obtenida de organismos adultos viables es menor a la esperada y éstos presentan defectos en la fertilidad. Se observó que la falta de p8 provoca esterilidad en machos y disminución de la fertilidad en hembras, mientras que la disminución de p52 produce esterilidad en ambos sexos [32,33]. Estos resultados indican que p8 y p52 son esenciales para la fertilidad en *Drosophila*. Adicionalmente, se observó que embriones provenientes de madres que no expresan p8 mueren en las primeras etapas del desarrollo, lo cual sugiere que esta proteína tiene un papel esencial en la embriogénesis.

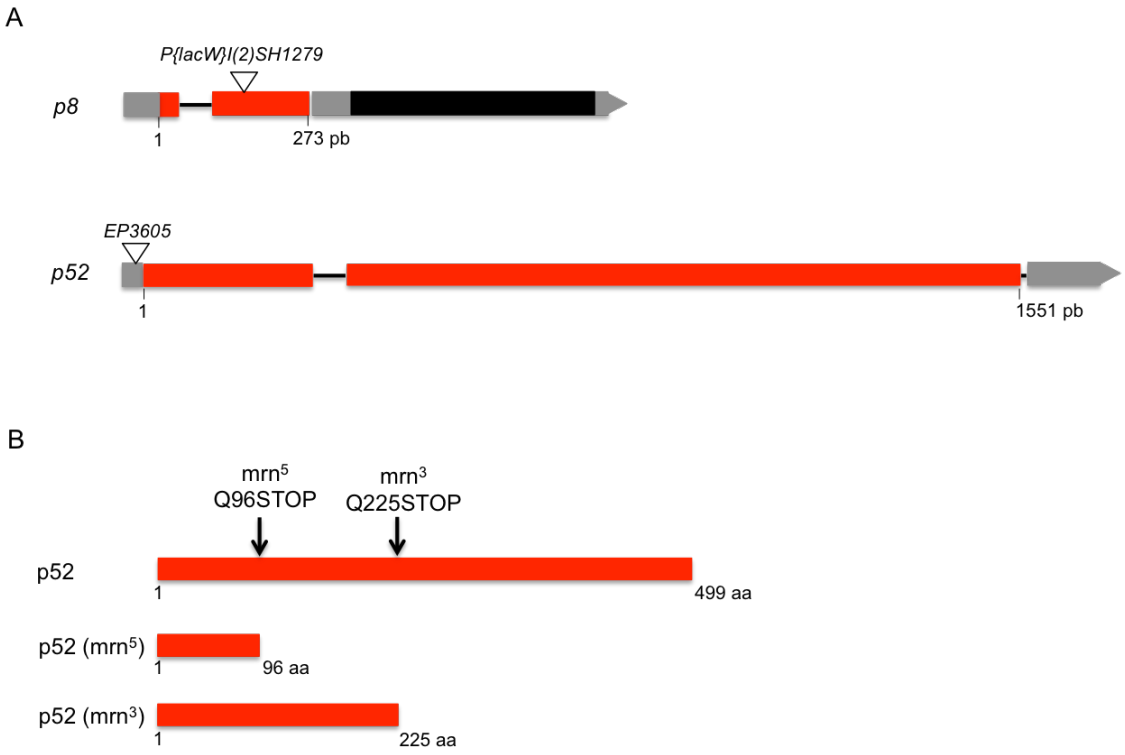

Figura 6. Representación de los alelos de *p8* y *p52* utilizados en este estudio. A. Las secuencias de *p8* (273 pb) y *p52* (1551 pb) incluyen dos exones (cajas rojas) y un intrón (línea). El alelo nulo de p8 tiene insertado un elemento P (*P{lacW}l(2)SH179*) en el segundo exón. p8 está codificado en un transcrito bicistrónico que incluye también la secuencia codificante de p18 (caja negra), sin embargo, este alelo sólo afecta la expresión de p8 [33]. El alelo hipomorfo de p52 tiene insertado un elemento P (*EP3605*) en la región 5' no traducida. Los triángulos representan los elementos P insertados en las secuencias de *p8* y *p52*, mientras que las cajas grises representan las regiones no traducidas. B. La proteína p52 consiste de 499 aminoácidos (aa), mientras que los alelos mutantes $p52^{mrn^5}$ y $p52^{mrn^3}$ codifican proteínas truncas de 96 y 225 aa respectivamente [32].

El presente trabajo aborda el estudio de la participación de TFIIH en dos procesos celulares fundamentales en el desarrollo: la diferenciación celular y la activación del genoma en la embriogénesis. En la primera parte de este escrito se presenta la caracterización del fenotipo de esterilidad de machos afectados en las subunidades p8 y p52 de TFIIH. La segunda parte se centra en el estudio de la dinámica de TFIIH en la embriogénesis temprana y el análisis de embriones tempranos provenientes de madres nulas en *p8*.

A continuación se describen brevemente los eventos relevantes para este estudio que ocurren durante la espermatogénesis y la embriogénesis temprana de *Drosophila melanogaster*.

2.2 La espermatogénesis en *Drosophila melanogaster*

La espermatogénesis en *Drosophila* inicia en la zona apical del testículo, denominada centro de proliferación germinal, en la cual se localizan células madre y células de origen somático que acompañan a las primeras durante la diferenciación. La espermatogénesis inicia cuando una célula progenitora de la línea germinal se divide asimétricamente para producir una nueva célula madre y una espermatogonia. Esta última sufre cuatro rondas de división mitótica sin citocinesis generando 16 células interconectadas denominadas espermatocitos primarios, los cuales tienen un periodo de crecimiento y elevada expresión genética, mismo que abandonan para entrar en dos rondas sucesivas de meiosis que producen un quiste de 64 células haploides denominadas espermátidas redondas. Las espermátidas permanecen interconectadas y sufren cambios morfológicos dramáticos hasta su elongación. Finalmente, las espermátidas completamente elongadas se individualizan, se enrollan en la base del testículo y se transfieren a la vesícula seminal (Figura 7).

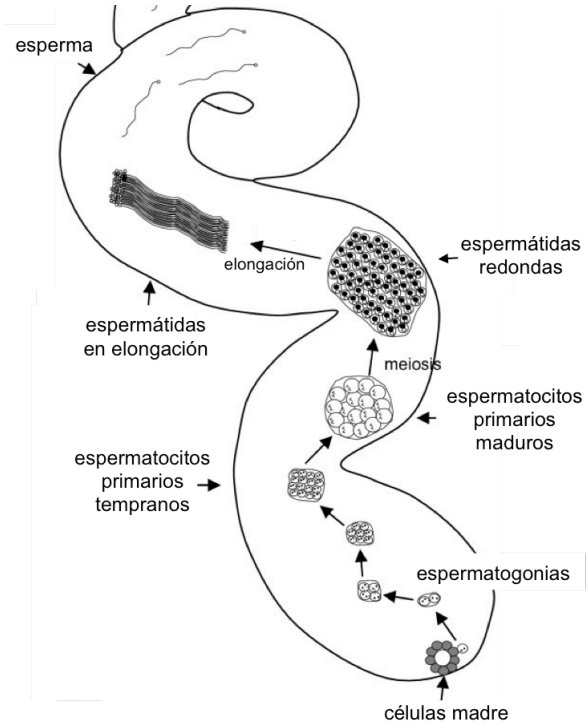

Figura 7. La espermatogénesis en el testículo de *Drosophila melanogaster*. La división asimétrica de una célula madre genera una espermatogonia que tras cuatro divisiones mitóticas alcanza el estadio de espermatocito primario, el cual sufre dos rondas de meiosis y se convierte en espermátida redonda. La remodelación celular conlleva a la elongación de las espermátidas y finalmente, tiene lugar la individualización del esperma (Figura adaptada de [35]).

2.3 La embriogénesis temprana de Drosophila melanogaster.

El desarrollo embrionario temprano de *Drosophila* comprende un periodo de 3h después de la fertilización del huevo. Las dos primeras horas del desarrollo corresponden al estadio denominado pre-blastodermo o blastodermo sincicial, debido a que el embrión es un sincicio en el que los núcleos se dividen rápida y sincrónicamente durante 13 ciclos que comprenden solamente las fases de síntesis y mitosis sin división celular. En las etapas más tempranas (ciclos 1-7) no hay transcripción y el embrión utiliza para su desarrollo ARNs y proteínas heredados maternamente. La activación del genoma del cigoto ocurre en dos etapas. La primera de ellas tiene lugar a partir del ciclo de división nuclear ocho y corresponde a la transcripción de sólo un pequeño grupo de genes (por ejemplo, los genes de histonas y los genes GAP). Posteriormente, al inicio del ciclo 14 cesan las divisiones nucleares sincrónicas, los núcleos migran hacia la periferia del embrión y ocurre la división celular, este proceso se denomina celularización del blastodermo y el estadio que se alcanza se denomina blastodermo celular. En esta etapa ocurre la transición de la blástula media (TBM) durante la cual se activa la transcripción global del genoma del cigoto, lo cual le permite continuar con su desarrollo hacia la gastrulación, etapa en la cual se generan las capas germinales a partir de las cuales se originan los órganos y tejidos del organismo (Figura 8) [36].

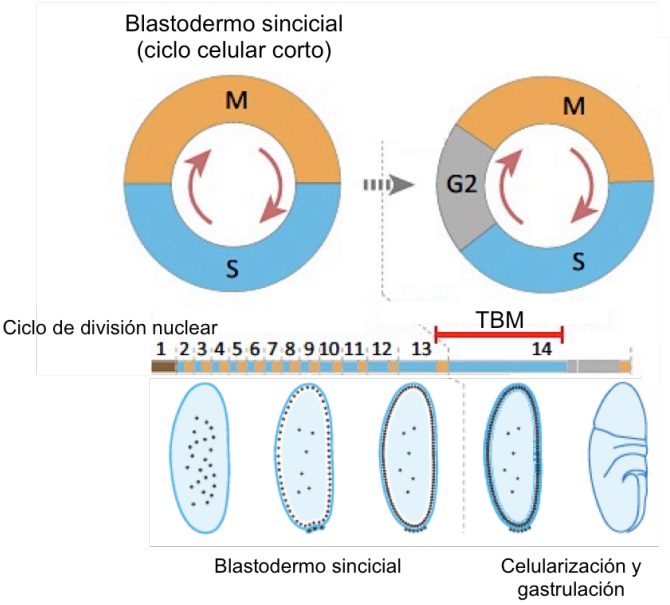

Figura 8. La embriogénesis temprana de *Drosophila melanogaster*. El blastodermo sincicial comprende los primeros 13 ciclos de división nuclear en el embrión, los cuales incluyen solamente las fases de síntesis (S) y mitosis (M). Al inicio del ciclo 14 ocurre la transición de la

blástula media (TBM). Durante la celularización tiene lugar la individualización de los núcleos a través de la formación de la membrana celular, las divisiones nucleares se alargan y el desarrollo continúa para alcanzar la gastrulación en donde los ciclos de división incluyen las fases S, M y G2 (Figura adaptada de [36].

3. HIPÓTESIS

Mutaciones en las subunidades p8 y p52 de TFIIH afectan la viabilidad y la fertilidad de *Drosophila melanogaster*, por lo tanto, estas proteínas podrían tener un papel esencial en el desarrollo embrionario y la gametogénesis.

4. OBJETIVOS

4.1 Objetivo general

Entender el papel de las subunidades p8 y p52 del factor basal de transcripción TFIIH durante el desarrollo, usando como modelo a *Drosophila melanogaster.*

4.2 Objetivos particulares

a) Determinar el papel de p8 y p52 en la diferenciación de las células germinales durante la espermatogénesis.

b) Evaluar el papel de TFIIH durante la activación de la transcripción del genoma del cigoto en el blastodermo sincicial.

5. MATERIALES Y METODOLOGÍA

Cepas de mosca. La línea *Ore R* se usó como cepa silvestre ($p8^{+}/p8^{+}$ y $p52^{+}/p52^{+}$). Las líneas transgénicas *Pc-GFP* (BL9593) y *H2Av-mRFP* (BL23250 y BL23251) se obtuvieron de la colección de Bloomington stock center. Las líneas con alelos mutantes de *p52* ($p52^{EP3605}$, $p52^{mrn5}$, $p52^{mrn3}$), *XPB* (XPB^{haync2}) y *p8* ($p8^{-}$) se describieron en trabajos previos [28,32,33].

ADN recombinante para generar fusiones de subunidades de TFIIH con proteínas fluorescentes. Se generaron construcciones de ADN recombinante con las secuencias codificantes de p8, XPB y p52 y las secuencias codificantes de las proteínas fluorescentes ECFP,

EGFP y EYFP respectivamente. Las construcciones p8-ECFP (etiqueta en el carboxilo de p8), XPB-EGFP (etiqueta en el carboxilo de XPB) y EYFP-p52 (etiqueta en el amino de p52) se clonaron en el vector pCaSper-Hsp83 con el cual se microinyectaron embriones tempranos de la línea silvestre W^{1118} siguiendo un protocolo estándar para la generación de moscas transgénicas (Genetic Services). Se obtuvieron y mapearon al menos cinco líneas transgénicas de cada construcción.

Rescate del fenotipo de letalidad asociado a alelos mutantes de p8 y p52. Se cruzaron individuos adultos heterocigóticos del alelo nulo de *p8* ($p8^{+}/p8^{-}$) con líneas transgénicas que expresan la construcción p8-ECFP insertada en el cromosoma 3. La progenie de esta cruza generó organismos con una copia del alelo nulo de *p8* y una copia del transgen *p8-ECFP*, los cuales se cruzaron entre sí para generar organismos homocigóticos para el alelo nulo de *p8* ($p8^{-}/p8^{-}$) con una o dos copias del transgen *p8-ECFP*. Cruzas similares se realizaron para evaluar la funcionalidad de líneas que expresan el transgen *EYFP-p52* insertado en el cromosoma 2, en el rescate del fenotipo de semiletalidad asociado a la disminución de p52 en la combinación de alelos $p52^{EP3605}$ y $p52^{mrn5}$. Los organismos adultos se contabilizaron y después de identificar la clase más sana, se determinaron los porcentajes de supervivencia de cada genotipo a partir del cociente de los organismos observados y los organismos esperados para cada clase. Estos ensayos se realizaron por triplicado.

Microscopía de contraste de fases y microscopía confocal de testículos. Se obtuvieron testículos de machos de 0-1 día después de su eclosión y se disecaron en buffer para testículo (183 mM KCl, 47 mM NaCl y 10 mM Tris pH 6.8). Para identificar los distintos estadios de la espermatogénesis mediante microscopía de contraste de fases, las muestras se colocaron en una gota del mismo buffer sobre la superficie de un portaobjetos, posteriormente se cubrieron con un cubreobjetos de 22x22 mm y se observaron en un microscopio invertido Axiovert 200 (Zeiss). Para observar las proteínas fluorescentes mediante microscopía confocal, los testículos se prepararon siguiendo el mismo protocolo y se observaron en el sistema confocal de Zeiss LSM 510 META acoplado a un microscopio invertido Axiovert 200 (Zeiss). Se analizaron al menos veinte pares de testículos de cada genotipo obtenidos de cinco replicas biológicas independientes.

Western Blotting. Se obtuvieron testículos de machos disecados en PBS con los cuales se prepararon extractos de proteína total en buffer de lisis (1 % SDS, 250 mM sacarosa, 50 mM Tris pH 7.5, 25 mM KCl, 5 mM $MgCl_2$ y 5 mM EDTA) con inhibidores de proteasas (complete, Roche). Los extractos de proteína de embriones se obtuvieron siguiendo el protocolo reportado por Tin Tin Su [37]. En cualquiera de los casos, las proteínas se sometieron a electroforesis en geles desnaturalizantes de acrilamida-bisacrilamida (Biorad) (gel concentrador al 5 % y gel separador al 7.5-15 %) y se transfirieron a una membrana de nitrocelulosa de 0.2 µm de diámetro del poro (Biorad). La membrana se bloqueó durante 12 h a 4 °C con leche semidescremada (a una concentración de 10-20 %) en PBST (PBS con 0.1 % tween 20). Posteriormente se incubó durante 2 h con el anticuerpo primario diluido en PBST con leche semidescremada al 5 %. Se eliminó con PBST el exceso de anticuerpo primario y se incubó con un anticuerpo secundario (1:3500; Invitrogen). La membrana se lavó con PBST y las proteínas se detectaron por quimioluminiscencia (Thermo Scientific Pierce ECL). Anticuerpos primarios: 8WG16 (1:1500; Covance), H14 (1:1500; Covance), XPD (1:1500; [38]), XPB (1:2000; [38]), p52 (1:1500; [33]), p8 (1:1000; [33]), Cdk7 (1:1000, Santa Cruz Biotechnology), TBP (1:500; Santa Cruz Biotechnology), E7 (1:2000; DSHB), A12 (1:1500; DSHB), F2F4 (1:1500; DSHB), JLA20 (1:3000; DSHB), GFP (1:2500; GenScript); p18 (1:1000; [33]). Se realizaron ensayos con tres replicas biológicas independientes.

Análisis de expresión relativa. Se obtuvo ARN total de testículos de machos disecados en PBS 0-1 día después de su eclosión. Se utilizó Trizol (Invitrogen) y se siguieron las instrucciones de la compañía fabricante durante la extracción del ARN. Se utilizó la misma cantidad de ARN de cada genotipo y las mismas condiciones de reacción para sintetizar ADN complementario (ADNc) mediante transcripción reversa, utilizando la transcriptasa MVL-V (Invitrogen). Se realizaron análisis de expresión mediante PCR en tiempo real (qPCR) utilizando el sistema LightCycler Fast Start DNA Master^{PLUS} SYBR Green I y el equipo LightCycler 1.5 (Roche). El nivel de expresión relativa de cada gen analizado se calculó empleando la siguiente fórmula: 2^{-ddCt}, donde ddCt=(Ct gen blanco-Ct gen control). *CycA* se usó como control interno. Las secuencias de los oligonucleótidos empleados en estos ensayos se indican a continuación (en dirección 5'-3'): *Mst87F*: sentido, AACTTTTACGAATTAATCATGTGCTG; antisentido, CAGGGTCCACATCCTCCTC. *dj*: sentido, AACTGAAAAAGAAATGCAAGGAA;

antisentido, TTTGCAAGGGTCTTTCTTCG. *fzo*: sentido, CAATGTCTCTCCATACCCCTACA; antisentido, AGTTGCCAATCGCAAGAGTT. *twe*: sentido, AAGACCAAGTCCTGGCAATG; antisentido, CAGTCGTGAACGTGATTTCC. *CycA*: sentido, GCTGGAGGAGATCACGACTT; antisentido, CCATCATAGCCACCTTCTTGT. Se realizaron triplicados técnicos de dos replicas biológicas independientes.

Inmunoprecipitación de cromatina de testículos. Para cada ensayo se utilizaron 100 pares de testículos, los cuales se obtuvieron de machos de 0-1 día después de su eclosión. Los machos se disecaron en PBS con inhibidores de proteasas (Roche), se fijaron durante 15 minutos a 37 °C en 1 % de paraformaldehído (EMS) y se lavaron con PBS. Grupos de 50 pares de testículos se procesaron simultáneamente y se almacenaron a -80 °C en PBS. Los testículos se homogenizaron en 130 µL de buffer de lisis con SDS (1 % SDS, 50 mM Tris, pH 8.0 y 10 mM EDTA) con inhibidores de proteasas (Roche) y se sonicaron durante seis ciclos (30 s ON/60 s OFF por cada ciclo) en tubos de pared delgada (Axygen PCR-05-C) a alta potencia en un sonicador Bioruptor (Diagenode). La cromatina se diluyó diez veces con buffer de dilución (0.01 % SDS, 1.1 % Triton X-100, 1.2 mM EDTA, 16.7 mM Tris, pH 8.0 y 167 mM NaCl) y se incubó con IgG de conejo acoplada a Dynabeads Protein G (Life Technologies). El 10 % del lisado se reservó como input y el resto se incubó con 7.5 µg de anticuerpo (anti-Pc o anti-XPB; Santa Cruz Biotechnology) o IgG de conejo (anticuerpo irrelevante o "mock") (Invitrogen) durante 12 h a 4 °C. Los complejos anticuerpo-cromatina fueron recuperados con 50 µL de Dynabeads Protein G. La resina se lavó una vez con cada una de las siguientes soluciones: buffer con baja concentración de sal (0.1 % SDS, 1 % Triton X-100, 2 mM EDTA, 20 mM Tris, pH 8.0 y 150 mM NaCl), buffer con alta concentración de sal (0.1 % SDS, 1 % Triton X-100, 2 mM EDTA, 20 mM Tris, pH 8.0 y 500 mM NaCl), buffer de LiCl (0.25 M LiCl, 1 % NP40, 1 % deoxicolato de sodio, 1 mM EDTA, y 10 mM Tris, pH 8.0) y dos veces con buffer TE (10 mM Tris, pH 8.0 y 1 mM EDTA). La cromatina inmunoprecipitada se recuperó con buffer de elusión (1 % SDS, 0.1 M $NaHCO_3$, 10 mM Tris, pH 8.0 y 1 mM EDTA). El entrecruzamiento se revirtió a 65 °C durante 12 h. Se incubó con 0.2 µg/µL de RNAsa A (Roche) durante 1 h a 37 °C y posteriormente con Proteinasa K (Roche) a una concentración final de 0.2 µg/µL durante 2 h a 55 °C. El ADN se recuperó con un protocolo estándar de extracción con fenol y cloroformo y

precipitación con etanol y glucógeno (Roche). El ADN recuperado se analizó mediante qPCR, para lo cual se emplearon secuencias de oligonucleótidos reportados en trabajos previos [39,40]. El enriquecimiento relativo al anticuerpo irrelevante o "mock" (IgG de conejo) se calculó empleando la siguiente fórmula: $E^{(-ddCt)}$, donde E representa la eficiencia de cada par de oligonucleótidos, y ddCt=[(Ct muestra-Ct input)-(Ct mock-Ct input)] [41,42]. Se realizaron ensayos de al menos dos y hasta tres replicas biológicas independientes.

RNA-seq de testículo y análisis bioinformático. Se obtuvo ARN total de organismos *Ore R* (genotipo silvestre), $p8^{-}/p8^{-}$ y $p52^{EP3605}/p52^{mrn5}$ utilizando Trizol (Invitrogen). El Beijing Genomic Institute (BGI) realizó la secuenciación masiva de ARN y parte del análisis bioinformático. En resumen, se prepararon bibliotecas de ARNm utilizando Illumina TruSeq RNA library construction kit v2. Las bibliotecas se purificaron utilizando Agencourt AMPure XP (Beckman Coulter) y se secuenciaron en un equipo Illumina HiSeq 2000. Para determinar el enriquecimiento en la expresión genética, se examinaron los valores de "Reads Per Kilobase of transcript per Million mapped reads" (RPKM) [43]. La corrección para errores por falsos positivos y falsos negativos se realizó usando el método de "False Discovery Rate" (FDR) descrito por Benjamini y colaboradores [44]. Los genes diferencialmente expresados en los testículos mutantes de TFIIH respecto al genotipo silvestre se representan a través de mapas de calor. Estos mapas se generaron con el software Cluster 3.0 [45]. El Log_2 del cambio en el nivel de expresión >1 indica el aumento (de al menos el doble), mientras que el Log_2 del cambio en el nivel de expresión <1 indica la disminución (al menos a la mitad) en la expresión de un gen respecto al nivel silvestre.

Inmunotinción de embriones. Se colectaron embriones en platos de agar piloncillo y se decorionaron con una solución de hipoclorito de sodio al 2.5 %. Para realizar inmunotinciones de tubulina, los embriones se fijaron durante 1 minuto con metanol, para el resto de las tinciones las muestras se fijaron durante 20 minutos en formaldehido al 4 % en PBS:heptano (1:1) y se devitelinizaron con metanol. Posteriormente, los embriones se hidrataron con un gradiente de metanol:TBST (20 mM Tris, 150 mM NaCl y 0.5 % tween 20) y se trataron con 10 µg/mL de RNAsa A (Roche) en TBST durante 1h a temperatura ambiente, se lavaron con TBST y se bloquearon durante 9 h con suero de cabra (Invitrogen) al 10 %. Después del bloqueo los

embriones se incubaron 12 h a 4 °C con el anticuerpo primario diluido en TBST con suero de cabra al 5 %. El exceso de anticuerpo primario se lavó con TBST y posteriormente se incubó durante 1 h con el anticuerpo secundario. Para teñir el ADN, los embriones se incubaron con 15 nM sytox green (Roche) durante 15 minutos. Finalmente las muestras se montaron en citifluor (ACF). Anticuerpos primarios: p8 (1:100;[33]), $H3S_{10}P$ (1:1500; Santa Cruz Biotechnology), AA4.3 (1:800; DSHB), ADL67 (1:600; DSHB), H14 (1:500; Covance), TBP (1:100; Santa Cruz Biotechnology), CTD4H8 (1:100; Santa Cruz Biotechnology), GTU-88 (1:500, abcam) y Ciclina H (1:500; Santa Cruz Biotechnology). Anticuerpos secundarios: Alexa-Fluor dyes (1:300-1:800; Invitrogen).

Visualización de embriones in vivo. Se colectaron embriones después de 2 horas de oviposición, se decorionaron y se lavaron con abundante agua. Se colocaron individualmente con un pincel delgado sobre un cubreobjetos cubierto con pegamento preparado con heptano y cinta adhesiva de doble cara. Los embriones se cubrieron con una gota de aceite de halocarbono 700 (Sigma) y finalmente se visualizaron con un equipo confocal Olympus FV1000 acoplado a un microscopio invertido. Se visualizaron embriones de al menos dos líneas transgénicas diferentes de cada construcción.

Inmunoprecipitación de cromatina de embriones. Se utilizaron 250 µL de embriones para cada ensayo de inmunoprecipitación. Se colectaron embriones silvestres en platos de agar piloncillo y se decorionaron con una solución de hipoclorito de sodio al 2.5 %. Los embriones se incubaron en una interfase de PBS:heptano (embriones en interfase) o PBS con 500 µM de colchicina (Sigma):heptano (embriones en mitosis) y se fijaron durante 15 minutos a temperatura ambiente con 1.8 % de paraformaldehído (EMS) en buffer de fijado (50 mM Hepes pH 7.5, 1 mM EDTA, 0.5 mM, EGTA y 100 mM NaCl). Para detener el fijado, los embriones se lavaron una vez con 125 mM glicina y 0.1 % Triton X-100 en PBS y una vez con 0.1 % Triton X-100 en PBS. Los embriones se devitelinizaron con heptano y metanol, se lavaron dos veces con metanol y se almacenaron en metanol a -20 °C. Los embriones se rehidrataron secuencialmente en un gradiente de metanol:PBST (PBS con 0.1 % triton X-100), se lavaron dos veces con PBST y se homogenizaron en 1 mL de buffer A1 (15 mM Hepes pH 7.5, 15 mM NaCl, 60 mM KCl, 4 mM $MgCl_2$, 0.5 mM DTT y 0.5 % triton X-100). El homogenizado se centrifugó a 2000 rpm durante

3 minutos a 4 ºC. Se descartó el sobrenadante y la pastilla se lavó una vez con 5 mL de buffer A1 y una vez con 5 mL de buffer A2 (15 mM Hepes pH 7.5, 140 mM NaCl, 1 mM EDTA, 0.5 mM EGTA, 1 % triton X-100, 0.1 % deoxicolato de sodio, 0.1 % SDS y 0.5 % sarcosil). La pastilla se resuspendió en 900 µL de buffer A2 y se sometió a 60 ciclos de sonicación (30 s ON/60 s OFF por cada ciclo) a alta potencia en un sonicador Bioruptor (Diagenode) en tubos TPX de 1.5 mL (Diagenode). El extracto sonicado se centrifugó a 13000 rpm durante 10 minutos a 4 ºC y se incubó con IgG de conejo o de ratón acoplada a Dynabeads Protein G (Life Technologies). El 10 % del lisado se reservó como input y el resto se incubó con 7.5 µg de anticuerpo (anti-TBP, Santa Cruz Biotechnology; anti-RNAP II, Covance o anti-XPB, Santa Cruz Biotechnology) o IgG de conejo o ratón (anticuerpo irrelevante o "mock") (Invitrogen) durante 12 h a 4 °C. Los complejos anticuerpo-cromatina se recuperaron con 25 µL de Dynabeads Protein G. El sobrenadante se descartó y la resina se lavó cinco veces durante 10 minutos con 1 mL de buffer de lavado (50 mM Hepes pH 7.5, 1 mM EDTA, 0.7 % deoxicolato de sodio, 1% Igepal y 500 mM LiCl) y una vez con 50 mM de NaCl en buffer TE (10 mM Tris pH 8.0 y 1 mM EDTA). La cromatina inmunoprecipitada se recuperó con 200 µL de buffer de elusión (1 % SDS, 0.1 M $NaHCO_3$, 10 mM Tris pH 8.0 y 1 mM EDTA) incubando a 65 ºC y 1500 rpm durante 20 minutos. La elusión se combinó con 0.5 volúmenes de buffer TE y el entrecruzamiento se revirtió a 65 °C durante 12 h. Se incubó con 0.2 µg/µL de RNAsa A (Roche) durante 2 h a 37 °C y posteriormente se incubó con Proteinasa K (Roche) a una concentración final de 0.2 µg/µL durante 2 h a 55 °C. El ADN se recuperó con un protocolo estándar de extracción con fenol y cloroformo y precipitación con 200 mM de NaCl, etanol y glucógeno (Roche). El ADN recuperado se analizó mediante PCR punto final, para lo cual se emplearon las siguientes secuencias de oligonucleótidos (anotados en dirección 5'-3'): H3 sentido, CACGTTCACTACTTCACGTTTG; H3 antisentido, GGCCTCTGTTTTTCTCTCTCTC. H4 sentido, ATTATACACGCACAGCACGAAAG; H4 antisentido, CTCTCGGGTTTTTGTCGTTTTAC. rover sentido, CAACCAAGACCAACCTACCC; rover antisentido, GCTCATTTTAGTCTGTCCGC [46]. Se realizaron ensayos con dos replicas biológicas independientes.

RNA-seq de embriones. Se colectaron embriones ovipositados por hembras heterocigóticas (dos embriones) u homocigóticas (tres embriones) del alelo nulo de *p8* que expresan la construcción

His2Av-RFP. Los embriones se colocaron en un cubreobjetos limpio y se cubrieron con una gota de agua mili Q. Se visualizaron mediante microscopía confocal y el número de núcleos en el embrión se determinó al analizar con el software Image J las imágenes de proyecciones derivadas de la reconstrucción de los planos adquiridos en Z. Después de la adquisición de las imágenes cada embrión se sometió a la extracción de ARN total con Trizol (Invitrogen). BGI realizó la secuenciación masiva de ARN siguiendo el protocolo para células individuales. En resumen, se prepararon bibliotecas de ARNm utilizando SMART-seq Ultra Low Input RNA kit. Las bibliotecas se purificaron utilizando Agencourt AMPure XP (Beckman Coulter) y se secuenciaron en un equipo Illumina HiSeq 2000.

6. RESULTADOS

Parte I: TFIIH es esencial en la diferenciación de células germinales en el testículo de *Drosophila melanogaster*

6.1 Las subunidades p8 y p52 de TFIIH son esenciales en la meiosis de las células germinales en el testículo

Con la finalidad de entender la causa del fenotipo de esterilidad asociado a la falta de p8 y la disminución de p52 se analizaron los testículos de estos organismos y de aquellos con fenotipo silvestre a través de microscopía de contraste de fases. Con esta técnica es posible observar los diferentes estadios de diferenciación que ocurren durante la espermatogénesis en el testículo de la mosca, a través de las características morfológicas de cada tipo celular. De esta forma, con excepción de algunas células que avanzan aberrantemente en la diferenciación y que se localizan en zonas del testículo próximas al ducto testicular, en ambas mutantes de TFIIH se observó la detención de la diferenciación de las células germinales en el estadio de espermatocito primario (Figura 9) una etapa transcripcionalmente muy activa previa a la entrada a meiosis. En espermatocitos provenientes de testículos con fenotipo silvestre ($p8^{+}/p8^{-}$) se observa el huso acromático durante la metafase de la meiosis, contrariamente, no se detectan células en meiosis en los testículos afectados en TFIIH (Figura 10A). Así mismo, la acumulación de espermatocitos

primarios antes de su entrada a meiosis es consistente con la acumulación de Ciclina A en los testículos mutantes (Figura 10B).

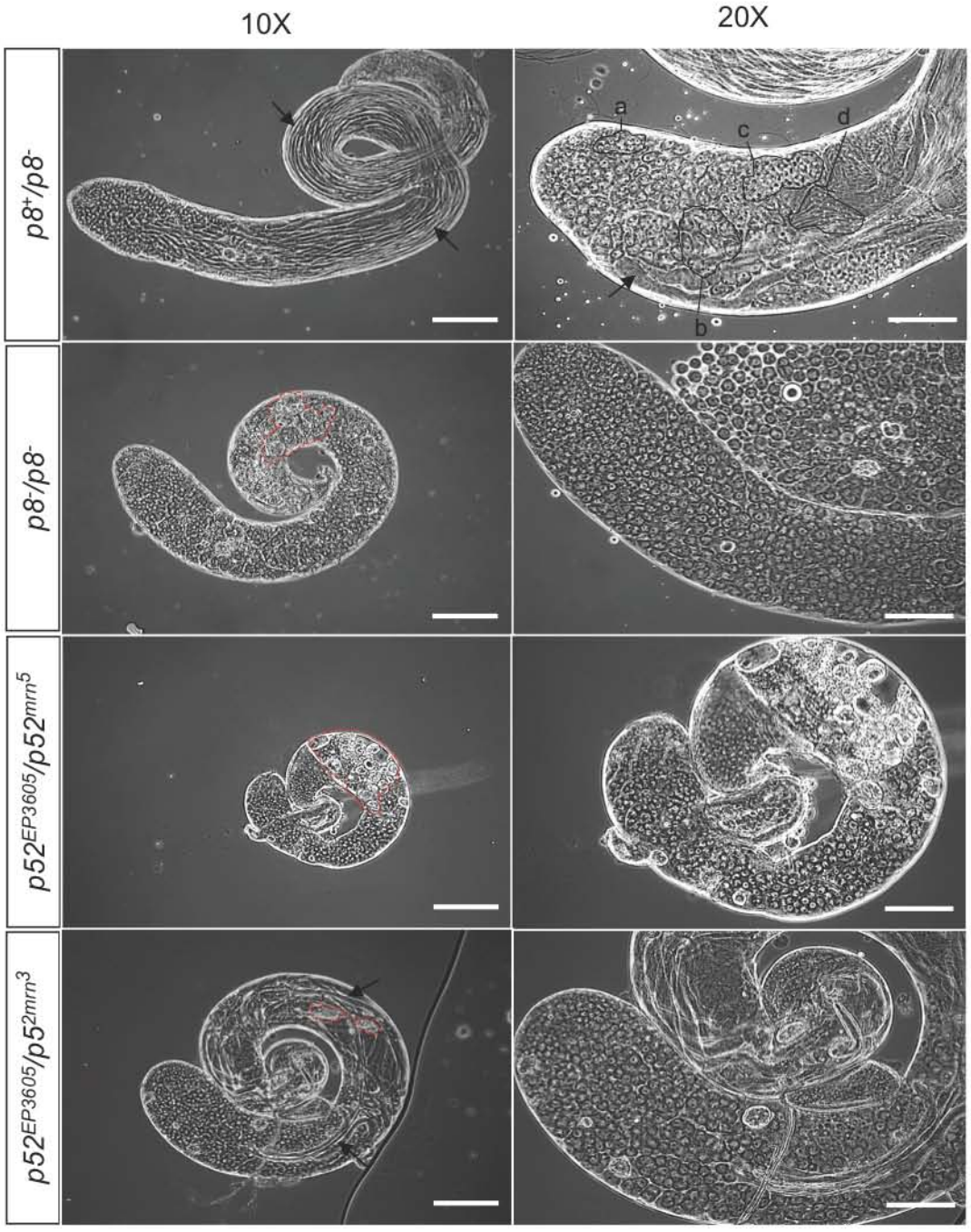

Figura 9. La falta de p8 al igual que la disminución de p52 causa la detención de la diferenciación de las células germinales en el estadio de espermatocito primario. Microscopía de contraste de fases (objetivos 10X y 20X) de testículos de machos fértiles ($p8^{+}/p8^{-}$) o bien machos que muestran fenotipo de esterilidad debido a mutaciones en las

subunidades *p8* y *p52* de TFIIH (*p8*$^{-}$/*p8*$^{-}$, *p52*^{EP3605}/*p52*^{mrn5} y *p52*^{EP3605}/*p52*^{mrn3}). En los testículos con fenotipo silvestre se aprecian células en distintas etapas de la diferenciación, incluyendo espermatocitos primarios tempranos (a), espermatocitos primarios maduros (b), espermátidas redondas (c), espermátidas en elongación (d) y una proporción considerable de espermatozoides (las flechas señalan flagelos). Por otra parte, los testículos mutantes presentan enriquecimiento anormal de células en el estadio de espermatocito primario y sólo en uno de los genotipos mutantes de *p52* (*p52*^{EP3605}/*p52*^{mrn3}) las células avanzan a estadios de diferenciación más tardíos. Además, en todos los casos se observan grupos de células en degeneración (regiones delimitadas en color rojo). La barra de escala representa 100 μm en imágenes en 10X (izquierda) y 50 μm en imágenes en 20X (derecha).

El fenotipo observado es similar entre los genotipos mutantes de TFIIH, sin embargo, es más severo en los testículos de machos afectados con la combinación de alelos *p52*^{mrn5} y *p52*^{EP3605} cuyos testículos son mucho más pequeños que los silvestres y están enriquecidos con espermatocitos primarios más jóvenes que aquellos que se acumulan en los testículos nulos de *p8* que muestran además de la acumulación de Ciclina A, un nivel elevado de Ciclina B, dos reguladores del ciclo celular que deben degradarse para salir de mitosis (Figura 10B). Estos resultados indican que la falta de p8 o la disminución de p52 impiden la entrada a meiosis y como consecuencia la diferenciación de las células germinales en el testículo.

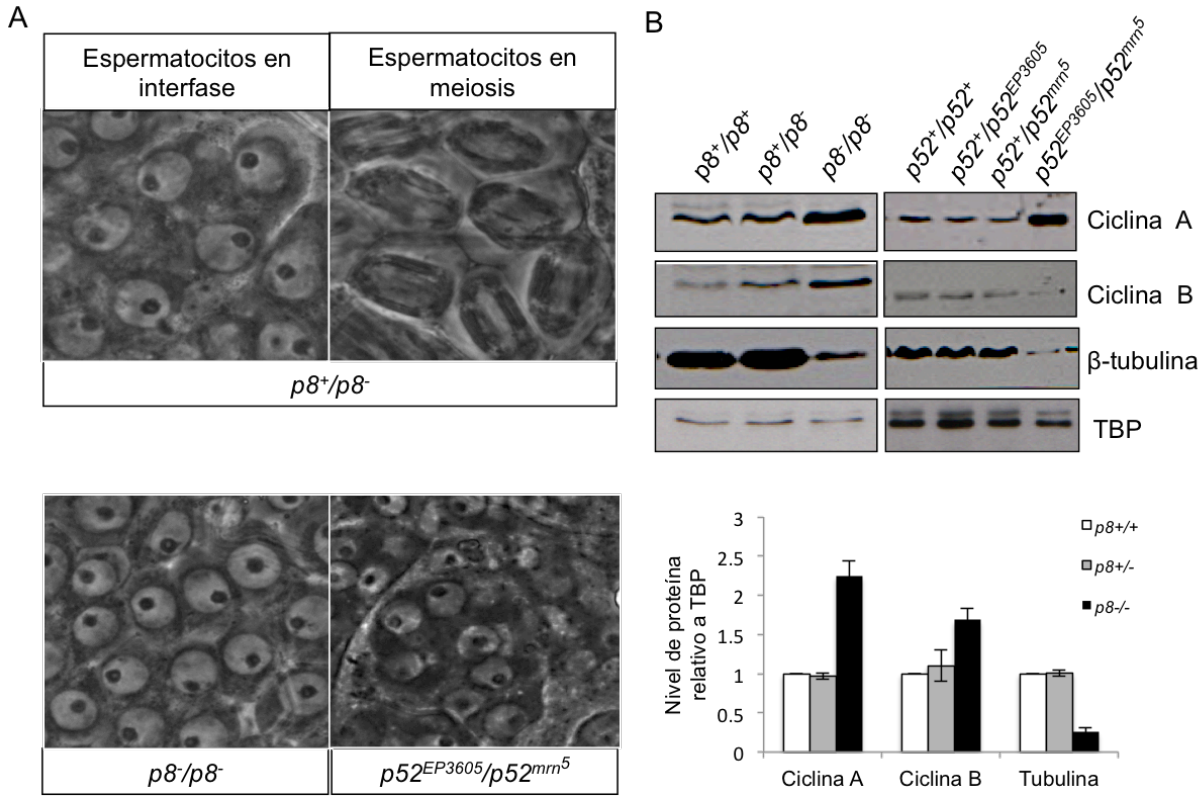

Figura 10. La diferenciación de los espermatocitos primarios en las mutantes de TFIIH se detiene antes de su entrada a meiosis. A. En los testículos control ($p8^{+}/p8^{-}$) se observan espermatocitos primarios tanto en interfase como en meiosis. Por el contrario, los testículos mutantes ($p8^{-}/p8^{-}$ y $p52^{EP3605}/p52^{mrn5}$) no contienen células en meiosis. B. Los testículos de las mutantes de TFIIH muestran niveles más altos de Ciclina A que los organismos control. Adicionalmente, los testículos nulos en *p8* muestran también un nivel más elevado de Ciclina B. En ambos casos, las mutantes muestran niveles más bajos de tubulina que los organismos control. El panel inferior en "B" muestra la cuantificación del nivel de proteína de los genotipos indicados relativo a la proteína TBP (el nivel de TBP fue normalizado a 1 para el genotipo silvestre). La gráfica de barras muestra el promedio y la desviación estándar de la cuantificación por densitometría de los niveles de proteína de tres ensayos independientes. "A" corresponde a imágenes de contraste de fases y "B" a ensayos tipo western blot de testículos. En "B" , las mutantes de TFIIH corresponden a los siguientes genotipos: $p8^{-}/p8^{-}$ y $p52^{EP3605}/p52^{mrn5}$, mientras que los organismos control corresponden a $p52^{+}/p52^{+}$, $p52^{+}/p52^{EP3605}$ y $p52^{+}/p52^{mrn5}$.

6.2 La localización subcelular de p8 en espermatocitos primarios depende de p52

Con la finalidad de determinar el patrón de localización de p8, p52 y XPB durante la espermatogénesis, se generaron moscas transgénicas que expresan fusiones de éstas con

proteínas fluorescentes (p8-ECFP, EYFP-p52 y XPB-EGFP). La expresión de estas proteínas en la mosca se corroboró mediante western blot y su funcionalidad se demostró a través de ensayos de rescate (Tablas 1 y 2), en los cuales la expresión del transgen suprimió los fenotipos de letalidad e infertilidad asociados a la falta de p8 o la disminución de p52. Por lo tanto estas proteínas son capaces de suplementar la dosis necesaria y las funciones de p8 y p52 para el desarrollo normal de la mosca y constituyen una herramienta útil en el estudio de la dinámica de estas proteínas durante el desarrollo.

Tabla 1. Rescate de mutantes heteroalélicas de *p52* con la expresión del transgen *EYFP-p52*.

Genotipo	% Sobrevivencia* (individuos observados/individuos esperados)
Sp/Cyo_{Cy}; $p52^{EP3605}/p52^{mrn5}$	57 % (263/462)
EYFP-p52/EYFP-p52; $p52^{EP3605}/p52^{mrn5}$	100 % (468/468)

* Número de organismos que alcanzan la etapa adulta. Sólo se muestran las clases relevantes. Tabla adaptada de [47].

En los testículos de las moscas transgénicas se observó, a través de microscopía confocal, que p8-ECFP, EYFP-p52 y XPB-EGFP se enriquecen en las etapas tempranas de la espermatogénesis, en las que se observa su distribución homogénea en el núcleo de las espermatogonias y un patrón más dinámico durante la etapa de espermatocito primario (Figura 11), estadio en el cual se detiene la diferenciación en los fondos mutantes de estas proteínas. En los espermatocitos primarios más jóvenes, las subunidades de TFIIH se enriquecen en los cromosomas bivalentes en el núcleo y muestran un patrón de puntos en la periferia del nucléolo. Posteriormente, se observa su enriquecimiento con un patrón punteado también en el nucleoplasma de espermatocitos maduros, mientras que su localización perinucleolar se define más claramente con un patrón en forma de anillo (Figura 12).

Tabla 2. Rescate de mutantes homocigóticas del alelo nulo de *p8* con la expresión del transgen *p8-ECFP*.

Genotipo	% Sobrevivencia* (individuos observados/individuos esperados)
p8⁻/p8⁻; TM2, $_{Ubx}$/MKRS, $_{Sb}$	26 % (102/387)
p8⁻/p8⁻; p8-ECFP/p8-ECFP	58 % (108/186)

* Número de organismos que alcanzan la etapa adulta. Sólo se muestran las clases relevantes.

En un trabajo previo se demostró la interacción física de las subunidades p8 y p52 en la mosca [33]. Debido a que el patrón de localización observado es común entre estas subunidades de TFIIH se decidió analizar si su localización es mutuamente dependiente, para ello se expresó el transgen de p8 (*p8-ECFP*) en la mutante de *p52* y el transgen de p52 (*EYFP-p52*) en la mutante de *p8*. De manera interesante, se observó que la localización de EYFP-p52 no se afecta en ausencia de p8 en el testículo, sin embargo, la disminución de p52 provoca la deslocalización de p8-ECFP en los espermatocitos primarios (Figura 13). Estos resultados sugieren que la interacción física de p8 con p52 podría ser necesaria para localizar a p8 en estas células, pero es dispensable para la localización de p52. Aunado a la mayor severidad del fenotipo observado en testículos en la mutante de *p52*, este resultado sugiere que mutaciones en esta subunidad tienen un efecto más deletéreo que la falta de p8, el cual puede afectar el comportamiento de otras subunidades del complejo.

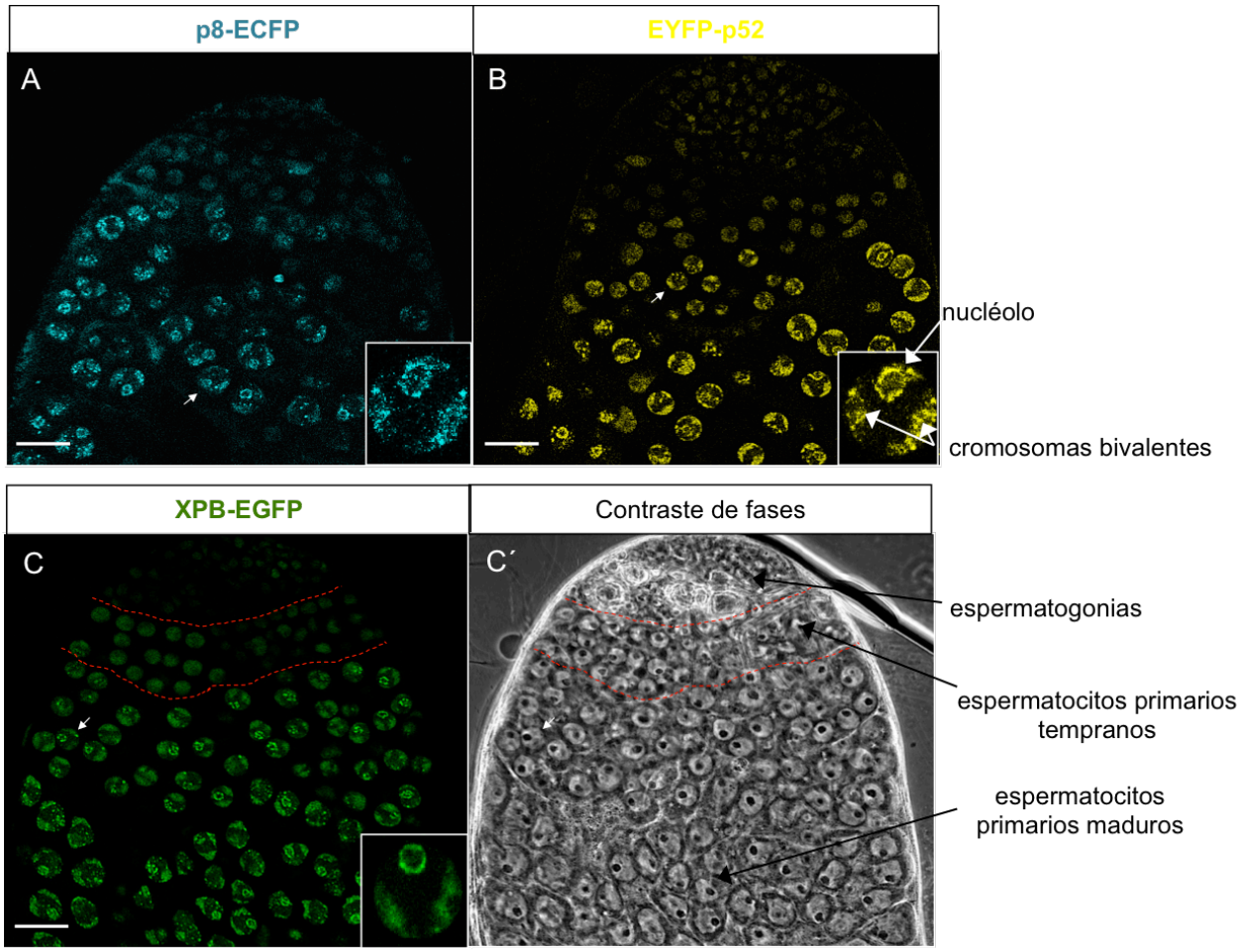

Figura 11. Las subunidades p8, p52 y XPB se enriquecen en espermatocitos primarios. A-C. p8-ECFP, EYFP-p52 y EGFP-XPB se enriquecen en las células de la zona apical del testículo en los estadios tempranos de la diferenciación de las células germinales. El mayor enriquecimiento se observa en los cromosomas bivalentes y la periferia del nucléolo de los espermatocitos primarios (ver recuadro en la esquina inferior derecha de cada imagen A-C). "A", "B" y "C" corresponden a imágenes de microscopía confocal, mientras que "C´" corresponde al mismo campo que "C" en microscopía de contraste de fases. Las líneas punteadas en "C" y "C´" delimitan regiones de enriquecimiento de espermatogonias (en la sección superior), espermatocitos primarios tempranos (en la sección media) y espermatocitos primarios maduros (en la sección inferior). El recuadro en la esquina inferior derecha de "A", "B" y "C" muestra la amplificación de una región de cada imagen de confocal en la que se observa un espermatocito primario. La barra de escala representa 25 μm.

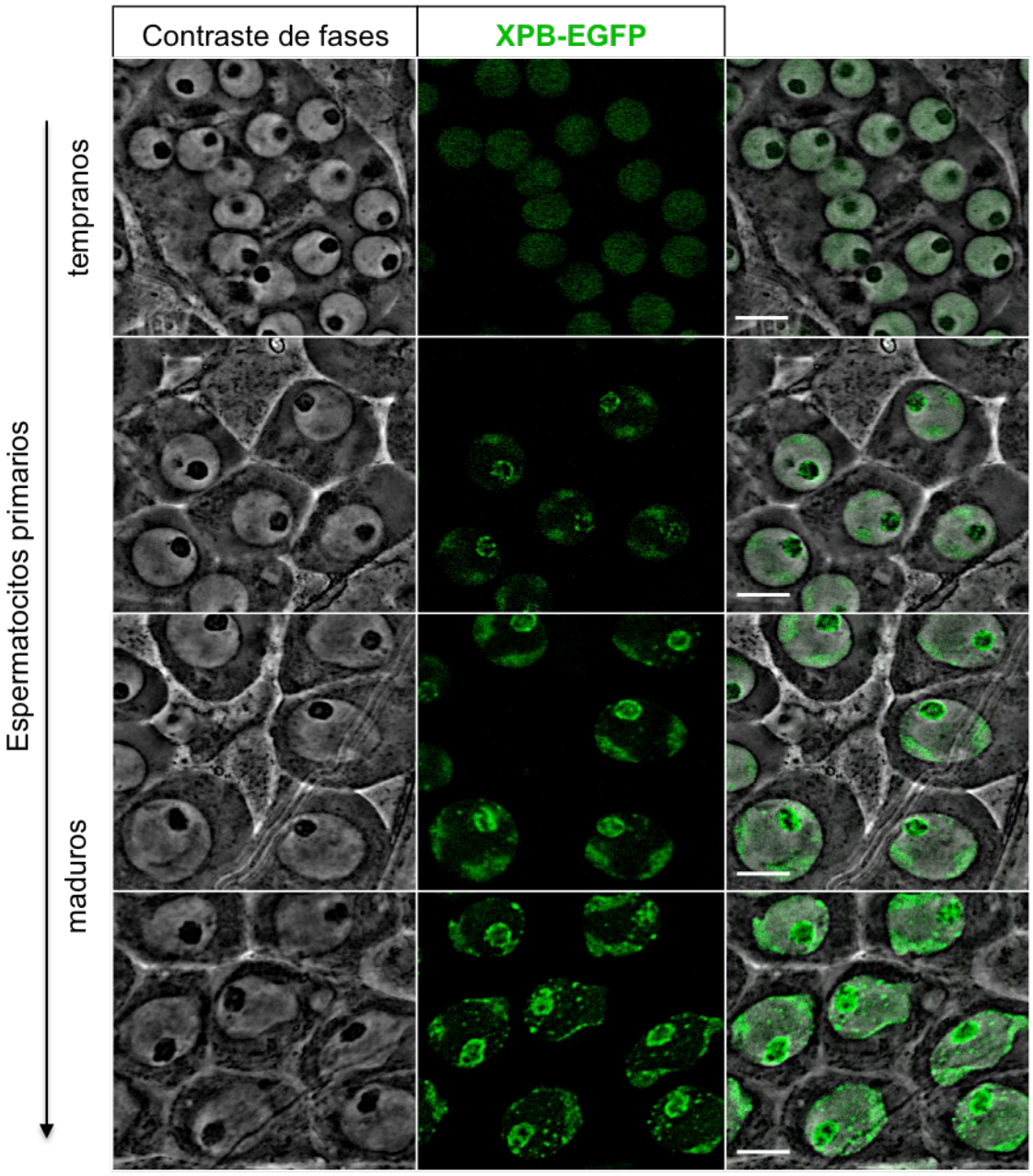

Figura 12. Dinámica de XPB-EGFP durante la maduración de los espermatocitos primarios. En la etapa más temprana de los espermatocitos primarios XPB-EGFP se localiza homogéneamente en el nucleoplasma (panel superior). Conforme estas células aumentan su volumen al avanzar en la maduración, XPB-EGFP se enriquece en regiones específicas en el núcleo y el nucléolo (paneles inferiores). Imágenes de testículos adquiridas mediante microscopía de contraste de fases y microscopía confocal. Izquierda: imágenes de contraste de fases. En medio: imágenes de confocal. Derecha: superposición de contraste de fases y confocal. La barra de escala representa 10 μm.

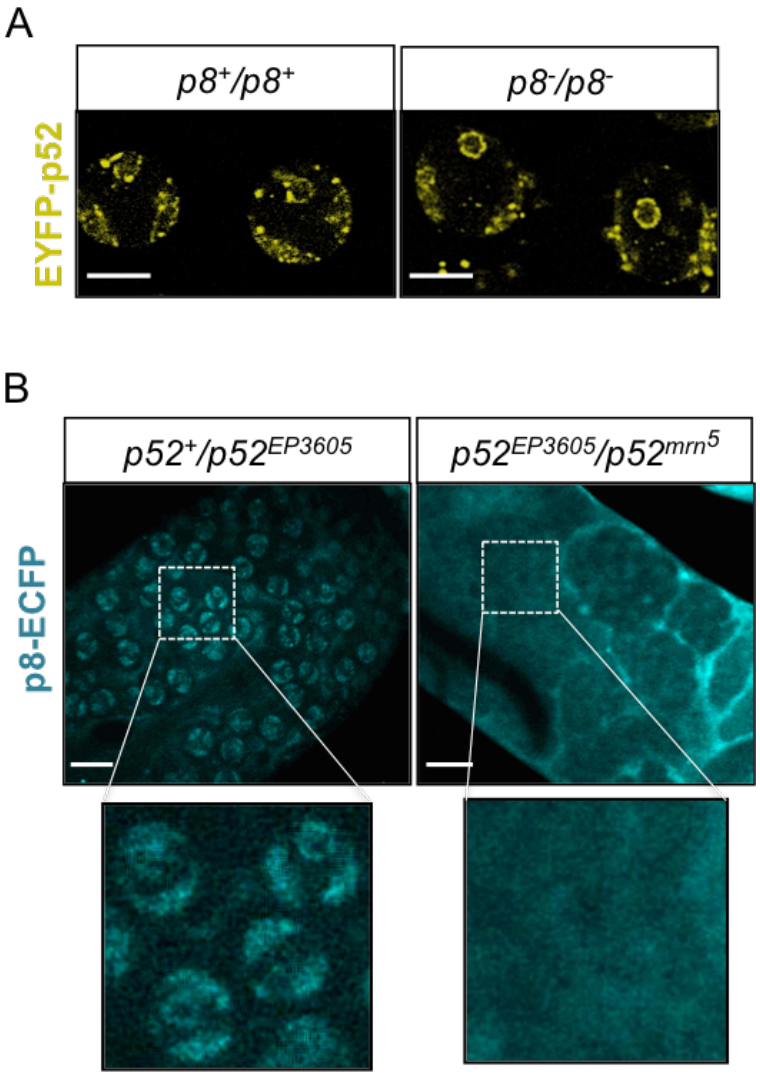

Figura 13. La localización subcelular de p8 depende de p52. A. En la mutante nula de *p8* (*p8*$^{-}$*/p8*$^{-}$), EYFP-p52 muestra el patrón de localización silvestre de enriquecimiento en los cromosomas bivalentes y la periferia del nucléolo. B. En la mutante hipomorfa de *p52* (*p52*^{EP3605}*/p52*^{mrn5}), p8-ECFP se distribuye homogéneamente en el nucleoplasma de los espermatocitos primarios, mientras que en un fondo con nivel silvestre de *p52* (*p52*$^{+}$*/p52*^{EP3605}) p8-ECFP se enriquece en el núcleo y el nucléolo de estas células. Los recuadros inferiores en "B" corresponden a una amplificación de las zonas indicadas con línea punteada en cada imagen. Imágenes adquiridas mediante microscopía confocal de testículos. La barra de escala en "A" representa 10 μm y en "B" 25 μm. El panel "B" de esta figura fue adaptado de [47].

6.3 La subunidad p52 es indispensable para mantener el nivel basal de TFIIH en testículo.

De manera interesante, a pesar de que ninguna de las mutaciones identificadas en células provenientes de pacientes con TTD afectados en p8 corresponde a un alelo nulo, en estas células se han observado niveles reducidos de otros componentes de TFIIH [48–50].

Para determinar si los defectos observados durante la espermatogénesis en las moscas mutantes de *p8* y de *p52* están asociados a niveles bajos de TFIIH se determinó el efecto de la ausencia de p8 o la disminución de p52 en la estabilidad de otras subunidades del complejo en testículo. Para esto, se comparó la abundancia de subunidades del "core" y del CAK entre testículos control ($p8^{+}/p8^{+}$, $p8^{+}/p8^{-}$, $p52^{+}/p52^{+}$, $p52^{+}/p52^{EP3605}$, $p52^{+}/p52^{mrn3}$ y $p52^{+}/p52^{mrn5}$) que muestran fenotipo silvestre y testículos mutantes de *p8* y de *p52* ($p8^{-}/p8^{-}$, $p52^{EP3605}/p52^{mrn3}$ y $p52^{EP3605}/p52^{mrn5}$) que muestran fenotipo de detención de la diferenciación en meiosis. De manera inesperada se encontró que la ausencia de p8 no afecta el nivel de las subunidades XPB, XPD o p52 en testículo (Figura 14A). En contraste, las mutantes en *p52* presentan niveles de XPB y p8 dramáticamente más bajos que los testículos control (Figura 14B). Por otra parte, en ambos casos hay un ligero aumento de Cdk7 (Figura 14).

Adicionalmente, se observó que los niveles de otros componentes de la maquinaria basal de transcripción (TBP y la ARNP II) y la forma activa de la ARNP II (ARNP II S_5P) son muy similares entre testículos silvestres y mutantes (Figura 14).

Estos resultados indican que la disminución de p52 tiene un efecto más dramático que la falta de p8 en la estabilidad de otros componentes de TFIIH en el testículo de la mosca. Además, estos datos sugieren que la disminución del nivel de TFIIH en los testículos mutantes de *p52* no es la causa principal del fenotipo de detención de la diferenciación de las células germinales, sin embargo, podría contribuir a la severidad del mismo.

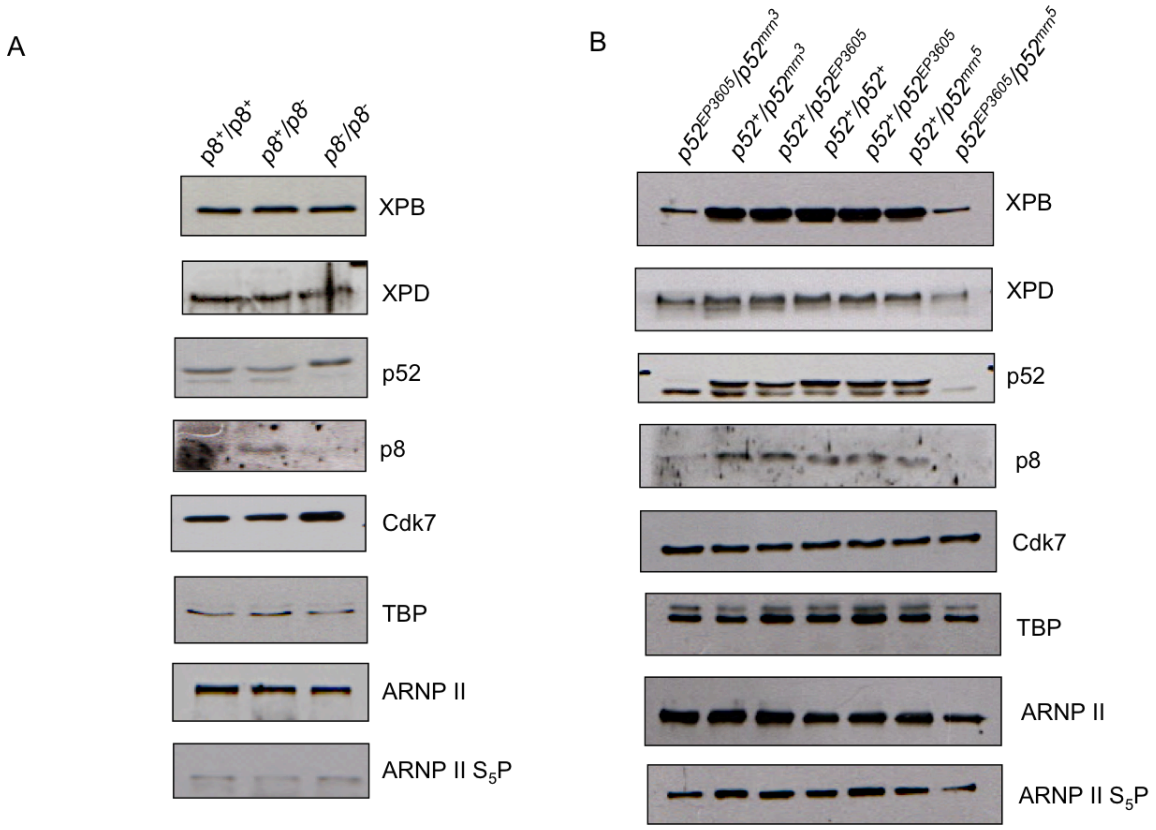

Figura 14. La subunidad p52 es indispensable para mantener la concentración de TFIIH en testículo. Se detectó mediante western blot, el nivel de algunas de las subunidades de TFIIH (XPB, XPD, p52, Cdk7 y p8) y proteínas de la maquinaria basal de transcripción (ARNP II y TBP) en testículos de machos silvestres ($p8^{+}/p8^{+}$), heterocigóticos ($p8^{+}/p8^{-}$) y nulos para *p8* ($p8^{-}/p8^{-}$) (izquierda) y machos silvestres ($p52^{+}/p52^{+}$), heterocigóticos ($p52^{+}/p52^{EP3605}$, $p52^{+}/p52^{mrn3}$, $p52^{+}/p52^{mrn5}$) e hipomorfos de *p52* ($p52^{EP3605}/p52^{mrn3}$ y $p52^{EP3605}/p52^{mrn5}$) (derecha). Se observa que de manera contraria a la falta de p8, la disminución de p52 afecta considerablemente el nivel de otras subunidades de TFIIH y tiene un efecto también sobre el nivel de la ARNP II.

6.4 Las mutantes de TFIIH con fenotipo de detención en meiosis muestran niveles de expresión silvestre de los genes de las clases *aly* y *can*

El fenotipo de detención en meiosis durante la diferenciación de las células germinales en el testículo se ha observado en mutantes de un grupo denominado "genes de detención en meiosis", la mayoría de los cuales codifican versiones específicas de testículo de factores de transcripción que participan en la activación del programa de expresión genética que permite las divisiones meióticas y la diferenciación de las espermátidas [39,51–54]. Estos genes se clasifican en dos

clases principales: la clase *aly* (componentes del complejo de transcripción tMAC) y la clase *can* (componentes de TFIID, denominados tTAFs) [52–58]. Algunos genes requeridos para la diferenciación terminal de las células germinales tales como *don juan* (*dj*), *fuzzy onions* (*fzo*) y *Male-specific RNA87F* (*Mst87F*) son blancos comunes entre las clases *aly* y *can*. Sin embargo, la transcripción de genes requeridos para el control del ciclo celular tales como *Cyclin B* (*CycB*), *boule* (*bol*) y *twine* (*twe*) depende sólo de la clase *aly* [59]. De esta manera, aunque las mutantes de ambas clases comparten el fenotipo de detención en meiosis, en mutantes de la clase *aly* se observa la disminución de la expresión de genes de diferenciación tardía y de control de ciclo celular, mientras que mutantes de la clase *can* muestran niveles silvestres de expresión de genes involucrados en el control del ciclo celular.

Para investigar si la transcripción en las mutantes de TFIIH tiene un comportamiento similar al reportado para las mutantes de la clase *aly* o de la clase *can*, se cuantificó la expresión de algunos de sus blancos mediante ensayos de PCR en tiempo real (qRT-PCR) a partir de ADNc de testículos silvestres, heterocigóticos, y nulos de *p8*. Se encontró que la falta de p8 afecta negativamente la expresión de *dj* y *Mst87F*, pero no de *fzo* y *twe* (Figura 15A). Estos datos sugieren que las mutantes de TFIIH muestran defectos en la transcripción, pero éstos no son idénticos a aquellos observados en testículos mutantes de factores transcripcionales específicos de testículo.

Debido a que TFIIH es un componente central de la maquinaria basal de transcripción de la ARNP II que se expresa de manera ubicua, se determinó el efecto de las mutantes de TFIIH en la transcripción global en testículo mediante RNA-seq. Se secuenciaron los transcriptomas de organismos silvestres y mutantes de *p8* ($p8^{-}/p8^{-}$) y *p52* ($p52^{EP3605}/p52^{mrn^5}$) y para identificar los genes diferencialmente expresados se compararon los niveles de expresión de los transcritos en los genotipos mutantes con el genotipo control. El cambio en la expresión de un gen se consideró significativo cuando se detectó un aumento de al menos el doble o bien la disminución al menos a la mitad del nivel de un transcrito en las mutantes respecto al nivel silvestre. Como se esperaba, los transcriptomas de ambas mutantes de TFIIH son muy semejantes (Figura 15B), sin embargo, el número genes desregulados es mayor en la mutante de *p52*. De manera sorprendente, el nivel de expresión de la mayor parte de los transcritos secuenciados mantiene el nivel silvestre, de tal forma que sólo 1,701 del total de 15,000 transcritos identificados mostraron cambio respecto al

genotipo silvestre (Figura 15C). El análisis ontológico de los genes desregulados mostró, entre otras cosas, la disminución de transcritos específicos de testículo y el aumento en la expresión de genes que regulan la transcripción o la estructura de la cromatina y genes involucrados en el control del ciclo celular. De manera importante, los testículos mutantes mostraron niveles silvestres de los transcritos de los genes de las clases *aly* y *can* (Figura 15C). Lo cual sugiere que el fenotipo de detención en meiosis de los testículos mutantes de TFIIH no está asociado a la desregulación de estos genes.

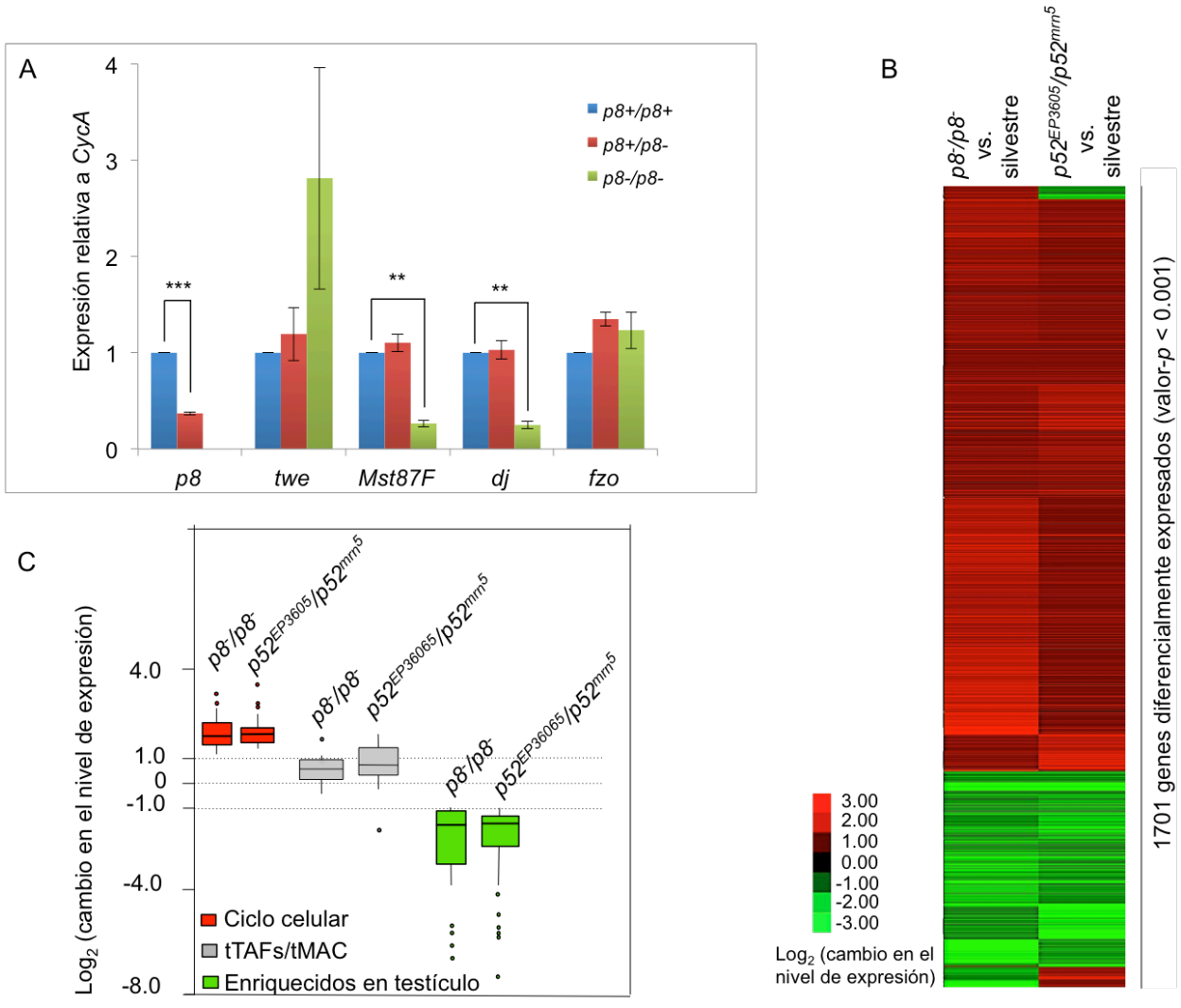

Figura 15. Las subunidades p8 y p52 de TFIIH son esenciales para la transcripción de genes necesarios para la diferenciación de las células germinales. A. La falta de p8 (*p8⁻/p8⁻*) afecta significativamente (**, valor $p < 0.001$) la expresión de algunos de los genes de diferenciación tardía, como *Mst87F* y *dj*. El nivel de expresión de estos y otros transcritos se

determinó mediante PCR en tiempo real. El nivel de cada transcrito se normalizó respecto a *CycA*, cuya expresión se mantiene homogénea entre los distintos genotipos. B. La comparación del transcriptoma de organismos mutantes de *p8* ($p8^{-}/p8^{-}$) o *p52* ($p52^{EP3605}/p52^{mrn^5}$) con el transcriptoma de organismos silvestres muestra la desregulación de 1701 genes en el testículo. Este mapa de calor muestra el nivel de expresión de todos los genes que mostraron un cambio significativo (valor $p < 0.001$) en ambos genotipos mutantes de TFIIH, respecto al genotipo silvestre. El Log_2 del cambio en el nivel de expresión >1 indica el aumento (rojo), mientras que el Log_2 del cambio en el nivel de expresión <1 indica la disminución (verde) en la expresión de un gen respecto al nivel silvestre. C. Gráfica de cajas generada a partir de los datos de genes diferencialmente expresados entre los transcriptomas de testículo de organismos silvestres y mutantes de TFIIH. En los transcriptomas de las mutantes ($p8^{-}/p8^{-}$ y $p52^{EP3605}/p52^{mrn^5}$) se observa el aumento en la expresión de genes cuyos productos están involucrados en el ciclo celular (cajas rojas) y la disminución de transcritos específicos o enriquecidos normalmente en testículo (cajas verdes). Por otra parte, no se afecta la expresión de los genes de la clase *aly* o *can* (cajas grises). En esta gráfica de cajas, el Log_2 del cambio en el nivel de expresión >1 indica aumento, mientras que el Log_2 del cambio en el nivel de expresión <1 indica disminución en la expresión de un gen respecto al nivel silvestre.

6.5 La represión de los genes de diferenciación en testículo en la mutante de *p8* es independiente de Pc

El modelo de regulación transcripcional en el testículo establece que los genes requeridos para la diferenciación durante la espermatogénesis son reprimidos a través de Pc en los precursores de las células germinales, hasta que se expresan los genes *tTAFs* cuyos productos se localizan preferencialmente en el nucléolo de espermatocitos primarios. Debido a que las mutantes de los *tTAFs* muestran deslocalización de Pc del nucléolo de los espermatocitos primarios, se propuso que parte del mecanismo de acción de estos factores transcripcionales consiste en secuestrar a Pc al nucléolo para permitir la expresión de los genes involucrados en la espermatogénesis (Figura 16A) [51].

El fenotipo de detención en meiosis observado en las mutantes de TFIIH y la localización de los componentes del complejo en la periferia del nucléolo nos llevó a investigar si el reclutamiento de Pc al nucléolo depende también de este factor basal de la transcripción. De manera interesante, al utilizar una línea de mosca que expresa una fusión de Pc con la proteína verde fluorescente (Pc-GFP) se observó que en ausencia de p8, el enriquecimiento de Pc en el nucléolo de los espermatocitos primarios disminuye significativamente (Figura 16B). Esto indica que la deslocalización de Pc es un aspecto común entre las mutantes de los factores de

transcripción específicos de testículo y mutantes de factores basales de la transcripción que muestran fenotipo de detención en meiosis.

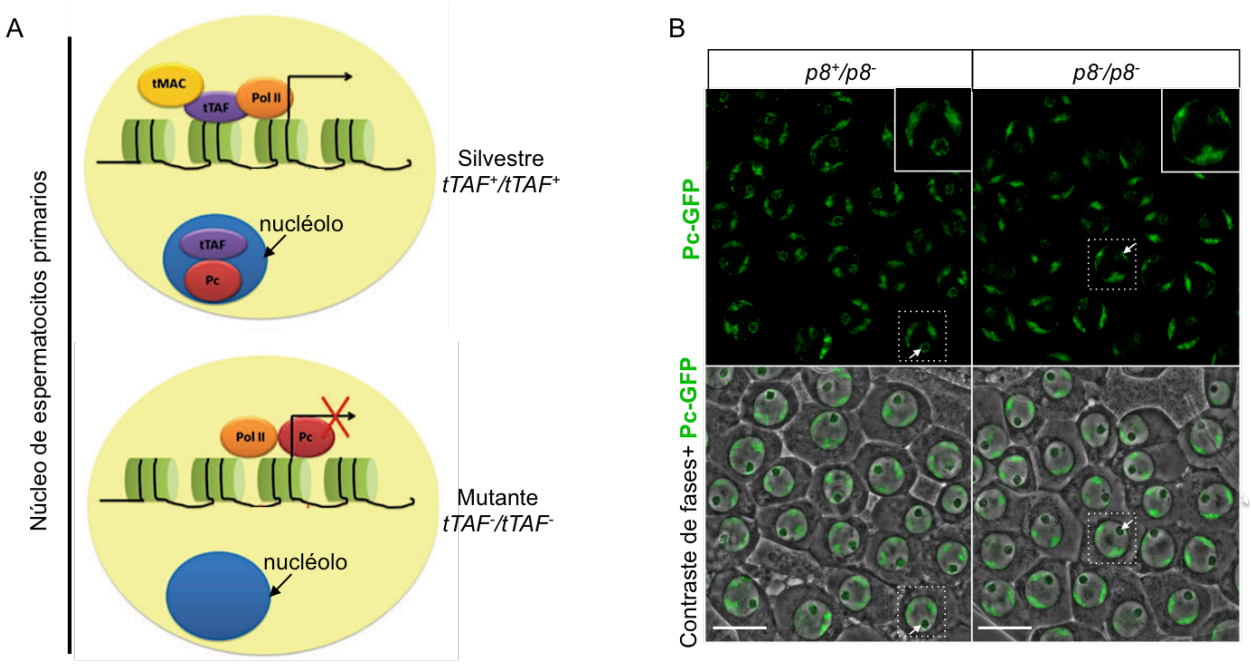

Figura 16. La localización de Pc en el nucléolo de espermatocitos primarios depende de p8. A. Modelo de la regulación de la transcripción mediada por los tTAFs y Pc en los espermatocitos primarios. En espermatocitos silvestres los tTAFs reclutan a Pc al nucléolo para permitir la transcripción de los genes de diferenciación en el núcleo. En mutantes de *tTAFs*, Pc se queda en el núcleo y reprime la expresión de los genes de diferenciación al unirse a la secuencia de ADN del promotor de los mismos (Figura adaptada de [39]). B. En un fondo de *p8* con fenotipo silvestre ($p8^{+}/p8^{-}$), Pc-GFP se localiza en los cromosomas bivalentes y el nucléolo (ver flechas) en los espermatocitos primarios. En ausencia de *p8* ($p8^{-}/p8^{-}$), Pc-GFP se mantiene en los cromosomas bivalentes, pero disminuye su localización en el nucléolo. Los recuadros en la esquina superior derecha de los panales superiores en "B" corresponden a amplificaciones de las regiones delimitadas por los recuadros en las imágenes de los paneles inferiores. Imágenes adquiridas mediante microscopía confocal y de contraste de fases de testículos. La barra de escala en "B" representa 25 μm.

Para determinar si la represión de la expresión de genes de diferenciación afectados en las mutantes de TFIIH depende de un mecanismo mediado por Pc, se realizaron ensayos de inmunoprecipitación de cromatina, en los cuales se analizó la unión de esta proteína al promotor de dos de los genes de diferenciación silenciados (*dj* y *Mst87F*) en las mutantes de TFIIH. En estos ensayos se incluyó un control positivo (*bxd*) que posee un elemento de respuesta a Pc y un control negativo de la unión de Pc a la cromatina (*CycA*). Como se esperaba, se detectó el

enriquecimiento de Pc en la secuencia blanco empleada como control positivo en la cromatina de testículos heterocigóticos u homocigóticos del alelo nulo de *p8*. Por otra parte, el nivel de Pc en los promotores de los genes de diferenciación es similar al detectado en el control negativo tanto en organismos heterocigóticos como homocigóticos del alelo nulo de *p8*. Por lo tanto, la disociación de Pc de la periferia del nucléolo no tiene efecto en la unión de esta proteína a los promotores de los genes de diferenciación, reportados previamente como blancos de los tTAFs que se encuentran silenciados en los testículos mutantes de *p8* (Figura 17A,B). Adicionalmente, se detectó enriquecimiento de XPB en los promotores de los genes de diferenciación y de *CycA* pero no en *bxd* en testículos control y testículos nulos de *p8* (Figura 17C,D), lo cual indica que aún en ausencia de p8, otros componentes de TFIIH pueden reclutarse a los promotores de estos genes.

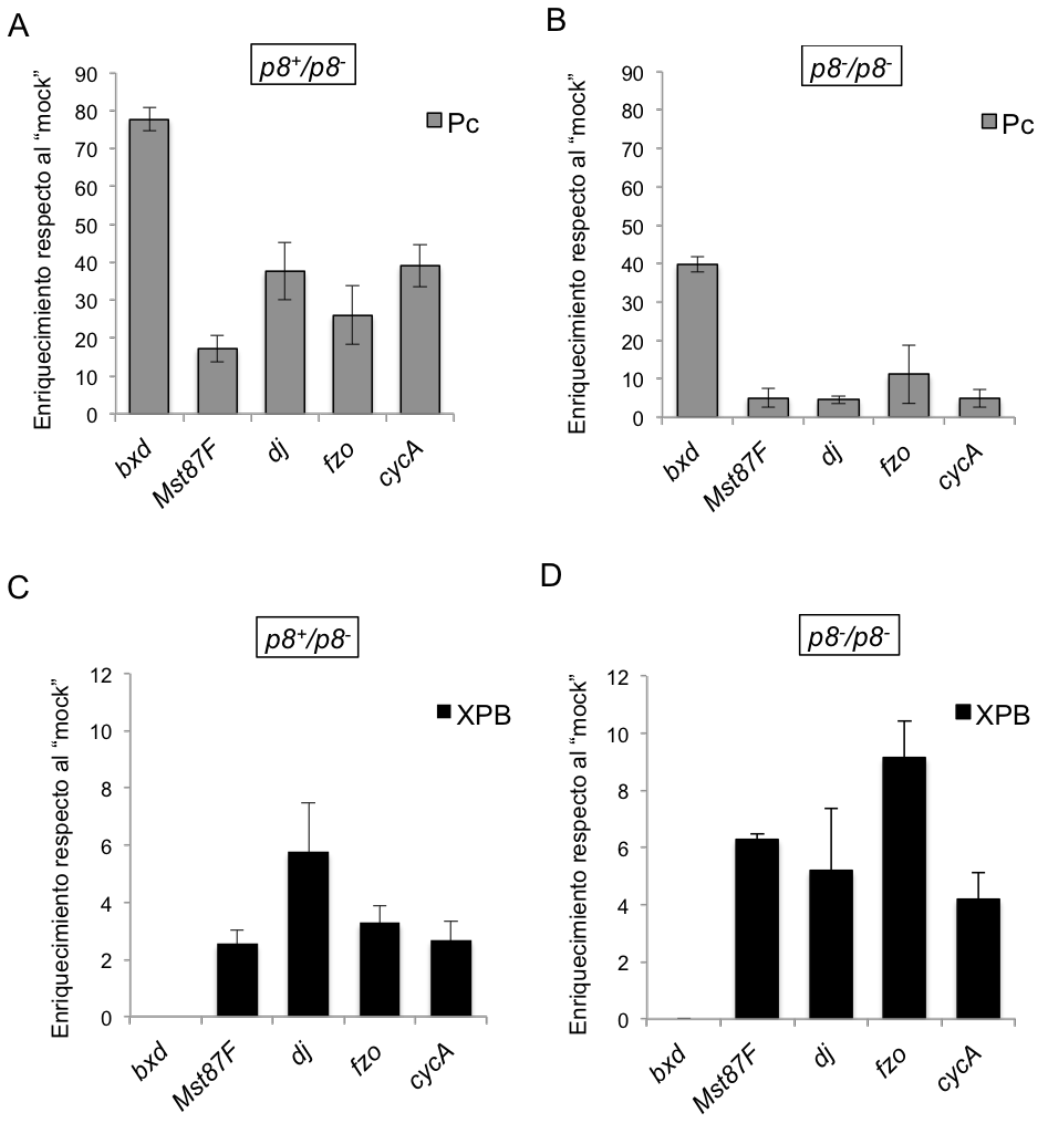

Figura 17. El silenciamiento de la expresión de los genes de diferenciación en ausencia de p8 es independiente de Pc. A, B. Pc se enriquece notablemente en *bxd* (control positivo) respecto al control negativo (promotor de *CycA*) pero no en los promotores de los genes de diferenciación (*Mst87F*, *dj*, *fzo*) en la cromatina de testículos control ($p8^{+}/p8^{-}$) y testículos nulos en *p8* ($p8^{-}/p8^{-}$). C, D. La falta de p8 ($p8^{-}/p8^{-}$) no afecta el reclutamiento de XPB a los promotores. Las barras representan el enriquecimiento de Pc o XPB cuantificado mediante ensayos de PCR en tiempo real del ADN inmunoprecipitado con anticuerpos contra estas proteínas a partir de cromatina de testículos heterocigóticos u homocigóticos del alelo nulo de *p8*. *Bxd*, el cual es un ARN largo no codificante que posee un elemento de respuesta a Pc y no se expresa en testículo, representa un control positivo de la unión de Pc y un control negativo de la unión de XPB a la cromatina. El promotor de *CycA* representa un control negativo de la unión de Pc y positivo de unión de XPB a la cromatina.

Parte II: TFIIH es un "bookmark" en los cromosomas en mitosis durante la activación de la transcripción del genoma del cigoto

De manera sorprendente, la activación de la transcripción de los primeros genes cigóticos en el embrión de *Drosophila* ocurre cuando los núcleos del embrión se dividen aproximadamente cada 9 minutos, en el ciclo de división nuclear 8. El mecanismo que permite que la transcripción de estos genes se lleve acabo en un periodo de tiempo tan corto se ha explorado muy poco.

El análisis de la dinámica de los factores que participan en la transcripción de estos genes puede contribuir a entender el mecanismo que permite la activación del genoma del cigoto, por ello, se decidió estudiar la dinámica y las funciones de componentes de TFIIH durante los primeros ciclos de división nuclear en etapas previas a la transición de la bástula media en el embrión de *Drosophila*.

6.6 TFIIH presenta un comportamiento dinámico durante las divisiones nucleares que ocurren en el estadio de blastodermo sincicial

Este estudio inició con el análisis de la dinámica de la subunidad p8 de TFIIH en los ciclos de división nuclear rápidos del blastodermo sincicial. De manera interesante se observó que durante profase, p8 se enriquece en el núcleo y muestra un patrón de localización semejante al ADN (Figura 18A). Posteriormente, en metafase p8 parece rodear a los cromosomas pero no se localiza en la periferia nuclear, lo cual indica que mantiene su localización en el lumen del núcleo (Figura 18B,C). Este patrón en metafase se observa con mayor claridad a través de la tinción simultánea de p8, tubulina (marcador del huso mitótico) y ADN (Figura 18D). Así mismo, p8 presenta un patrón muy similar a los cromosomas en anafase (Figura 18E).

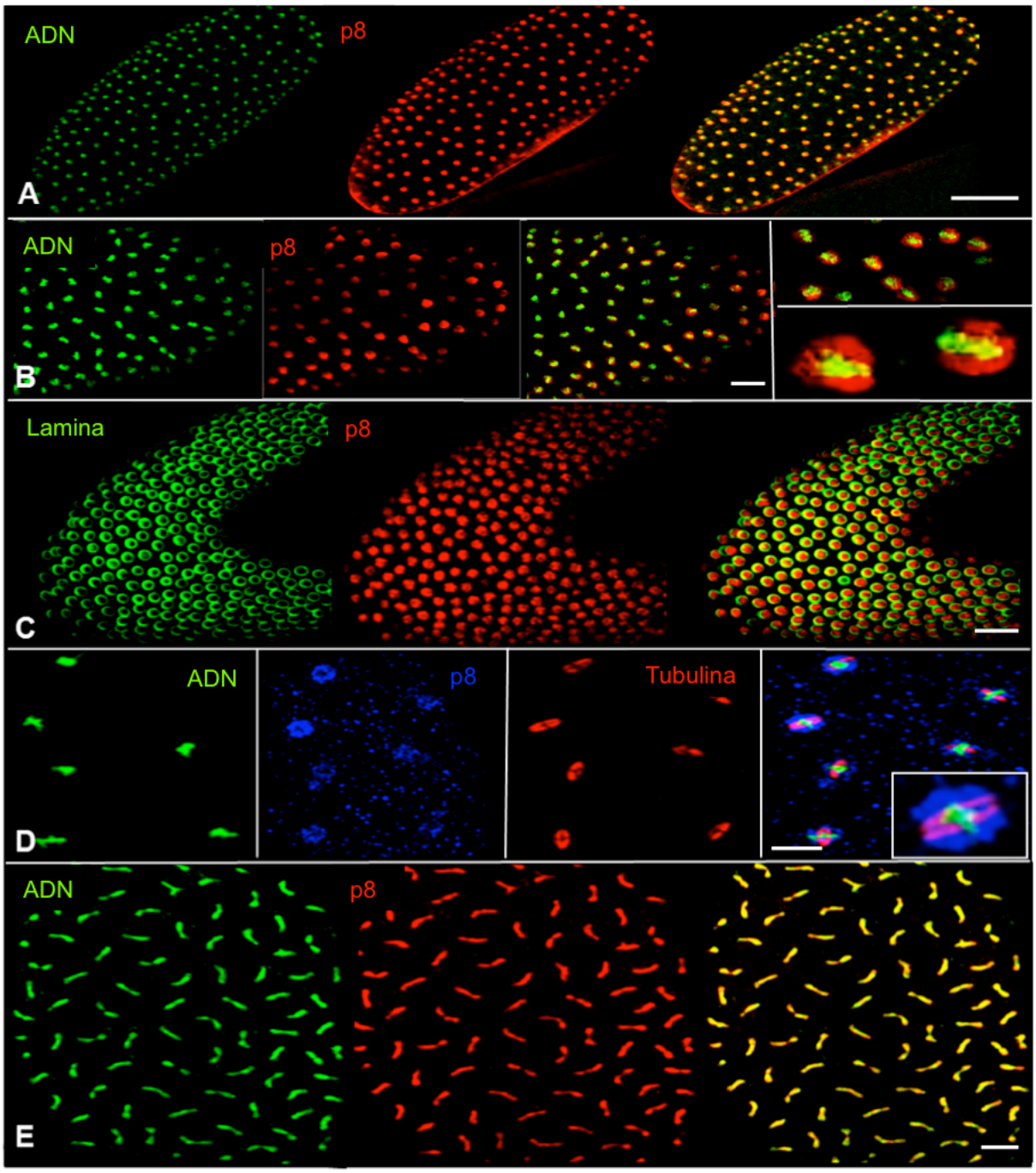

Figura 18. p8 es nuclear durante la mitosis en el blastodermo sincicial. Dinámica de la subunidad p8 de TFIIH durante el desarrollo temprano de *Drosophila*. Para determinar la distribución de p8 en estadios tempranos del desarrollo se utilizó un anticuerpo contra p8 en combinación con anticuerpos anti-lamina (proteína de la membrana nuclear), anti-α-tubulina (proteína de microtúbulos) y/o sytox green (tinción de ADN). A. p8 (rojo) colocaliza con el ADN (verde) en núcleos en profase durante el estadio de blastodermo sincicial. B. En núcleos mitóticos, p8 (rojo) extiende su localización en el núcleo mas allá del ADN (verde). C. p8 (rojo)

se excluye de la membrana nuclear (verde). D, E. En metafase y anafase p8 mantiene su localización nuclear. "A-E" corresponden a imágenes de microscopía confocal de embriones inmunoteñidos. La barra de escala en "A" representa 100 μm, en "B", "C" y "E" 25 μm y en "D" 10 μm.

Múltiples estudios han documentado que la mayoría de los factores de transcripción son excluidos del núcleo durante la mitosis debido a que la compactación de la cromatina en esta etapa del ciclo celular es altamente restrictiva para la transcripción [60–62]. Por lo tanto, la localización observada para p8 durante mitosis resultó muy interesante.

Como se mencionó en secciones previas de este documento, p8 interacciona físicamente con p52 y en el presente estudio se encontró que esta interacción es importante para localizar a p8 en las células germinales en testículo. Por ello se decidió analizar también la dinámica de p52 en esta etapa del desarrollo.

Para ello se visualizó simultáneamente la dinámica de ambas proteínas *in vivo* en embriones que expresan p8-ECFP y EYFP-p52, en los cuales se observó que estas proteínas colocalizan en todas las etapas del ciclo de división nuclear y muestran oscilaciones semejantes en su enriquecimiento en el núcleo y el citoplasma (Figura 19).

La localización nuclear de p8 y p52 durante la mitosis no se ha reportado previamente. Por lo tanto, se decidió analizar si este comportamiento es particular de estas dos subunidades de TFIIH o corresponde a la dinámica del holocomplejo. La subunidad p52 es esencial para el anclaje de XPB al complejo [14], por lo tanto, si el "core" de TFIIH se mantiene ensamblado durante la mitosis sería posible que XPB muestre una dinámica similar a p8 y p52. Esta hipótesis se corroboró al analizar la dinámica *in vivo* de XPB-EGFP en embriones en blastodermo sincicial (Figura 19).

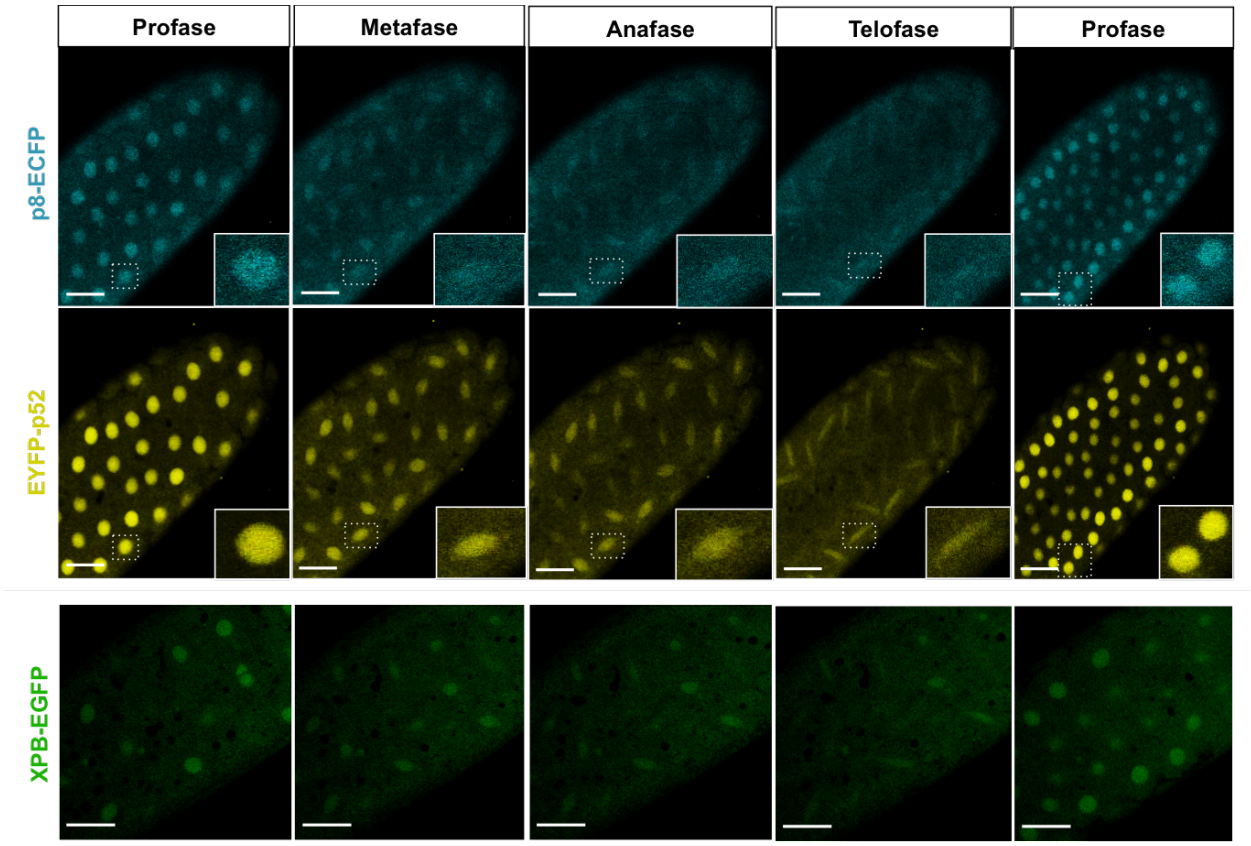

Figura 19. Dinámica, *in vivo,* de EYFP-p52, p8-ECFP y XPB-EGFP durante la mitosis en el blastodermo sincicial. EYFP-p52 (amarillo), p8-ECFP (cian) y XPB-EGFP (verde) siguen exactamente la misma dinámica durante cada ciclo de división nuclear; son principalmente nucleares durante la profase de cada ciclo, posteriormente se observa la disminución gradual de ambas proteínas en el núcleo y su enriquecimiento en el citoplasma al avanzar durante metafase y anafase, sin embargo, la señal nuclear se mantiene también en estos estadios. En telofase las proteínas son mayoritariamente citoplasmáticas y se enriquecen nuevamente en el núcleo al iniciar el ciclo siguiente. La figura muestra una secuencia de imágenes obtenida mediante microscopía confocal en el mismo plano de cada embrión a lo largo del tiempo. El recuadro en la esquina inferior derecha de las imágenes de p8-ECFP y EYFP-p52 corresponde a la amplificación de una región de cada imagen en la que aparece el mismo núcleo en las distintas etapas de su división. La barra de escala representa 25 μm. Los paneles superior (p8-ECFP) y medio (EYFP-p52) de esta figura fueron adaptados de [47].

La misma dinámica se observó en el blastodermo sincicial para los componentes del CAK, a través la detección de Ciclina H mediante inmunotición (Figura 20) y empleando embriones transgénicos que expresan fusiones de Cdk7, Ciclina H y MAT1 con proteínas fluorescentes (Valerio, 2017, Tesis de Maestría en preparación).

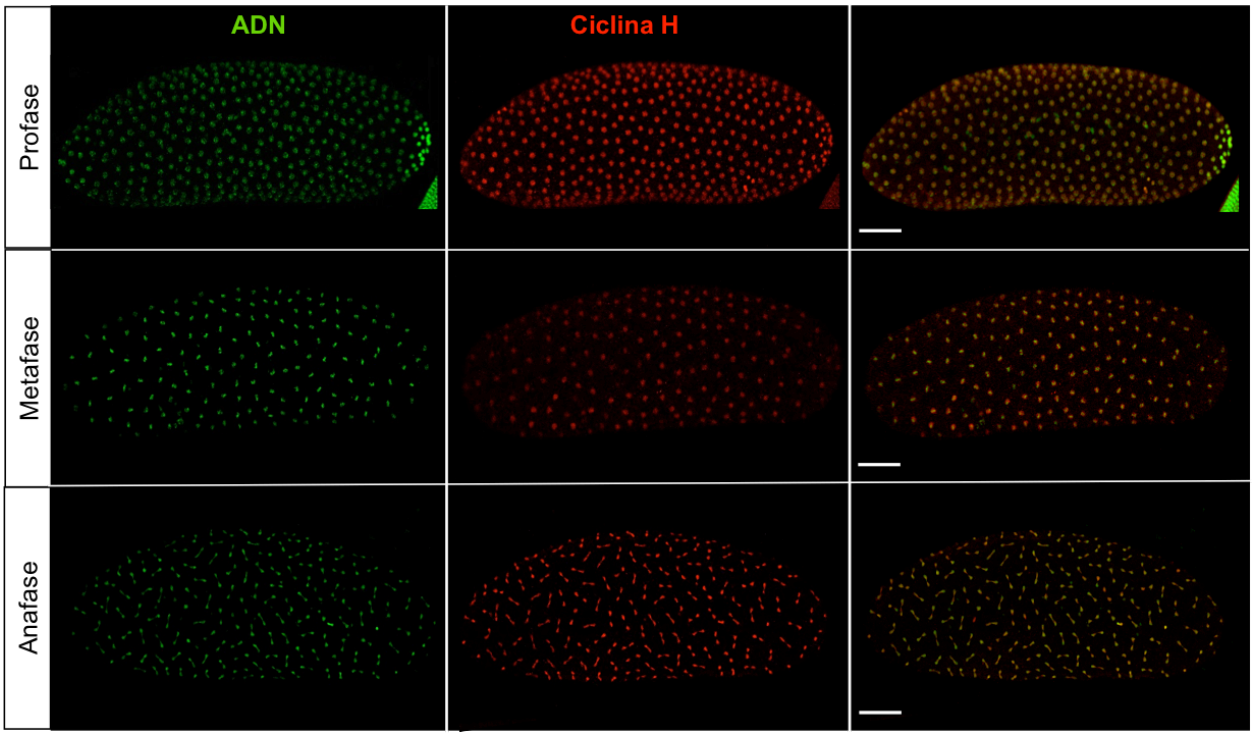

Figura 20. Ciclina H es nuclear durante la mitosis en el blastodermo celular. La detección de Ciclina H (rojo) mediante inmunotinción muestra que esta proteína tiene un patrón similar al de los cromosomas (verde) durante la profase, la metafase y la anafase. Imágenes obtenidas mediante microscopía confocal. La barra de escala representa 50 μm.

Estos resultados sugieren que el holocomplejo TFIIH permanece en el núcleo durante las divisiones mitóticas del embrión en blastodermo sincicial, una etapa en la que la maquinaria de transcripción debe transcribir algunos genes del cigoto en lapsos de tiempo muy cortos.

6.7 TFIIH y la forma activa de la ARNP II coinciden en zonas de enriquecimiento (foci) en el núcleo

De manera interesante, durante el estudio de la dinámica *in vivo* de las subunidades de TFIIH en los embriones en blastodermo sincicial se detectó el enriquecimiento de EYFP-p52 y XPB-EGFP en estructuras granulares en el núcleo de embriones en mitosis en blastodermo sincicial (Figura 21A).

La activación de la transcripción de los genes de histonas en el ciclo de división nuclear 8 ocurre en un par de estructuras denominadas "Histone Locus Bodies" (HLBs) las cuales se observan en el núcleo como dos puntos que muestran además enriquecimiento de TBP y la

ARNP II [63]. Un patrón de puntos similar al de los HLBs, se observa para XPB-EGFP y EYFP-p52.

De manera importante, los foci de EYFP-p52 no colocalizan con el estado de cromatina más compacta en el núcleo (Figura 21B), por el contrario, coinciden con la forma activa de la ARNP II (Figura 21C) sugiriendo que estos foci podrían ser sitios donde ocurre la transcripción en el núcleo durante interfase y al inicio de la profase.

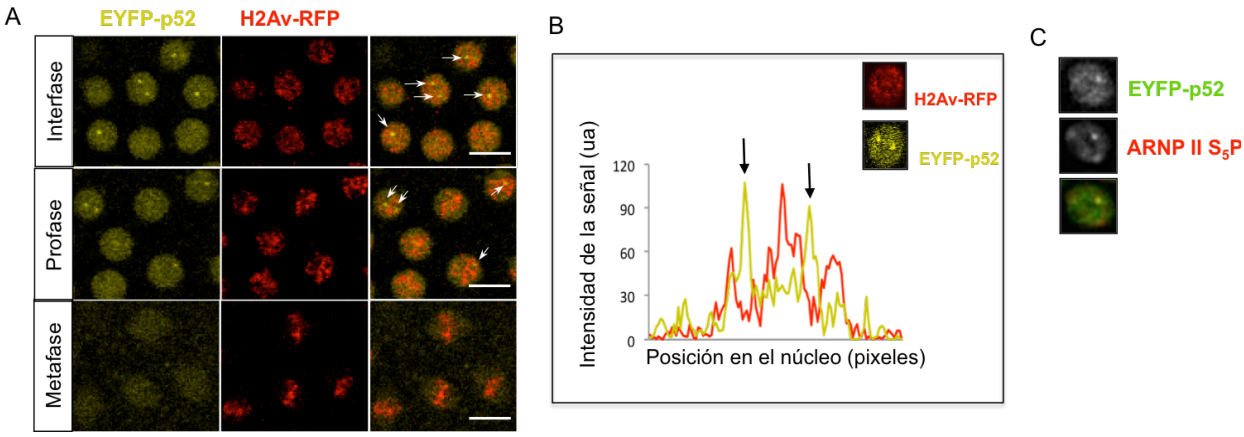

Figura 21. EYFP-p52 muestra un patrón de gránulos que colocalizan con la forma activa de la ARNP II en el núcleo. A. La presencia de foci de EYFP-p52 (indicados con flechas) se observa en núcleos en profase. La dinámica de la cromatina a lo largo de la mitosis se observa a través de la histona H2Av-RFP (en rojo). B. Los foci de EYFP-p52 se excluyen de los sitios de mayor condensación de la cromatina. Las flechas indican los sitios de mayor intensidad de la señal de EYFP-p52 cuantificada en el núcleo mostrado en la esquina superior de la gráfica. u.a: unidades arbitrarias. C. Imagen representativa de núcleos de embriones que expresan el transgen *EYFP-p52* (panel superior) y fueron teñidos con un anticuerpo que reconoce la forma fosforilada de la serina 5 de la ARNP II (panel medio). Los foci de EYFP-p52 colocalizan con la ARNP II (superposición de los paneles superior y medio en el panel inferior). El panel "A" de esta figura fue adaptado de [47]. La barra de escala en "A" representa 10 μm.

6.8 La maquinaria basal de transcripción está unida a la cromatina durante la mitosis en el blastodermo sincicial

La localización nuclear de TFIIH en los ciclos mitóticos del blastodermo sincicial, en los cuales la transcripción de los primeros genes cigóticos debe lograrse en lapsos muy cortos, sugiere que componentes de la maquinaria basal de transcripción podrían mantenerse en la cromatina en

mitosis para garantizar la rápida activación de la transcripción después de la mitosis en cada ciclo.

Para abordar esta hipótesis, se realizaron inmunotinciones de TBP (un componente de TFIID) y de ARNP II en embriones en blastodermo sincicial. Al igual que para TFIIH, se observó que TBP y la ARNP II colocalizan con los cromosomas a lo largo de la mitosis (Figura 22).

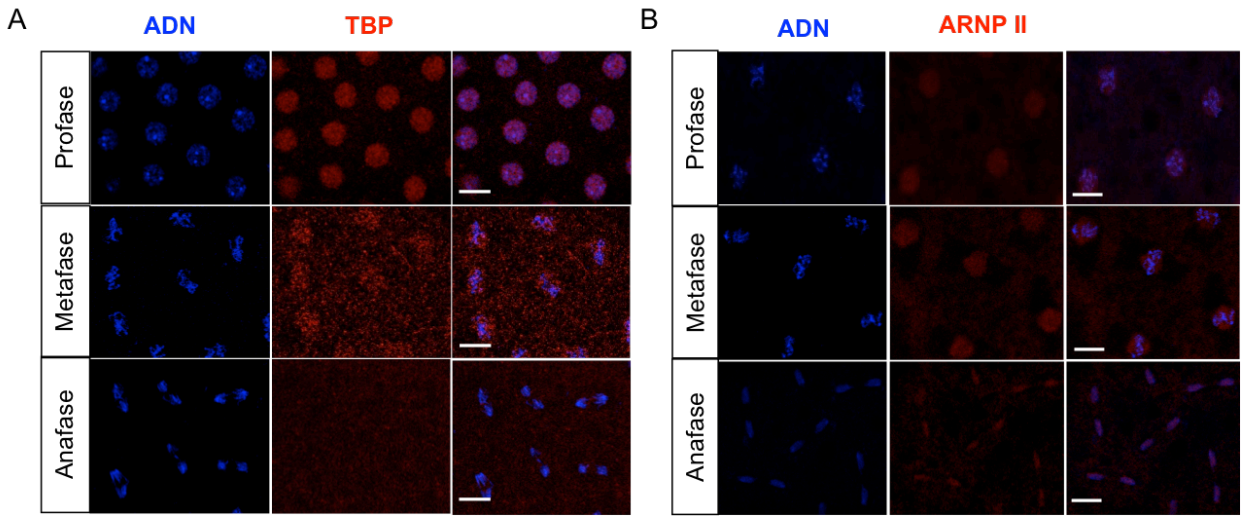

Figura 22. TBP y la ARNP II son nucleares durante mitosis de los embriones en blastodermo sincicial. La dinámica determinada mediante inmunotinciones de TBP y la ARNP II, los cuales son componentes de la maquinaria de transcripción basal, muestra el enriquecimiento de TBP en el núcleo durante profase y metafase, mientras que la ARNP II se detecta además durante la anafase de la mitosis. Imágenes adquiridas mediante microscopía confocal de embriones silvestres en blastodermo sincicial. La barra de escala representa 10 μm.

Para determinar si estos factores se encuentran unidos a la cromatina, se realizaron ensayos de inmunoprecipitación de cromatina de embriones sin tratamiento y embriones tratados con colchicina (la cual detiene el ciclo de división durante la mitosis). Debido a que la transcripción de los genes de histonas ocurre en el ciclo 8 del blastodermo sincicial, se analizó la presencia de XPB, TBP y la ARNP II en los promotores de los genes de las histonas H3 y H4, así como los promotores de rover y TAHRE, dos elementos repetidos que no se transcriben en este momento del desarrollo.

Se detectó enriquecimiento de XPB, TBP y la ARNP II en el promotor de H3 y el promotor de H4 en la cromatina de embriones en interfase y en mitosis. Se observó además el

enriquecimiento de estos factores en la secuencia de rover en interfase y mitosis, pero no en THARE (Figura 23) Estos resultados, sugieren que la maquinaria basal de transcripción permanece unida a diferentes regiones de la cromatina en mitosis durante el blastodermo sincicial posiblemente para activar rápidamente la transcripción durante el siguiente ciclo de división nuclear.

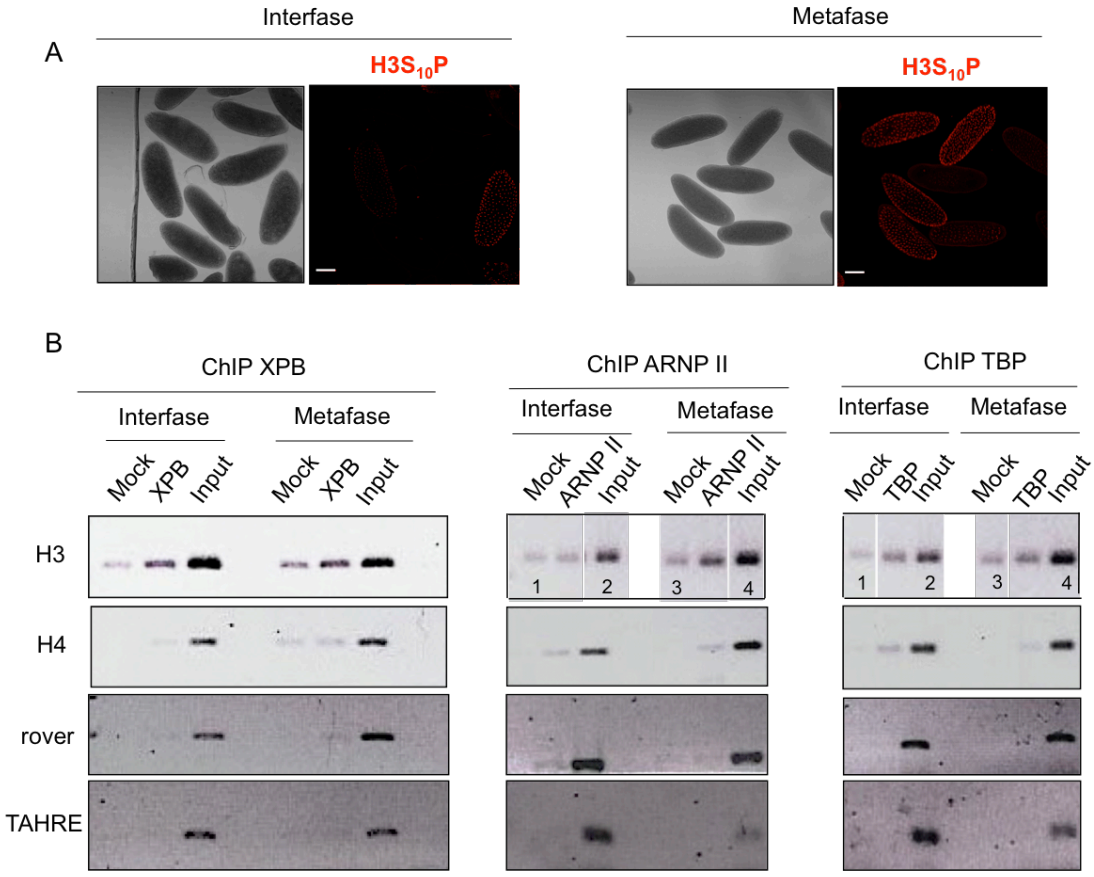

Figura 23. Componentes de la maquinaria basal de transcripción se mantienen unidos a la cromatina en mitosis. A. Muestras de las poblaciones de embriones empleados en los ensayos de inmunoprecipitación de cromatina (ChIP). El enriquecimiento de la población de embriones en metafase después de su tratamiento con colchicina se observa por el mayor número de embriones positivos a la tinción de serina diez fosforilada de la histona H3 (rojo) (derecha) respecto a embriones no tratados (izquierda). B. A través de ensayos de inmunoprecipitación de cromatina y PCR punto final se detectó el enriquecimiento de XPB, la ARNP II y TBP en la cromatina (promotores de las histona H3 y H4 y los elementos repetidos rover y TAHRE) de embriones tanto en interfase como en mitosis. El "mock" corresponde a una IgG irrelevante empleada en los ensayos de ChIP como control negativo. El "input" corresponde a una proporción del total de la cromatina a partir de la cual se realizaron los ensayos de ChIP. Los números 1, 2, 3 y 4 indican que las mismas muestras se presentan en dos paneles diferentes de

imágenes (debido a que el "mock" y el "input" en la inmunoprecipitación de TBP y la ARNP II son los mismos). La barra de escala en "A" representa 100 μm.

6.9 La ausencia de p8 afecta la mitosis en el desarrollo embrionario temprano

En *Drosophila*, al igual que en humano, el subcomplejo CAK tiene un papel esencial en la progresión del ciclo celular. Mutaciones en la subunidad Cdk7 afectan la modulación de la mitosis [64]. De manera interesante la falta de XPD en la embriogénesis causa defectos en la mitosis que se han asociado a la desregulación de Cdk7 [65]. Sin embargo, un reporte reciente muestra que XPD forma con galla y crumbs un complejo involucrado en la segregación de los cromosomas durante la mitosis en *Drosophila* [66]. De manera interesante, un complejo similar se aisló en células de humano, sugiriendo que la subunidad XPD podría tener funciones en mitosis que son independientes de su interacción con TFIIH [22]. Por otra parte, la participación de otros componentes del "core" de TFIIH en mitosis no se ha determinado.

En este trabajo se describe la localización nuclear de subunidades del "core" y del CAK de TFIIH durante la mitosis en el blastodermo sincicial. De manera interesante se observó además que XPB y otros componentes de la maquinaria basal están unidos a la cromatina en mitosis en esta etapa, sugiriendo que esta localización está relacionada a una función en la transcripción. Sin embargo, debido a que en esta etapa del desarrollo, el embrión está principalmente dedicado a cumplir rondas sucesivas de mitosis, la participación de otros componentes de TFIIH, además de Cdk7 y XPD, en mitosis no puede descartarse.

Con base en esto se decidió estudiar cuáles son los defectos en el desarrollo embrionario que causan la letalidad de los embriones provenientes de madres que no tienen p8 (por lo tanto, estos embriones no tienen contribución materna de p8).

Para estudiar el efecto de la ausencia de p8 en el desarrollo de estos organismos se realizaron tinciones de ADN y tubulina en el blastodermo sincicial. Se observó que estos embriones presentan desincronización de la mitosis, centrosomas libres, deformación del huso mitótico, husos monopolares y la falta de condensación del ADN durante los ciclos de división nuclear tempranos (Figura 24A). Adicionalmente, se observaron defectos en el patrón de localización de serina diez fosforilada de la histona H3 ($H3S_{10}P$) durante la mitosis. En embriones silvestres esta marca aparece en profase tardía, se mantiene durante metafase y es

eliminada en anafase, sin embargo, en los embriones mutantes de *p8* esta marca se observa incluso en la cromatina de núcleos en anafase tardía (Figura 24B).

Por otra parte, mediante western blot se determinó que la falta de p8 no afecta el nivel basal de otras subunidades de TFIIH o el nivel de fosforilación de la serina cinco del CTD de la ARNP II (Figura 24C), sugiriendo que el fenotipo observado en mitosis podría ser independiente de defectos causados por una reducción en los niveles de otras subunidades de TFIIH, en particular XPD o Cdk7, en estos embriones.

Adicionalmente, se encontraron defectos similares en la mitosis de embriones mutantes de la subunidad XPB (Figura 24D) o con baja dosis de Cdk7 (Valerio 2017, Tesis de Maestría en proceso). Por lo tanto, la deficiencia de subunidades del "core" y del CAK de TFIIH causa mitosis catastróficas en la embriogénesis de *Drosophila*.

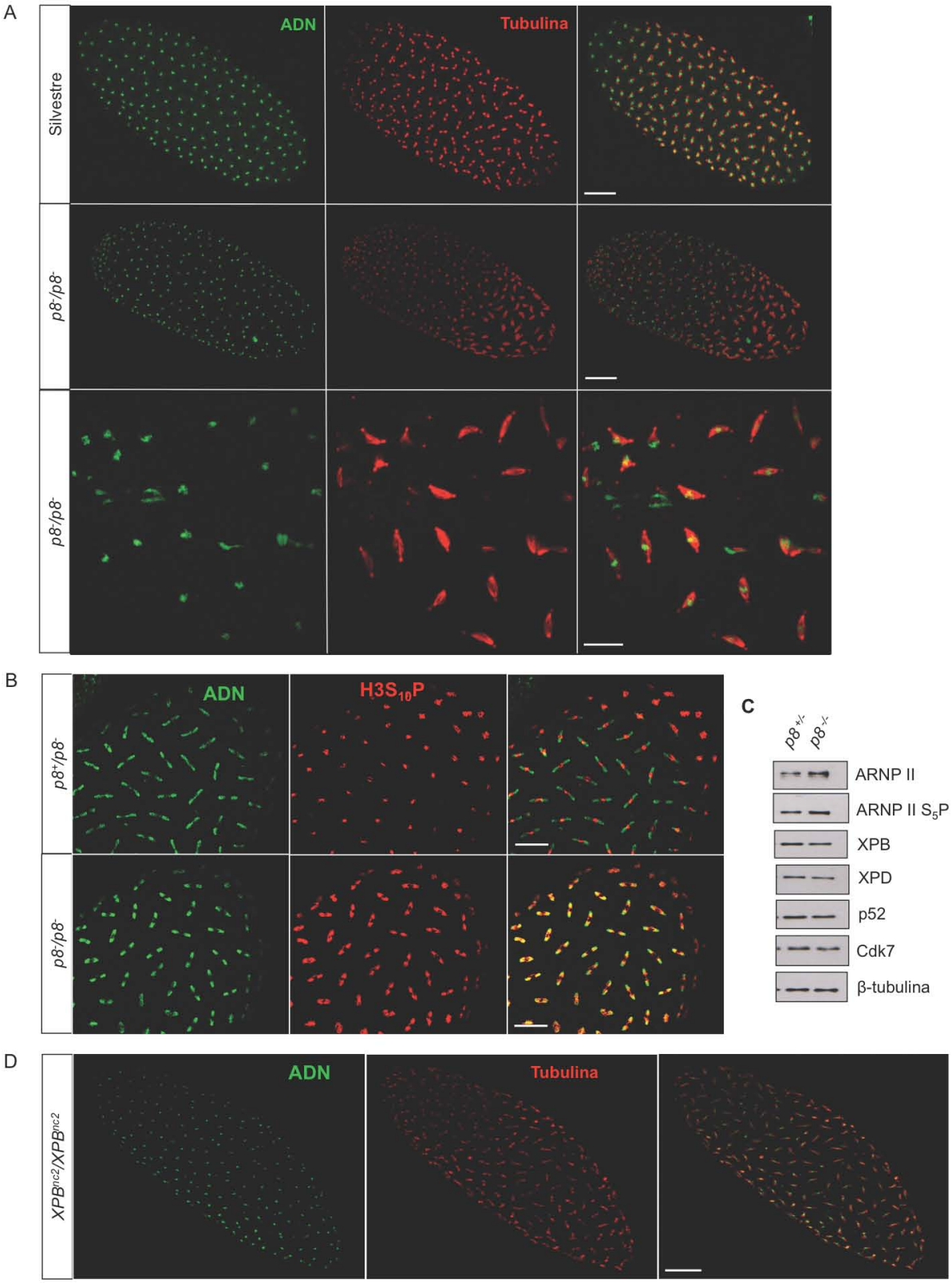
A
Silvestre
p8-/p8-
p8-/p8-
ADN
Tubulina
B
p8+/p8-
p8-/p8-
ADN
H3S10P
C
p8+/-
p8-/-
ARNP II
ARNP II S5P
XPB
XPD
p52
Cdk7
β-tubulina
D
XPBmc2/XPBmc2
ADN
Tubulina

Figura 24. Embriones con mutaciones en subunidades del "core" de TFIIH presentan defectos durante mitosis. A. En un embrión con fenotipo silvestre ($p8^{+}/p8^{-}$) se observan núcleos mitóticos en sincronía; el embrión nulo en *p8* ($p8^{-}/p8^{-}$) presenta núcleos mitóticos asincrónicos y deformación del huso en algunos núcleos, falta de condensación del ADN y husos monopolares. B. La fosforilación de la serina diez de la histona H3 ($H3S_{10}P$) se extiende a la cromatina de núcleos en anafase tardía en ausencia de p8 ($p8^{-}/p8^{-}$). C. Embriones nulos en *p8* ($p8^{-}/p8^{-}$) muestran niveles silvestres de otras subunidades de TFIIH y la fosforilación de la serina cinco del CTD de la ARNP II (ARNP II S_5P). El nivel de estas proteínas se determinó mediante western blot. D. Embriones homocigóticos (XPB^{nc2}/XPB^{nc2}) para un alelo mutante de *XPB* presentan mitosis catastróficas que causan la falta de compactación del ADN y husos mitóticos deformes. La tinción con tubulina muestra el patrón de los microtúbulos en el huso. La barra de escala representa 25 μm en B y 50 μm en A y D.

6.10 La presencia de defectos en mitosis causada por la falta de p8 en el embrión temprano correlaciona con la desregulación de la expresión de transcritos de contribución materna

Durante el inicio de la transcripción, TFIIH se encarga de la apertura del ADN en la región promotora y fosforila la serina 5 del CTD de la ARNP II [8,16]. En los embriones nulos de *p8* se observó un nivel silvestre de serina 5 fosforilada, sin embargo debido a que p8, al igual que p52, modula la actividad ATPasa de XPB [14,48], la falta de p8 podría tener un efecto en la función de XPB en la apertura del ADN y por lo tanto, afectar la transcripción en el embrión, lo cual a su vez podría ocasionar defectos en mitosis.

Para explorar esta posibilidad se analizó, mediante RNA-seq, el transcriptoma de embriones en blastodermo sincicial en ciclos de división nuclear 9-10 (determinado por el número de núcleos en el embrión visualizados a través de la proteína H2Av-RFP) heterocigóticos u homocigóticos para el alelo nulo de *p8*. Para este análisis se seleccionaron dos embriones heterocigóticos ($p8^{+}/p8^{-}$), los cuales mostraron fenotipo silvestre y tres embriones homocigóticos ($p8^{-}/p8^{-}$) con distinto grado de severidad en el fenotipo de mitosis catastróficas (Figura 25A). El ARN total de cada embrión se secuenció individualmente.

El análisis de correlación de las muestras control (embriones a y b) reveló niveles de expresión muy semejantes en la mayoría de los transcritos detectados (coeficiente de correlación: 0.98) y algunas diferencias debidas probablemente a la variabilidad intrínseca de las muestras biológicas.

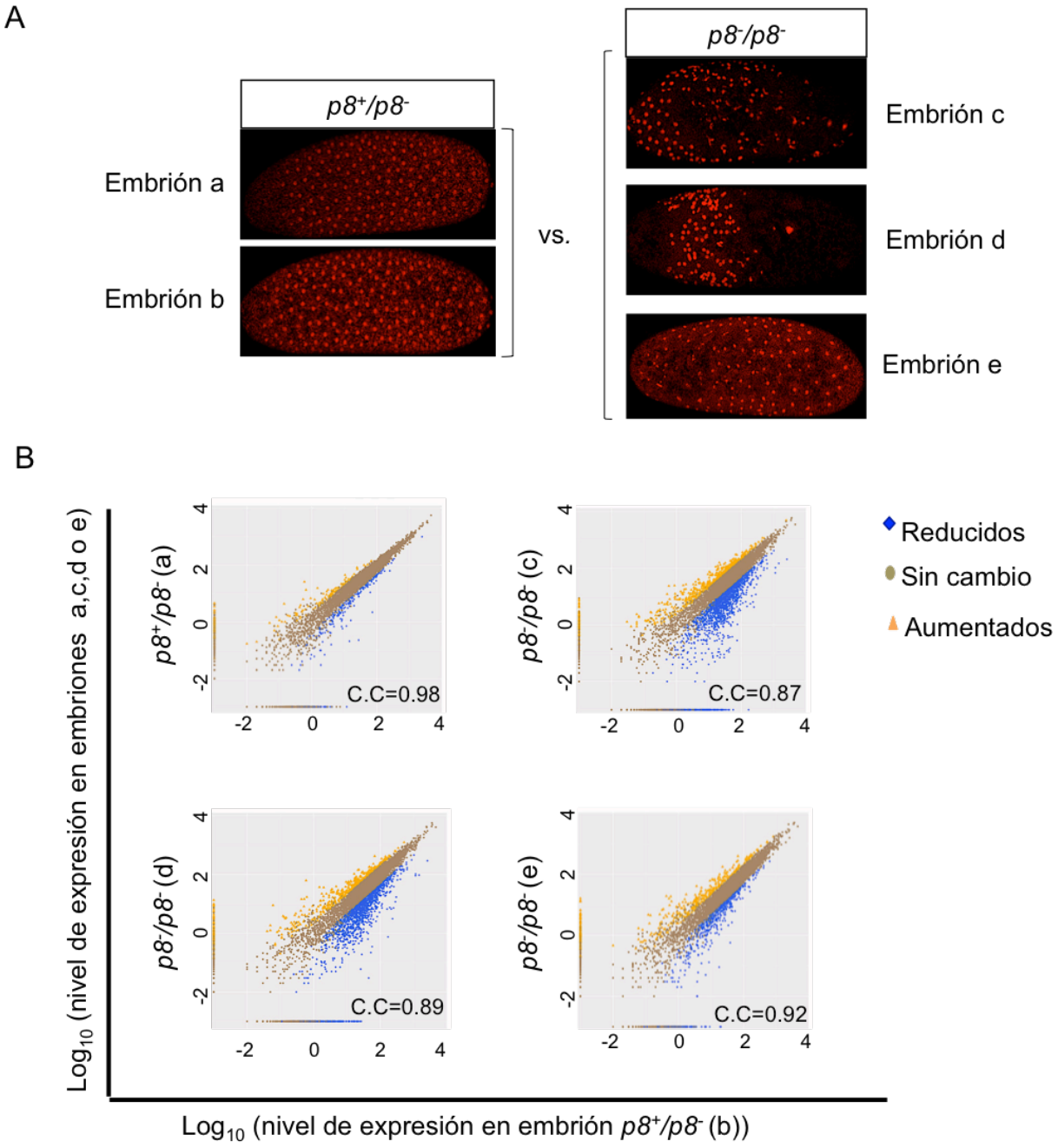

Figura 25. La severidad en el fenotipo de mitosis catastróficas en embriones nulos en *p8* El grado de afectación de la transcripción. A. Imágenes de microscopía confocal de los embriones heterocigóticos ($p8^{+}/p8^{-}$) y homocigóticos ($p8^{-}/p8^{-}$) del alelo nulo de *p8* sometidos a un análisis global de expresión genética mediante RNA-seq. Los embriones nulos (derecha) muestran mitosis catastróficas (desincronización de los núcleos en mitosis y falta de compactación de la cromatina) con distintos grados de severidad. Los núcleos se observan a través de la señal de la histona H2Av fusionada a RFP (rojo). B. Comparación de los transcriptomas de los embriones heterocigóticos ($p8^{+}/p8^{-}$) y homocigóticos ($p8^{-}/p8^{-}$) del alelo

nulo de *p8*. En el eje X de cada gráfica de dispersión se presentan los valores del Log_{10} del nivel de expresión de los genes en el embrión con fenotipo silvestre que corresponde a la muestra embrión b del panel A. En el eje Y se presenta el Log_{10} del nivel del expresión de los mismos genes en el resto de los embriones (a, c, d y e). Las muestras control que corresponden a embriones con fenotipo silvestre (a y b) presentan un patrón de expresión genética muy semejante entre sí. Por el contrario, este patrón difiere en distinto grado con las muestras de embriones mutantes (c, d y e). En azul se representan los transcritos que muestran una disminución, en café aquellos que se mantienen invariables y en amarillo los que aumentan al comparar el transcriptoma del embrión b (eje X) con cada uno de los embriones indicados en el eje Y . El coeficiente de correlación (C.C) es una medida del grado de variación en el patrón de expresión genética entre las muestras comparadas (C.C=1 indica una relación lineal).

Por otra parte, la comparación entre los transcriptomas de los embriones control (a y b) y cada uno de los embriones mutantes (c, d y e) muestra una gran variación en el nivel de expresión de una cantidad considerable de transcritos (Figura 25B). El nivel de afectación de la transcripción en los embriones mutantes correlaciona además con la severidad del fenotipo en mitosis, es decir, la transcripción global está menos afectada en el embrión con fenotipo menos severo.

Se detectó un nivel menor de expresión en un grupo de 270 genes que es común entre todos los embriones mutantes, esto sugiere que algunos genes son particularmente sensibles a la desregulación transcripcional causada por la ausencia de p8. En concordancia con el fenotipo observado durante mitosis, el análisis ontológico mostró que entre los genes afectados se encuentran algunos de los factores que participan en la replicación del ADN y en mitosis (Figura 26) Sin embargo, la mayoría de los transcritos afectados son depositados maternamente en el embrión, lo cual sugiere que durante la ovogénesis de las hembras nulas en *p8* ocurren aberraciones transcripcionales que afectan el desarrollo temprano del embrión.

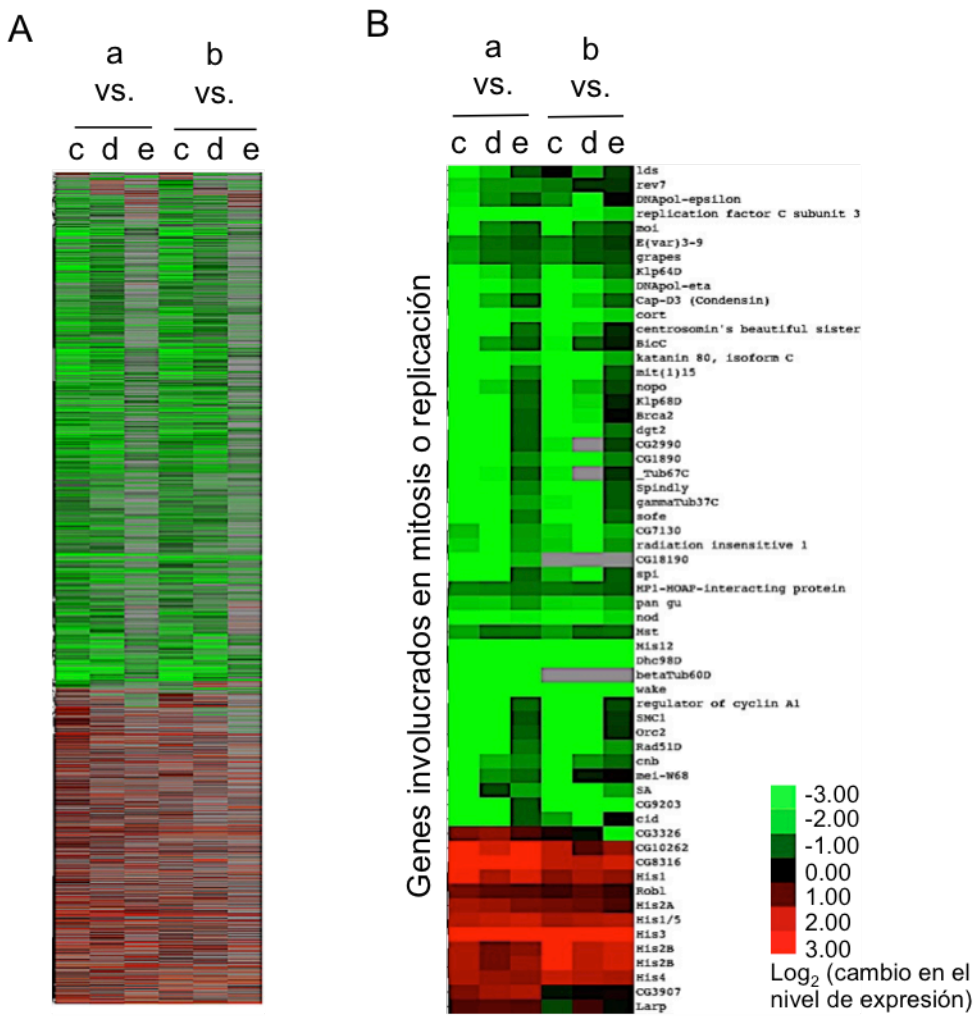

Figura 26. Genes diferencialmente expresados (valor-*p* < 0.001) entre embriones con fenotipo silvestre y mutante de *p8*. A. Comparación de los transcriptomas de embriones heterocigóticos (a y b) y homocigóticos (c, d y e) del alelo nulo de *p8* con fenotipo en la mitosis silvestre y mutante respectivamente. El mapa de calor muestra la variación en la expresión de los mismos genes en los dos embriones control (a y b) contra cada uno de los embriones mutantes (c, d y e). La menor variación se observa al comparar la expresión genética del embrión e con los embriones control (las columnas a vs. e y b vs. e). En contraste, los embriones c y d muestran mayor variación con los niveles de expresión de los mismos genes en los embriones a y b. B. Los genes desregulados en los embriones nulos de *p8* (c, d y e) incluyen genes involucrados en la mitosis y la replicación del ADN, este mapa de calor representa una porción del mapa de calor del panel A que sólo incluye estos genes. El Log_2 del cambio en el nivel de expresión >1 indica el aumento, mientras que el Log_2 del cambio en el nivel de expresión <1 indica la disminución en la expresión de un gen respecto al nivel silvestre.

7. DISCUSIÓN

Parte I

7.1 Las funciones no descritas de p8 y p52: su participación en transcripción y en el mantenimiento de la estabilidad de TFIIH

En el presente trabajo se determinó que la falta de p8 en *Drosophila* produce un fenotipo de infertilidad en machos debido a la detención de la diferenciación de las células germinales en el estadio de espermatocito primario. Ésta es la etapa más activa transcripcionalmente durante la diferenciación de las células germinales en el testículo, lo cual sugiere que la falta de p8 puede afectar el papel de TFIIH en transcripción y con ello afectar el programa de expresión genética que dirige la diferenciación. Esta hipótesis se confirmó a través del análisis del transcriptoma de testículos que no tienen p8, en los cuales se observó la desregulación de aproximadamente el 10% de los genes que se expresan en testículos silvestres, incluyendo la disminución de transcritos necesarios para la diferenciación. Esta observación resultó interesante debido a que varios estudios argumentan que la subunidad p8 de TFIIH es dispensable durante la transcripción y se requiere sólo durante la reparación de daño al ADN a través del mecanismo de NER [13,48,67]. Adicionalmente, la participación de p8 en transcripción está sustentada por un reporte reciente en el que se encontraron defectos transcripcionales en embriones de ratones nulos de p8, los cuales mueren durante el desarrollo temprano [50].

Por otra parte, en estudios previos realizados con cultivos celulares derivados de pacientes afectados en p8 se observó la disminución del nivel basal de TFIIH y se propuso que esta subunidad es fundamental para la estabilidad del complejo [5,68–70]. Sin embargo, trabajos recientes mostraron que ninguna de las mutaciones presentes en estas células corresponde a un alelo nulo de p8 y generan versiones truncas de esta proteína que son capaces de ensamblarse en el complejo [50,71]. Debido a esto, se decidió investigar el efecto de la falta de p8 en la estabilidad de TFIIH en el testículo. En este estudio se detectaron niveles silvestres de las subunidades de TFIIH analizadas en los testículos nulos de p8, lo que sugiere que la disminución en el nivel basal de este complejo en las células de pacientes con mutaciones en p8 es una consecuencia de la incorporación de las versiones truncas de la proteína al complejo, lo cual de alguna manera podría perturbar su estabilidad. Esta posibilidad podría analizarse a través del

modelamiento de la estructura del complejo en presencia de las proteínas truncas de p8, para determinar si existen impedimentos estéricos en las interacciones entre las subunidades de TFIIH.

Por otra parte, se observó que mutaciones en la subunidad p52 provocan la disminución dramática del nivel de XPB y p8 (con las cuales p52 interacciona físicamente) en testículo. Esto sugiere que p52 tiene un papel fundamental en mantener la estabilidad de estas proteínas al favorecer su integración al complejo a través de la formación del heterotrímero XPB/p52/p8 que a su vez interacciona físicamente con el heterodímero formado por las subunidades p34 y p44 del "core" de TFIIH. Así mismo, al analizar la espermatogénesis de organismos mutantes de *p52*, se observaron fenotipos de detención en meiosis semejantes a los ocasionados por la falta de p8 y la desregulación de la transcripción de un grupo muy similar de genes. Indicando que estas proteínas participan conjuntamente en la regulación del programa transcripcional que permite la diferenciación de las células germinales.

7.2 El modelo de silenciamiento de la transcripción de los genes de diferenciación mediado por Polycomb no es un mecanismo generalizado en mutantes con fenotipo de detención en meiosis

El fenotipo de detención en meiosis se caracterizó por primera vez durante el estudio de machos mutantes con defectos en la fertilidad. De esta forma se identificaron alelos de genes cuyos productos codifican versiones específicas de testículo de factores transcripcionales que forman parte del complejo TFIID, denominados tTAFs [72]. El estudio de estos factores contribuyó a establecer un modelo para la regulación de la transcripción de los genes requeridos durante la diferenciación de las células germinales en testículo [39,51]. Este modelo propone que los tTAFs regulan positivamente la expresión de los genes de diferenciación en el estadio de espermatocito primario, etapa en la cual estos factores reclutan a Pc al nucléolo para anular la represión de estos genes. En mutantes de los *tTAFs* se observó la deslocalización de Pc del nucléolo de espermatocitos primarios y su enriquecimiento en los promotores de genes de diferenciación que se encuentran silenciados en estas mutantes [51].

El transcriptoma de testículo de la mutante de p8 mostró que los niveles de transcrito de los *tTAFs* se mantienen en el orden silvestre, lo cual sugiere que el fenotipo de detención en

meiosis de la mutante de *p8* no es consecuencia de la desregulación de la transcripción de estos genes.

Al analizar el patrón de localización de Pc en los espermatocitos primarios en ausencia de p8, en este estudio se observó la disminución de esta proteína en el nucléolo. Este comportamiento resulta interesante, debido a que Pc y TFIIH presentan el mismo patrón de localización durante la espermatogénesis, sugiriendo que la localización de Pc en el nucléolo depende también de TFIIH, por lo que sería interesante determinar si existe interacción física entre estos factores, ya que hasta ahora se desconoce si esto ocurre con Pc y los tTAFs y por lo tanto se desconoce el mecanismo preciso a través del cuál se regula la localización de Pc en estas células. Así mismo, resulta intrigante observar que la localización de Pc en los cromosomas bivalentes aparentemente no presenta cambios por la falta de p8 o de los tTAFs, indicando que la localización de estas proteínas en el nucléolo está regulada finamente, lo cual podría ser relevante en las funciones de estos factores en este compartimento subcelular.

Por otra parte, Pc no se recluta a los promotores de los genes de diferenciación que se encuentran silenciados en la mutante de *p8*. Este resultado contradice el modelo establecido para la activación de la transcripción de los genes de diferenciación en los espermatocitos primarios, sin embargo, coincide con los datos publicados por El-Sharnouby y colaboradores (2013) que cuestionan el modelo debido a que al realizar un análisis global de la unión de Pc en el genoma, no se observó su enriquecimiento en ninguno de los promotores de los genes de diferenciación en los testículos de mutantes de *tTAFs* o en los precursores de las células germinales [40]. Por lo tanto, la participación de Polycomb en el silenciamiento de los genes de diferenciación en las mutantes de detención en meiosis es un tema controversial.

Parte II

7.3 La distribución subcelular de TFIIH es altamente dinámica durante la embriogénesis temprana

Las dinámicas subcelular y molecular de TFIIH durante la transcripción se ha estudiado extensivamente en células en interfase [38,67,73–75]. Por otra parte, se sabe muy poco de estas dinámicas a lo largo del ciclo celular.

Aguilar-Fuentes y colaboradores (2006) reportaron la dinámica del “core” y el CAK de TFIIH en el desarrollo temprano de *Drosophila*. Mostraron que proteínas de ambos subcomplejos se localizan en el citoplasma de embriones en blastodermo sincicial hasta su entrada al núcleo durante el ciclo de división nuclear número diez y sugieren que estos subcomplejos interaccionan físicamente sólo cuando se encuentran en el núcleo durante el inicio de la transcripción de los genes cigóticos [38]. Sin embargo, en este estudio sólo se analizaron embriones en blastodermo sincicial con núcleos en interfase.

El presente trabajo describe la dinámica de componentes del "core" y del CAK de TFIIH en las diferentes etapas de los ciclos de división nuclear en el blastodermo sincicial. Los resultados de este estudio, obtenidos *in vivo* e *in vitro*, mostraron que los componentes de este complejo se mantienen en núcleos mitóticos de embriones en blastodermo sincicial. La ARNP II sigue la dinámica nuclear de TFIIH durante la mitosis en la embriogénesis temprana, lo cual podría deberse a que la rapidez con la que ocurren los ciclos de división nuclear en el blastodermo sincicial, requiere que estos factores se mantengan asociados al ADN, listos para el inicio de la transcripción después de la mitosis de cada ciclo.

Un estudio previo describió la localización de algunos factores de transcripción en células HeLa durante la transición de las fases M/G1. En este análisis se observó que a diferencia de TBP, el cual colocaliza con los cromosomas durante la mitosis, otros factores basales incluyendo la ARNP II, XPB y XPD se excluyen de la cromatina en mitosis [76]. Por lo tanto, el comportamiento de la maquinaria basal de transcripción en el embrión de *Drosophila* podría ser parte de un mecanismo involucrado particularmente en la regulación de la transcripción durante los ciclos de división nuclear cortos que ocurren en el blastodermo sincicial.

Sin embargo, un reporte reciente muestra que diferentes protocolos empleados para analizar la localización de las proteínas en la cromatina en mitosis pueden generar resultados dramáticamente diferentes. De tal forma que el análisis de la localización de varios factores transcripcionales durante la mitosis en células madre embrionarias de ratón, a través de inmunotinciones empleando formaldehído como agente fijador resultó en la ausencia de señal nuclear durante la mitosis. Contrariamente, el análisis de las mismas proteínas *in vivo* mostró su enriquecimiento en cromosomas mitóticos y este resultado se confirmó mediante ensayos bioquímicos [77].

Así mismo, la observación de la colocalización de los componentes del CAK con los cromosomas durante la mitosis descrita en este trabajo contradice un reporte reciente que propone que en embriones silvestres en blastodermo sincicial el CAK es nuclear durante la interfase pero se excluye completamente del núcleo durante la mitosis a través de un mecanismo dependiente de XPD, de tal manera que la falta de XPD en la embriogénesis ocasiona la localización de Cdk7 en los cromosomas en anafase y como consecuencia defectos en mitosis [65]. La discrepancia entre estos resultados podría deberse, como sugiere Teves y colaboradores (2016) a la estrategia usada en la detección de las proteínas [77]. Durante el desarrollo de este trabajo se probaron diferentes anticuerpos para detectar a Cdk7 a través de inmunotinciones, sin embargo, no fue posible detectar señal con ninguno de ellos. Debido a esto se recurrió al uso de moscas transgénicas que expresan una fusión de Cdk7 con EGFP (EGFP-Cdk7), la cual es nuclear durante la mitosis de embriones con dosis silvestres de XPD. Estas moscas rescatan fenotipos causados por la disminución de la dosis de Cdk7, lo que indica que esta proteína de fusión es funcional y tiene una localización similar a la silvestre (Valerio, 2017, tesis de maestría). Adicionalmente, el patrón de localización nuclear del CAK durante mitosis fue confirmado mediante la inmunotinción de Ciclina H y el uso de una mosca transgénica que expresa la fusión EYFP-Ciclina H. Así mismo, en acuerdo con nuestras observaciones, Ito y colaboradores reportaron la localización nuclear de XPD en metafase en células de humano [22].

En los últimos años, un número creciente de estudios han señalado el "bookmarking" en mitosis por algunos factores transcripcionales. Las evidencias mostradas en este trabajo sobre la dinámica de TFIIH sugieren que ese podría ser el caso para TFIIH durante el desarrollo temprano del embrión de *Drosophila*.

7.4 "Bookmarking" por TFIIH y otros componentes de la maquinaria basal durante la mitosis en el embrión temprano

Durante años de investigación se ha postulado que la transcripción se apaga durante la mitosis y que los factores transcripcionales se excluyen del núcleo [60–62,78]. Sin embargo, la colocalización de TFIIH con los cromosomas en núcleos mitóticos en el blastodermo sincicial sugiere que TFIIH actúa como "bookmark" para la rápida activación de la transcripción después de la mitosis. Esta propuesta está respaldada por la publicación cada vez más frecuente, de trabajos que sugieren que la unión de algunos factores transcripcionales al ADN se mantiene

durante la mitosis para garantizar la activación de la transcripción de ciertos genes después de la división celular. Por ejemplo, se ha reportado el "bookmarking" por GATA1 en los genes de globina durante la mitosis; de igual forma Runx 2, RBPJ y Myc se mantienen en la cromatina en mitosis de células en cultivo de *Drosophila* [79–82].

Adicionalmente, un estudio realizado mediante microscopía confocal de 4 dimensiones para determinar la elasticidad de los cromosomas, sugiere que los cromosomas mitóticos están mucho menos compactados en el embrión de *Drosophila* que los cromosomas analizados en otros organismos, lo que podría favorecer el acceso de los factores de transcripción a la cromatina durante los ciclos de división nuclear en el blastodermo sincicial [83].

De manera interesante, TBP y la ARNP II siguen una dinámica semejante y al igual que la subunidad XPB de TFIIH se localizan en los promotores de las histonas H3 y H4 en la cromatina en mitosis. En conjunto, los datos presentados en este trabajo sugieren que componentes de la maquinaria basal de transcripción se mantienen en los promotores de algunos genes para lograr la rápida activación de la transcripción después de la mitosis, como un mecanismo de memoria transcripcional a corto plazo en el blastodermo sincicial.

7.5 Mutaciones en subunidades de TFIIH causan mitosis catastróficas y defectos en la transcripción en el embrión temprano

El papel del CAK en la modulación del ciclo celular está documentado en un gran número de estudios [18,19,64]. Adicionalmente, reportes recientes muestran que XPD forma parte de complejos involucrados en la segregación de los cromosomas durante la mitosis en *Drosophila* y células de humano en cultivo [22,66]. De manera consistente, Ito y colaboradores (2010) mostraron que las células de pacientes con mutaciones en XPD presentan defectos durante la mitosis, incluyendo husos mitóticos anormales [22].

En el presente trabajo, se muestra que embriones con mutaciones en las subunidades p8 y XPB también muestran defectos durante la mitosis, lo cual sugiere que este fenotipo es una característica común en mutantes de subunidades tanto del "core" como del CAK de TFIIH. De manera consistente con estas observaciones Matsuno y colaboradores (2007) encontraron que mutaciones en *p52*, *XPB* o *Cdk7* producen defectos muy semejantes en la progresión del ciclo celular durante el desarrollo del disco imaginal de ojo en *Drosophila*, por lo cual sugieren por primera vez la participación del holocomplejo en la regulación del ciclo celular [84].

Los datos presentados en este trabajo indican que la ausencia de p8 causa la desregulación de la transcripción de algunos genes durante de la ovogénesis, de tal forma que los defectos observados en la mitosis de los embriones que no tienen p8 pueden deberse a la falta de transcritos provenientes de herencia materna, a la desregulación de la transcripción de los primeros genes activados en el cigoto o a la participación directa de TFIIH en este proceso. Por lo tanto, discernir entre las funciones de TFIIH en la transcripción y su posible participación en mitosis representa un enorme reto para investigaciones futuras.

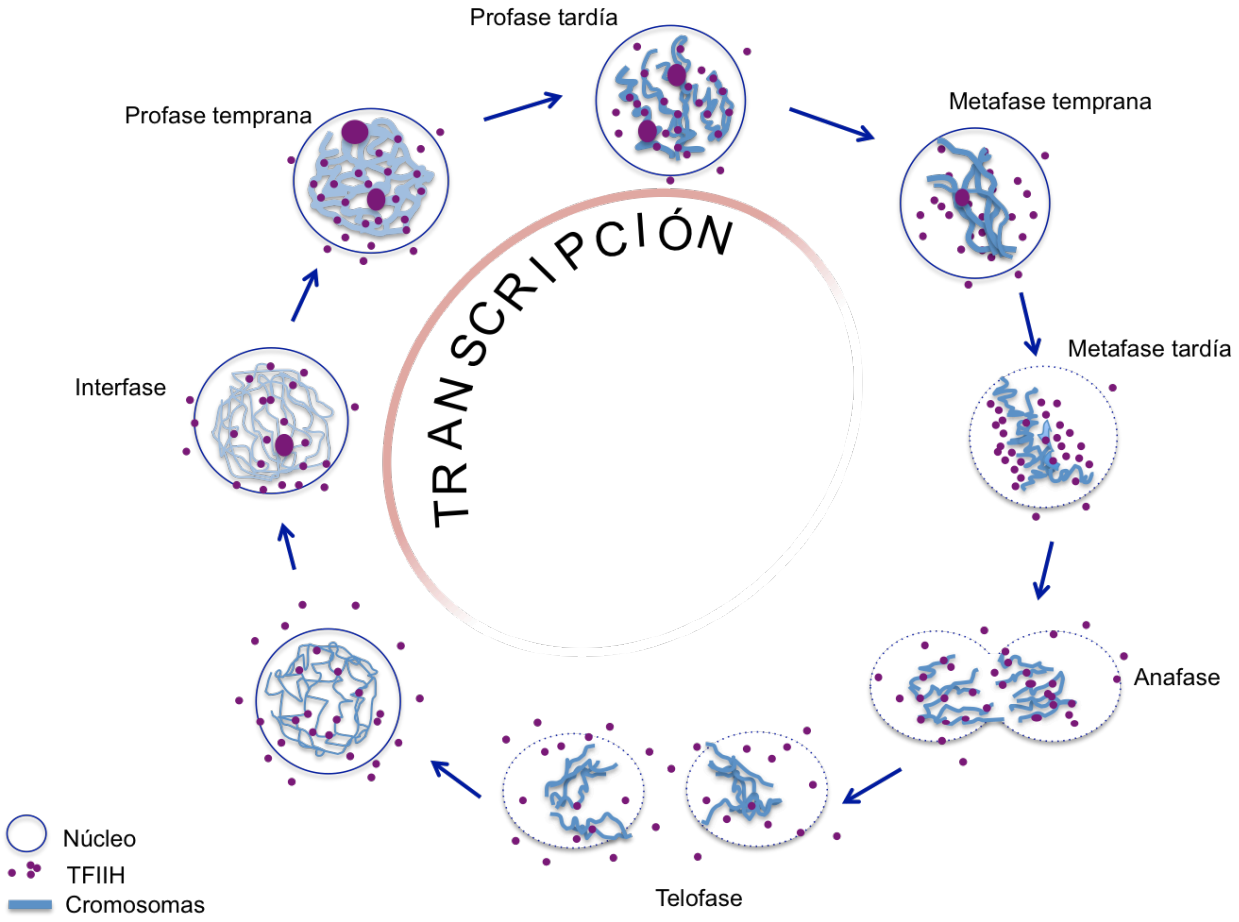

Figura 27. Modelo de la dinámica de TFIIH durante los ciclos de división nuclear rápidos en el blastodermo sincicial. En interfase TFIIH es principalmente nuclear y se enriquece en zonas (foci) en las que también se detecta el enriquecimiento de la forma activa de la ARNP II, por lo tanto, éstos podrían ser sitios transcripcionalmente activos. Estos foci se mantienen durante profase y desaparecen cuando la cromatina se encuentra más compacta en metafase tardía. La localización nuclear de TFIIH se mantiene en metafase y anafase, disminuye considerablemente en telofase y se recupera al inicio del siguiente ciclo de división nuclear.

8. CONCLUSIONES

Parte I

- Los testículos de los organismos mutantes de *p8* y *p52* presentan un fenotipo de detención en meiosis durante la diferenciación de las células germinales debido a la disminución de la expresión de genes de diferenciación en los espermatocitos primarios.
- p8, p52 y XPB colocalizan en los cromosomas bivalentes y la periferia del nucléolo de los espermatocitos primarios.
- La subunidad p52 de TFIIH es indispensable para mantener los niveles basales de otros componentes del complejo en testículo. Mientras que la falta de p8 no afecta la estabilidad de las otras subunidades.
- La disminución de p52 o la falta de p8 en testículo no abaten la transcripción global
- No hay reclutamiento del represor transcripcional Pc a los promotores de los genes de diferenciación en la mutante de *p8*.

Parte II

- La localización de TFIIH durante la embriogénesis temprana es altamente dinámica, estas proteínas se mantienen principalmente nucleares durante la fase de síntesis y la profase y una fracción continúa en el núcleo durante la metafase y anafase, se excluyen mayoritariamente durante telofase y se enriquecen nuevamente en el núcleo en el ciclo siguiente.
- TFIIH, TBP y la ARNP II se mantienen unidos a la cromatina en mitosis en el blastodermo sincicial.
- p8 y XPB son esenciales para la mitosis sincrónica y la estabilidad del huso mitótico durante la embriogénesis temprana.
- La falta de p8 afecta el programa de expresión genética durante la ovogénesis y la activación de la transcripción de los primeros genes cigóticos.

9. PERSPECTIVAS

De los resultados generados en este trabajo se plantean algunas interrogantes que podrían abordarse en investigaciones futuras para estudiar las funciones de TFIIH durante el desarrollo.

- ¿Cuál es la función de TFIIH en la periferia del nucléolo de los espermatocitos primarios? Debido a que TFIIH participa también en la transcripción mediada por la ARNP I pero se desconoce cuál es su papel en este mecanismo, será interesante investigar la función de TFIIH en el nucléolo de los espermatocitos primarios.

- ¿Cuál es la localización de la maquinaria basal de transcripción en el genoma durante la mitosis? El enriquecimiento de TFIIH (XPB), la ARNP II y TBP en algunas regiones del genoma durante la mitosis sugiere que estas proteínas permanecen unidas a la cromatina como "bookmarks" para la activación de la transcripción durante los ciclos de división nuclear rápidos que ocurren en el embrión temprano. Analizar la distribución de estas proteínas mediante ensayos de ChIP-seq de embriones tempranos en mitosis permitirá determinar si su unión a la cromatina es específica de regiones promotoras o se distribuyen aleatoriamente en el genoma.

- ¿El holo-TFIIH tiene un papel directo en la mitosis independiente de sus funciones en la transcripción en el embrión temprano? Hasta ahora, sólo se ha reportado la participación de la subunidad XPD del "core" durante mitosis, sin embargo, la dinámica de subunidades tanto del "core" como del CAK de TFIIH durante la mitosis en el embrión temprano de *Drosophila* y el fenotipo de mitosis catastróficas observado en embriones mutantes, sugieren la participación del holo-complejo en mitosis.

10. BIBLIOGRAFÍA

1. Maldonado E, Ha I, Cortes P, Weis L, Reinberg D. Factors Involved in Specific Transcription by Mammalian RNA Polymerase II: Role of Transcription Factors IIA, IID, and IIB during Formation of a Transcription-Competent Complex. Mol. Cell. Biol. 1990;10:6335–47.

2. Louder R, He Y, Lopez-Blanco J, Fang J, Chacon P, Nogales E. Structure of promoter-bound TFIID and model of human pre-initiation complex assembly. Nature. 2016;531:604–9.

3. Compe E, Egly J-M. Nucleotide excision repair and transcriptional regulation: TFIIH and beyond. Annu. Rev. Biochem. 2016;85:265–90.

4. Gerard M, Fischer L, Moncollin V, Chipoulet JM, Chambon P, Egly JM. Purification and interaction properties of the human RNA polymerase B(II) general transcription factor BTF2. J. Biol. Chem. 1991;266:20940–5.

5. Giglia-Mari G, Coin F, Ranish J a, Hoogstraten D, Theil A, Wijgers N, et al. A new, tenth subunit of TFIIH is responsible for the DNA repair syndrome trichothiodystrophy group A. Nat. Genet. 2004;36:714–9.

6. Luo J, Cimermancic P, Viswanath S, Ebmeier CC, Kim B, Dehecq M, et al. Architecture of the Human and Yeast General Transcription and DNA Repair Factor TFIIH. Mol. Cell. Elsevier Inc.; 2015;59:794–806.

7. He Y, Yan C, Fang J, Inouye C, Tjian R, Ivanov I, et al. Near-atomic resolution visualization of human transcription promoter opening. Nature. 2016;533:1–21.

8. Bradsher J, Coin F, Egly JM. Distinct roles for the helicases of TFIIH in transcript initiation and promoter escape. J. Biol. Chem. 2000;275:2532–8.

9. Tirode F, Busso D, Coin F, Egly J-M. Reconstitution of the Transcription Factor TFIIH. Mol. Cell. 1999;3:87–95.

10. Lainé J, Mocquet V, Egly J. TFIIH Enzymatic Activities in Transcription and Nucleotide Excision Repair. METHODS Enzymol. 1999;81:139–46.

11. Fishburn J, Tomko E, Galburt E, Hahn S. Double-stranded DNA translocase activity of transcription factor TFIIH and the mechanism of RNA polymerase II open complex formation. Proc. Natl. Acad. Sci. U. S. A. 2015;112:3961–6.

12. Kuper J, Braun C, Elias A, Michels G, Sauer F, Schmitt DR, et al. In TFIIH, XPD Helicase Is Exclusively Devoted to DNA Repair. PLoS Biol. 2014;12:doi:10. 1371/journal.pbio.1001954.

13. Singh A, Compe E, Le May N, Egly JM. TFIIH subunit alterations causing xeroderma

pigmentosum and trichothiodystrophy specifically disturb several steps during transcription. Am. J. Hum. Genet. 2015;96:194–207.

14. Jawhari A, Lainé JP, Dubaele S, Lamour V, Poterszman A, Coin F, et al. p52 mediates XPB function within the transcription/repair factor TFIIH. J. Biol. Chem. 2002;277:31761–7.

15. Tremeau-Bravard A, Perez C, Egly JM. A Role of the C-terminal Part of p44 in the Promoter Escape Activity of Transcription Factor IIH. J. Biol. Chem. 2001;276:27693–7.

16. Akhtar MS, Heidemann M, Tietjen JR, Zhang DW, Chapman RD, Eick D, et al. TFIIH Kinase Places Bivalent Marks on the Carboxy-Terminal Domain of RNA Polymerase II. Mol. Cell. 2009;34:387–93.

17. Lu H, Zawel L, Fisher L, Egly JM, Reinberg D. Human general transcription factor IIH phosphorylates the C-terminal domain of RNA polymerase II. Nature. 1992;358:641–5.

18. Fesquet D, Labbé JC, Derancourt J, Capony JP, Galas S, Girard F, et al. The MO15 gene encodes the catalytic subunit of a protein kinase that activates cdc2 and other cyclin-dependent kinases (CDKs) through phosphorylation of Thr161 and its homologues. EMBO J. 1993;12:3111–21.

19. Schachter MM, Merrick KA, Larochelle S, Hirschi A, Zhang C, Shokat KM, et al. A Cdk7-Cdk4 T-Loop Phosphorylation Cascade Promotes G1 Progression. Mol. Cell. 2013;50:250–60.

20. Yankulov KY, Bentley DL. Regulation of CDK7 substrate specificity by MAT1 and TFIIH. EMBO J. 1997;16:1638–46.

21. Takagi Y, Masuda C a, Chang W-H, Komori H, Wang D, Hunter T, et al. Ubiquitin ligase activity of TFIIH and the transcriptional response to DNA damage. Mol. Cell. 2005;18:237–43.

22. Ito S, Tan LJ, Andoh D, Narita T, Seki M, Hirano Y, et al. MMXD, a TFIIH-Independent XPD-MMS19 Protein Complex Involved in Chromosome Segregation. Mol. Cell. 2010;39:632–40.

23. Hwang JR, Moncollin V, Vermeulen W, Seroz T, Van Vuuren H, Hoeijmakers JHJ, et al. A

3’ → 5’ XPB helicase defect in repair/transcription factor TFIIH of xeroderma pigmentosum group B affects both DNA repair and transcription. J. Biol. Chem. 1996;271:15898–904.

24. Weeda G, van Ham RCA, Vermeulen W, Bootsma D, van der Eb AJ, Hoeijmakers JHJ. A presumed DNA helicase encoded by ERCC-3 is involved in the human repair disorders xeroderma pigmentosum and Cockayne’s syndrome. Cell. 1990;62:777–91.

25. Egly J-M. The 14th Datta Lecture TFIIH: from transcription to clinic. FEBS Lett. . 2001;498:124–8.

26. Schärer OD. The molecular basis for different disease states caused by mutations in TFIIH and XPG. DNA Repair (Amst). 2008;7:339–44.

27. Zurita M, Cruz-Becerra G. TFIIH: New Discoveries Regarding its Mechanisms and Impact on Cancer Treatment. J. Cancer. 2016;7:2258–65.

28. Regan CL, Fuller MT. Interacting genes that affect microtubule function: the nc2 allele of the haywire locus fails to complement mutations in the testis-specific beta-tubulin gene of Drosophila. Genes Dev. 1988;2:82–92.

29. Merino C, Reynaud E, Vazquez M, Zurita M. DNA Repair and Transcriptional Effects of Mutations in TFIIH in Drosophila Development. Mol. Biol. Cell. 2002;13:3246–56.

30. Castro J, Merino C, Zurita M. Molecular characterization and developmental expression of the TFIIH factor p62 gene from Drosophila melanogaster: Effects on the UV light sensitivity of a p62 mutant fly. DNA Repair (Amst). 2002;1:359–68.

31. Aguilar-Fuentes J, Fregoso M, Herrera M, Reynaud E, Braun C, Egly JM, et al. p8/TTDA Overexpression Enhances UV-Irradiation Resistance and Suppresses TFIIH Mutations in a Drosophila Trichothiodystrophy Model. PLoS Genet. 2008;4:e1000253.

32. Fregoso M, Lainé J-P, Aguilar-Fuentes J, Mocquet V, Reynaud E, Coin F, et al. DNA repair and transcriptional deficiencies caused by mutations in the Drosophila p52 subunit of TFIIH generate developmental defects and chromosome fragility. Mol. Cell. Biol. 2007;27:3640–50.

33. Herrera-Cruz M, Cruz G, Valadez-Graham V, Fregoso-Lomas M, Villicaña C, Vázquez M, et al. Physical and functional interactions between Drosophila homologue of Swc6/p18hamlet subunit of the SWR1/SRCAP chromatin-remodeling complex with the DNA repair/transcription factor TFIIH. J. Biol. Chem. 2012;287:33567–80.

34. Villicaña C, Cruz G, Zurita M. The genetic depletion or the triptolide inhibition of TFIIH in p53-deficient cells induces a JNK-dependent cell death in Drosophila. J. Cell Sci. 2013;126:2502–15.

35. Hirst J, Carmichael J. A potential role for the clathrin adaptor GGA in Drosophila spermatogenesis. BMC Cell Biol. 2011;12:22.

36. Yuan K, Seller CA, Shermoen AW, O'Farrell PH. Timing the Drosophila Mid-Blastula Transition: A Cell Cycle-Centered View. Trends Genet. 2016;32:496–507.

37. Sullivan W, Ashburner M, Hawley S, editors. Drosophila Protocols. Cold Spring Harbor, NY, USA.: Cold Spring Harbor Laboratory Press; 2000.

38. Aguilar-Fuentes J, Valadez-Graham V, Reynaud E, Zurita M. TFIIH trafficking and its nuclear assembly during early Drosophila embryo development. J Cell Sci. 2006;119:3866–75.

39. Chen X, Lu C, Prado JRM, Eun SH, Fuller MT. Sequential changes at differentiation gene promoters as they become active in a stem cell lineage. Development. 2011;138:2441–50.

40. El-Sharnouby S, Redhouse J, White RAH. Genome-Wide and Cell-Specific Epigenetic Analysis Challenges the Role of Polycomb in Drosophila Spermatogenesis. PLoS Genet. 2013;9:e1003842.

41. Mukhopadhyay A, Deplancke B, Walhout AJM, Tissenbaum HA. Chromatin immunoprecipitation (ChIP) coupled to detection by quantitative real-time PCR to study transcription factor binding to DNA in Caenorhabditis elegans. Nat. Protoc. 2008;3:698–709.

42. Lin X, Tirichine L, Bowler C. Protocol: Chromatin immunoprecipitation (ChIP) methodology to investigate histone modifications in two model diatom species. Plant Methods.

2012;8:48.

43. Mortazavi A, Williams BA, McCue K, Schaeffer L, Wold B. Mapping and quantifying mammalian transcriptomes by RNA-Seq. Nat. Methods. 2008;5:621–8.

44. Benjamini Y, Yekutieli D. THE CONTROL OF THE FALSE DISCOVERY RATE IN MULTIPLE TESTING UNDER DEPENDENCY. Ann. Stat. 2001;29:1165–88.

45. de Hoon MJL, Imoto S, Nolan J, Miyano S. Open source clustering software. Bioinformatics. 2004;20:1453–4.

46. Palomera-Sanchez Z, Bucio-Mendez A, Valadez-Graham V, Reynaud E, Zurita M. Drosophila p53 is required to increase the levels of the dKDM4B demethylase after UV-induced DNA damage to demethylate histone H3 lysine 9. J. Biol. Chem. 2010;285:31370–9.

47. Juárez M. Dinámica de las subunidades DmP8 y DmP52 de TFIIH durante el desarrollo y en respuesta a daño al ADN en Drosophila melanogaster. Universidad Nacional Autónoma de México; 2014.

48. Coin F, De Santis LP, Nardo T, Zlobinskaya O, Stefanini M, Egly JM. p8/TTD-A as a repair-specific TFIIH subunit. Mol. Cell. 2006;21:215–26.

49. Vermeulen W, Bergmann E, Auriol J, Rademakers S, Frit P, Appeldoorn E, et al. Sublimiting concentration of TFIIH transcription/DNA repair factor causes TTD-A trichothiodystrophy disorder. Nat. Genet. 2000;26:307–13.

50. Theil AF, Nonnekens J, Steurer B, Mari PO, de Wit J, Lemaitre C, et al. Disruption of TTDA Results in Complete Nucleotide Excision Repair Deficiency and Embryonic Lethality. PLoS Genet. 2013;9:e1003431.

51. Chen X, Hiller M, Sancak Y, Fuller M. Tissue-Specific TAFs Counteract Polycomb to Turn on Terminal Differentiation. Science (80-.). 2005;310:869–72.

52. Perezgasga L, Jiang J, Bolival B, Hiller M, Benson E, Fuller MT, et al. Regulation of transcription of meiotic cell cycle and terminal differentiation genes by the testis-specific Zn-

finger protein matotopetli. Development. 2004;131:1691–702.

53. Jiang J, White-Cooper H. Transcriptional activation in Drosophila spermatogenesis involves the mutually dependent function of aly and a novel meiotic arrest gene cookie monster. Development. 2003;130:563–73.

54. Jiang J, Benson E, Bausek N, Doggett K, White-Cooper H. Tombola, a tesmin/TSO1-family protein, regulates transcriptional activation in the Drosophila male germline and physically interacts with always early. Development. 2007;134:1549–59.

55. White-Cooper H, Leroy D, MacQueen A, Fuller MT. Transcription of meiotic cell cycle and terminal differentiation genes depends on a conserved chromatin associated protein, whose nuclear localisation is regulated. Development. 2000;127:5463–73.

56. Beall EL, Lewis PW, Bell M, Rocha M, Jones DL, Botchan MR. Discovery of tMAC: A Drosophila testis-specific meiotic arrest complex paralogous to Myb-Muv B. Genes Dev. 2007;21:904–19.

57. Hiller MA, Lin TY, Wood C, Fuller MT. Developmental regulation of transcription by a tissue-specific TAF homolog. Genes Dev. 2001;15:1021–30.

58. Hiller M, Chen X, Pringle MJ, Suchorolski M, Sancak Y, Viswanathan S, et al. Testis-specific TAF homologs collaborate to control a tissue-specific transcription program. Development. 2004;131:5297–308.

59. White-Cooper H, Schäfer M a, Alphey LS, Fuller MT. Transcriptional and post-transcriptional control mechanisms coordinate the onset of spermatid differentiation with meiosis I in Drosophila. Development. 1998;125:125–34.

60. Martínez-Balbás MA, Dey A, Rabindran SK, Ozato K, Wu C. Displacement of sequence-specific transcription factors from mitotic chromatin. Cell. 1995;83:29–38.

61. Parsons GG, Spencer C a. Mitotic repression of RNA polymerase II transcription is accompanied by release of transcription elongation complexes. Mol. Cell. Biol. 1997;17:5791–

802.

62. Esposito E, Lim B, Guessous G, Falahati H, Levine M. Mitosis-associated repression in development. Genes Dev. 2016;30:1503–8.

63. Guglielmi B, LaRochelle N, Tjian R. Gene-specific transcriptional mechanisms at the histone gene cluster revealed by single-cell imaging. Mol. Cell. 2013;51:480–92.

64. Larochelle S, Merrick KA, Terret ME, Wohlbold L, Barboza NM, Zhang C, et al. Requirements for Cdk7 in the Assembly of Cdk1/Cyclin B and Activation of Cdk2 Revealed by Chemical Genetics in Human Cells. Mol. Cell. 2007;25:839–50.

65. Li X, Urwyler O, Suter B. Drosophila Xpd regulates Cdk7 localization, mitotic kinase activity, spindle dynamics, and chromosome segregation. PLoS Genet. 2010;6:e1000876.

66. Yeom E, Hong S-T, Choi K-W. Crumbs interacts with Xpd for nuclear division control in Drosophila. Oncogene. 2015;34:2777–89.

67. Giglia-Mari G, Miquel C, Theil AF, Mari PO, Hoogstraten D, Ng JMY, et al. Dynamic interaction of TTDA with TFIIH is stabilized by nucleotide excision repair in living cells. PLoS Biol. 2006;4:0952–63.

68. Botta E, Nardo T, Lehmann AR, Egly J, Pedrini AM, Stefanini M. Reduced level of the repair/transcription factor TFIIH in trichothiodystrophy. Hum. Mol. Genet. 2002;11:2919–28.

69. Hashimoto S, Egly JM. Trichothiodystrophy view from the molecular basis of DNA repair/transcription factor TFIIH. Hum. Mol. Genet. 2009;18:224–30.

70. Stefanini M, Botta E, Lanzafame M, Orioli D. Trichothiodystrophy: From basic mechanisms to clinical implications. DNA Repair (Amst). 2010;9:2–10.

71. Nonnekens J, Cabantous S, Slingerland J, Mari P-O, Giglia-Mari G. In vivo interactions of TTDA mutant proteins within TFIIH. J. Cell Sci. 2013;126:3278–83.

72. Lin TY, Viswanathan S, Wood C, Wilson PG, Wolf N, Fuller MT. Coordinate

developmental control of the meiotic cell cycle and spermatid differentiation in Drosophila males. Development. 1996;122:1331–41.

73. Santagati F, Botta E, Stefanini M, Pedrini AM. Different dynamics in nuclear entry of subunits of the repair/transcription factor TFIIH. Nucleic Acids Res. 2001;29:1574–81.

74. Hoogstraten D, Nigg AL, Heath H, Mullenders LHF, Van Driel R, Hoeijmakers JHJ, et al. Rapid switching of TFIIH between RNA polymerase I and II transcription and DNA repair in vivo. Mol. Cell. 2002;10:1163–74.

75. Giglia-Mari G, Theil AF, Mari PO, Mourgues S, Nonnekens J, Andrieux LO, et al. Differentiation driven changes in the dynamic organization of basal transcription initiation. PLoS Biol. 2009;7.

76. Prasanth K V., Sacco-Bubulya PA, Prasanth SG, Spector DL. Sequential Entry of Components of Gene Expression Machinery into Daughter Nuclei. Mol. Biol. Cell. 2003;14:1043–57.

77. Teves SS, An L, Hansen AS, Xie L, Darzacq X, Tjian R. A Dynamic Mode of Mitotic Bookmarking by Transcription Factors. Elife. 2016;5:e22280.

78. Hartl P, Gottesfeld J, Forbes DJ. Mitotic repression of transcription in vitro. J. Cell Biol. 1993;120:613–24.

79. Ali SA, Zaidi SK, Dobson JR, Shakoori AR, Lian JB, Stein JL, et al. Transcriptional corepressor TLE1 functions with Runx2 in epigenetic repression of ribosomal RNA genes. Proc. Natl. Acad. Sci. U. S. A. 2010;107:4165–9.

80. Lake RJ, Tsai PF, Choi I, Won KJ, Fan HY. RBPJ, the Major Transcriptional Effector of Notch Signaling, Remains Associated with Chromatin throughout Mitosis, Suggesting a Role in Mitotic Bookmarking. PLoS Genet. 2014;10.

81. Kadauke S, Blobel G. Mitotic bookmarking by transcription factors. Epigenetics Chromatin. 2013;6:6.

82. Yang J, Sung E, Donlin-Asp PG, Corces VG. A subset of Drosophila Myc sites remain associated with mitotic chromosomes co-localized with insulator proteins. Nat. Commun. 2013;4:1464.

83. Marshall WF, Marko JF, Agard DA, Sedat JW. Chromosome elasticity and mitotic polar ejection force measured in living Drosophila embryos by four-dimensional microscopy-based motion analysis. Curr. Biol. 2001;11:569–78.

84. Matsuno M, Kose H, Okabe M, Hiromi Y. TFIIH controls developmentally-regulated cell cycle progression as a holocomplex. Genes to Cells. 2007;12:1289–300.

11. ANEXOS

11.1 Publicación

- Analysis of *Drosophila p8* and *p52* mutants reveals distinct roles for the maintenance of TFIIH stability and male germ cell differetiation.

11.2 Manuscrito en preparación

- Mitotic bookmarking by TFIIH during zygotic genome activation in Drosophila suggests the existence of a short-term transcriptional memory mechanism.

11.3 Otras publicaciones generadas durante el curso de los estudios de doctorado

- TFIIH: New Discoveries Regarding its Mechanisms and Impact on Cancer Treatment.
- The basal transcription machinery as a target for cancer therapy.
- The genetic depletion or the triptolide inhibition of TFIIH in p53-deficient cells induces a JNK-dependent cell death in *Drosophila.*
- Physical and Functional Interactions between Drosophila Homologue of Swc6/p18Hamlet Subunit of the SWR1/SRCAP Chromatin-remodeling Complex with the DNA Repair/Transcription Factor TFIIH.

OPEN BIOLOGY

rsob.royalsocietypublishing.org

Research

Cite this article: Cruz-Becerra G, Juárez M, Valadez-Graham V, Zurita M. 2016 Analysis of *Drosophila p8* and *p52* mutants reveals distinct roles for the maintenance of TFIIH stability and male germ cell differentiation. *Open Biol.* **6**: 160222.
http://dx.doi.org/10.1098/rsob.160222

Received: 26 July 2016
Accepted: 18 September 2016

Subject Area:
developmental biology/genetics/molecular biology/cellular biology

Keywords:
TFIIH, transcription, cell differentiation, spermatogenesis, meiotic arrest, *Drosophila*

Author for correspondence:
Mario Zurita
e-mail: marioz@ibt.unam.mx

Electronic supplementary material is available online at https://dx.doi.org/10.6084/m9.figshare.c.3500376.

THE ROYAL SOCIETY PUBLISHING

Analysis of *Drosophila p8* and *p52* mutants reveals distinct roles for the maintenance of TFIIH stability and male germ cell differentiation

Grisel Cruz-Becerra, Mandy Juárez, Viviana Valadez-Graham and Mario Zurita

Departamento de Genética del Desarrollo, Instituto de Biotecnología, Universidad Nacional Autónoma de México, Av Universidad 2001, Cuernavaca Morelos 62250, Mexico

MZ, 0000-0002-8404-2173

Eukaryotic gene expression is activated by factors that interact within complex machinery to initiate transcription. An important component of this machinery is the DNA repair/transcription factor TFIIH. Mutations in TFIIH result in three human syndromes: xeroderma pigmentosum, Cockayne syndrome and trichothiodystrophy. Transcription and DNA repair defects have been linked to some clinical features of these syndromes. However, how mutations in TFIIH affect specific developmental programmes, allowing organisms to develop with particular phenotypes, is not well understood. Here, we show that mutations in the p52 and p8 subunits of TFIIH have a moderate effect on the gene expression programme in the *Drosophila* testis, causing germ cell differentiation arrest in meiosis, but no Polycomb enrichment at the promoter of the affected differentiation genes, supporting recent data that disagree with the current Polycomb-mediated repression model for regulating gene expression in the testis. Moreover, we found that TFIIH stability is not compromised in p8 subunit-depleted testes that show transcriptional defects, highlighting the role of p8 in transcription. Therefore, this study reveals how defects in TFIIH affect a specific cell differentiation programme and contributes to understanding the specific syndrome manifestations in TFIIH-afflicted patients.

1. Introduction

Proliferation and cell differentiation are linked to cell cycle modulation, global gene expression and genome maintenance. Several factors mediate the crosstalk among these mechanisms. One of these is the DNA repair and basal transcription factor TFIIH, which participates in transcription with RNA polymerases I and II (RNAPI and RNAPII), nucleotide excision repair (NER) and cell cycle regulation in metazoans [1,2]. TFIIH is composed of a core and cyclin-dependent activating kinase (CAK) subcomplexes. The core includes XPB and XPD as well as the p62, p52, p44, p34 and p8 subunits. Cdk7, cyclin H and MAT1 constitute the CAK subcomplex [3]. Several enzymatic activities have been identified in components of the TFIIH complex. Recently, a DNA translocase activity was attributed to XPB [4]. In addition, XPB and XPD are DNA helicases/ATPases essential for transcription and DNA repair, while Cdk7 is one of the major kinases involved in transcription activation and cell cycle regulation [5,6]. On the other hand, most TFIIH subunits, including p52, p8, p34, Cyc H and Mat1, have been described as key modulators of these enzymatic activities [7–9]. Additionally, a main role in maintaining steady-state TFIIH levels has been attributed to the p8 subunit [10].

Mutations in TFIIH are associated with complex human diseases, including cancer. Mutations in the XPB and XPD subunits may cause xeroderma

pigmentosum (XP), Cockayne syndrome (CS) and trichothiodystrophy (TTD) [11]. In the case of p8, the different mutations described in humans have been related only to TTD-A, which is caused by reduced TFIIH levels in p8 mutant cells [10]. Cutaneous photosensitivity is a shared feature among these syndromes, but other manifestations are syndrome-specific. For example, XP patients may develop skin cancer. TTD is characterized by mental and physical retardation, sterility, ichthyosis and brittle hair. By contrast, CS is characterized by premature ageing, growth failure and progressive neurological dysfunction [12]. As expected, some clinical symptoms in XP, CS and TTD patients have been strongly linked to DNA repair defects as well as transcriptional deficiencies [13]. In this regard, it is intriguing how individuals affected by a general transcription factor that also has a role in cell cycle control and NER are able to complete development showing very specific phenotypes. This may be explained by considering that the mutations observed in human patients are not null, but rather partially affect TFIIH functions [13,14]. Additionally, specific cell types or specific gene expression programmes could be more susceptible to these defects. For example, male sterility is a common feature among several TFIIH mutants in *Drosophila* [15–17] and some TFIIH-afflicted patients [2]. Therefore, the study of how TFIIH mutations affect global transcription in different cell types and how this may affect proliferation or differentiation programmes during the development of model organisms will contribute to an understanding of the basis of the clinical features demonstrated by TFIIH-afflicted patients.

Drosophila spermatogenesis consists of a multi-step differentiation programme that involves easily observable cellular morphology changes and a well-defined gene expression programme that allows stem cells to become highly specialized sperm cells in the testis. Germ cell differentiation requires the transcriptional activation of approximately 2000 genes in the *Drosophila* testis [18]. The model proposed to explain how germ cell differentiation is achieved involves the participation of testis-specific TBP-associated factors (tTAFs) and some components of the testis-specific meiotic arrest complex (tMAC), which are encoded by some meiotic arrest genes [19] that positively regulate the expression of their targets by interacting with the mediator complex and by sequestering Polycomb (Pc) in a particular compartment of the nucleolus to counteract the repression of differentiation genes in the primary spermatocyte stage during differentiation [19–21]. Here, we report that mutations in the core subunits of the general transcription factor TFIIH generate a meiotic arrest phenotype similar to that observed in testis-specific TAF mutants. A TFIIH mutation delocalizes Pc from the nucleolus in primary spermatocytes. However, Pc binding is not enhanced at the promoter of the repressed differentiation genes in the TFIIH mutant testes, which supports recent genome-wide data that challenge the participation of Pc in the repression of tTAFs targets [22]. Interestingly, our data show that mutations in the p8 and p52 subunits of TFIIH do not affect the transcription of most genes in the *Drosophila* testis. Instead, genes required for terminal differentiation, but not their testis-specific transcriptional regulators, are downregulated, suggesting a gene-specific requirement for TFIIH in transcription during this cell differentiation programme. Furthermore, contrary to the effects of the mutations in p8 observed in cells from TTD-A patients [10], the analysis of p8-depleted testes, which showed transcriptional defects, revealed that the stability of other TFIIH subunits is not compromised, highlighting a role for p8 in transcription beyond its role in TFIIH stability maintenance.

2. Material and methods

2.1. Fly stocks

Ore R was used as wild-type strain ($p8^{+}/p8^{+}$ and $p52^{+}/p52^{+}$), except when indicated. The *Pc-GFP* transgenic line (BL9593) was obtained from the Bloomington Stock Center. The $p52^{EP3605}$, $p52^{mrn5}$, $p52^{mrn3}$ and $p8^{-}$ alleles were previously described [15,16].

2.2. Phase-contrast and confocal microscopy

Testes from 0 to 1 day post eclosion were dissected in testis buffer [23] and examined by phase-contrast and confocal microscopy. Visualization of fluorescently tagged proteins was performed using the Zeiss LSM 510 META confocal system coupled to an Axiovert 200 inverted microscope.

2.3. Transgenic constructs

DNA recombinant constructs of p8-ECFP, XPB-EGFP and EYFP-p52 were generated by tagging the full-length open reading of p8, p52 and XPB, in frame with the DNA sequence of the Enhanced-Cyan, Enhanced-Green or the Enhanced-Yellow Fluorescent Proteins. These constructs were cloned into the pCaSper-Hsp83 vector.

2.4. Rescue experiments

Rescue of the semi-lethality phenotype of homozygous *p8* mutant flies was performed by crossing heterozygotes ($p8^{+}/p8^{-}$) mutants with pCaSper-Hsp83 transgenic lines expressing the p8-ECFP recombinant protein. The F_1 progeny was intercrossed to generate homozygous $p8^{-}/p8^{-}$ flies containing one or two copies of the p8-ECFP transgene. Similar crosses were performed to rescue the semi-lethality phenotype of the heteroallelic combination of *p52* mutants ($p52^{EP3605}/p52^{mrn5}$) with transgenic lines expressing EYFP-p52.

2.5. Western blotting

Testes were dissected in ice-cooled PBS with protease inhibitors (complete, Roche). Total protein extracts were analysed by immunoblotting using standard procedures. Primary antibodies used were: 8WG16 (1 : 1500; Covance), H14 (1 : 1500; Covance), XPD (1 : 1500; our own preparation), XPB (1 : 2000; our own preparation), p52 (1 : 1500 [16]), p8 (1 : 1000 [16]), Cdk7 (1 : 1000, Santa Cruz Biotechnology), TBP (1 : 500; Santa Cruz Biotechnology), E7 (1 : 2000; DSHB), A12 (1 : 1500; DSHB), F2F4 (1500; DSHB), JLA20 (1 : 3000; DSHB), GFP (1 : 2500; GenScript); p18 (1 : 1000; [16]) HRP-coupled secondary antibodies (1 : 3500; Invitrogen) were used for chemioluminiscence detection with Thermo Scientific Pierce ECL. Densitometric analyses in western blots were performed using ImageJ software. Protein levels among the different genotypes were normalized to TBP and quantified with respect to the correspondent

wild-type ($p8^+/p8^+$ and $p52^+/p52^+$genotypes) protein amount set to 1.

2.6. qPCR expression analysis

Total RNA from testes was extracted with Trizol (Invitrogen). Equal quantity of RNA from each genotype was used to synthetize cDNA with MVL-V reverse transcriptase (Invitrogen). qPCR analyses were performed with LightCycler Fast Start DNA Master^{PLUS} SYBR Green I and the LightCycler 1.5 Instrument (Roche). The relative expression level of each analysed gene was calculated by 2^{-ddCt}, where ddCt = (Ct target gene-Ct control gene) using *CycA* as internal control. Primer sequences (5′-3′) for *Mst87F*: forward, aacttttacgaattaatcatgtgctg; reverse, cagggtccacatcctcctc. *dj*: forward, aactgaaaa agaaatgcaaggaa; reverse, tttgcaagggtctttcttcg. *fzo*: forward, caatgtctctccataccctaca; reverse, agttgccaatcgcaagagtt. *twe*: forward, aagaccaagtcctggcaatg; reverse, cagtcgtgaacgtgatttcc. *CycA*: forward, gctggaggagatcacgactt; reverse, ccatcata gccaccttcttgt.

2.7. Chromatin immunoprecipitation-qPCR

Chromatin immunoprecipitation from testes was performed as reported previously [20] with small modifications. Briefly, 100 pairs of testes were used per assay. Cross-linking was performed with 1% formaldehyde in PBS for 15 min at 37°C, followed by washing with PBS. Testes were disrupted in 130 µl of SDS-lysis buffer (1% SDS, 50 mM Tris-HCl, pH 8.0, 10 mM EDTA) and sonicated in thin wall 0.6 ml tubes (Axygen PCR-05-C) for 6 cycles (1 cycle is: 30 s ON/60 s OFF) at high setting using a Diagenode Bioruptor. Chromatin was diluted 1 : 10 with ChIP dilution buffer (0.01% SDS, 1.1% Triton X-100, 1.2 mM EDTA, 16.7 mM Tris-HCl, pH 8.0, 167 mM NaCl) and pre-cleared with rabbit IgG coupled to Dynabeads Protein G (Life Technologies). After pre-clearing, 10% of the lysate was reserved as input. The lysate was incubated with 7.5 µg of the antibody (anti-Pc or anti-XPB; Santa Cruz Biotechnology) or irrelevant rabbit IgG (Invitrogen) overnight at 4°C. The antibody-chromatin complexes were pulled-down with 50 µl of Dynabeads Protein G. Beads were washed once with low-salt wash buffer (0.1% SDS, 1% Triton X-100, 2 mM EDTA, 20 mM Tris-HCl, pH 8.0 and 150 mM NaCl), once with high-salt wash buffer (0.1% SDS, 1% Triton X-100, 2 mM EDTA, 20 mM Tris-HCl, pH 8.0 and 500 mM NaCl), once with LiCl wash buffer (0.25 M LiCl, 1% NP40, 1% sodium deoxycholate, 1 mM EDTA, and 10 mM Tris-HCl, pH 8.0) and twice with TE (10 mM Tris-HCl, pH 8.0 and 1 mM EDTA). Immunoprecipitated chromatin was eluted with elution buffer (1% SDS, 0.1 M $NaHCO_3$ in 1xTE). Reverse cross-linking was performed at 65°C, followed by RNA and protein digestion. The DNA was recovered by phenol/chloroform extraction and ethanol/glycogen precipitation. Immunoprecipitated DNA was analysed by qPCR, using the primers reported previously [21,22]. The fold enrichment relative to mock was calculated by $E^{(-ddCt)}$, where E represents the efficiency of each gene primers, and ddCt = [(Ct sample − Ct input) − (Ct mock − Ct input)] [24,25].

2.8. RNA-seq and bioinformatics analysis

Total RNA from *Ore R*, $p8^-/p8^-$ and $p52^{EP3605}/p52^{mrn^5}$ testes were prepared with trizol. The Beijing Genomic Institute (BGI) performed the RNA-seq and part of the data analysis. In summary, libraries for RNA sequencing were prepared with poly-A-selected mRNA using the Illumina TruSeq RNA library construction kit v2. Libraries were purified using the Agencourt AMPure XP (Beckman Coulter) and run as 50 bp single-end lanes on an Illumina HiSeq 2000 instrument. To test the gene expression enrichment, BGI examined the reads per kilobase transcriptome per million mapped reads (RPKM) [26] values in the different samples. Correction for false positive and false negative errors was performed by using the FDR method [27].

2.9. Transcriptome comparison between TFIIH mutants and other meiotic arrest mutants

The significant $\log_2$-fold change values for the DEGs in the transcriptomes of *sa*, *aly*, *Med22* and *Ubi-p63E* were obtained from the data in the GEO database with the GEO accession numbers previously reported [19,28,29]. In the case of the *bam* transcriptome, the $\log_2$-fold change values were calculated from the reported RPKM data for each analysed gene [30].

3. Results

3.1. TFIIH core subunits are required for meiotic divisions during spermatogenesis

Similar to humans, mutations in TFIIH subunits in the fly cause complex and pleiotropic phenotypes [31]. We have previously reported a *p8* gene null allele ($p8^-$), which is semilethal, though the males are sterile [16]. Semi-lethality and sterile organisms were also observed from heteroallelic combinations between a P-element insertion allele ($p52^{EP3605}$) and point mutation alleles ($p52^{mrn^3}$ and $p52^{mrn^5}$) in the p52 subunit of TFIIH [15]. To better understand the function of TFIIH during cell differentiation, we investigated the cellular and molecular processes affected during spermatogenesis in the *p8* and *p52* mutant testes.

In wild-type organisms, spermatogenesis is initiated at the apical tip of the testis with the asymmetrical division of a stem cell to produce a daughter stem cell and a spermatogonial precursor cell, which after four rounds of mitotic divisions undergoes premeiotic S phase and becomes a 16-primary spermatocyte cyst. At the primary spermatocyte stage, the transcriptional programme required for the meiotic divisions and terminal differentiation is activated, allowing postmeiotic spermatid differentiation [18].

To gain insights into the $p8^-/p8^-$, $p52^{EP3605}/p52^{mrn^3}$ and $p52^{EP3605}/p52^{mrn^5}$ male sterility phenotypes, we analysed their testes by phase-contrast microscopy. We noticed that TFIIH mutant testes were smaller than wild-type (figure 1*a*). Furthermore, squash preparations from live mutant testes showed an arrest of germ cell differentiation at the primary spermatocyte stage, while groups of degenerating cells were observed at the base of the testes (figure 1*a*). Unlike wild-type primary spermatocytes, which showed nucleolus break down and metaphasic spindle assembly at meiosis I, the TFIIH mutant primary spermatocytes failed to enter meiosis, arresting at the G2/M transition (figure 1*b*). Although these phenotypes were similar between

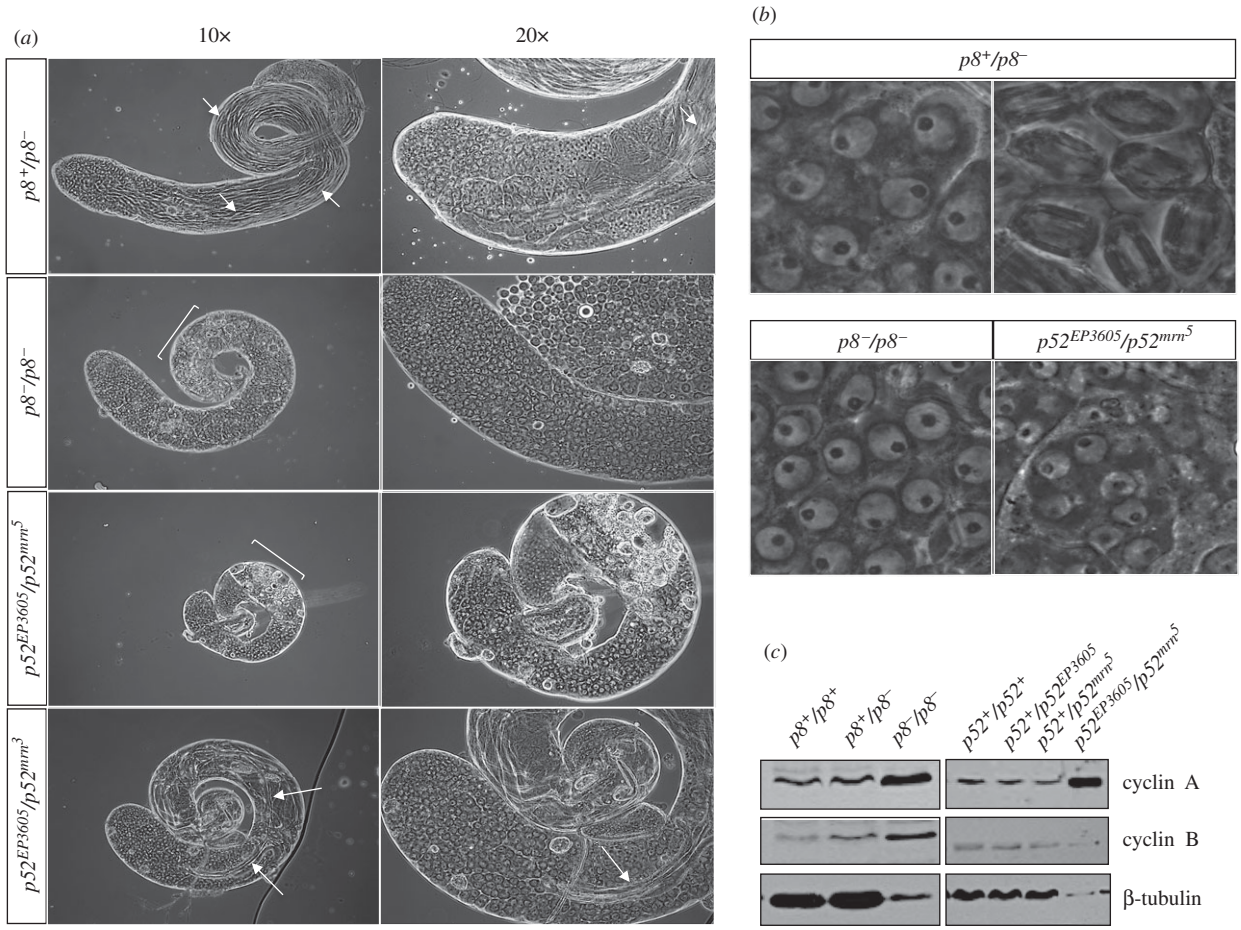

Figure 1. Meiotic arrest phenotype in *p8* and *p52* mutant testes. (*a*) Phase contrast of squash testes from heterozygous *p8* mutant ($p8^{+}/p8^{-}$), homozygous *p8* mutant ($p8^{-}/p8^{-}$) and heteroallelic *p52* mutants ($p52^{EP3605}/p52^{mrn5}$ and $p52^{EP3605}/p52^{mrn3}$). Note that all the TFIIH mutant testes are smaller than control ($p8^{+}/p8^{-}$): $p8^{-}/p8^{-}$, $p52^{EP3605}/p52^{mrn5}$ and $p52^{EP3605}/p52^{mrn3}$ testes represent about 0.67×, 0.3× and 0.8× the wild-type size, respectively. The $p8^{+}/p8^{-}$ testes show all the stages of spermatogenesis and flagella bundles (small arrows) are easily observed. By contrast, $p8^{-}/p8^{-}$ and $p52^{EP3605}/p52^{mrn5}$ testes are filled with primary spermatocytes and some degenerating cells (square bracket). Similarly, the $p52^{EP3605}/p52^{mrn3}$ testes are mostly enriched with primary spermatocytes; however, some bundles of flagella (big arrows) are also observed. (*b*) Primary spermatocytes at metaphase of meiosis I are observed in control ($p8^{+}/p8^{-}$, top right panel), but not in $p8^{-}/p8^{-}$ or $p52^{EP3605}/p52^{mrn5}$ testes. (*c*) Western blots for the indicated proteins in $p8^{-}/p8^{-}$, $p52^{EP3605}/p52^{mrn5}$ and control ($p8^{+}/p8^{+}$, $p8^{+}/p8^{-}$, $p52^{+}/p52^{+}$, $p52^{+}/p52^{mrn5}$ and $p52^{+}/p52^{EP3605}$) testes. The same number of testes was loaded for each genotype.

the mutant testes from the two different TFIIH subunits, we observed an effect on the severity of the phenotype that depended on the allele combination in the *p52* mutant organisms. For example, despite primary spermatocyte enrichment, some flagella bundles were observed in the $p52^{EP3605}/p52^{mrn3}$ testes (figure 1*a*), indicating that spermatogenesis proceeded aberrantly in some cells even though it was not successfully completed. Moreover, the $p52^{EP3605}/p52^{mrn3}$ mutant shows the less dramatic effect on testis size (i.e. 0.2× smaller than wild-type). On the other hand, the strongest phenotype was observed in the $p52^{EP3605}/p52^{mrn5}$ males, which showed the smallest testis size (representing only about one-third of the wild-type size) and were filled with early primary spermatocytes (figure 1*a*). In agreement with the accumulation of premeiotic primary spermatocytes, the protein levels of some cell cycle regulators, such as cyclin A (Cyc A) and cyclin B (Cyc B), were highly increased in the $p8^{-}/p8^{-}$ testes, while only Cyc A was increased in the $p52^{EP3605}/p52^{mrn5}$ testes (figure 1*c*), suggesting that primary spermatocytes arrested at different stages during meiosis in $p8^{-}/p8^{-}$ and $p52^{EP3605}/p52^{mrn5}$ testes. Altogether these data indicate that the absence or reduction of some TFIIH proteins resulted in a meiotic arrest phenotype that impairs primary spermatocyte differentiation. Intriguingly, these phenotypes were very similar to those observed in mutant testes from the meiotic arrest genes, which only produce primary spermatocytes that fail to continue meiosis or spermatid differentiation. Most meiotic arrest genes encode testis-specific transcription factors, including tTAFs, and some components of the tMAC, which are required for the activation of several genes during differentiation [19].

3.2. The core subunits of TFIIH are located in the nucleus and the nucleolus periphery of primary spermatocytes

The localization pattern of several meiotic arrest gene products during spermatogenesis has been shown to be relevant to their function. For example, tTAFs are poorly detected in euchromatin but are enriched in the nucleolus of primary spermatocytes, where they have been proposed to sequester Pc to counteract Pc-mediated repression of terminal differentiation genes [20]. By contrast, *tMAC* gene products are mainly located in the bivalent chromosomes of primary spermatocytes, suggesting a major role in transcriptional activation [32,33].

Because we observed that TFIIH mutant testes showed a meiotic arrest phenotype, we investigated the distribution of TFIIH during spermatogenesis. We generated transgenic flies expressing p8-ECFP or EYFP-p52. Importantly, these recombinant proteins partially rescued the *p8* and *p52* semilethal mutants, respectively (see the electronic supplementary material, tables S1 and S2). Using confocal microscopy on unfixed squashed testes from these transgenic flies, we observed restricted localization of these TFIIH core subunits to the early stages of spermatogenesis (figure 2*a*,*b*). Accordingly, an identical pattern for the XPB subunit was observed in the testes of transgenic flies expressing XPB-EGFP (figure 2*c*). There was also a weak signal and a homogeneous distribution in the nucleus of spermatogonial cells, but a more dynamic pattern during the spermatocyte stage (figure 2*a–c*,*e*). TFIIH fluorescently tagged proteins were enriched at bivalent chromosomes and showed a ring-shaped foci pattern at the nucleolus periphery in early spermatocytes (figure 2*d*,*e*). Later, an additional foci pattern was also observed throughout the nucleoplasm of mature spermatocytes (figure 2*e*). Thus, the localization pattern of the TFIIH subunits correlated with the stages of active transcription required to conduce germ cell differentiation in the testis.

3.3. The reduction of p52 levels, but not the ablation of p8, affects the stability of other TFIIH components in the *Drosophila* testis

The strength of the defect severity showed by the $p52^{EP3605}/p52^{mrn5}$ mutant in spermatogenesis suggests that mutations in *p52* have a more deleterious effect on TFIIH functions than the absence of *p8* in the fly testes. Interestingly, the p8 mutant alleles reported in TTD-A afflicted-humans are linked to a reduction in the basal levels of TFIIH [10]. However, recent reports revealed that none of the p8 mutations found in humans are null [14,34]. To determine whether the spermatogenesis defects observed in the *p8* and *p52* mutants are related to globally reduced levels of TFIIH components, we analysed the effect of the absence of p8 or the mutation of p52 on the stability of other TFIIH subunits. We compared, by western blot, the protein amount of some components of the core and CAK subcomplexes from control testes that show wild-type phenotype ($p8^{+}/p8^{+}$, $p8^{+}/p8^{-}$, $p52^{+}/p52^{+}$, $p52^{+}/p52^{EP3605}$, $p52^{+}/p52^{mrn3}$, $p52^{+}/p52^{mrn5}$) with *p8* as well as *p52* mutant testes, which show meiotic arrest phenotype. Unexpectedly, we detected p52, XPB and XPD protein levels similar to wild-type, with only a slight increase in Cdk7 in the $p8^{-}/p8^{-}$ testes (figure 3*a*). By contrast, testes from mutant heteroallelic combinations of *p52* ($p52^{EP3605}/p52^{mrn3}$ and $p52^{EP3605}/p52^{mrn5}$) showed dramatically reduced amounts (less than half) of p52, XPB and p8 compared with wild-type or heterozygotes genotypes (figure 3*b*). Furthermore, there were no significant changes in the levels of other components of the basal transcription machinery, like TBP and the RNAPII or the CAK-mediated serine 5 phosphorylation of the RNAPII-CTD (RNAPII-S_5P-CTD) in the TFIIH mutant testes (figure 3*a*,*b*).

To better understand the effect of the *p52* mutants on the stability of the other TFIIH components, we decided to determine whether the localization of p8-ECFP was affected in the $p52^{EP3605}/p52^{mrn5}$ testes, which showed reduced amounts of endogenous p52, p8 and XPB proteins. The level of p8-ECFP in testes, which was determined by immunoblotting, was unaffected in the *p52* mutant compared with p8-ECFP transgenic flies that showed normal p52 levels (figure 3*c*). However, confocal microscopy revealed that unlike to the observed enrichment in bivalent chromosomes and the nucleolus periphery of primary spermatocytes in control testes ($p52^{+}/p52^{EP3605}$), p8-ECFP was homogeneously distributed in the cytoplasm and the nucleoplasm in the $p52^{EP3605}/p52^{mrn5}$ primary spermatocytes (figure 3*d*). By contrast, EYFP-p52 localization during spermatogenesis was unaffected in $p8^{-}/p8^{-}$ testes (figure 3*e*). Thus, mutations in *p52* not only affected endogenous p8 protein levels but also the p8-ECFP cellular distribution. These data showed that reduced levels of p52 have a more dramatic effect on the stability of the core TFIIH components than the absence of p8 in the fly testes. Moreover, as there was no change in TFIIH subunit levels in $p8^{-}/p8^{-}$ other than p8, while the testes displayed a meiotic arrest phenotype similar to *p52* mutants, this suggests that a global reduction in TFIIH subunits is not the main cause for this phenotype, but it could account for the stronger penetrance observed in *p52*-affected testes. On the other hand, since the absence of p8 does not affect the stability of TFIIH or the p52 cellular localization, we cannot discard the possibility that the meiotic arrest phenotype in the *p8* mutant is generated by its interaction with other proteins or complexes besides TFIIH. Indeed, we have previously demonstrated that p8 interacts with the $p18^{(Hamlet)}$ subunit of the SWR1 complex [16]. However, by western blot experiments we did not find any affection in $p18^{(Hamlet)}$ levels in the $p8^{-}/p8^{-}$ testes (figure 3*a*).

3.4. TFIIH mutants, with meiotic arrest phenotype, showed no reduced expression in the *aly* and *can* classes of meiotic arrest genes

Depending on their targets, most meiotic arrest genes have been classified into the following two general groups: the *always early* (*aly*) class (including *aly, comr, achi, vis, topi, mip40* and *tomb*), some of which are components of the tMAC [23,32,33,35,36] and the cannonball (*can*) class (including *can, sa, mia, rye* and *nht*), which encode for tTAFs [37,38]. The *aly* and *can* classes of genes have been proposed to be the major regulators of the testis-specific gene expression programme that allows meiotic divisions and postmeiotic spermatid differentiation. Some genes required for terminal differentiation, such as *don juan* (*dj*), *fuzzy onions* (*fzo*) and *Male-specific RNA 87F* (*Mst87F*), are common targets between the *aly* and *can* classes. However, the transcription of some cell cycle control genes, such as *Cyclin B* (*CycB*), *boule* (*bol*) and *twine* (*twe*), only depends on *aly* class genes [39]. To investigate whether transcription in TFIIH mutant testes behaves similarly to the *aly* or *can* classes of meiotic arrest mutants, we analysed the expression of some of these terminal differentiation and cell cycle control genes in $p8^{-}/p8^{-}$ and control testes by qPCR. Strikingly, we observed reduced expression of the *dj* and *Mst87F* transcripts, but no change in the levels of the *fzo* transcript in $p8^{-}/p8^{-}$ compared with wild-type ($p8^{+}/p8^{+}$) or heterozygote ($p8^{+}/p8^{-}$) testes (see the electronic supplementary material, figure S1). By contrast, $p8^{-}/p8^{-}$ testes showed slightly increased *twe* mRNA expression (see the electronic supplementary material, figure S1). These data suggest that the transcriptional defects

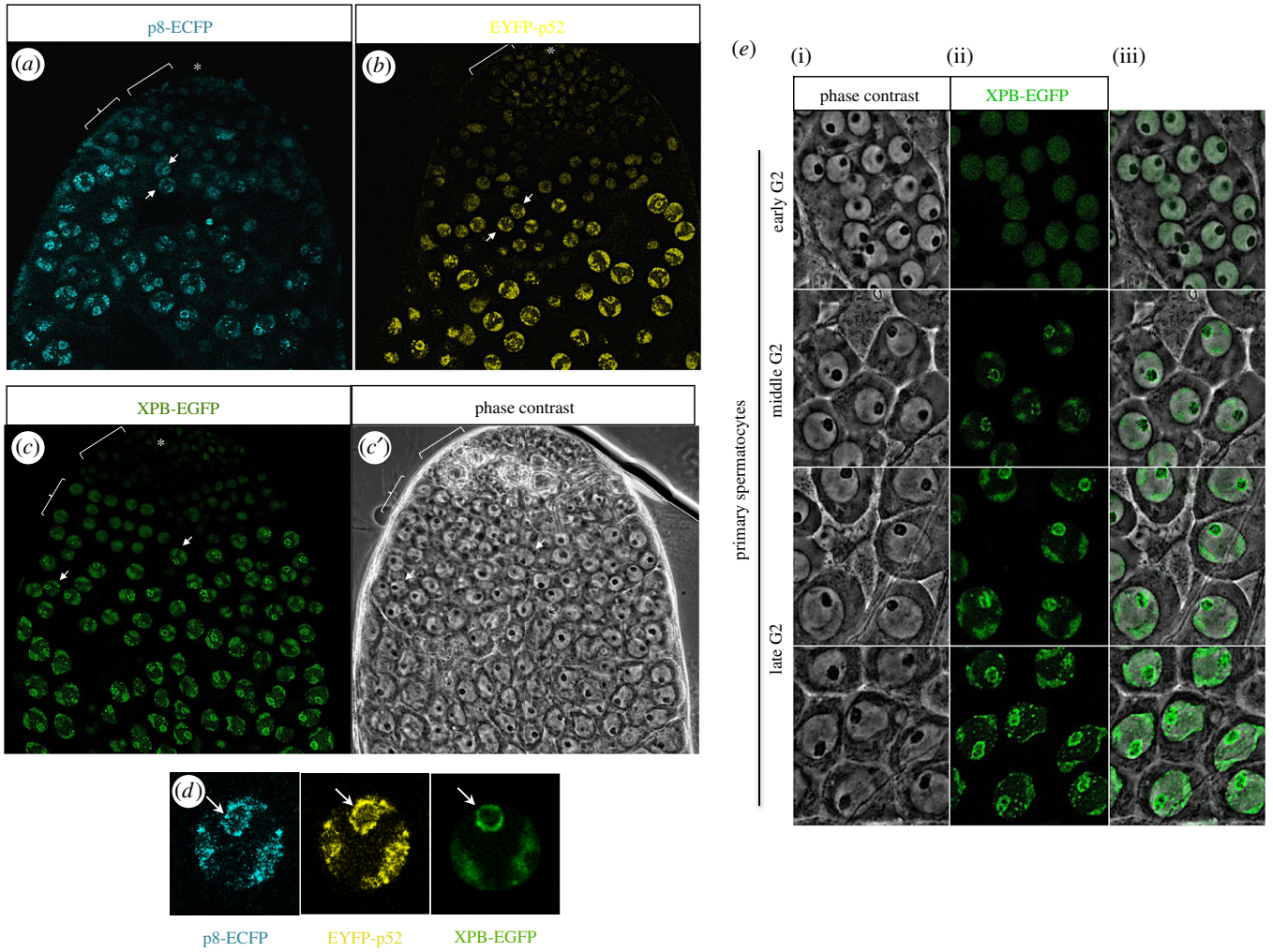

Figure 2. p8, p52 and XPB are enriched in primary spermatocytes. Confocal microscopy images from (*a*) p8-ECFP, (*b*) EYFP-p52 and (*c*) XPB-EGFP in the apical tip of testes. Low levels of these proteins are detected in very early germ cells and gradual enrichment is observed at the primary spermatocyte stage. (*c*′) Phase-contrast image from the XPB-EGFP testis. Asterisk: somatic cells and stem cells niche; square bracket: spermatogonium cells zone; curly brackets: very early spermatocytes zone; arrows: early spermatocytes. (*d*) p8-ECFP, EYFP-p52 and XPB-EGFP are localized at the periphery of the nucleolus (arrows) and the autosomal bivalents in mature primary spermatocytes. Images from p8-ECFP and EYFP-p52 correspond to the same primary spermatocyte obtained from testes expressing both proteins. (*e*) Dynamic of XPB-EGFP in primary spermatocytes. At the earliest stage of primary spermatocytes, XPB-EGFP is homogeneously distributed through the nucleus. As spermatocytes advance in G2, the XPB-EGFP distribution switches to particular enriched regions. In middle G2 spermatocytes, XPB-EGFP shows a foci pattern at the nucleolar periphery and it is enriched in the somatic bivalents. In mature spermatocytes, the localization of XPB-EGFP at the nucleolus periphery become ring-shaped, the enrichment at the bivalents is enhanced and foci enrichment in the nucleoplasm is observed. Panel (i) corresponds to phase-contrast images, (ii) corresponds to XPB-EGFP signal and (iii) shows the merge between them.

in TFIIH mutants were not identical to those observed in mutant testes for some testis-specific transcription factors.

Considering that TFIIH is a ubiquitously expressed central component in the basal transcription machinery for RNAPII, we aimed to analyse how TFIIH mutants affected the transcription programme required for cell differentiation in the testes. Thus, we performed global gene expression analyses (RNA-seq) of total RNA from $p8^{-}/p8^{-}$, $p52^{EP3605}/p52^{mrn5}$ and wild-type testes. In agreement with a previously reported transcriptome analysis of *D. melanogaster* wild-type testes [30], the total number of transcripts identified in the wild-type and TFIIH mutant testes was approximately 15 000 (see the electronic supplementary material, tables S3–S5). Unexpectedly, when the two TFIIH mutants were compared to wild-type only 1701 genes were significantly differentially expressed in the *p52* and *p8* mutants (figure 4*a*; see the electronic supplementary material, table S6). The change in gene expression was very similar between both TFIIH mutants, although it was not identical, with a strongest phenotype observed in the $p52^{EP3605}/p52^{mrn5}$ testes (figure 4*a*; see the electronic supplementary material, tables S7 and S8). Intriguingly, there were more upregulated ($\log_2$-fold change ≥ 1) than downregulated transcripts ($\log_2$-fold change ≤ -1) in both of the TFIIH mutants (figure 4*a*; see the electronic supplementary material, table S6). There were a few genes that were upregulated in $p8^{-}/p8^{-}$ testes, but downregulated in the $p52^{EP3605}/p52^{mrn5}$ testes and vice versa (figure 4*a*; see the electronic supplementary material, figure S2). This difference may be due to an indirect effect on gene expression between the two mutants, since the meiotic arrest phenotype is more severe in the *p52* mutant organisms.

Importantly, we found no significant changes in the transcript level of the *aly* (*tMAC*) or *can* (*tTAF*s) classes of genes in $p8^{-}/p8^{-}$ testes (figure 4*b*). By contrast, some *can* and *aly* genes were slightly upregulated in the $p52^{EP3605}/p52^{mrn5}$ testes (figure 4*b*), indicating that the meiotic arrest phenotype of the TFIIH mutant testes is not caused by decreased expression of the *aly* or *can* classes of genes.

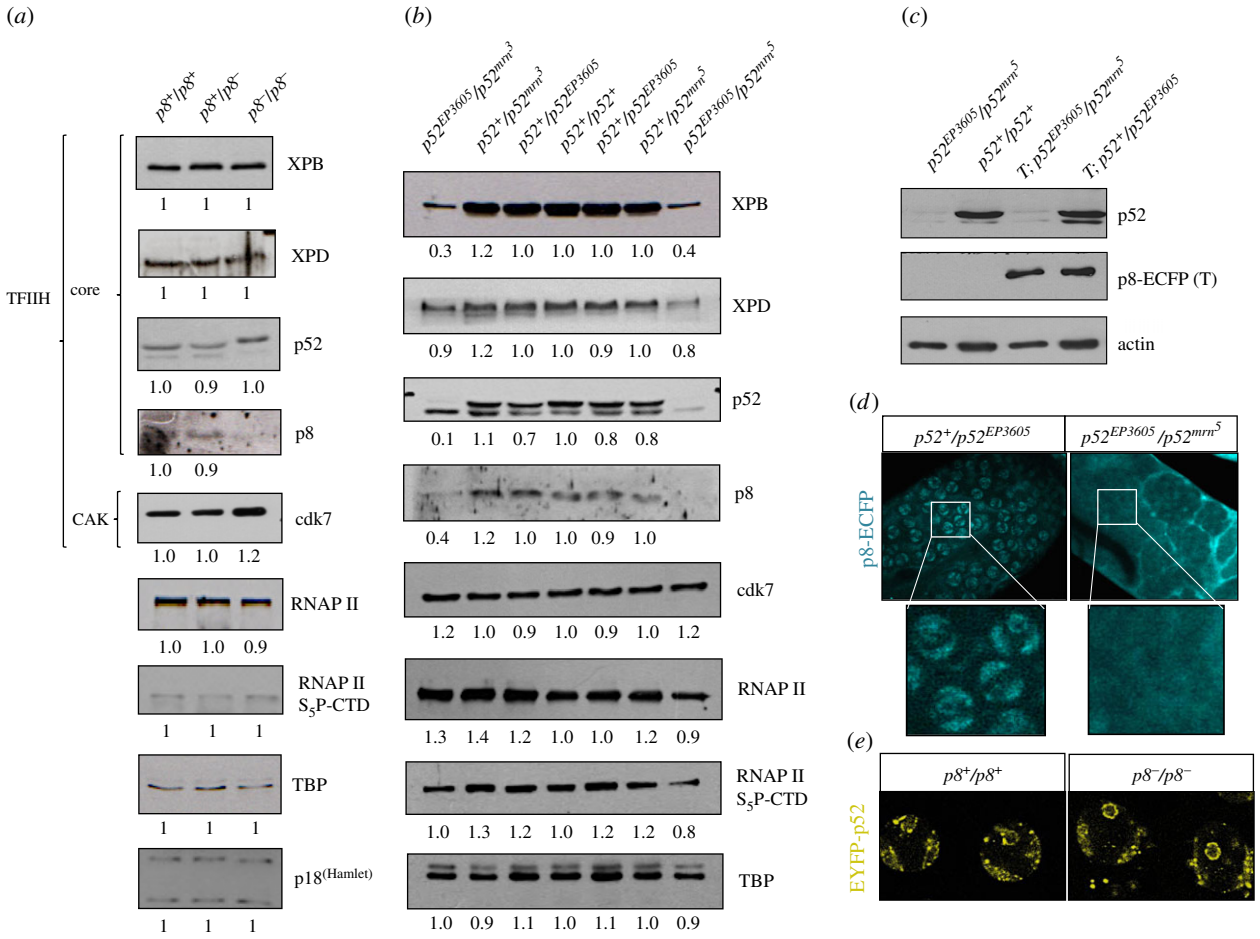

Figure 3. Effect on the stability of TFIIH subunits in *p8* and *p52* mutant testes. (*a*) Western blots from wild-type ($p8^{+}/p8^{+}$), heterozygous ($p8^{+}/p8^{-}$) and homozygous ($p8^{-}/p8^{-}$) *p8* mutant testes. (*b*) Western blots from wild-type ($p52^{+}/p52^{+}$), heterozygous ($p52^{+}/p52^{EP3605}$, $p52^{+}/p52^{mrn^{3}}$ and $p52^{+}/p52^{mrn^{5}}$) and heteroallelic combinations ($p52^{EP3605}/p52^{mrn^{3}}$ and $p52^{EP3605}/p52^{mrn^{5}}$) of *p52* mutant testes. Note that the heteroallelic *p52* mutants show affected levels of several components of TFIIH. Densitometric analyses were performed using TBP as a loading control; the relative quantification is indicated under each blot. (*c*) Western blots in heterozygous ($p52^{+}/p52^{EP3605}$) and heteroallelic ($p52^{EP3605}/p52^{mrn^{5}}$) *p52* mutant testes expressing the *p8-ECFP* transgene show no difference in p8-ECFP protein levels. The *p8-ECFP* transgene is indicated as a *T* in the genotypes. (*d*,*e*) Localization of EYFP-p52 and p8-ECFP recombinant proteins in *p8* and *p52* mutant primary spermatocytes, respectively.

To better understand how the misregulated genes in the TFIIH mutant testes could affect the normal cell differentiation programme in spermatogenesis, we used the demonstrated or putative function reported in the Fly Base database (http://flybase.org/) to ontologically classify the 1701 differentially expressed genes (DEGs) common to $p8^{-}/p8^{-}$ and $p52^{EP3605}/p52^{mrn^{5}}$ testes. The DEGs were distributed in a wide range of ontological classes, suggesting that several processes were affected. In agreement with the accumulation of premeiotic primary spermatocytes observed in the TFIIH mutant testes, we found that upregulated genes included factors that regulate transcription and chromatin structure as well as genes implicated in cell cycle control (figure 4*c*; see the electronic supplementary material, tables S9 and S10). By contrast, transcripts that encode for testis-enriched proteins were notoriously reduced in the TFIIH mutant genotypes (figure 4*c*; see the electronic supplementary material, table S11). Taken together, these results show that the meiotic arrest phenotype generated by these two mutations in TFIIH subunits was not caused by the reduced expression of *aly* or *can* classes of genes, though many of their target genes were affected, suggesting that general transcription factors and testis-specific transcription factors act in coordination to regulate the specific gene programme required for normal germ cell differentiation in the testis.

3.5. tTAFs and TFIIH share several target genes

Meiotic arrest gene mutants other than the *aly* and *can* classes have been reported [19,28,29,40–42]. Available microarrays data were used to compare our TFIIH mutant transcriptomes with the *sa* (from the *can* class), *aly* (from the *aly* class) and the unclassified *Med22* and the *Ubi-p63E* meiotic arrest mutants. We also compared our data with the transcriptome of *bag of marbles* (*bam*) mutant testes, in which the transition from spermatogonial to primary spermatocyte is abolished and testes are enriched with over-proliferating spermatogonial cells [30]. Although these studies have been performed using different platforms, it is acceptable to compare the $\log_2$-fold change data obtained by RNA-seq with the geometric mean of the $\log_2$-fold change obtained by microarrays [43]. Therefore, the comparisons between these analyses were only at the level of what genes were upregulated or downregulated compared with the wild-type based on the significant $\log_2$-fold change values obtained from the GEO datasets for each mutant [19,28,29]. We focused on genes that participate in transcription, chromatin remodelling or cell cycle

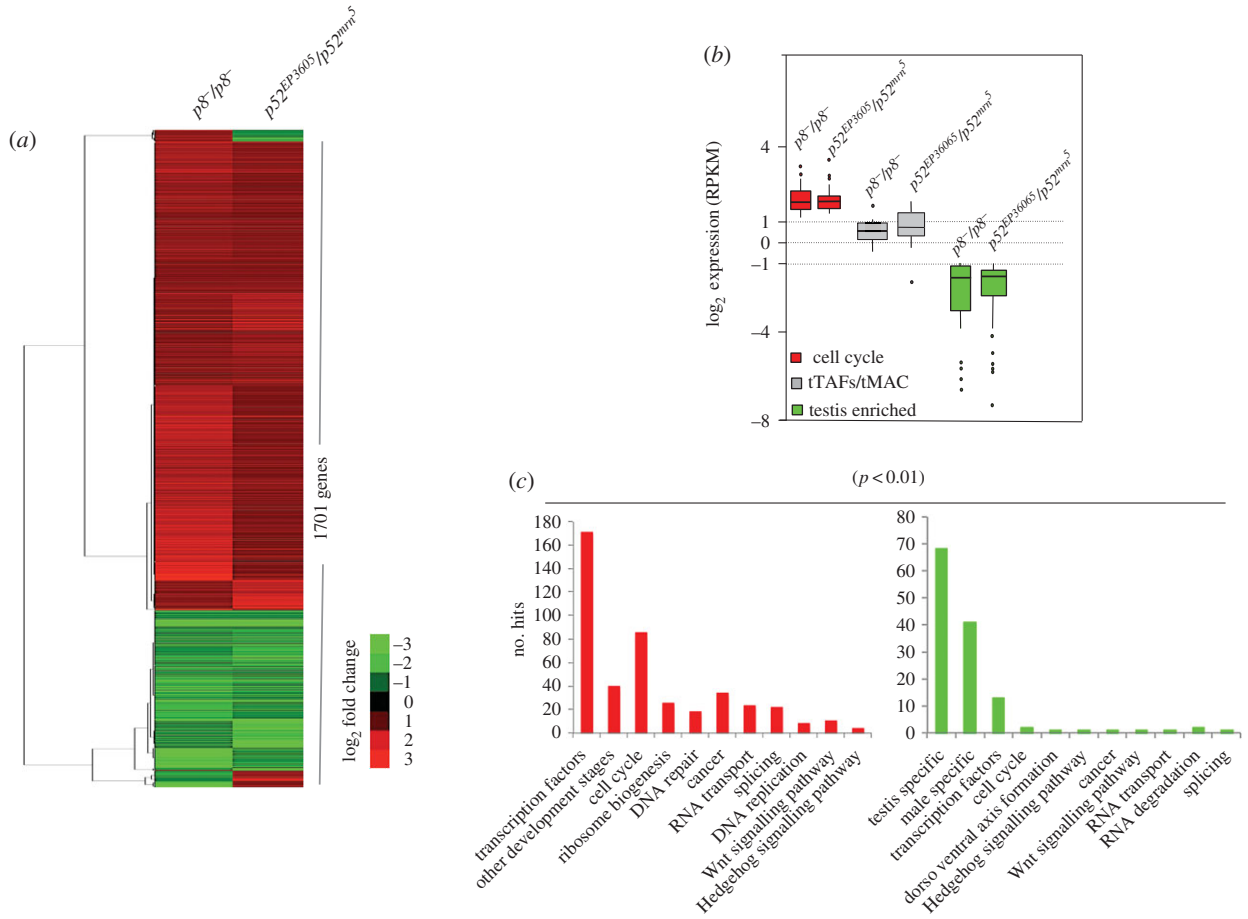

Figure 4. Global gene expression analyses in the *p8* and *p52* mutant testes. (*a*) Heat map of the DEGs with significant $\log_2$-fold change ($p < 0.01$) when compared with wild-type testes, shared between the $p8^{-}/p8^{-}$ and $p52^{EP3605}/p52^{mrn5}$ testes. (*b*) The box plot shows groups of genes of interest that were upregulated (cell cycle involved genes; red boxes), genes whose expression did not significantly change (*tTAFs* and *tMAC* genes; grey boxes) and genes that were downregulated (testis-enriched genes; green boxes) in TFIIH mutant testes. (*c*) Gene ontology analysis of selected functions of DEGs common between the *p8* and *p52* mutant transcriptomes when compared with wild-type ($p < 0.01$). Upregulated (red bars) and downregulated (green bars) groups of genes are shown.

	% *sa*/TFIIH	% *aly*/TFIIH	% *Ubi-p63E*/TFIIH	% *Med22*/TFIIH	% *bam*/TFIIH
transcription	73 (122/166)	59 (99/166)	57 (95/166)	58 (97/166)	62 (103/166)
cell cycle	72 (59/81)	56 (46/81)	51 (42/81)	54 (44/81)	44 (36/81)
testis enriched	91 (64/70)	71 (50/70)	61 (43/70)	81 (57/70)	87 (61/70)

0 100%

Figure 5. Gene expression comparison among TFIIH, *sa*, *aly*, *Med22*, *Ubi-p63E* and *bam* mutants. The percentage of misregulated genes involved in transcription, cell cycle or testis-enriched genes shared between the TFIIH mutants and *sa*, *aly*, *Med22*, *Ubi-p63E* and *bam* mutants in the *Drosophila* testis is shown. The numbers in the parentheses correspond to the number of genes misregulated in the column-correspondent mutant and TFIIH mutants between the total genes misregulated in the TFIIH mutants for each group.

regulation that were upregulated and the testis-enriched genes that were downregulated in the TFIIH mutants.

In the case of the mRNAs that encode for transcription and chromatin remodelling factors, of the transcripts that increased in TFIIH mutants, 73% also increased in *sa*, 59% in *aly*, 57% in *Ubi-p63E*, 58% in *Med22* and 62% in *bam* mutant testes (figure 5). For transcripts that encode factors involved in cell cycle, of the mRNAs that are enriched in the TFIIH mutants, 72% are also increased in *sa*, 56% in *aly*, and 51%, 54% and 44% in *Ubi-p63E*, *Med22* and *bam* mutants, respectively (figure 5). When we compared the reduction in the transcript levels from the testis-enriched genes in the TFIIH mutants, we found that 91%, 71%, 61%, 81% and 87% are also reduced in the *sa*, *aly*, *Ubi-p63E*, *Med22* and *bam* mutants, respectively (figure 5). This analysis suggests that the transcriptome of the TFIIH mutant testes is more similar to the *sa* mutant and less similar to the *aly*, *Med22* and *Ubi-p63E* mutants, which also generate a meiotic arrest phenotype and accumulate primary spermatocytes. The transcriptome of the *bam* mutant that arrests spermatogenesis at the spermatogonial stage is more similar in the effect on the expression of transcription factors and differentiation genes to the TFIIH mutants than the *aly*,

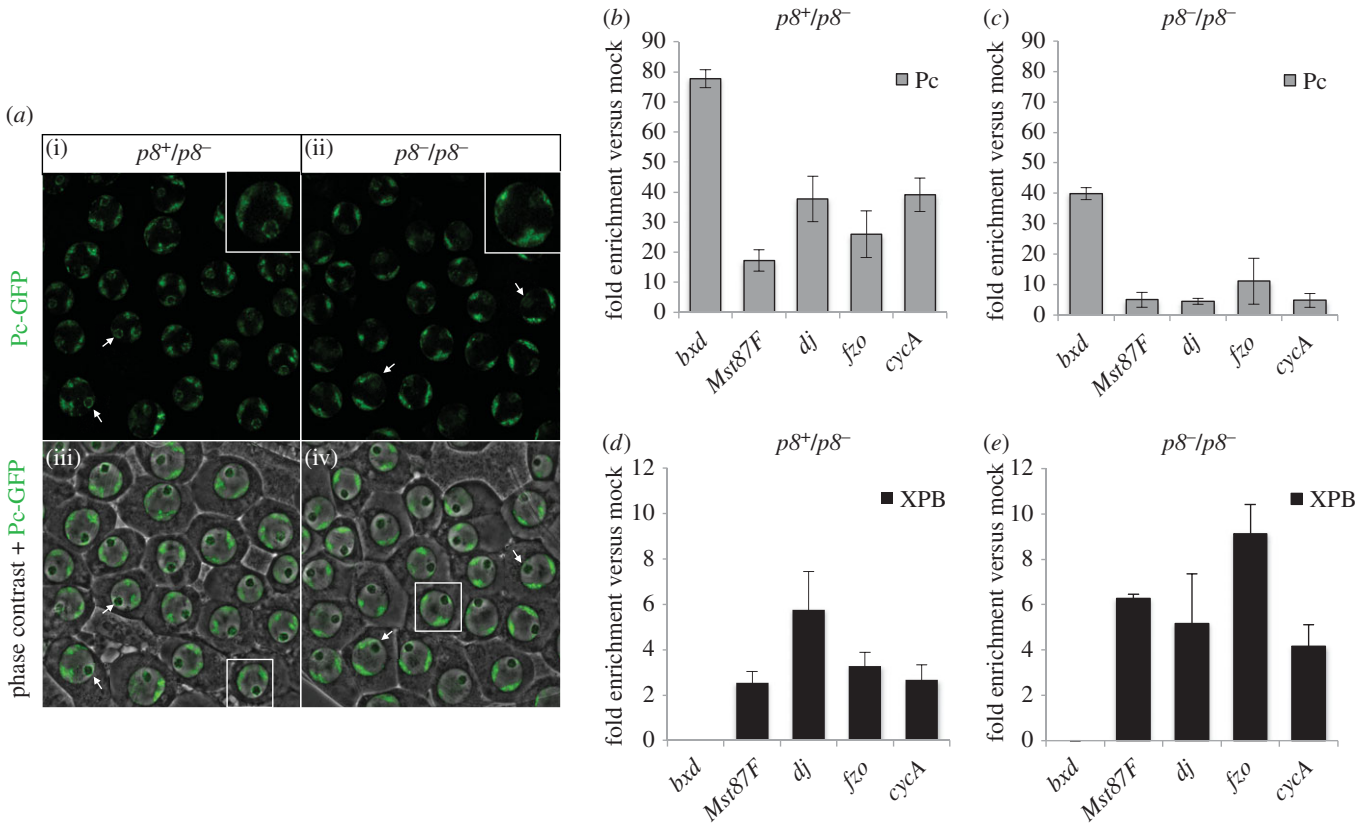

Figure 6. Pc is delocalized from the nucleolus in *p8* mutant testes, but does not occupy the spermatid differentiation gene promoters. (*a*) Confocal microscopy images from heterozygous ($p8^{+}/p8^{-}$) and homozygous ($p8^{-}/p8^{-}$) *p8* mutant unfixed testes show the location of Pc-GFP in mature primary spermatocytes. In $p8^{+}/p8^{-}$ testes ((i) and (iii)), Pc is located in the bivalent chromosomes and the nucleolus periphery in primary spermatocytes. By contrast, in $p8^{-}/p8^{-}$ testes ((ii) and (iv)), Pc is highly reduced from the nucleolus periphery in the primary spermatocytes. The arrows indicate the nucleolus in some cells. (*b–e*) qPCR from ChIP assays show the occupancy of (*b*,*c*) Pc and (*d*,*e*) XPB at the promoters of several spermatid differentiation genes in heterozygous ($p8^{+}/p8^{-}$) and homozygous ($p8^{-}/p8^{-}$) *p8* mutant testes. No Pc signal higher than background levels is observed in the analysed region of the promoters of *dj*, *Mst87F* and *fzo* in control or ($p8^{-}/p8^{-}$) testes. The *bxd* element was used as positive control and negative control for Pc and XPB binding, respectively. The *CycA* promoter is a non-target control for Pc binding. The percentage input enrichment for Pc and XPB in the analysed promoters was normalized to the mock signal detected for each sequence. Each bar shows the average and standard deviation from three biological replicates in (*b–d*) and two biological replicates for (*e*).

Ubi-p63E and *Med22* meiotic arrest mutants (figure 5). The strong effect on differentiation genes in the *bam* mutant is expected, since these genes are only expressed in primary spermatocytes and the *bam* mutant germ cells fail to enter this stage. On the other hand, defects in TFIIH functions may have a more general effect in gene expression than the *aly*, *Med22* and *Ubi-p63E* mutants, something that may be expected for a basal transcription factor. In summary, the TFIIH mutants displayed gene expression misregulation during spermatogenesis, which partially resemble a testis-specific TAF mutant (the *sa* mutant), suggesting that the disturbance of transcription at different levels may generate a meiotic arrest phenotype during spermatogenesis.

3.6. TFIIH mutant causes Pc delocalization from the nucleolus in primary spermatocytes, but not Pc-enhanced enrichment at differentiation gene promoters

The current model for transcription regulation in the testis establishes that spermatogenesis genes are repressed by Pc in germ cell precursors until the expression of tTAFs in the nucleolus of the primary spermatocytes [20,21]. As mutants in *tTAFs* genes show de-localization of Pc from the nucleolus in primary spermatocytes, it has been proposed that part of the tTAFs mechanism of action is to sequester Pc in the nucleolus to allow the expression of the genes involved in spermatogenesis [20]. The meiotic arrest phenotype observed in TFIIH mutant testes (figure 1) and the localization of TFIIH components in the nucleolus periphery of primary spermatocytes (figure 2) prompted us to investigate whether the recruitment of Pc to the nucleolus depends on this basal transcription factor. Therefore, using the Pc-GFP transgenic fly reported previously [20,22,44], we analysed Pc localization in control ($p8^{+}/p8^{-}$) and $p8^{-}/p8^{-}$ testes. Consistent with previous reports [22,44], confocal microscopy of live squashed testes showed Pc location at bivalent chromosomes and the nucleolar periphery in control primary spermatocytes (figure 6*a*(i),(iii)). By contrast, although localization in the bivalent chromosomes was unaffected, Pc was highly reduced in the nucleolar periphery of $p8^{-}/p8^{-}$ primary spermatocytes (figure 6*a*(ii),(iv)). This suggests that irregular Pc localization is a common feature among tTAFs and general transcription factors mutants with meiotic arrest phenotypes.

The next aim was to determine whether the repression of the affected differentiation genes relied on Pc binding to their promoters in the TFIIH mutant testes. We performed ChIP experiments, followed by qPCR, to analyse the binding of Pc

and the TFIIH subunit XPB at the promoters of two repressed genes (*dj* and *Mst87F*) and one unaffected gene (*fzo*) in $p8^{-}/p8^{-}$ testes. Additionally, positive (a known target sequence in the *bxd* long non-coding RNA) and negative (the *CycA* promoter) controls for Pc binding were included in our analyses. As expected, high Pc enrichment was detected at its known canonical target (*bxd*) in both $p8^{+}/p8^{-}$ and $p8^{-}/p8^{-}$ testes (figure 6*b*,*c*). On the other hand, Pc levels in the promoters of *dj*, *Mst87F* and *fzo* were similar to the negative control (*CycA* promoter) in the $p8^{+}/p8^{-}$ and $p8^{-}/p8^{-}$ testes (figure 6*b*,*c*). Therefore, Pc dissociation from the nucleolar periphery had no effect on Pc binding to the promoters of these tTAFs target genes, which were repressed in $p8^{-}/p8^{-}$ testes. Moreover, we detected XPB occupancy at the promoter of *dj*, *fzo*, *Mst87F* and *CycA* in control ($p8^{+}/p8^{-}$) and $p8^{-}/p8^{-}$ testes, suggesting that TFIIH recruitment to the promoters of these genes was not affected (figure 6*d*,*e*). Taken together, these data indicate that the p8 subunit of TFIIH is required for Pc localization to the nucleolus in primary spermatocytes, but that Pc is not enriched at the promoters of the differentiation genes repressed in $p8^{-}/p8^{-}$ testes.

4. Discussion

4.1. The stability of TFIIH components in the *Drosophila* testis does not rely on p8 function, suggesting an unrevealed role for p8 in transcription

Intriguingly, to date, mutations affecting only the XPB, XPD and p8 subunits have been identified in human patients afflicted with XP, CS or TTD [10–13], suggesting that mutations in other TFIIH subunits in humans may be more deleterious, or are indistinguishable from the wild-type phenotype. We have previously reported that *p52* mutant heteroallelic combinations and p8 depletion are compatible with life in *Drosophila*, but cause male sterility [15,16]. In this study, we determined that *p52* mutant or p8-depleted organisms show a meiotic arrest phenotype during spermatogenesis. This phenotype was very similar between the two mutants, though more penetrating in p52-affected testes. Further analysis of the mutant testes revealed that *p52* mutants cause an important decrease in the levels of other TFIIH core subunits, including XPB and p8. Interestingly, physical interactions among XPB, p52 and p8 have been reported [45,46]. Furthermore, p52 modulates the ATPase activity of XPB and is required for anchoring this subunit into TFIIH [7], suggesting that when p52 is affected, XPB becomes unstable and more susceptible to degradation. Strikingly, the absence of p8 in the *Drosophila* testis has no effect on the levels of other TFIIH subunits. These data seem to be against the proposed role for p8 in maintaining TFIIH stability and in contrast to the observation of lower levels of the TFIIH subunits in human cells derived from patients, who suffer from TTD-A. However, the p8 mutations described in these patients seem not to be null, and it has recently been reported that they still may interact with TFIIH [14,34]. Thus, it is possible that these mutations may generate p8 proteins that have some toxic effect when they are assembled into TFIIH, generating instability in the complex. In comparison with our analysis in the p8-depleted organism, it has been reported that XPB levels in cells derived from p8 knock-out mice, which were measured by the expression of exogenous XPB-YFP, were reduced [34]. However, it is possible that if global transcription is affected in these p8-depleted cells the expression of the transgene also might be reduced since it has been observed that the expression of transgenes is preferentially affected in comparison with endogenous genes when the basal transcription machinery is not completely functional [47]. In fact, the RNA-seq analysis from these p8-depleted early mouse embryos showed that there is a significant effect on gene expression, in particular in genes required for terminal differentiation [34], which correlates with the deregulation of transcription that we observed in the p8-depleted testes, although normal levels of other TFIIH subunits were observed.

Intriguingly, we observed that XPB is still recruited to the promoter sequences and that the global level of CAK-mediated RNAPII-Ser_5P-CTD phosphorylation remains unaffected in p8-depleted testis. In agreement with these results, it has been recently reported that different mutations in p8 did not affect either the recruitment of TFIIH to promoters or the phosphorylation of the RNAPII-CTD in human cells [48]. Therefore, a more direct role for p8 in transcription should be considered. For instance, a possibility that might explain the effect on transcription by p8 depletion is that the interaction between p8 and p52 could be relevant for the regulatory role of p52 on XPB ATPase activity, which is required for transcription initiation by RNAPII. This is supported by recent evidence that shows that both p8 and p52 directly interact with XPB lock-N and lock-C domains [46]. Moreover, this correlates with our previous observations of enhanced transcription when p8 is added to *in vitro* transcription assays [49]. Thus, it will be relevant to analyse how XPB ATPase activity is affected by p8 and how this could affect promoter opening during transcription.

4.2. No Pc recruitment at spermatid differentiation gene promoters in TFIIH meiotic arrest mutants argues against the current model for transcription repression in testis

The cellular and molecular analyses of the meiotic arrest phenotype observed in the TFIIH mutant testes revealed some similarities with the main characteristics of *can* class meiotic arrest genes, though some differences can also be noted. For example, the expression of many spermatid differentiation genes, such as *Mst87F* and *dj*, were downregulated in TFIIH mutant testes, but other tTAFs targets, such as *fzo*, remained unaffected, suggesting that meiosis arrest in TFIIH primary spermatocytes was caused, at least in part, by the reduced expression levels of key spermatid differentiation gene products, some of which are common targets between tTAFs and TFIIH. Interestingly, we detected no difference in XPB recruitment at the promoters of some downregulated or unaffected spermatid differentiation genes in p8-depleted testes, suggesting that the downregulated genes identified in the TFIIH mutant testes transcriptomes represent targets that are more sensitive to TFIIH-reduced functions. Furthermore, contrary to the *aly* class but similar to the *can* class of meiotic arrest genes, the transcripts from many cell cycle regulators were not reduced in the TFIIH mutant testes. We also observed normal or even increased cyclin A and cyclin B protein levels in the TFIIH

mutant testes, suggesting that the meiosis arrest in these testes was not caused by the deficiency in these key cell cycle modulators.

Interestingly, TFIIH localization in bivalent chromosomes and at the periphery of the nucleolus at the primary spermatocyte stage is very similar to the localization observed for other transcription factors, including tTAFs [22], TAF1 [50], the mediator complex [19] and the elongating form of RNAPII [22], suggesting that these regions are permissive sites for transcription. However, no evidence of transcription was detected at the nucleolar periphery of primary spermatocytes in a previous study [22]. Intriguingly, the same localization pattern has been observed for the transcriptional repressor Polycomb [22,44]. In fact, it has been proposed that nucleolar Polycomb localization in primary spermatocytes is essential to counteract its repressor role in the transcription of several tTAFs targets genes [20,21]. Intriguingly, similar to the *tTAF*s mutants, we observed Pc dissociation from the nucleolus in p8-depleted primary spermatocytes. By contrast, we did not detect Pc binding higher than the background levels observed at the non-target gene (*CycA*), in the promoter of downregulated spermatid differentiation genes in p8-depleted testes. Thus, our results agree with a recent genome-wide analysis of Pc binding sites in whole *Drosophila* testes or germline precursors that suggests that Pc is not directly involved in the regulation of tTAFs target genes during spermatogenesis, as no Pc enrichment was detected at the promoters of these genes [22]. This is further supported by a previous study that showed that the *thoc5* meiotic arrest mutant, which shows nucleolar structure disruption and concomitant Pc delocalization from the nucleolus, showed normal *Mst87F*, *dj* and *fzo* transcript expression levels, suggesting that the perinucleolar localization of Pc is not required for the expression of these spermatid differentiation genes [41]. Therefore, the evidence suggests that mutants in any of the tTAFs or components of the basal transcription machinery cause a deregulation of gene expression in primary spermatocytes that could indirectly affect Pc localization from the periphery of the nucleolus without enhancing Pc recruitment at the promoters of spermatid differentiation genes. Thus, it would be relevant to determine whether Pc localization is also affected in mutants of the recently characterized *Med22* meiotic arrest gene [19], which is a component of the mediator complex.

In conclusion, this study provides important insights about the role of TFIIH in a cell differentiation programme and how a reduction in the activities of a basal transcription factor generates specific phenotypes.

Authors' contributions. M.Z. and G.C.-B. conceived and designed the experiments; G.C.-B. and M.J. performed the experiments; M.Z., G.C.-B. and V.V.-G. analysed the data and M.Z. and G.C.-B. wrote the paper.

Competing interests. We have no competing interest.

Funding. This work was supported by the grants from CONACyT 219673 and DGAPA UNAM number IN200315 to M.Z. G.C.-B. received a scholarship from CONACyT, as a student of the Programa de Doctorado en Ciencias Bioquímicas at the Universidad Nacional Autónoma de México and the Hugo Aréchiga Urtuzuástegui Fellowship from El Colegio de Sinaloa.

Acknowledgements. We thank Martha Vazquez for discussions during the development of this work. We also thank Arturo Pimentel, Andres Saralegui, Chris Wood and the LNMA for advice in the use of the confocal microscopes.

References

1. Zurita M, Merino C. 2003 The transcriptional complexity of the TFIIH complex. *Trends Genet.* **19**, 578–584. (doi:10.1016/j.tig.2003.08.005)
2. Compe E, Egly JM. 2012 TFIIH: when transcription met DNA repair. *Nat. Rev. Mol. Cell Biol.* **13**, 476. (doi:10.1038/nrm3377)
3. Egly JM, Coin F. 2011 A history of TFIIH: two decades of molecular biology on a pivotal transcription/repair factor. *DNA Repair* **10**, 714–721. (doi:10.1016/j.dnarep.2011.04.021)
4. Fishburn J, Tomko E, Galburt E, Hahn S. 2015 Double-stranded DNA translocase activity of transcription factor TFIIH and the mechanism of RNA polymerase II open complex formation. *Proc. Natl Acad. Sci. USA* **112**, 3961–3966. (doi:10.1073/pnas.1417709112)
5. Fisher RP. 2012 The CDK network: linking cycles of cell division and gene expression. *Genes Cancer* **3**, 731–738. (doi:10.1177/1947601912473308)
6. Tirode F, Busso D, Coin F, Egly JM. 1999 Reconstitution of the transcription factor TFIIH. *Mol. Cell* **3**, 87–95. (doi:10.1016/S1097-2765(00)80177-X)
7. Coin F, Oksenych V, Egly JM. 2007 Distinct roles for the XPB/p52 and XPD/p44 subcomplexes of TFIIH in damaged DNA opening during nucleotide excision repair. *Mol. Cell* **26**, 245–256. (doi:10.1016/j.molcel.2007.03.009)
8. Giglia-Mari G, Miquel C, Theil AF, Mari PO, Hoogstraten D, Ng JMY, Dinant C, Hoeijmakers JHJ, Vermeulen W. 2006 Dynamic interaction of TTDA with TFIIH is stabilized by nucleotide excision repair in living cells. *PLoS Biol.* **4**, 0952–0963. (doi:10.1371/journal.pbio.0040156)
9. Busso D, Keriel A, Sandrock B, Poterszman A, Gileadi O, Egly JM. 2000 Distinct regions of MAT1 regulate cdk7 kinase and TFIIH transcription activities. *J. Biol. Chem.* **275**, 22 815–22 823. (doi:10.1074/jbc.M002578200)
10. Giglia-Mari G *et al.* 2004 A new, tenth subunit of TFIIH is responsible for the DNA repair syndrome trichothiodystrophy group A. *Nat. Genet.* **36**, 714–719. (doi:10.1038/ng1387)
11. Egly JM. 2001 The 14th Datta Lecture TFIIH: from transcription to clinic. *FEBS Lett.* **498**, 124–128. (doi:10.1016/S0014-5793(01)02458-9)
12. Kraemer KH, Patronas NJ, Schiffmann R, Brooks BP, Tamura D, DiGiovanna JJ. 2007 Xeroderma pigmentosum, trichothiodystrophy and Cockayne syndrome: a complex genotype-phenotype relationship. *Neuroscience* **145**, 1388–1396. (doi:10.1016/j.neuroscience.2006.12.020)
13. Schärer OD. 2008 The molecular basis for different disease states caused by mutations in TFIIH and XPG. *DNA Repair* **7**, 339–344. (doi:10.1016/j.dnarep.2007.10.007)
14. Nonnekens J, Cabantous S, Slingerland J, Mari PO, Giglia-Mari G. 2013 *In vivo* interactions of TTDA mutant proteins within TFIIH. *J. Cell Sci.* **126**, 3278–3283. (doi:10.1242/jcs.126839)
15. Fregoso M, Lainé JP, Aguilar-Fuentes J, Mocquet V, Reynaud E, Coin F, Egly JM, Zurita M. 2007 DNA repair and transcriptional deficiencies caused by mutations in the *Drosophila* p52 subunit of TFIIH generate developmental defects and chromosome fragility. *Mol. Cell. Biol.* **27**, 3640–3650. (doi:10.1128/MCB.00030-07)
16. Herrera-Cruz M, Cruz G, Valadez-Graham V, Fregoso-Lomas M, Villicaña C, Vázquez M, Reynaud E, Zurita M. 2012 Physical and functional interactions between *Drosophila* homologue of Swc6/p18Hamlet subunit of the SWR1/SRCAP chromatin-remodeling complex with the DNA repair/transcription factor TFIIH. *J. Biol. Chem.* **287**, 33 567–33 580. (doi:10.1074/jbc.M112.383505)
17. Regan CL, Fuller MT. 1988 Interacting genes that affect microtubule function: the nc2 allele of the haywire locus fails to complement mutations in the testis-specific beta-tubulin gene of *Drosophila*. *Genes Dev.* **2**, 82–92. (doi:10.1101/gad.2.1.82)

18. White-Cooper H. 2010 Molecular mechanisms of gene regulation during *Drosophila* spermatogenesis. *Reproduction* **139**, 11–21. (doi:10.1530/REP-09-0083)
19. Lu C, Fuller MT. 2015 Recruitment of mediator complex by cell type and stage-specific factors required for tissue-specific TAF dependent gene activation in an adult stem cell lineage. *PLoS Genet.* **11**, e1005701. (doi:10.1371/journal.pgen.1005701)
20. Chen X, Hiller M, Sancak Y, Fuller MT. 2005 Tissue-specific TAFs counteract polycomb to turn on terminal differentiation. *Science* **310**, 869–872. (doi:10.1126/science.1118101)
21. Chen X, Lu C, Prado JRM, Eun SH, Fuller MT. 2011 Sequential changes at differentiation gene promoters as they become active in a stem cell lineage. *Development* **138**, 2441–2450. (doi:10.1242/jcs.093971)
22. El-Sharnouby S, Redhouse J, White RAH. 2013 Genome-wide and cell-specific epigenetic analysis challenges the role of polycomb in *Drosophila* spermatogenesis. *PLoS Genet.* **9**, e1003842. (doi:10.1371/journal.pgen.1003842)
23. Perezgasga L, Jiang J, Bolival B, Hiller M, Benson E, Fuller MT, White-Cooper H. 2004 Regulation of transcription of meiotic cell cycle and terminal differentiation genes by the testis-specific Zn-finger protein matotopetli. *Development* **131**, 1691–1702. (doi:10.1242/dev.01032)
24. Mukhopadhyay A, Deplancke B, Walhout AJM, Tissenbaum HA. 2008 Chromatin immunoprecipitation (ChIP) coupled to detection by quantitative real-time PCR to study transcription factor binding to DNA in *Caenorhabditis elegans*. *Nat. Protoc.* **3**, 698–709. (doi:10.1038/nprot.2008.38)
25. Lin X, Tirichine L, Bowler C. 2012 Protocol: chromatin immunoprecipitation (ChIP) methodology to investigate histone modifications in two model diatom species. *Plant Methods* **8**, 48. (doi:10.1186/1746-4811-8-48)
26. Mortazavi A, Williams BA, McCue K, Schaeffer L, Wold B. 2008 Mapping and quantifying mammalian transcriptomes by RNA-Seq. *Nat. Methods* **5**, 621–628. (doi:10.1038/nmeth.1226)
27. Benjamini Y, Yekutieli D. 2001 The control of the false discovery rate in multiple testing under dependency. *Ann. Stat.* **29**, 1165–1188. (doi:10.1214/aos/1013699998)
28. Doggett K, Jiang J, Aleti G, White-Cooper H. 2011 Wake-up-call, a lin-52 paralogue, and always early, a lin-9 homologue physically interact, but have opposing functions in regulating testis-specific gene expression. *Dev. Biol.* **355**, 381–393. (doi:10.1016/j.ydbio.2011.04.030)
29. Lu C, Kim J, Fuller MT. 2013 The polyubiquitin gene Ubi-p63E is essential for male meiotic cell cycle progression and germ cell differentiation in *Drosophila*. *Development* **140**, 3522–3531. (doi:10.1242/dev.098947)
30. Gan Q, Chepelev I, Wei G, Tarayrah L, Cui K, Zhao K, Chen X. 2010 Dynamic regulation of alternative splicing and chromatin structure in *Drosophila* gonads revealed by RNA-seq. *Cell Res.* **20**, 763–783. (doi:10.1038/cr.2010.64)
31. Merino C, Reynaud E, Vazquez M, Zurita M. 2002 DNA repair and transcriptional effects of mutations in TFIIH in *Drosophila* development. *Mol. Biol. Cell* **13**, 3246–3256. (doi:10.1091/mbc.E02-02-0087)
32. Jiang J, White-Cooper H. 2003 Transcriptional activation in *Drosophila* spermatogenesis involves the mutually dependent function of aly and a novel meiotic arrest gene cookie monster. *Development* **130**, 563–573. (doi:10.1242/dev.00246)
33. Jiang J, Benson E, Bausek N, Doggett K, White-Cooper H. 2007 Tombola, a tesmin/TSO1-family protein, regulates transcriptional activation in the *Drosophila* male germline and physically interacts with always early. *Development* **134**, 1549–1559. (doi:10.1242/dev.000521)
34. Theil AF *et al.* 2013 Disruption of TTDA results in complete nucleotide excision repair deficiency and embryonic lethality. *PLoS Genet.* **9**, e1003431. (doi:10.1371/journal.pgen.1003431)
35. White-Cooper H, Leroy D, MacQueen A, Fuller MT. 2000 Transcription of meiotic cell cycle and terminal differentiation genes depends on a conserved chromatin associated protein, whose nuclear localisation is regulated. *Development* **127**, 5463–5473.
36. Beall EL, Lewis PW, Bell M, Rocha M, Jones DL, Botchan MR. 2007 Discovery of tMAC: a *Drosophila* testis-specific meiotic arrest complex paralogous to Myb-Muv B. *Genes Dev.* **21**, 904–919. (doi:10.1101/gad.1516607)
37. Hiller MA, Lin TY, Wood C, Fuller MT. 2001 Developmental regulation of transcription by a tissue-specific TAF homolog. *Genes Dev.* **15**, 1021–1030. (doi:10.1101/gad.869101)
38. Hiller M *et al.* 2004 Testis-specific TAF homologs collaborate to control a tissue-specific transcription program. *Development* **131**, 5297–5308. (doi:10.1242/dev.01314)
39. White-Cooper H, Schäfer M, Alphey LS, Fuller MT. 1998 Transcriptional and post-transcriptional control mechanisms coordinate the onset of spermatid differentiation with meiosis I in *Drosophila*. *Development* **125**, 125–134.
40. Kwon SY, Xiao H, Wu C, Badenhorst P. 2009 Alternative splicing of NURF301 generates distinct NURF chromatin remodeling complexes with altered modified histone binding specificities. *PLoS Genet.* **5**, e1000574. (doi:10.1371/journal.pgen.1000574)
41. Moon S, Cho B, Min S, Lee D, Chung D. 2011 The THO complex is required for nucleolar integrity in *Drosophila* spermatocytes. *Development* **138**, 3835–3845. (doi:10.1242/dev.056945)
42. Caporilli S, Yu Y, Jiang J, White-Cooper H. 2013 The RNA export factor, Nxt1, Is required for tissue specific transcriptional regulation. *PLoS Genet.* **9**, e1003526. (doi:10.1371/journal.pgen.1003526)
43. Trost B, Moir CA, Gillespie ZE, Kusalik A, Mitchell JA, Eskiw CH. 2015 Concordance between RNA-sequencing data and DNA microarray data in transcriptome analysis of proliferative and quiescent fibroblasts. *R. Soc. open sci.* **2**, 150402. (doi:10.1098/rsos.150402)
44. Dietzel S, Niemann H, Brückner B, Maurange C, Paro R. 1999 The nuclear distribution of polycomb during *Drosophila melanogaster* development shown with a GFP fusion protein. *Chromosoma* **108**, 83–94. (doi:10.1007/s004120050355)
45. Kainov DE, Vitorino M, Cavarelli J, Poterszman A, Egly JM. 2008 Structural basis for group A trichothiodystrophy. *Nat. Struct. Mol. Biol.* **15**, 980–984. (doi:10.1038/nsmb.1478)
46. Luo J *et al.* 2015 Architecture of the human and yeast general transcription and DNA repair factor TFIIH. *Mol. Cell* **59**, 794–806. (doi:10.1016/j.molcel.2015.07.016)
47. Gutierrez L, Merino C, Vazquez M, Reynaud E, Zurita M. 2004 RNA polymerase II 140wimp mutant and mutations in the TFIIH subunit XPB differentially affect homeotic gene expression in *Drosophila*. *Genesis* **40**, 58–66. (doi:10.1002/gene.20066)
48. Singh A, Compe E, Le May N, Egly JM. 2015 TFIIH subunit alterations causing xeroderma pigmentosum and trichothiodystrophy specifically disturb several steps during transcription. *Am. J. Hum. Genet.* **96**, 194–207. (doi:10.1016/j.ajhg.2014.12.012)
49. Aguilar-Fuentes J, Fregoso M, Herrera M, Reynaud E, Braun C, Egly JM, Zurita M. 2008 p8/TTDA overexpression enhances UV-irradiation resistance and suppresses TFIIH Mutations in a *Drosophila* trichothiodystrophy model. *PLoS Genet.* **4**, e1000253. (doi:10.1371/journal.pgen.1000253)
50. Metcalf CE, Wassarman DA. 2007 Nucleolar colocalization of TAF1 and testis-specific TAFs during *Drosophila* spermatogenesis. *Dev. Dyn.* **236**, 2836–2843. (doi:10.1002/dvdy.21294)

Mitotic bookmarking by TFIIH during zygotic genome activation in *Drosophila* suggests the existence of a short-term transcriptional memory mechanism

Grisel Cruz-Becerra, Mandy Juárez, Saraí Valerio-Cabrera and Mario Zurita*.

Departamento de Genética del Desarrollo y Fisiología Molecular, Instituto de Biotecnología. Universidad Nacional Autónoma de México. Av. Universidad 2001, Cuernavaca Morelos 62250, México.

*Correspondence to: marioz@ibt.unam.mx

Zygotic Genome Activation (ZGA) allows development to proceed by transcribing the embryo genome. In *Drosophila,* ZGA takes place at the pre-blastoderm embryo during a phase of rapid mitotic divisions. How the transcription machinery is coordinated to achieve this goal in a very short time span is still poorly understood. TFIIH is a component of the basal transcription machinery that is fundamental for transcription initiation by RNA polymerase II (RNAPII). Here, we show for the first time the *in vivo* dynamics of TFIIH components at the onset of transcription in the early *Drosophila* embryo. Interestingly, TFIIH shows a highly oscillatory behaviour between the nucleus and cytoplasm in the pre-Mid-Blastula-Transition (pre-MBT) embryo. From interphase to early metaphase, TFIIH foci are observed, and at prophase, these foci co-localize with the serine-5-phosphorylated form of RNAPII (RNAPII-S5P), suggesting that transcription overlaps with the first mitotic phases in this embryonic stage. Intriguingly, TFIIH, as well as TBP and the RNAPII, remain associated with mitotic chromatin, enriched at the promoters of the histone genes, acting as possible bookmarks for the fast activation of transcription after mitosis in the pre-blastoderm and syncytial blastoderm embryo. Furthermore, we found an essential role for TFIIH core subunits during mitosis in the pre-blastoderm embryo, as mutant organisms show several mitotic phenotypes, including free centrosomes, multipolar spindles and uncompacted DNA. Intriguingly, the RNAPII-S5P was detected at the wild type level in these embryos; thus, a direct role for the core of TFIIH in mitosis cannot be ruled out. However, the transcriptome analysis of these embryos shows transcriptional deficiencies of maternal genes that participate in mitosis in the early embryo. These results provide important insights regarding the role of one of the components of the basal transcription machinery at the pre-MBT, when the zygotic genome is activated in the embryo.

Introduction

In many organisms, the initial stages of embryonic development are directed by the action of maternal products deposited in the egg during oogenesis. Maternal mRNAs encoding factors that are required for the first developmental stages are eventually degraded; simultaneously, the expression of the zygotic genes takes place in transcriptional waves (Zurita et al., 2008; Lee et al., 2014). In *Drosophila,* after fertilization, the embryo is a syncytium in which the nucleus undergoes a series of rapid synchronized mitotic divisions, consisting of S-M phases only, with little or no transcription (Mazumdar and Mazumdar, 2002). At nuclear division eight, the first expression wave of zygotic genes is observed at the pre-Mid-Blastula-Transition (pre-MBT) (Lu et al., 2009). Nonetheless, it has been recently suggested that the transcription of some zygotic genes could be detected as early as the second nuclear division (All-Murthy et al., 2013). After division 10, nuclear division cycles slow down and by division 14 the expression of most of the zygotic genome is activated at the Mid-Blastula-Transition (MBT; Farrell and O'Farrell, 2014).

In *Drosophila*, Zygotic Genome Activation (ZGA) is at least mediated by the transcription factor vielfälting/zelda (Staudt et al., 2006; Li et al., 2014) in coordination with components of the basal transcription machinery that must be recruited at the promoters of the genes expressed either at the pre-MBT or at the MBT (Satija and Bradley, 2012). At pre-MBT approximately 100 genes have been reported to be expressed (Lott et al., 2011) and a recent study showed that during the pre-MBT stages, RNAPII is detected on the promoters of 117 genes, in most of them without pausing, probably because these genes should be transcribed in a very short time span (Chen et al., 2013). Therefore, the analysis of the dynamic of factors that activate transcription is fundamental to understand the mechanism of ZGA.

A central component of the basal transcription machinery is TFIIH, a multi protein complex constituted of the core (composed of the XPB, XPD, p62, p52, p44, p34 and p8 subunits) and CAK (composed of the Cdk7, CycH and MAT1 subunits) sub-complexes. The core and CAK form the holo-TFIIH complex, which participates in transcription by RNAPII (Zurita and Merino, 2003; Compe and Egly, 2012). The XPB and XPD subunits are DNA helicases/ATPases, while XPB is also a DNA translocase required for transcription initiation (Egly and Coin, 2011; Fishburn et al., 2015). Additionally, serine 5

and 7 phosphorylation of the Carboxi-Terminal Domain (CTD) of the largest subunit of RNA polymerase II (RNAPII) by Cdk7 is required for RNAPII promoter escape and recruitment of mRNA modification and processing factors during transcription elongation (Hsin and Manley, 2012). In addition, the core of TFIIH participates in the DNA repair mechanism of Nucleotide Excision Repair (Coin et al., 2007), while the CAK participates cell cycle control as the main activating kinase for the cyclin-dependent kinase complexes (Reviewed in Schachter and Fisher, 2013).

Furthermore, a transitory complex between the CAK and the XPD subunit can also be isolated (Aguilar-Fuentes et al., 2006; Abdulrahman et al., 2013). In accordance with this interaction, it has been reported that XPD regulates Cdk7 localization and negatively modulates its function in cell cycle regulation in the *Drosophila* embryo (Chen et al., 2003; Li et al., 2010). However, it has been demonstrated in human cells, that XPD is a component of the MMXD complex involved in chromosome segregation; thus, XPD depletion produces catastrophic mitosis (Ito et al., 2010). Furthermore, in *Drosophila*, XPD physically and genetically interacts with Galla, the fly homologue of one component of the human MMXD complex, which also causes catastrophic mitosis when defective in early embryo nuclear divisions (Yeom et al., 2014).

Therefore, the general transcription factor TFIIH is involved in three fundamental cellular processes: transcription, DNA repair and cell cycle regulation. Although several studies have concentrated efforts on the analysis of TFIIH functions *in vitro* and *in vivo*, there remain fundamental questions that have to be answered, for instance, whether other subunits of the core of TFIIH are also involved in mitosis, whether all the TFIIH subunits have the same dynamics during early embryo development and how they participate in zygotic gene activation. In this work, we have addressed these questions by analysing the functions and *in vivo* dynamics of the core subunits of TFIIH during early mitotic division cycles in the fly embryo as well as the effect of the absence of TFIIH components at the syncytial blastoderm stage.

Results

TFIIH shows highly dynamic behaviour at the onset of transcription in the syncytial blastoderm.

We have previously reported the localization of the XPB, XPD, Cdk7 and MAT1 subunits of TFIIH during early *Drosophila* embryo development (Aguilar-Fuentes et al., 2006). By using immunostaining, we showed that during the pre-blastoderm stage, at interphase, XPB and XPD are preferentially cytoplasmic; however, after nuclear division 10, when ZGA had already taken place, some of the XPB and XPD signals were detected inside the nucleus, while most of the Cdk7 and MAT1 remain cytoplasmic at these stages, although Chromatin ImmunoPrecipitation (ChIP) experiments indicated that core and CAK are enriched in some promoters at the time of transcription onset (Aguilar-Fuentes et al., 2006). In contrast, a recent report showed by using a different protocol for embryo immunostaining preparation that Cdk7 was better visualized in the nucleus at interphases 13 and 14 (Li et al., 2013).

Based on this information, we decided to refine our previous analysis on TFIIH dynamics during early embryo development and determine, for the first time, the *in vivo* dynamics of TFIIH during the fast mitotic cycles at the pre-MBT stages using immunostaining and tagged fluorescent proteins.

p8 is the smallest TFIIH subunit; although it does have not enzymatic activity, it has been proposed that p8 plays an important role in TFIIH steady-state level maintenance in human fibroblasts, although recent results from our group suggest that it is not the case (Vermeulen et al., 2000; Giglia-Mari et al., 2004; Cruz-Becerra et al., 2016). Initially, we studied the dynamics of this protein by the time of ZGA during *Drosophila* embryo development. By immunostainings we found that at interphase of mitotic cycle 10, p8 is mostly nuclear and co-localizes with chromosomes (Figure 1A). Intriguingly, at metaphase, this co-localization is still observed, but most of p8 is apparently surrounding the chromosomes (Figures 1B, C). However, p8 does not co-localize with the nuclear envelope (which is not completely de-assembled during syncytial blastoderm mitosis (Foe and Alberts, 1983) as determined using anti-Lamin antibody staining (Figure 1D), indicating that at metaphase, most p8 is maintained inside the nuclear lumen. To better characterize p8 during metaphase, we visualized p8, DNA and tubulin (to observe the mitotic spindle),

confirming that p8 partially co-localizes with chromosomes in metaphase and also with the mitotic spindle (Figure 1E). In addition, at anaphase, p8 is still clearly visualized on the chromosomes (Figure 1F). This localization of p8 during mitosis was not observed before for any TFIIH subunit, suggesting that p8 could have a different dynamic than other TFIIH components.

In the context of TFIIH, p8 physically interacts with p52 and it has been reported that this interaction is important for the TFIIH functions (Kainov et al., 2008). Therefore, we decided to analyse whether the dynamic of p52 is similar to p8 during the syncytial blastoderm mitotic cycles. Although we have several anti-p52 antibodies that are very specific in western blot (Villicaña et al., 2013), none of them work well for immunostaining. Therefore, we decided to generate transgenic flies expressing a recombinant protein of p52 and the Enhanced Yellow Fluorescent Protein (EYFP). We have previously reported that this EYFP-p52 construct is able to rescue several lethal alleles of *p52* (Cruz-Becerra et al., 2016), suggesting that this fusion protein is functional. Furthermore, this result makes us confident that the dynamics of this protein seen *in vivo* are similar to wild type. To visualize the different phases of the mitotic cycle through chromatin dynamics, we took advantage of the previously reported histone H2Av fused to the Red Fluorescent Protein (H2Av-RFP) transgenic line (Schuh et al., 2007). Figure 2A (also see supplementary Movie 1 and Supp. Figure 1) shows an embryo expressing EYFP-p52 as well as H2Av-RFP; at interphase of cycle 11 although some signal is observed in the cytoplasm most EYFP-p52 co-localizes with the chromosomes and intriguingly, EYFP-p52 nuclear foci are clearly observed, (Figure 2A; Supp. Movie 1). During early prophase, EYFP-p52 signal is reduced in the cytoplasm and enriched in the nucleus. Furthermore, EYFP-p52 nuclear foci are increased (in general, 2 to 4 foci per nucleus can be observed) and are more evident at late prophase (Figure 2A; Supp. Movie 1). The nuclear signal of EYFP-p52 is reduced but surrounds chromosomes during metaphase and co-localizes with the chromosomes at anaphase. At telophase, nuclear EYFP-p52 is significantly decreased, however some EYFP-p52 co-localization with the chromosomes is always detected (Figure 2A; Supp. Movie 1; Supp. Figure 1).

The dynamic behaviour observed *in vivo* for EYFP-p52 was similar to the unexpected localization of p8 observed by immunostaining (Figure 1) during the early

embryo mitotic cycles, suggesting that these proteins follow the same dynamics at this stage of development. To confirm these results, we next analysed the dynamics of p8 *in vivo* by using transgenic flies that express a recombinant protein of p8 and the Enhanced Cyan Fluorescent Protein (ECFP). We successfully tested the p8-ECFP recombinant protein functionality by performing rescue experiments on a p8 null background (Cruz-Becerra et al., 2016). To directly compare the *in vivo* dynamics of p8 and p52, we generated flies that simultaneously expressed EYFP-p52 and p8-ECFP. Figure 2B (See also Supp. Movie 2) shows the time-lapse sequence of one mitotic cycle in an early syncytial blastoderm embryo expressing both transgenes. We observed that these proteins co-localize at all the nuclear division stages following identical highly dynamic oscillations between the nucleus and the cytoplasm. In particular, the chromosomal localization of p52 and p8 during mitosis, which has never been described before for these TFIIH subunits in any organism, was intriguing.

The p52 subunit of TFIIH is essential for XPB anchorage to the complex (Jawhari et al., 2002); in addition, its role in modulating the ATPase activity of XPB has been extensively documented (Coin et al., 2007; Fregoso et al., 2007). Then, we reasoned that if the core of TFIIH is assembled during mitosis, XPB could follow a similar behaviour as p8 and p52. In our previous studies, using an antibody against XPB, we observed the exclusion of this protein from mitotic chromosomes in gastrulated embryos (Aguilar-Fuentes et al., 2006); however, we did not analyse the localization of this protein on mitotic chromatin in the syncytial blastoderm embryo. At this point, we considered the possibility of having lost valuable information about the XPB dynamics during mitosis; therefore, we decided to analyse, as was done for p8 and p52, the *in vivo* dynamics of fluorescently tagged XPB in the syncytial blastoderm embryo. XPB-EGFP or XPB-mCherry recombinant proteins follow similar dynamics as p8 and p52 along the mitotic cycle (Supp. Movie 3 and Supp. Figure 2). Therefore, these *in vivo* results indicate that some of the core subunits of TFIIH are retained in the nuclear lumen and co-localizes with the chromosomes during mitosis.

As mentioned before, the holo-TFIIH complex (composed of the core and CAK) is required for transcription by RNAPII. Considering that ZGA takes place during the pre-MBT stages, we expected to observe core and CAK co-localization in transcriptionally active nuclei in pre-blastoderm and syncytial blastoderm embryos (e.g., at the interphase of

nuclear cycle 8 and onwards). Interestingly, we noted that the TFIIH core subunits co-localize with chromosomes during mitosis in early syncytial blastoderm embryos (Figures 1 and 2). Thus, we considered the possibility of CAK localization on mitotic chromosomes. To answer this question, we tested several antibodies against Cdk7, Mat1 and CycH for immunostaining in wild type embryos (data not shown; Supp. Figure 3). Intriguingly, CycH, one CAK component for which localization has not been analysed in the early fly embryo, shows exactly the same dynamics observed for the core components of TFIIH. As expected, some CycH is detected in the cytoplasm, in addition, CycH co-localizes with chromosomes during mitosis (Supp. Figure 3). Furthermore, we constructed flies that express a recombinant protein Cdk7-EGFP which show exactly the same dynamics as the core subunits TFIIH (Supp. Movie 4). Altogether these data indicate that both core and CAK remain nuclear during mitotic divisions and co-localizes with the mitotic chromosomes at the pre-MBT stages in wild type embryos.

TFIIH foci are present in most of the syncytial blastoderm mitotic cycle and co-localize with active transcriptional foci.

As indicated before, EYFP-p52 was observed in granular structures in the nuclei of syncytial blastoderm embryos. These nuclear foci can also be visualized in the *mCherry-XPB* or *EGFP-XPB* transgenic embryos (Supp. Movie 3 and data no shown). Interestingly, these EYFP-p52 foci do not co-localize with the highest chromatin compaction, (indicated by the low intensity of the H2Av-RFP nuclear signal in these regions) (Figure 3A, C), suggesting that transcription could be taking place in these foci. Furthermore, in syncytial blastoderm nuclei, the serine 5 phosphorylated form of RNAPII is enriched in two foci (Chen et al., 2013), which could correspond to the Histone Locus Bodies (HLBs) (Salzler et al., 2013) in which histone genes are transcribed during the Pre-MBT (Nizami et al., 2010). Thus, these foci could be sites of TFIIH enrichment. Furthermore, in the case of TFIIH, we observed 3 or 4 foci in some nuclei (Figure 3A; Supp. Movie 1 and Supp. Movie 3). Interestingly, during the pre-MBT stages, the transcription by RNA polymerase I (RNAPI) of rRNA genes (which as the histone genes are organized in several tandem repeats; Seydoux and Dunn, 1997) also requires TFIIH. Thus, the detection of two to four TFIIH foci in the pre-MBT embryos suggested the presence of regions where TFIIH could be

recruited to activate transcription by RNAPI (for the rRNA genes) and RNAPII (for the histone genes). Therefore, by following the dynamics of TFIIH foci in time-lapse experiments, we could visualize the time and sites of gene expression in the Pre-MBT. To support this idea, we performed immunostaining on EYFP-p52 early syncytial blastoderm embryos using an antibody against the serine 5 phosphorylated form of RNAPII. As expected, we observed that the active RNAPII co-localizes with some of the EYFP-p52 foci (Figure 3B), suggesting that these nuclear structures are sites where the basal transcription machinery is recruited for the zygotic transcription of pre-MBT genes. Interestingly, we were able to follow the presence of the same foci from interphase to late metaphase in mitotic nuclei of syncytial blastoderm embryos (arrows at Figure 3C). Although it is known that histone genes are highly transcribed at the S phase (Guglielmi et al., 2013), our data show that these TFIIH foci are maintained when mitosis has been initiated, suggesting that transcription might overlap with the first stages of mitosis at the pre-MBT.

The basal transcription machinery is bound to mitotic chromatin at the pre-MBT.

The co-localization of TFIIH with chromosomes along the fast mitotic cycles in the early embryo in which transcription has to be attempted in a very short span of time suggests that other components of the basal transcription machinery could be retained in the mitotic chromatin to ensure the rapid activation of transcription after mitosis at the pre-MBT stages. Figure 4A shows that, as expected at interphase, TBP and RNAPII are also enriched in two foci, in which RNAPII is phosphorylated at serine 5. Importantly, while most RNAPII and TBP are surrounding the DNA, some signal was co-localized with metaphase chromosomes (Figure 4A). However, at anaphase, although RNAPII co-localization with chromosomes is observed, RNAPII is not phosphorylated at serine 5 and TBP is homogeneously distributed through the nucleus and cytoplasm (Figure 4A). It is intriguing that a fraction of TFIIH, RNAPII and TBP does not exit the nuclear lumen during mitosis, suggesting the possibility that these factors are still bound to chromatin, probably at the promoter of genes that are transcribed during the pre-MBT ready to activate transcription in the next cycle or randomly maintained on chromatin, as a consequence of the fast division cycles at these developmental stages, which may facilitate the activation of transcription in a short time span.

The activation of transcription of the histone gene cluster during the pre-MBT in *Drosophila* has been well documented (Günesdogan et al., 2014). The transcription of histone genes, with the exception of H1, depends on TATA box promoters and TBP binding. Indeed, HLBs are sites of TBP and RNAPII enrichment (Isogai et al., 2007; Guglielmi et al., 2013). Importantly, HLBs has been observed from interphase until metaphase (Isogai et al., 2007), as we observed for TFIIH foci (Figure 3C). Thus, we decided to determine by ChIP experiments whether the basal transcription machinery was associated with chromatin during mitosis in early embryos. We collected wild type embryos in pre-MBT stages (nuclear cycles 8-11) at interphase or arrested at metaphase by colchicine treatment (Figure 4B, left) to perform ChIP experiments against the RNAPII, TBP and the XPB subunit of TFIIH. We next analysed the presence of these proteins in the promoters of actively transcribed genes (i.e., the histone H3 and H4 promoters) and multi copy DNAs that are not transcribed (the rover retro-transposon element and the THARE sequence) at the pre-MBT. Figure 4B shows that TBP, the RNAPII and TFIIH (XPB) occupy the H3 and H4 promoters in chromatin from embryos at interphase, as well as in the embryos in mitosis. Occupancy of XPB and RNAPII can be identified in the rover element in interphasic and metaphase chromosomes for XPB, but not in the THARE element (Figure 4B, right). These results show that during the fast and synchronized nuclear divisions, components of the basal transcription machinery remain bound at different sequences in the chromatin during mitosis, including the histone promoters, suggesting a mechanism of short term transcriptional memory or bookmarking that operates during the pre-MBT to rapidly activate transcription at the next nuclear division cycle. It will be relevant in future investigations to determine where, at the genomic level, TFIIH and RNAPII remain bound to chromosomes in mitosis.

Essential role of TFIIH for proper mitosis in the pre-MBT stages.

Next we analysed the effect on the syncytial blastoderm embryo of the absence of TFIIH subunits. The CAK sub-complex of TFIIH has an important role in the control of the cell cycle (reviewed in Schachter and Fisher, 2013). Mutations in Cdk7 indeed affect the correct modulation of mitosis (Larochelle et al., 2007). Furthermore, it has been reported that the depletion of XPD in *Drosophila* embryos causes mitotic defects by inducing Cdk7

localization on mitotic chromosomes. Nonetheless, a TFIIH-independent role for the XPD core subunit in chromosome segregation during mitosis has been suggested (Ito et al., 2010). However, whether core subunits of TFIIH other than XPD participate in mitosis remains an open question.

We have recently characterized a *p8* null allele that shows semi-lethality, as approximately 25% of the expected homozygous organisms develop into adults. Of these adults, the males are sterile and the females lay fewer eggs than wild type (Herrera-Cruz et al., 2012). Importantly, the embryos laid by homozygote *p8* null females do not have maternally deposited *p8* and are thus an excellent tool to analyse the phenotypes produced by the absence of *p8* in the early embryo. As we show in Figure 5A, in homozygous *p8 null* females, although oogenesis can be completed, in some organisms, the egg chambers and the laid eggs are smaller than wild type; this reduction in size suggests transcriptional deficiencies during oogenesis, as we have previously observed in other organs for mutants affecting TFIIH (Fregoso et al., 2007; Villicaña et al., 2013). We next analysed the effect of the absence of p8 in early syncytial blastoderm embryos, when the embryo is mainly committed to nuclear division cycles. By staining microtubules and chromosomes in *p8* null embryos, we observed mitotic defects after nuclear division cycle 8 (Figure 5C, D, E; Supp. Figure 4). The population of *p8* null embryos exhibiting mitotic defects can be classified as moderately severe (middle panel) and severe (lower panel) phenotypes (Figure Supp. 4). In *p8* null embryos with the severe phenotype, the coordination of the mitotic waves is clearly affected (Supp. Figure 4). At metaphase, the spindle is misaligned and longer than in wild type organisms; furthermore, some metaphase chromosomes are under-compacted (Figure 5C) and isolated centrosomes as well as isolated chromosomes are observed (Figure 5C, D). During anaphase, in wild type embryos, the localization of histone H3 serine 10 phosphorylated (H3S10P) is restricted to the telomeric region of the chromosomes (Figure 5E), while in the *p8* null embryos the localization of this mitosis marker is maintained throughout the chromosome bodies, even at telophase (Figure 5E). All these defects in mitosis are supressed in *p8* null embryos expressing the p8-ECFP recombinant protein (data not shown).

Importantly, it has been suggested that human cells derived from TTDA patients showed reduced levels of all the other subunits of TFIIH (Vermeulen et al., 2000; Giglia-

Mari et al., 2004). However, we have recently reported that the absence of p8 in the *Drosophila* testis does not affect the levels of other TFIIH subunits (Cruz-Becerra et al., 2016). To determine if the catastrophic mitosis observed in syncytial blastoderm embryos lacking p8 could be an indirect effect of the deficiency of other subunits of TFIIH, we analysed the level of some core and CAK subunits in egg chambers and embryos from *p8 null* flies. Intriguingly, we do not find a significant reduction in the levels of the TFIIH components analysed, neither changes in the levels of other transcription factors or the phosphorylation of Serine 5 in the CTD of the RNAPII were detected (Figure 5B, F and see ahead). Therefore, the mitotic catastrophes observed in the *p8 null* embryos are due to the absence of p8, suggesting a possible role for p8 in mitotic modulation.

The following question of whether mutations in other TFIIH subunits, besides p8 and XPD, also affect mitosis in the early embryo emerged. To answer this point, we used the XPB (*haywire* in the fly) mutant allele hay^{nc2} (Mounkes et al., 1992). This allele is also semi-lethal and homozygous females can lay few fecundated eggs. When we observed these embryos, we also found defects in mitosis, including free centrosomes, incompletely compacted chromosomes at metaphase and isolated chromosomes not attached to the mitotic spindle (Figure 5G). XPB as well as p8 are components of the core of TFIIH, thus it was relevant to analyse if affection in the CAK also generates embryos with defects in the synchronized mitosis. To achieve this we constructed flies that express an RNAi against the Cdk7 transcript during oogenesis, therefore generating embryos with reduced levels of this CAK component (Supp. Figure 5A). We also observed embryos that present desynchronization in the mitotic cycles, aberrant mitotic spindles and isolated chromosomes (Supp. Figure 5B). In summary, affecting XPB and Cdk7 functions in the pre-MBT embryo causes similar defects in mitosis as the depletion of XPD (Li et al., 2013) or p8 (this paper). Therefore, mutations in the core and CAK subunits of TFIIH in the early fly embryo cause catastrophic mitosis.

Misregulation of the expression of maternal transcripts caused by the depletion of p8 correlates with the penetrance of mitotic defects in the early embryo.

In addition to the fundamental TFIIH activity on CTD-RNAPII serine 5 phosphorylation, TFIIH is also necessary to open the DNA template during transcription initiation (Kouzine

et al., 2013). Therefore, although in the *p8 null* ovaries and early embryos we observed wild type levels of RNAPII phosphorylated at serine 5 (Figure 5B and 5D), we were intrigued by the possibility that the mitotic phenotypes observed were caused by transcriptional defects during oogenesis or in the pre-MBT stages. To determine the effect of the absence of p8 on global transcription, we performed RNA-seq analysis of individual *p8 null* ($p8^{-}/p8^{-}$) and p8 heterozygous ($p8^{+}/p8^{-}$) embryos, which show mitotic defects and wild type phenotypes, respectively (Figure 6A). Using this strategy, we would be able to find out whether there is a deregulation of maternal mRNAs that contribute to mitosis in the embryo or in the genes expressed at the pre-MBT in p8-depleted embryos.

Embryos from *p8 null* or heterozygous females expressing the H2Av-RFP protein, to determine the nuclear division cycle and to observe the penetrance of the mitotic defects, were collected between the nuclear cycles 9-10. Then, total RNA from two heterozygous (G and H) and three *p8 null* (A, B and E) embryos (Figure 6A) was submitted to single embryo transcriptome analyses following the single cell protocol for RNA-seq. These analyses showed genome map rates higher than 90 % and identified nearly 8,000 different expressed transcripts per embryo (Supp. Tables 3-8).

The correlation analysis of the two control embryo samples indicates similar levels of most of the detected transcripts, although as expected for biological samples, some variability is observed (embryos H vs G; Figure 6B). In contrast, the comparison between the control (G and H) and *p8 null* embryos (A, B and E) shows a large variation in the levels of many transcripts (Figure 6B; Supp. Figure 6). The *p8 null* embryos A and B clearly show a more severe mitotic phenotype than embryo E, which shows less dramatic defects (Figure 6A). Interestingly, the global gene expression in embryo E was less affected (Figures 6B, C, D), indicating that there is a correlation between the severity in the mitotic defect phenotype and the degree of influence on global gene expression. We identified a group of 270 down regulated genes shared among all of our p8-depleted samples, suggesting that these genes are particularly sensitive to the transcriptional deregulation caused by the absence of p8 (Figure 6E). The RNA-seq data show that most of the deregulated transcripts in the *p8 null* embryos come from maternal contribution (data not shown), suggesting aberrant transcription during the oogenesis of *p8 null* females. In agreement with the embryo phenotypes, the ontology analysis of the affected transcripts

shows the down-regulation of genes that encode for factors that participate in DNA replication or during mitosis (Figure 6D). Taken together, these observations support that deregulation in gene expression during oogenesis generated by mutations in TFIIH cause catastrophic mitosis in the early syncytial blastoderm embryo.

Discussion.

Zygotic genome activation in the *Drosophila* embryo occurs in two waves, the first involves the transcription of a small group of genes at the pre-MBT and the second includes the transcription of an important fraction of the zygotic genome at MBT (Lee et al., 2014). At these stages, the dynamics followed by the basal transcription machinery, which have to attempt transcription in a very short time span, have been poorly studied. In *Drosophila,* there are only few reports by our group and others for some TFIIH subunits (Aguilar-Fuentes et al., 2006; Li et al., 2013), and some studies for the RNAPII and TBP dynamics (Seydoux and Dunn, 1997; Wanz and Lindquist, 1998). In this work, we have extended our analysis on the dynamics of TFIIH by immunostaining and *in vivo* studies using recombinant fluorescent proteins and found that TFIIH co-localizes with mitotic chromosomes during the nuclear division cycles in the early syncytial blastoderm, indeed TFIIH and other basal transcription factors remain bound to the histone promoters on mitotic chromatin possibly acting as bookmarks for rapid transcriptional activation in the early embryo nuclear cycles. In addition, we found that mutations in some TFIIH core subunits cause catastrophic mitosis during early embryo development, resulting at least in part from the deregulation of global transcription during oogenesis.

Dynamic behaviour of TFIIH in the *Drosophila* early syncytial blastoderm nuclear division cycles.

Several studies have been performed to observe the subcellular and molecular dynamics of TFIIH during transcription and the DNA damage response in interphasic cells (Giglia-Mari et al., 2006; Nonnekens et al., 2013). Nonetheless, the dynamic of the TFIIH components throughout the cell cycle progression has been less extensively studied. Importantly, although there is a previous study that showed the dynamics of the XPB core subunit *in vivo* in a mouse XPB-YFP knock in model, this report is focused on the comparison of the

mobility of the fluorescently tagged XPB in interphasic cells that have the capacity to proliferate and in post-mitotic non-proliferative cells. By using FRAP, Giglia-Mari and colleagues showed that XPB mobility was lower in post-mitotic differentiated cells, suggesting that after differentiation, the cell transcription program is committed to a specific group of genes involved in cellular specialty and housekeeping functions without the requirement to continuously switch to transcribed genes that are involved in proliferation (Giglia-Mari et al., 2009). Thus, to our knowledge, our work is a pioneer study in the analysis of the *in vivo* dynamics of TFIIH throughout the cell cycle progression in the context of the whole organism. Here, we showed that TFIIH is highly dynamic during the fast nuclear division cycles in the early fly embryo. Our *in vivo* analyses show that although some TFIIH always co-localizes with the chromosomes, the intensity of the signal on chromatin changes with cell cycle progression. During interphase, some cytoplasmic localization was detected, but most of the TFIIH signal was observed in the nucleus. Interestingly, during chromatin condensation at prophase, the signal further increased inside the nucleus while decreasing in the cytoplasm, suggesting the translocation of TFIIH into the nucleus at this stage, in which TFIIH foci are clearly observed. During mitosis, although some TFIIH remains co-localized with the chromosomes, we observed the opposite behaviour: a reduction of the nuclear signal with increased signal in the cytoplasm. Thus, the concentration of TFIIH oscillated between the cytoplasm and the nucleus during the cell cycle in the early syncytial blastoderm embryos. A previous work described the localization of some transcription factors in HeLa cells at the transition of mitosis/G1, in this analysis, Prasanth and colleagues found that unlike TBP, which was found on chromosomes throughout mitosis, some other general transcription factors, including RNAPII, XPB and XPD, were localized in the daughter nuclei after mid-telophase (Prasanth et al., 2003). Hence, this intriguing behaviour observed for TFIIH in the fly embryo could be due to the mechanism involved in the regulation of transcription during the very short nuclear division cycles that occurred at the pre-MBT stages in which not even complete nuclear membrane breakdown was observed.

Importantly, the observation of CycH and Cdk7 co-localization with chromosomes during mitosis is in disagreement with a previous work that proposed that in wild type syncytial blastoderm embryos, the CAK is nuclear during interphase but it is excluded from

mitotic chromosomes through an XPD-dependent mechanism causing defects in mitosis in XPD-depleted syncytial blastoderm embryos in which Cdk7 co-localizes with chromosomes at anaphase (Li et al., 2010). Despite our efforts to analyse the Cdk7 localization pattern by immunostaining with several available antibodies, we were not able to observe any clear nuclear signal for this protein in any case during interphase in wild type embryos, only with the Cdk7-GFP protein we were able to observe an identical localization as the other TFIIH subunits during the replicative cycles in the syncytial blastoderm, including the presence of the CAK in mitotic chromosomes (Supp. Figure 4; Supp. Movie 4). Thus, this discrepancy could be explained because the antibodies that have been used to recognize Cdk7 do not generate a good signal in embryo immunostainings. Indeed, in agreement with our observations for other TFIIH subunits in the early fly embryo, Ito and colleagues reported that the XPD signal is spread in the nucleoplasm but enriched at the mitotic spindle at metaphase in human cells (Ito et al., 2010).

Recently, an increased number of studies have highlighted the existence of mitotic bookmarking by several transcription factors (reviewed in Kadauke and Blobel, 2013). Our observations on the TFIIH dynamics suggest that this could be the case for TFIIH during early embryo development.

Mitotic bookmarking by TFIIH and other components of the basal transcription machinery in the early fly embryo.

An interesting feature observed during TFIIH dynamics is its enrichment in nuclear foci that co-localize with the active RNAPII foci that correspond to the HLBs (White et al., 2007). As previously reported for the HLBs (Salzler et al., 2013), the TFIIH foci are maintained along the division cycle and disappear until late metaphase. Despite the generally accepted model of transcription shut off in mitotic nuclei (Gottesfeld and Forbes 1997), it has been reported that some transcription can take place during mitosis; for instance, for the *CycB* gene in Hela cells (Sciortino et al., 2001) and a-satellite DNA in the centromere (Chan et al., 2012). In the early fly embryo, the time period for transcription is very short, because the nuclear cycle only has a brief interphase and mostly consists of S and M phases (Farrell and O´Farrell, 2014). It is well documented that histone genes are transcribed during the S phase (Guglielmi et al., 2013). However, in the case of the

syncytial blastoderm, it could be possible that transcription has to be extended during the fast nuclear division cycle to achieve the amount of pre-MBT mRNA required during this developmental stage.

The co-localization of some TFIIH with the chromosomes in all stages of the nuclei division cycles in the early embryo suggest a mechanism to maintain TFIIH as bookmark for a fast transcriptional re-activation after mitosis. Interestingly, TBP and the RNAPII follow similar dynamics, and together with TFIIH, occupy the H3 and H4 promoters in metaphase. Then, we propose that components of the basal transcription machinery are maintained in the promoters of some genes for rapid transcriptional activation after mitosis, as a short-term memory transcription mechanism in the pre-blastoderm and syncytial blastoderm (Figure 7). This proposal is supported by the recent accumulating evidence that suggests that transcriptional activation of specific genes after cell division may be through the maintenance of different transcription factors bound to its target DNA elements during mitosis. In fact, the mitotic condensed chromatin is accessible for transcription factors (reviewed in Kadauke and Blobel, 2013). For instance, there is convincing evidence for bookmarking at mitosis in the globin genes by GATA1; the rRNA genes by Runx 2, RBPJ, and Myc in *Drosophila* cells, among many other examples (Kalaude et al., 2012; Ali et al., 2010; Yang el al., 2013; Lake et al., 2014). Furthermore, it has been found that TBP can be associated with mitotic chromosomes in highly transcribed regions preserving the memory of gene activity (Xing et al., 2008). Interestingly, Marshall and Colleagues analysed the *Drosophila* embryo chromosome elasticity by four-dimensional microscopy based-motion analysis which suggested that the *Drosophila* embryo mitotic chromosomes may be less tightly compacted than mitotic chromosomes analysed in other organisms (Marshall et al., 2001), which could facilitate the maintenance of many nuclear factors in the chromatin. Thus, with regard to the basal transcription machinery during the pre-blastoderm and syncytial blastoderm nuclear division cycles, because transcription has to be reactivated very fast after mitosis, some components of the basal transcription machinery remain bound to the promoters of some genes. Following this idea, it will be relevant in future works to determine if other general transcription factors as well as vielfältig/zelda have a similar behaviour in the early fly embryo mitotic chromosomes as well as to determine its occupancy at the global genome level.

Early embryo catastrophic mitosis and transcriptional defects caused by mutations in TFIIH core and CAK subunits.

Previous reports have suggested a role for the XPD subunit of TFIIH in the control of Cdk7 function in cell cycle modulation during early fly embryogenesis (Chen et al., 2003; Li et al., 2010). In addition, XPD has been found to be a component of the MMXD complex involved in chromosome segregation in human cells (Ito et al., 2010) and has an important role in transcriptional activation, because it is well documented that its ATPase activity is important for the formation of the open complex in RNAPII transcribed genes and as scaffold to maintain the integrity of TFIIH during transcription (Lainé et al., 2006; Kuper et al., 2014). Thus, further analyses to clarify the role of XPD in cell cycle regulation are required. Here, we showed that also mutations in p8 and the XPB core subunits of TFIIH as well as the depletion of Cdk7 caused defects in mitosis, suggesting that this phenotype is not exclusive to Cdk7 delocalization by XPD-depletion in the fly embryo. In accordance, Matsuno and colleagues reported that mutations of p52, XPB or Cdk7 produced similar defects in cell cycle progression during fly eye imaginal disc development, suggesting that CAK activity in cell cycle regulation is performed by the holo-TFIIH (Matsuno et al., 2007). However, although a direct role for the holo-TFIIH in mitosis cannot be discarded, the evidence presented in this work indicated that the absence of p8 produced a deregulation of global gene expression during oogenesis affecting the expression of many genes that participate in coordinated mitosis at the pre-blastoderm and syncytial blastoderm stages. Interestingly, it is known that embryos affected in the transcriptional activator vielfälting/zelda, which activates the onset of zygotic transcription, show mitotic defects that have some similarities to the reported XPD deficient embryo phenotypes and those observed in this work with *p8 null*, homozygous hay^{nc2} as well as Cdk7 depleted embryos (Staudt et al., 2006). It is thus difficult to distinguish a direct possible role for TFIIH subunits in mitosis from the obvious defects in gene expression that indirectly affect mitosis, particularly because some of the genes expressed at pre-MBT may also participate in mitosis.

Despite the fact that in human cells, an essential role for p8 in maintaining a steady-state level of cellular TFIIH has been proposed (Giglia-Mari, 2004), we did not observe a

significant reduction in the level of any of the other TFIIH subunits in p8-depleted ovaries or embryos (this work) and in our previous studies on spermatogenesis (Cruz-Becerra te al., 2016), suggesting that this role for p8 is not conserved in *Drosophila*. Furthermore, our transcriptome analyses of p8-depleted embryos highlight the importance of this protein in global transcription during development, as was recently observed in a p8 knock-out mouse model in which the absence of p8 caused embryonic lethality (Theil et al., 2013).

In conclusion, the analysis of TFIIH at the pre-MBT shows how this factor moves in waves in the chromosomes during the mitotic cycles, but some TFIIH as well as other components of the basal transcription machinery always remain bound to the promoters of genes that have to be rapidly transcribed after mitosis. In addition, defects in subunits of TFIIH that affect transcription during oogenesis cause catastrophic mitosis in the syncytial blastoderm embryo. This knowledge provides important insights into the functions of TFIIH during early embryo development.

Acknowledgments

We thank Martha Vazquez and Viviana Valadez for discussions during the development of this work. We also thank Andres Saralegui, Arturo Pimentel and Chris Wood and the LNMA for advice in the use of the confocal microscopes. This work was supported by the CONACyT grant 219673 and PAPIIT/UNAM grant IN200315 to M.Z. GC-B thanks to El Colegio de Sinaloa for the Hugo Aréchiga Urtuzuástegui scholarship.

References

Abdulrahman, W., Iltis, I., Radu., L, Braun, C., Maglott-Roth, A., Giraudon, C., Egly. J.M. and Poterszman A. (2013). ARCH domain of XPD, an anchoring platform for CAK that conditions TFIIH DNA repair and transcription activities. Proc. Natl. Acad. Sci. U S A. *110,* 633-642.

Aguilar-Fuentes, J., Valadez-Graham, V., Reynaud, E., and Zurita, M. (2006). TFIIH trafficking and its nuclear assembly during early Drosophila embryo development. J Cell Sci, *119*, 3866-3875.

Ali, S. A., Zaidi, S.K., Dobson, J.R., Shakoori, A.R., Lian, J.B., Stein, J.L., van Wijnen, A. J., and Stein, G. S. (2010). Transcriptional corepressor TLE1 functions with

Runx2 in epigenetic repression of ribosomal RNA genes. Proc. Natl. Acad. Sci. U S A *107*, 4165-

Ali-Murthy, Z., Lott, S.E., Eisen, M.B., and Kornberg, T. B. (2013). An essential role for zygotic expression in the pre-cellular Drosophila embryo. PLoS Genet. 9(4):e1003428. doi: 10.1371

Chan, F.L., Marshall, O. J., Saffery, R,. Kim, B.W., Earle, E. , Choo, K.H., and Wong, L.H. (2102). Active transcription and essential role of RNA polymerase II at the centromere during mitosis. Proc. Natl. Acad. Sci. U S A *109*, 1979-1984.

Chen, J., Larochelle, S., Li, X., and Suter, B. (2003). Xpd/Ercc2 regulates CAK activity and mitotic progression. Nature *424*, 228-232.

Chen, K., Johnston, J., Shao, W., Meier, S., Staber, C., and Zeitlinger, J. (2013). A global change in RNA polymerase II pausing during the Drosophila midblastula transition. Elife. 2:e00861. doi: 10.7554/eLife.00861.

Coin, F., Oksenych, V., and Egly, J.M. (2007). Distinct roles for the XPB/p52 and XPD/p44 subcomplexes of TFIIH in damaged DNA opening during nucleotide excision repair. Mol. Cell *272,* 245-256.

Compe, E., and Egly, J.M. (2012). TFIIH: when transcription met DNA repair. Nat. Rev. Mol. Cell. Biol. *13*, 343-354.

Egly, J.M., and Coin, F. (2011). A history of TFIIH: two decades of molecular biology on a pivotal transcription/repair factor. DNA Repair *10*, 714-721.

Farrell, J.A., and O'Farrell, P. H. (2014). From egg to gastrula: how the cell cycle is remodeled during the Drosophila mid-blastula transition. Annu. Rev. Genet. *48*, 269-294.

Foe, V.E., and Alberts, B.M. (1983) Studies of nuclear and cytoplasmic behaviour during the five mitotic cycles that precede gastrulation in Drosophila embryogenesis. J. Cell Sci. *61*, 31-70.

Fregoso, M., Lainé, J.P., Aguilar-Fuentes, J., Mocquet, V., Reynaud, E., Coin, F., Egly, J.M., and Zurita M. (2007). DNA repair and transcriptional deficiencies caused by mutations in the Drosophila p52 subunit of TFIIH generate developmental defects and chromosome fragility. Mol Cell. Biol. *27*, 3640-3650.

Giglia-Mari, G., Coin, F., Ranish, J.A., Hoogstraten, D., Theil, A., Wijgers, N., Jaspers, N.G., Raams, A., Argentini, M., van der Spek, P.J., Botta, E., Stefanini, M., Egly, J.M., Aebersold, R., Hoeijmakers, J.H. and Vermeulen, W. (2004). A new, tenth subunit of TFIIH is responsible for the DNA repair syndrome trichothiodystrophy group A. Nature Genet. *36*, 714-719.

Gottesfeld, J.M., and Forbes, D. J. (1997). Mitotic repression of the transcriptional machinery. Trends Biochem. Sci. *22,* 197-202.

Guglielmi, B., La Rochelle, N., and Tjian, R. (2013). Gene-specific transcriptional mechanisms at the histone gene cluster revealed by single-cell imaging. Mol. Cell *51*, 480-492.

Günesdogan, U., Jäckle, H., and Herzig, A. (2014). Histone supply regulates S phase timing and cell cycle progression. Elife *3:*e02443.

Herrera-Cruz, M., Cruz, G., Valadez-Graham, V., Fregoso-Lomas, M., Villicaña, C., Vázquez, M., Reynaud, E., and Zurita, M. (2012). Physical and functional interactions between Drosophila homologue of Swc6/p18Hamlet subunit of the SWR1/SRCAP chromatin-remodeling complex with the DNA repair/transcription factor TFIIH. J. Biol. Chem. *287*, 33567-33580.

Hsin, J.P., and Manley, J. L. (2012). The RNA polymerase II CTD coordinates transcription and RNA processing. Genes Dev. *26*, 2119-2137.

Isogai, Y., Keles, S., Prestel, M., Hochheimer, A., and Tjian, R. (2007). Transcription of histone gene cluster by differential core-promoter factors. Genes Dev. *21*, 2936-2949.

Kadauke, S., and Blobel, G.A. (2013). Mitotic bookmarking by transcription factors. Epigenetics Chromatin 6, 6. doi: 10.1186/1756-8935-6-6

Kadauke, S., Udugama, M.I., Pawlicki, J.M., Achtman, J.C., Jain, D.P., Cheng, Y., Hardison, R.C., and Blobel, G. A. (2012). Tissue-specific mitotic bookmarking by hematopoietic transcription factor GATA1. Cell. *150*, 725-737.

Kainov, D. E., Vitorino, M., Cavarelli, J., Poterszman, A., Egly, J. M. (2008). Structural basis for group A trichothiodystrophy. Nat. Struct. Mol. Biol. *15*, 980-984.

Kouzine, F., Wojtowicz, D., Yamane, A., Resch, W., Kieffer-Kwon, K.R., Bandle, R., Nelson, S., Nakahashi, H., Awasthi, P., Feigenbaum, L., Menoni, H., Hoeijmakers, J., Vermeulen, W., Ge, H., Przytycka, T.M., Levens, D., and Casellas, R. (2013). Global regulation of promoter melting in naive lymphocytes. Cell *153,* 988-999.

Kuper, J., Braun, C., Elias, A., Michels, G., Sauer, F., Schmitt, D.R., Poterszman, A., Egly, J.M. Kisker, C. (2014). In TFIIH, XPD helicase is exclusively devoted to DNA repair. PLoS Biol. *12*(9):e1001954.

Lainé, J.P., Mocquet, V. and Egly, J.M. (2006). TFIIH enzymatic activities in transcription and nucleotide excision repair. Methods Enzymol. 408, 246-263.

Lake, R.J., Tsai, P.F., Choi, I., Won, K.J., and Fan, H.Y. (2014). RBPJ, the major transcriptional effector of Notch signaling, remains associated with chromatin throughout mitosis, suggesting a role in mitotic bookmarking. PLoS Genet. 10(3):e1004204.

Larochelle, S., Merrick, K.A., Terret, M.E., Wohlbold, L., Barboza, N.M., Zhang, C., Shokat, K.M., Jallepalli, P.V., and Fisher, R.P. (2007). Requirements for Cdk7 in the assembly of Cdk1/cyclin B and activation of Cdk2 revealed by chemical genetics in human cells. Mol. Cell *25,* 839-850.

Li, X.Y., Harrison, M.M., Villalta, J.E., Kaplan, T., and Eisen, M.B. (2014) Establishment of regions of genomic activity during the Drosophila maternal to zygotic transition. Elife 14; 3. doi: 10.7554/eLife.03737.

Lee, M.T., Bonneau, A.R., and Giraldez, (2014). Zygotic genome activation during the maternal-to-zygotic transition. Annu. Rev. Cell Dev. Biol. *30*, 581-613.

Li, X., Urwyler, O., and Suter, B. Drosophila Xpd regulates Cdk7 localization, mitotic kinase activity, spindle dynamics, and chromosome segregation. PLoS Genet. 6(3):e1000876. doi: 10.1371

Lott, S.E., Villalta, J.E., Schroth, G.P., Luo, S., Tonkin, L.A., and Eisen M. B. (2011) Noncanonical compensation of zygotic X transcription in early *Drosophila melanogaster* development revealed through single-embryo RNA-seq. PLoS Biol. 8;9(2):e1000590.

Lu, X., Li, J.M., Elemento, O., Tavazoie, S., and Wieschaus, E.F. (2009). Coupling of zygotic transcription to mitotic control at the Drosophila mid-blastula transition. Development *136*, 2101-2110.

Mazumdar, A., and Mazumdar, M. (2002). How one becomes many: blastoderm cellularization in Drosophila melanogaster. Bioessays 24, 1012-1022.

Merino, C., Reynaud, E., Vázquez, M., and Zurita M. (2002). DNA repair and transcriptional effects of mutations in TFIIH in Drosophila development. Mol. Biol. Cell. *13*, 3246-3256.

Mounkes, L.C., Jones, R.S., Liang, B.C,. Gelbart, W., and Fuller, M.T. (1992). A Drosophila model for xeroderma pigmentosum and Cockayne's syndrome: haywire encodes the fly homolog of ERCC3, a human excision repair gene. Cell *71*, 925-937.

Nizami, Z.F., Deryusheva, S., and Gall, J.G. (2010). Cajal bodies and histone locus bodies in Drosophila and Xenopus. Cold Spring Harb. Symp. Quant. Biol. *75*, 313-320.

Nonnekens, J., Cabantous, S., Slingerland, J., Mari, P.O. and Giglia-Mari G. (2013). In vivo interactions of TTDA mutant proteins within TFIIH. J Cell Sci. *126*, 3278-3283.

Rapin, I. (2013). Disorders of nucleotide excision repair.. Handb. Clin. Neurol. *113*, 1637-1650.

Reynaud, E., Lomelí, H., Vázquez, M., and Zurita, M. (1999). The Drosophila melanogaster homologue of the Xeroderma pigmentosum D gene product is located in euchromatic regions and has a dynamic response to UV light-induced lesions in polytene chromosomes. Mol. Biol. Cell. *10*, 1191-1203.

Salzler, H.R., Tatomer, D.C., Malek, P.Y., McDaniel, S.L., Orlando, A.N., Marzluff, W.F., and Duronio, R. J. A. (2013). Sequence in the Drosophila H3-H4 Promoter triggers histone locus body assembly and biosynthesis of replication-coupled histone mRNAs. Dev. Cell *24*, 623-634.

Satija, R., and Bradley, R. K. (2012). The TAGteam motif facilitates binding of 21 sequence-specific transcription factors in the Drosophila embryo. Genome Res. *22*, 656-665.

Sciortino, S., Gurtner, A., Manni, I., Fontemaggi, G., Dey, A., Sacchi, A., Ozato, K., and Piaggio, G. (2001). The cyclin B1 gene is actively transcribed during mitosis in HeLa cells. EMBO Rep. *2,* 1018-1023.

Schachter, M.M., and Fisher, R-P. (2013). The CDK-activating kinase Cdk7: taking yes for an answer. Cell Cycle. *12*, 3239-3240.

Schuh, M., Lehner, C.F., and Heidmann, S. (2007). Supplemental Data. Incorporation of *Drosophila* CID/CENP-A and CENP-C into Centromeres during Early Embryonic Anaphase. Curr. Biol. *17*, 237—243.

Seydoux, G., and Dunn, M. A. (1997). Transcriptionally repressed germ cells lack a subpopulation of phosphorylated RNA polymerase II in early embryos of Caenorhabditis elegans and Drosophila melanogaster. Development. *124*, 2191-2201.

Staudt, N., Fellert, S., Chung, H.R., Jäckle, H., and Vorbrüggen, G. (2006). Mutations of the Drosophila zinc finger-encoding gene vielfältig impair mitotic cell divisions and cause improper chromosome segregation. Mol. Biol. Cell. 17, 2356-2365.

Titov, D.V., Gilman, B., He, Q.L., Bhat., S., Low, W.K., Dang, Y., Smeaton, M., Demain, A.L., Miller, P.S., Kugel, J.F., Goodrich, J.A., and Liu, J.O. (2011). XPB, a subunit of TFIIH, is a target of the natural product triptolide. Nat. Chem. Biol. 7, 182-188.

Villicaña, C., Cruz, G., and Zurita, M. (2013). The genetic depletion or the triptolide inhibition of TFIIH in p53-deficient cells induces a JNK-dependent cell death in Drosophila. J. Cell Sci. *126*, 2502-2515.

Wang, Z., and Lindquist, S. (1998). Developmentally regulated nuclear transport of transcription factors in Drosophila embryos enable the heat shock response. Development *125*, 4841-4850.

White, A.E., Leslie, M.E., Calvi, B.R., Marzluff, W.F. and Duronio, R.J. (2007) Developmental and cell cycle regulation of the Drosophila histone locus body. Mol Biol Cell 18, 2491-2502.

Xing, H., Vanderford, N.L., Sarge, K. D. (2008). The TBP-PP2A mitotic complex bookmarks genes by preventing condensin action. Nat. Cell Biol. *10*, 1318-1323.

Yang, J., Sung, E., Donlin-Asp, P.G., and Corces, V.G. (2013). A subset of Drosophila Myc sites remain associated with mitotic chromosomes colocalized with insulator proteins. Nat Commun. 4:1464. doi: 10.1038/ncomms2469.

Yeom, E., Hong, S.T., and Choi, K.W. (2014). Crumbs interacts with Xpd for nuclear division control in Drosophila. Oncogene *34*, 2777-2789.

Zurita, M., and Merino, E. (2003). The transcriptional complexity of the TFIIH Complex. Trends in Genet. 10, 578-584.

Zurita, M., Reynaud, E., and Aguilar-Fuentes, J. (2008). From the beginning: the basal transcription machinery and onset of transcription in the early animal embryo. Cell Mol, Life Sci. *65*, 212-227.

Figures

Figure 1. p8 is preferentially nuclear during the mitotic cycles in the syncytial blastoderm embryo. Immunostaining of syncytial blastoderm embryos shows the nuclear localization of p8 in mitosis.

(A) p8 is distributed in the nucleoplasm during interphase.

(B and C) Most of p8 surrounds the chromosomes, although some p8 co-localizes with the chromosomes at metaphase.

(D) Immunolocalization of laminin (green) and p8 (red) in syncytial blastoderm embryos at interphase (left) and mitosis (right) shows that p8 does not co-localize with the nuclear membrane during the nuclear division cycle.

(E) At metaphase p8 surrounds the mitotic structures, although also co-localizes with the chromosomes and the mitotic spindle. p8 (blue), b-tubulin (red) and DNA (green).

(F) p8 (red) co-localizes with chromosomes (green) at anaphase.

Figure 2. The Core and CAK subunits of TFIIH follow similar dynamics during the syncytial blastoderm stage.

(A) Visualization of an *EYFP-p52*/*H2Av-RFP* (yellow/red) transgenic syncytial blastoderm embryo during a nuclear division cycle. The different stages of the mitotic cycle were identified using H2Av-RFP.

(B) Time lapse analysis of a syncytial blastoderm embryo expressing EYFP-p52 (yellow) and p8-ECFP (cian). Note that the both TFIIH subunits follow identical dynamics during the syncytial blastoderm stage. The same dynamics was also observed with other core and CAK TFIIH subunits (see Movies 2 and 3 and Supp. Figure 1).

Figure 3. TFIIH is enriched at transcribed chromatin regions that are maintained in most of the mitotic cycle in the syncytial blastoderm.

(A) Nuclei at interphase expressing EYFP-p52 (yellow) and H2Av-RFP (red) recombinant proteins in which TFIIH bodies can be observed. The plots represent the signal quantification in a single confocal plane showing that regions of TFIIH enrichment are reduced in the H2Av-RFP signal.

(B) RNAPII enriched regions (Histone Locus Bodies) co-localize with TFIIH foci at the syncytial blastoderm. The plots show the location in a single plane of both signals.
(C) Time lapse analysis of TFIIH bodies during a replicative cycle. TFIIH (EYFP-p52) bodies, indicated by the arrows, were followed during a replicative cycle using as reference of the stage of the chromatin the H2Av-RFP recombinant protein. The time lapse shows nuclei from the beginning of the interphase to metaphase in a syncytial blastoderm embryo between the 10-11 replicative cycles.

Figure 4. Basal transcription machinery components follow similar dynamics in the syncytial blastoderm embryo and remain bound in active promoters during mitosis.
(A) Immunostained syncytial blastoderm embryos using antibodies against TBP (red signal, left panel), RNAPII (red signal, middle panel) and RNAPII-CTD-Serine 5-phosphorylated (red signal-right panel). Note the presence of bodies that correspond to the HLB´s with the three antibodies. In the case of TBP and RNAPII-CTD signal, co-localization with the mitotic chromosomes can be observed, but not the phosphorylated RNAPII-CTD.
(B) ChIP analyses of TBP, RNAPII and TFIIH (XPB) in syncytial blastoderm embryos at interphase or metaphase. An example of the embryos used for ChIPs experiments stained with the mitosis marker H3-serine 10 phosphorylated is shown. The sequences analysed after ChIP are the H3 and H4 promoters as well as the rover transposable element and the subtelomeric repetitive sequence TAHRE. The figure shows an example of at least duplicated experiments. For the H3 promoter ChIP analysis panel, the RNAPII and TBP mock and input are the same in each case for interphase and metaphase chromatin, indicated by numbers 1 to 4 in the figure.

Figure 5. The absence of functional TFIIH causes catastrophic mitosis in the syncytial blastoderm embryo.
(A) Wild type and p8 null ovaries stained with sytox-green to visualize the DNA and laid embryos from wild type and p8 null mothers. Note that the oogenesis is completed, but the ovaries and the embryos are smaller than heterozygous organisms.
(B) Western blot against different subunits of TFIIH, components of the basal transcription machinery as well as other proteins as control.

(C) Comparison of wt and p8 mutant mitosis. The mitotic spindle is identified with an anti b-tubulin antibody (red) DNA with sytox-green.

(D) Detection of centrosomes in wt and p8 null embryos using a γ-tubulin antibody (red) and DNA with sytox-green.

(E) Alterations in mitosis cycle timing in p8 null embryos if compared to wt organisms by visualizing the presence of H3-serine 10 phosphorylated.

(F) Western blot analysis from p8 mutant or wt embryos to determine the levels of different TFIIH subunits and the RNAPII-CTD phosphorylated at serine 5.

(G) Syncytial blastoderm embryos from heterozygous hay^{nc2}/+ females and embryos from homozygous hay^{nc2} females stained with the anti b-tubulin antibody and with sytox-green. The panel shows a desynchronized embryo in the middle and an amplification showing catastrophic mitosis in a homozygous hay^{nc2} embryo. All the genotypes and used antibodies are indicated in the figure.

Figure 6. Transcriptome analysis of independent $p8^{-/-}$ (null) or $p8^{-/+}$ (heterozygote) embryos.

(A) $p8^{+/-}$; H2Av-$RFP^{/+}$ embryos with wild type phenotype (embryos G and H) and $p8^{-/-}$; H2Av-$RFP^{/+}$ embryos, with defects in mitosis (embryos A, B, and E) at division cycle 9-10, used for single embryo RNA-seq analysis.

(B) Correlation plots indicating the variations in gene expression between p8+/- control embryos (G vs H) and with the mutant embryos (A, B, and E).

(C) Heat map showing the variations in gene expression of the same genes between the two control embryos and the three mutants. Note that the low variation in embryo E if compared with embryos A and B with more severe mutant phenotype.

(E) Heat map showing the variation in gene expression in mutated embryos as well a between the two control embryos of genes that participate in mitosis and DNA replication. Again the affliction in gene expression of these genes in mutant embryo E is not a severe as in the other mutant embryos with more dramatic mutant phenotype.

Figure 7. Model on the dynamics of TFIIH at the ZGA in the mitotic cycles of the *Drosophila* syncytial blastoderm. At interphase must of TFIIH is bound to the

chromosomes and concentrated in the HLB as part of the transcription pre-initiation complex (PIC). At metaphase must of TFIIH is maintained in the nuclear lumen, but some remains bound to the chromatin and in the promoter of some genes. In the cytoplasm the core and the CAK subcomplexes do not interact, only in the nucleus both subcomplexes form the 10 subunits TFIIH (Aguilar et al., 2006, and data not shown). At anaphase and telophase, TFIIH start to move form the nuclear lumen and the core and the CAK from the cytoplasm to the chromosomes and in the next interphase, must of TFIIH is now located in the chromatin and transcription is restarted from the PIC poised at the promoters during mitosis. The different TFIIH complexes are indicated.

Supplementary Figures

Supp. Figure 1. Oscillatory behaviour of the TFIIH dynamics during a replicative cycle. This example shows the dynamics of EYFP-p52 (grey) during a replicative cycle having H2Av-RFP (red) as reference to visualize the chromatin. The plots represent the signal intensity for each channel of the same plane. Note that the intensity signal of EYFP-p52 on the chromosomes changes depending of the mitotic phase, although always there is some signal on the chromosomes.

Supp. Figure 2. Visualization of XPB-EGFP in embryos at cycles 8 and 10. The presence of TFIIH foci can be detected (indicated by arrows).

Supp. Figure 3. Detection by immunostaining of CycH in syncytial blastoderm embryos. Different phases of the mitotic cycle are indicated in the figure. Note that the CycH signal (red) is preferentially located on the chromosomes (green), although some CycH also is cytoplasmic.

Supp. Figure 4. Syncytial blastoderm embryos deficient in p8 have desynchronized mitotic cycles. The figure shows two embryos with low (middle embryo) and severe (bottom embryo) mutant phenotype. The genotype is indicated in the figure as well as DNA and alpha tubulin staining.

Supp. Figure 5. The depletion of Cdk7 during oogenesis causes catastrophic mitosis in the syncytial blastoderm embryo.

(A) Western blot showing the reduction of the Cdk7 levels in embryos from mothers that express RNAi against Cdk7 (Cdk7i) during oogenesis. Note that the maximum reduction of Cdk7 occurs in double homozygous females for the RNAi and the driver.

(B) Example of embryos depleted in Cdk7 showing different mitotic defects. The mother genotypes are indicated. Note that there is a desynchronization in the mitotic cycles, aberrant spindles, and isolated chromosomes among other mitotic defects.

Supp. Figure 6. Correlation values of the transcriptome between a wild type embryo (G) and mutant embryos (A, B, and E).

(A) Correlation plots between mutant and wild type embryos.

(B) RNA-seq correlation values between the different embryos analysed.

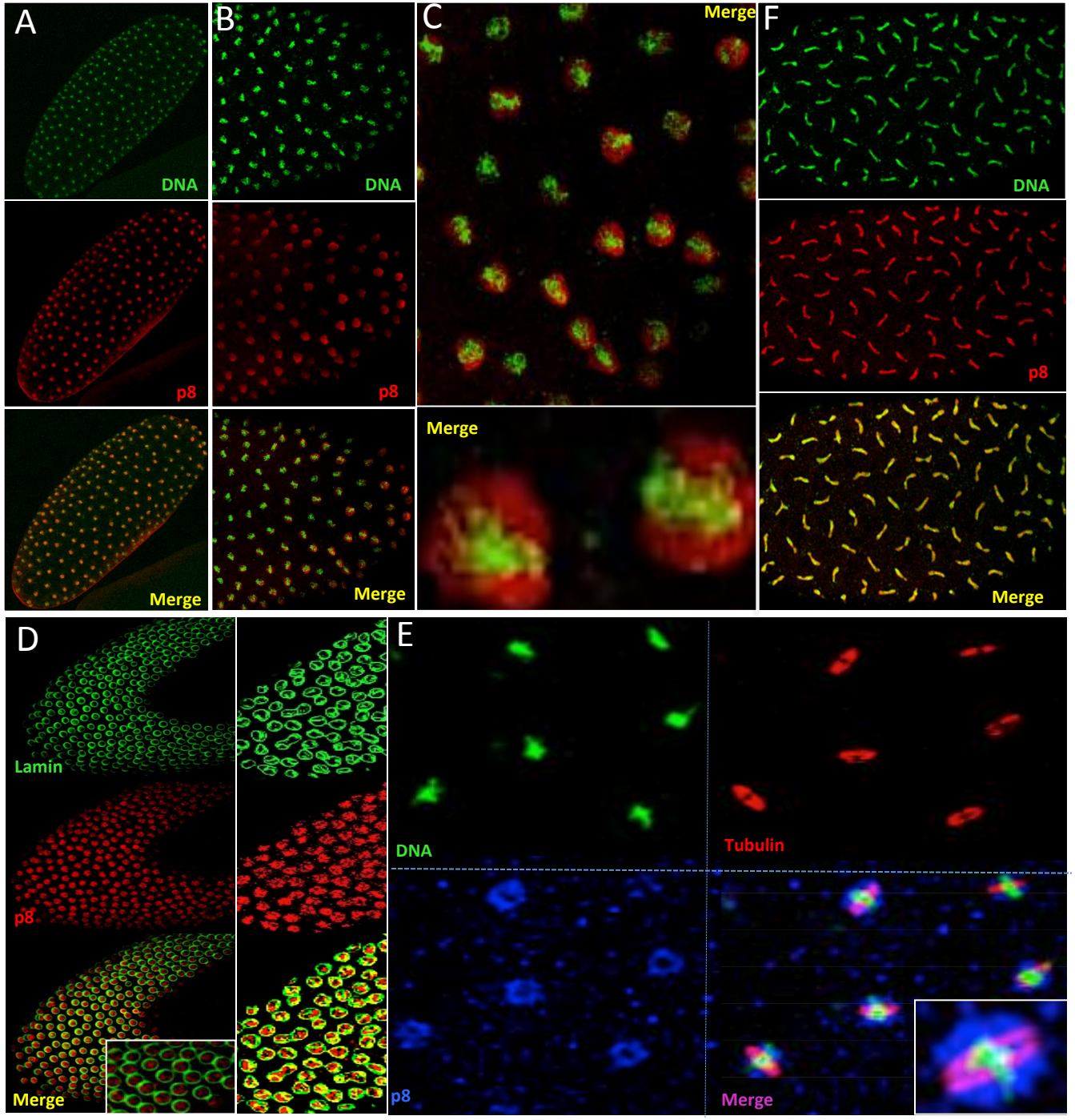
A
DNA
p8
Merge
B
DNA
p8
Merge
C
Merge
Merge
F
DNA
p8
Merge
D
Lamin
p8
Merge
E
DNA
p8
Tubulin
Merge

Fig. 1

Fig. 2

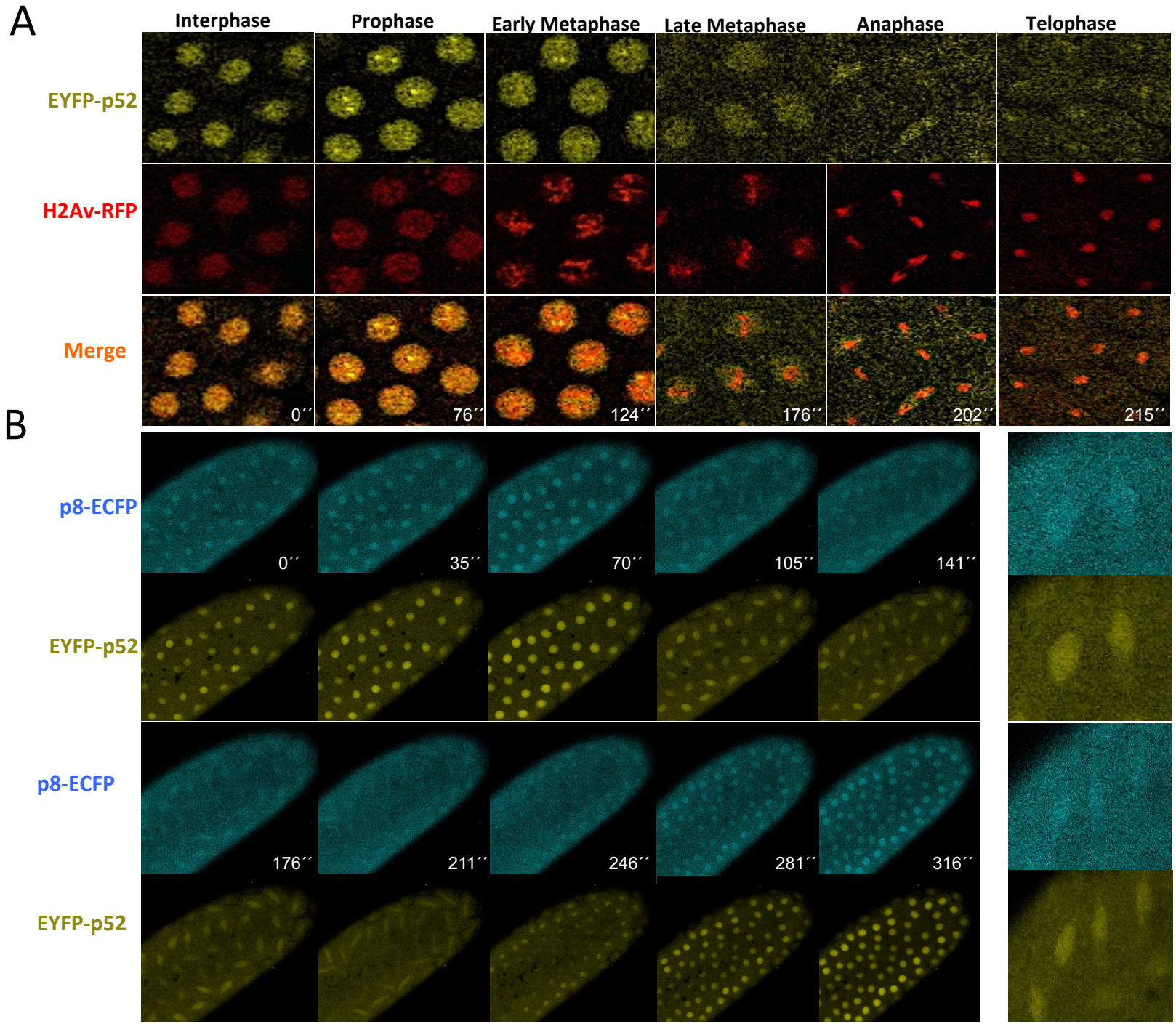
A
Interphase
Prophase
Early Metaphase
Late Metaphase
Anaphase
Telophase
EYFP-p52
H2Av-RFP
Merge
0´´
76´´
124´´
176´´
202´´
215´´
B
p8-ECFP
0´´
35´´
70´´
105´´
141´´
EYFP-p52
p8-ECFP
176´´
211´´
246´´
281´´
316´´
EYFP-p52

Fig. 3

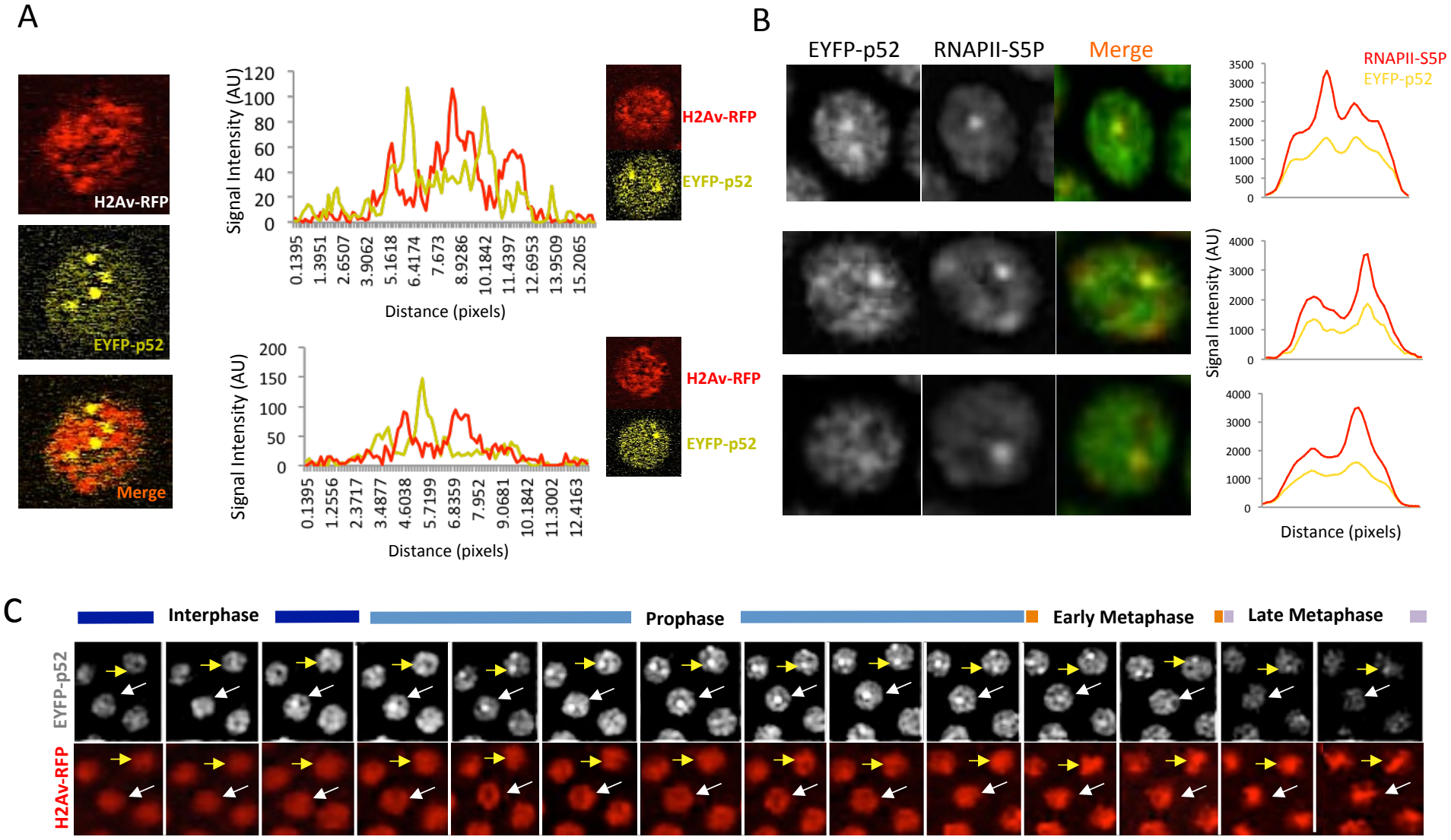
A
H2Av-RFP
EYFP-p52
Merge
Signal Intensity (AU)
Distance (pixels)
H2Av-RFP
EYFP-p52
B
EYFP-p52
RNAPII-S5P
Merge
RNAPII-S5P
EYFP-p52
Signal Intensity (AU)
Distance (pixels)
C
Interphase
Prophase
Early Metaphase
Late Metaphase
EYFP-p52
H2Av-RFP

Fig. 4

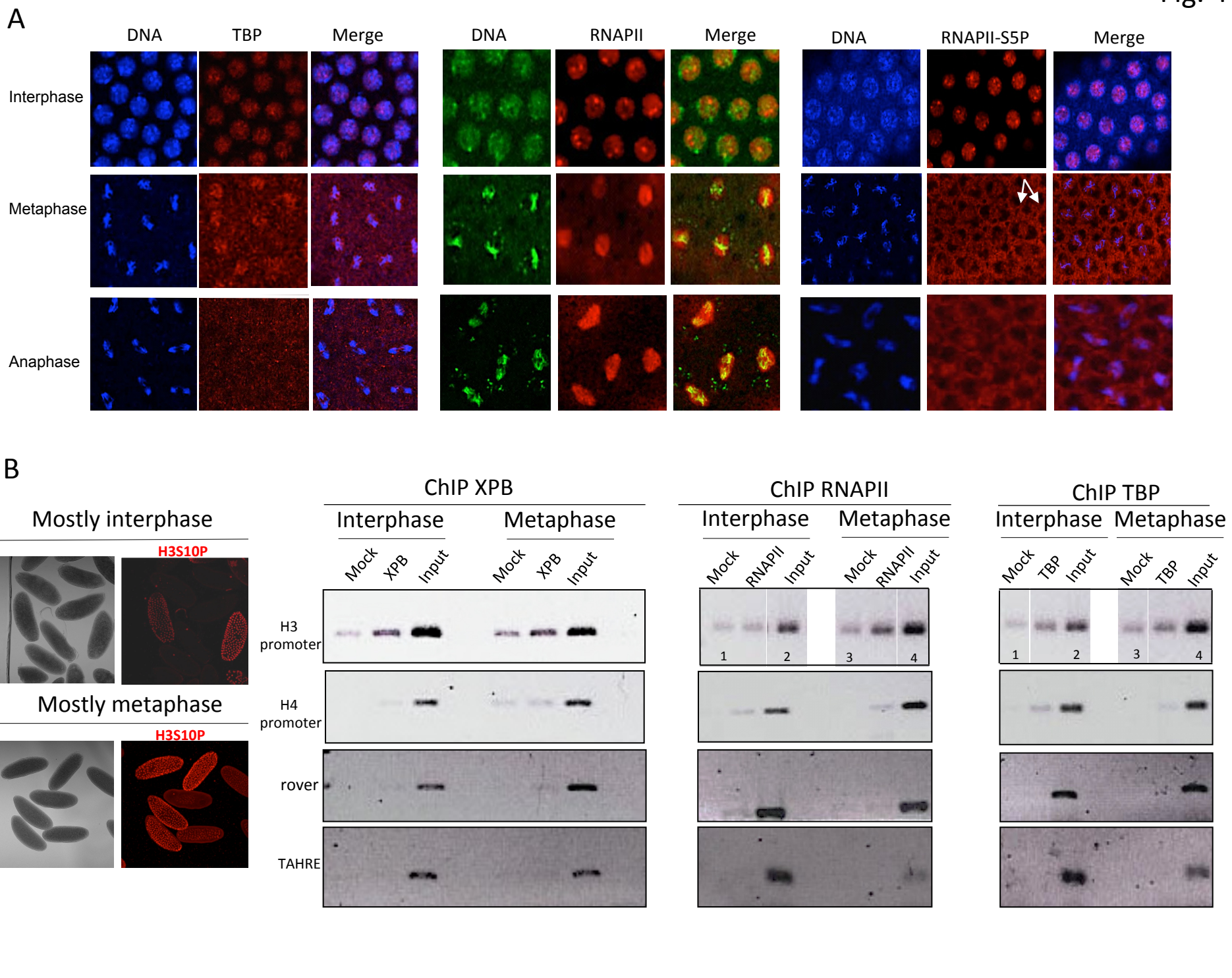
A
DNA
TBP
Merge
DNA
RNAPII
Merge
DNA
RNAPII-S5P
Merge
Interphase
Metaphase
Anaphase
B
Mostly interphase
H3S10P
Mostly metaphase
H3S10P
ChIP XPB
Interphase
Metaphase
Mock
XPB
Input
Mock
XPB
Input
ChIP RNAPII
Interphase
Metaphase
Mock
RNAPII
Input
Mock
RNAPII
Input
ChIP TBP
Interphase
Metaphase
Mock
TBP
Input
Mock
TBP
Input
H3 promoter
H4 promoter
rover
TAHRE
1
2
3
4

Fig. 5

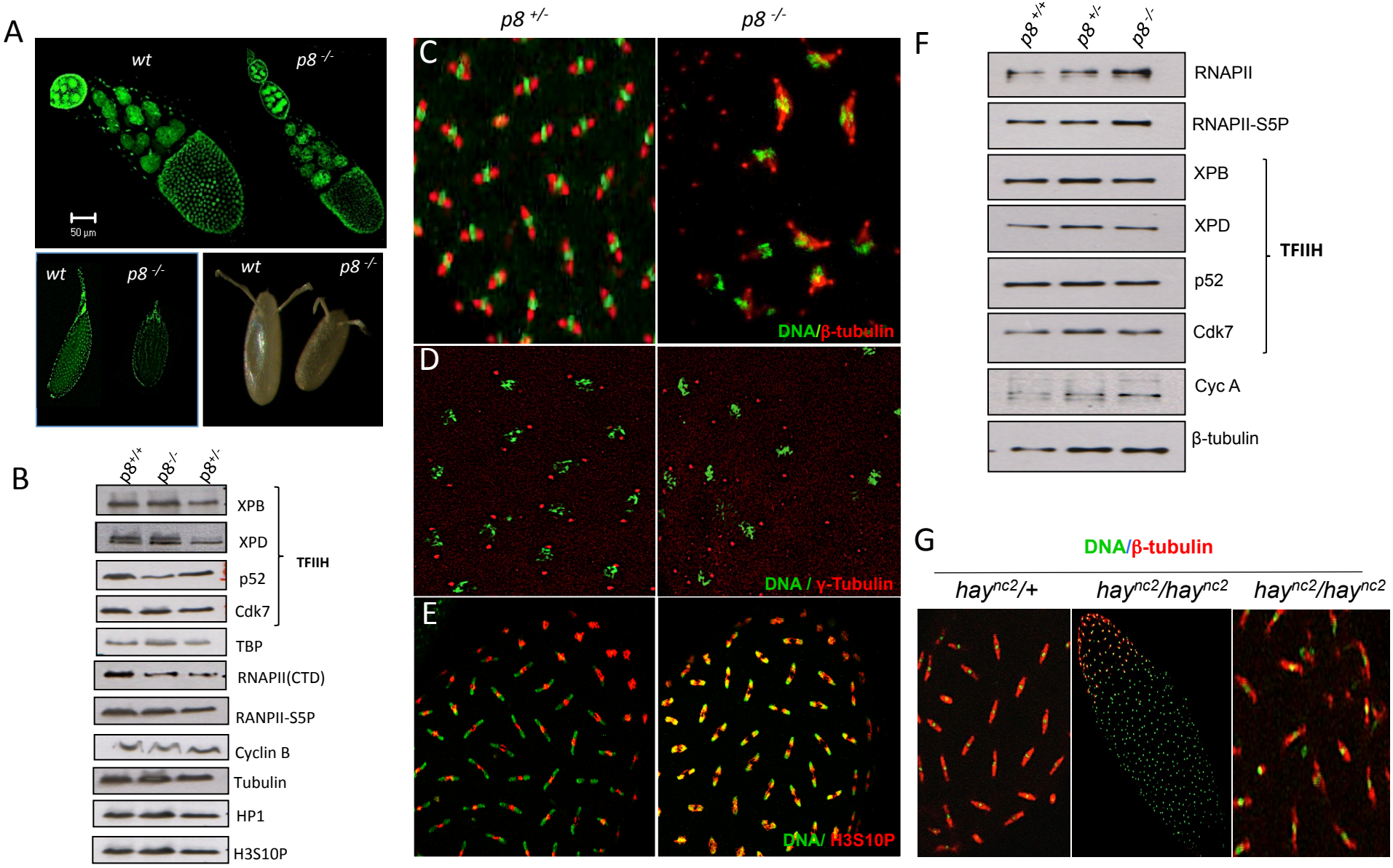
A
wt
p8 -/-
50 µm
wt
p8 -/-
wt
p8 -/-
B
p8+/+
p8-/-
p8+/-
XPB
XPD
p52
Cdk7
TFIIH
TBP
RNAPII(CTD)
RANPII-S5P
Cyclin B
Tubulin
HP1
H3S10P
p8 +/-
p8 -/-
C
DNA/β-tubulin
D
DNA / γ-Tubulin
E
DNA/ H3S10P
F
p8 +/+
p8 +/-
p8 -/-
RNAPII
RNAPII-S5P
XPB
XPD
p52
Cdk7
TFIIH
Cyc A
β-tubulin
G
DNA/β-tubulin
hay nc2/+
hay nc2/hay nc2
hay nc2/hay nc2

Fig. 6

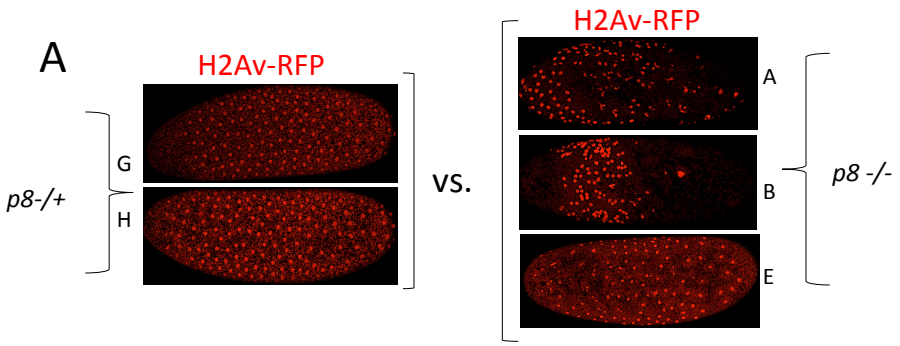
A
H2Av-RFP
p8-/+
G
H
vs.
H2Av-RFP
A
B
E
p8 -/-

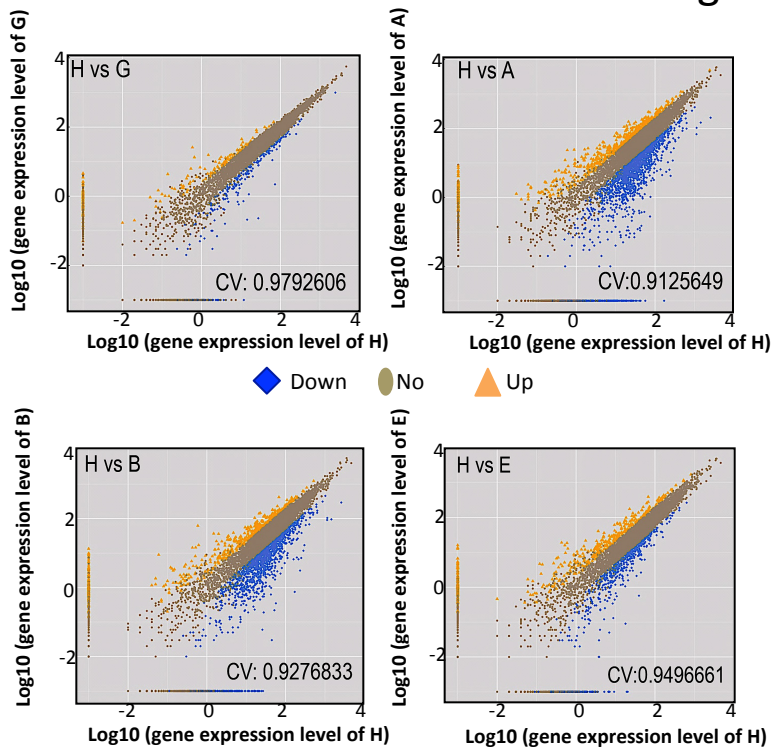
B
H vs G
CV: 0.9792606
H vs A
CV:0.9125649
H vs B
CV: 0.9276833
H vs E
CV:0.9496661
Log10 (gene expression level of G)
Log10 (gene expression level of A)
Log10 (gene expression level of B)
Log10 (gene expression level of E)
Log10 (gene expression level of H)
Down
No
Up

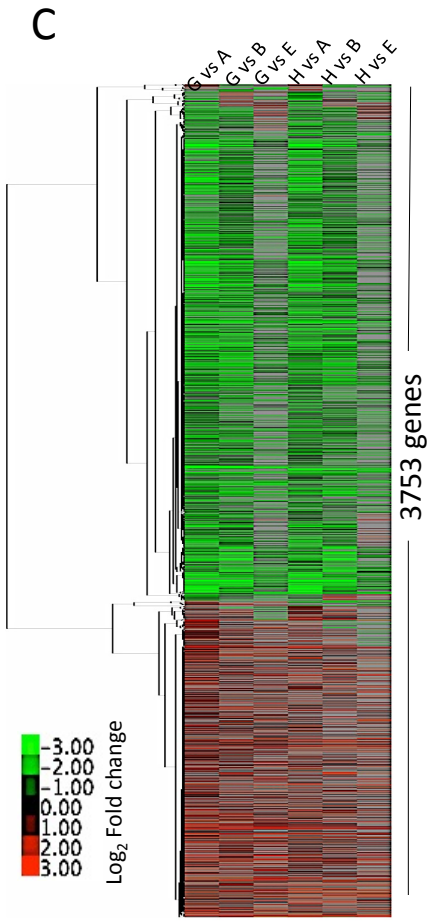
C
G vs A
G vs B
G vs E
H vs A
H vs B
H vs E
3753 genes
-3.00
-2.00
-1.00
0.00
1.00
2.00
3.00
Log2 Fold change

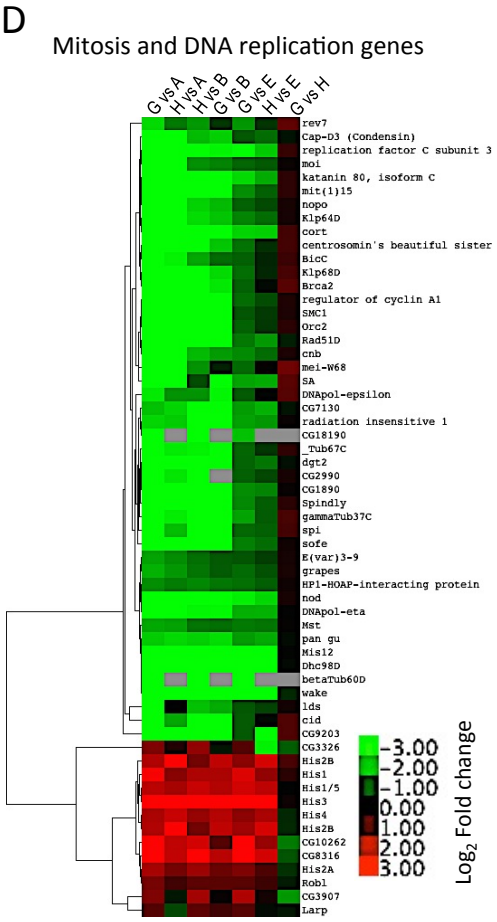
D
Mitosis and DNA replication genes
G vs A
H vs A
H vs B
G vs B
G vs E
H vs E
G vs H
rev7
Cap-D3 (Condensin)
replication factor C subunit 3
mol
katanin 80, isoform C
mit(1)15
nopo
Klp64D
cort
centrosomin's beautiful sister
BicC
Klp68D
Brca2
regulator of cyclin A1
SMC1
Orc2
Rad51D
cnb
mei-W68
SA
DNApol-epsilon
CG7130
radiation insensitive 1
CG18190
_Tub67C
dgt2
CG2990
CG1890
Spindly
gammaTub37C
spi
sofe
E(var)3-9
grapes
HP1-HOAP-interacting protein
nod
DNApol-eta
Mst
pan gu
Mis12
Dhc98D
betaTub60D
wake
lds
cid
CG9203
CG3326
His2B
His1
His1/5
His3
His4
His2B
CG10262
CG8316
His2A
Robl
CG3907
Larp
-3.00
-2.00
-1.00
0.00
1.00
2.00
3.00
Log2 Fold change

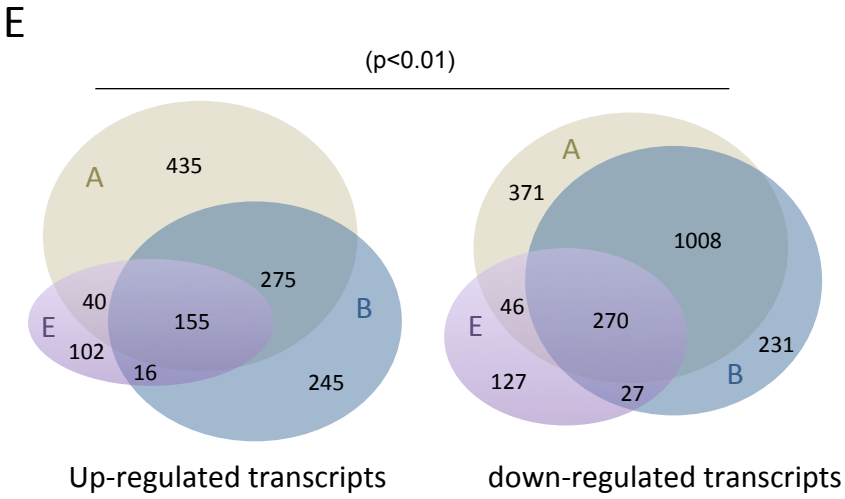
E
(p<0.01)
A
435
275
40
155
B
E
102
16
245
A
371
1008
46
270
231
E
B
127
27
Up-regulated transcripts
down-regulated transcripts

Fig. 7

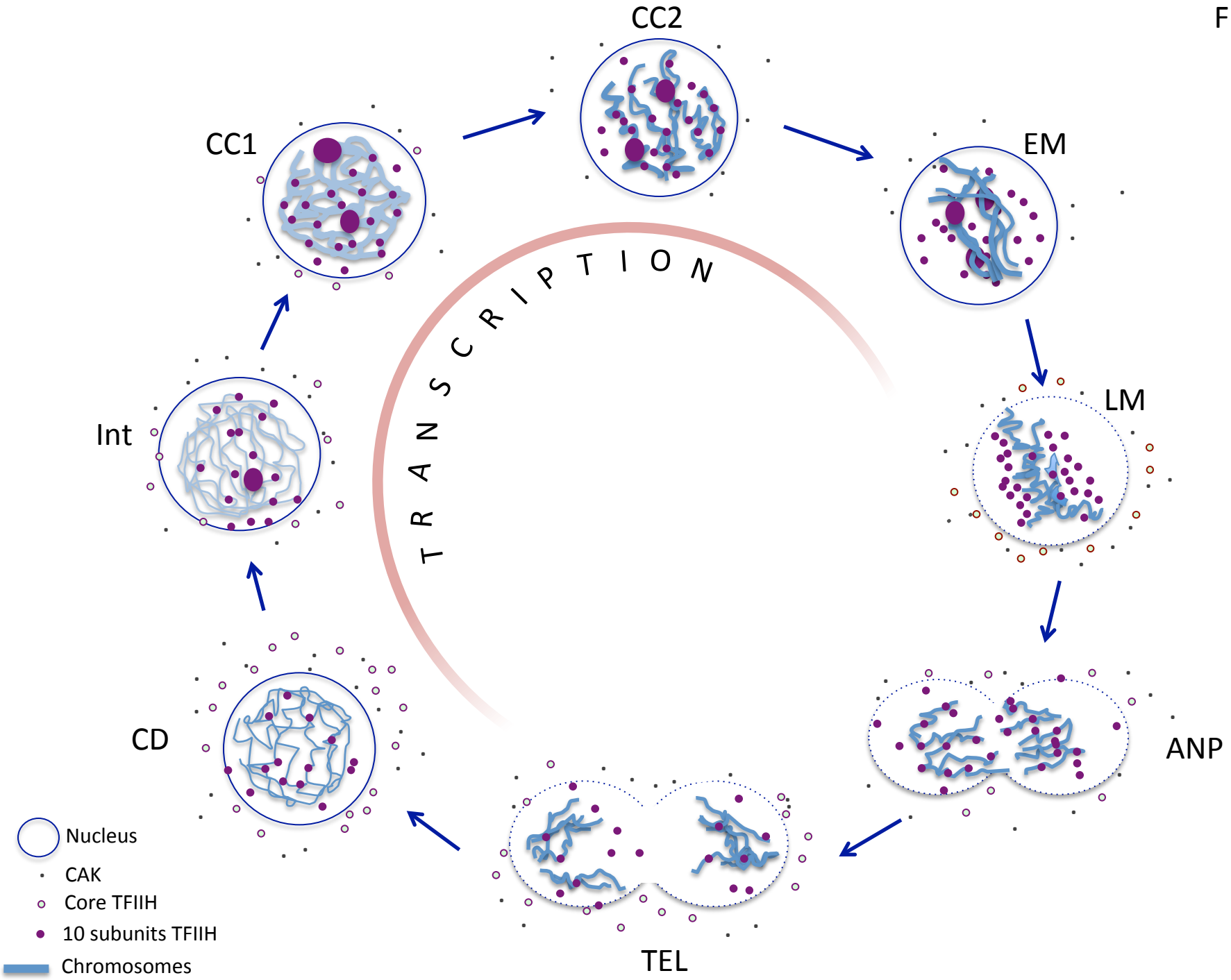
CC2
CC1
EM
TRANSCRIPTION
Int
LM
CD
ANP
TEL
Nucleus
CAK
Core TFIIH
10 subunits TFIIH
Chromosomes

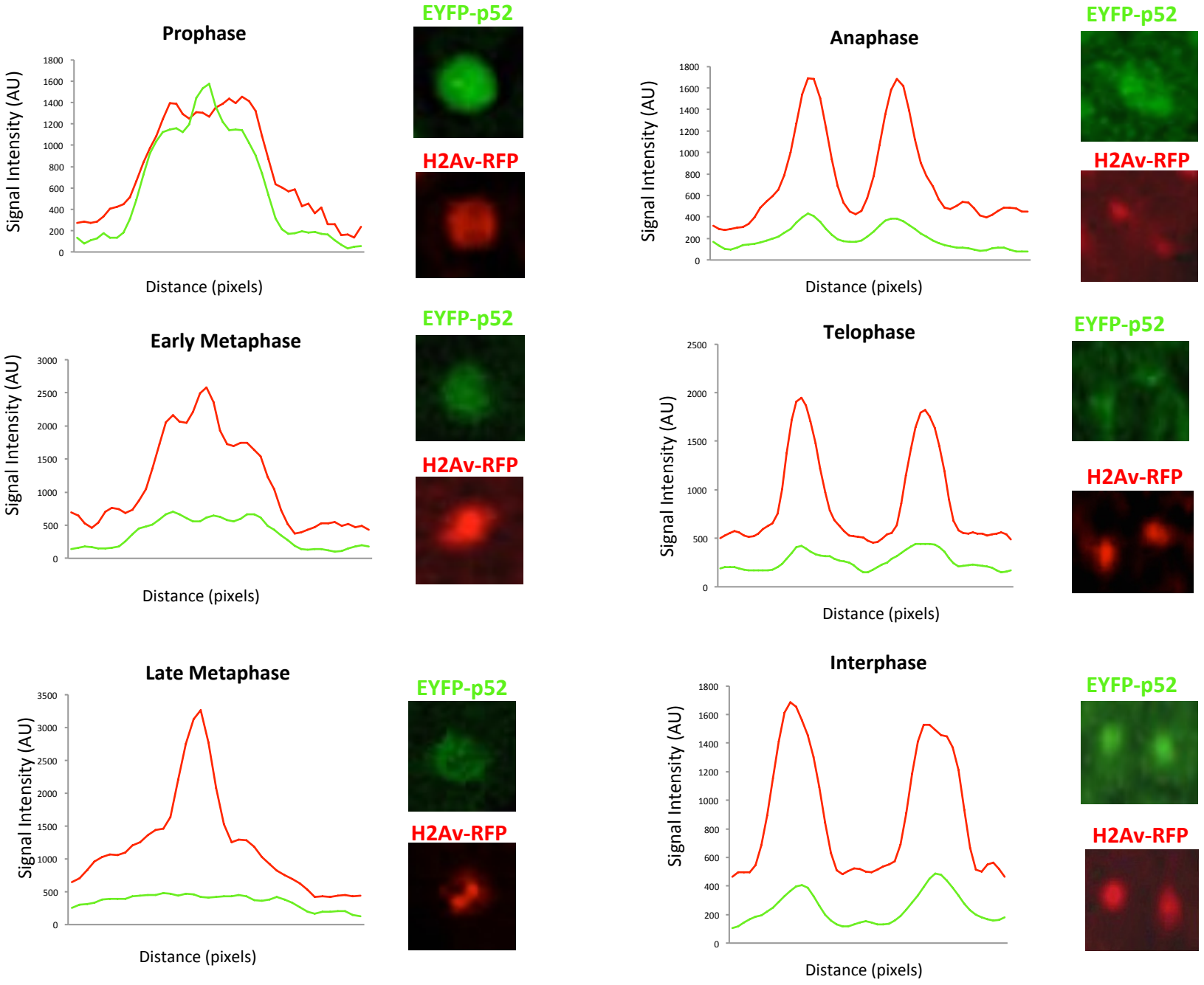
Prophase
Signal Intensity (AU)
Distance (pixels)
EYFP-p52
H2AV-RFP
Anaphase
Signal Intensity (AU)
Distance (pixels)
EYFP-p52
H2Av-RFP
Early Metaphase
Signal Intensity (AU)
Distance (pixels)
EYFP-p52
H2Av-RFP
Telophase
Signal Intensity (AU)
Distance (pixels)
EYFP-p52
H2Av-RFP
Late Metaphase
Signal Intensity (AU)
Distance (pixels)
EYFP-p52
H2Av-RFP
Interphase
Signal Intensity (AU)
Distance (pixels)
EYFP-p52
H2Av-RFP

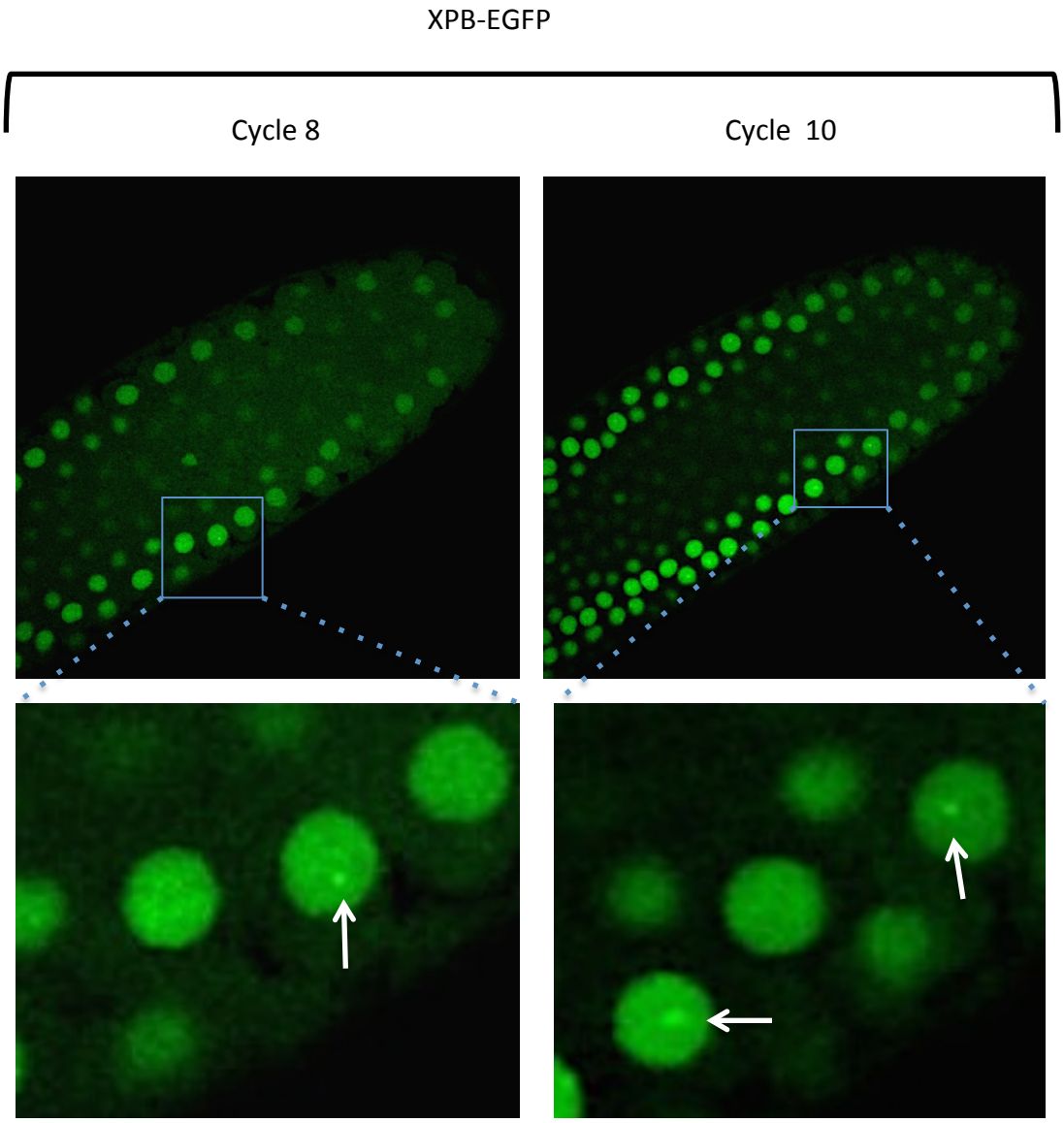
XPB-EGFP
Cycle 8
Cycle 10

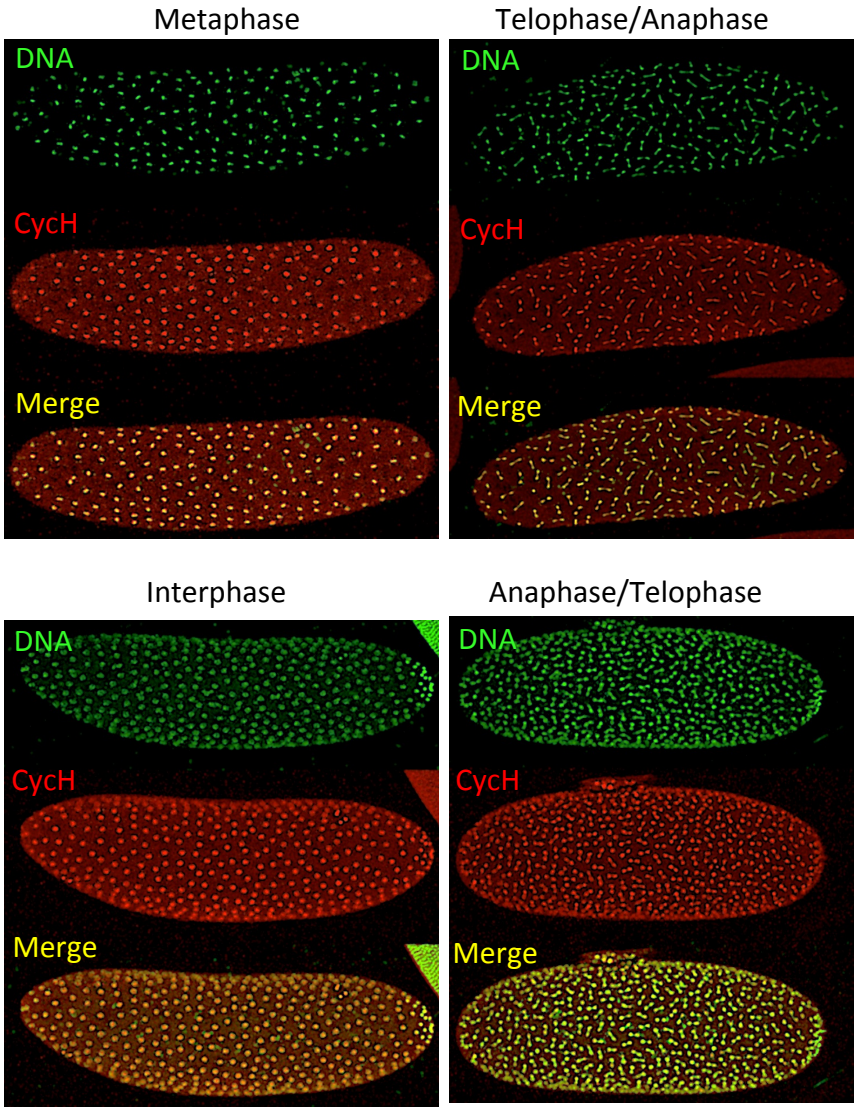
Metaphase
DNA
CycH
Merge
Telophase/Anaphase
DNA
CycH
Merge
Interphase
DNA
CycH
Merge
Anaphase/Telophase
DNA
CycH
Merge

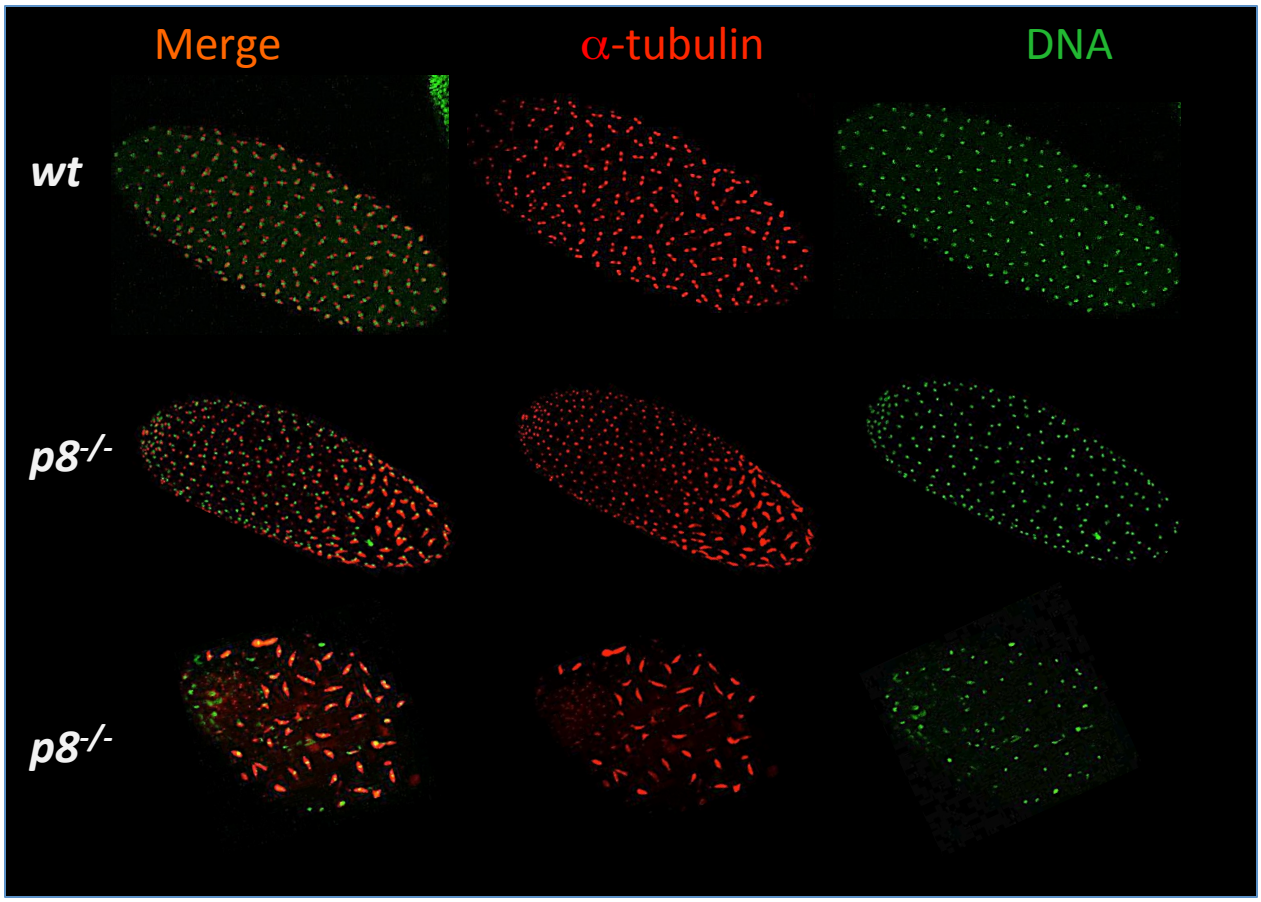
Merge
α-tubulin
DNA
wt
p8-/-
p8-/-

A

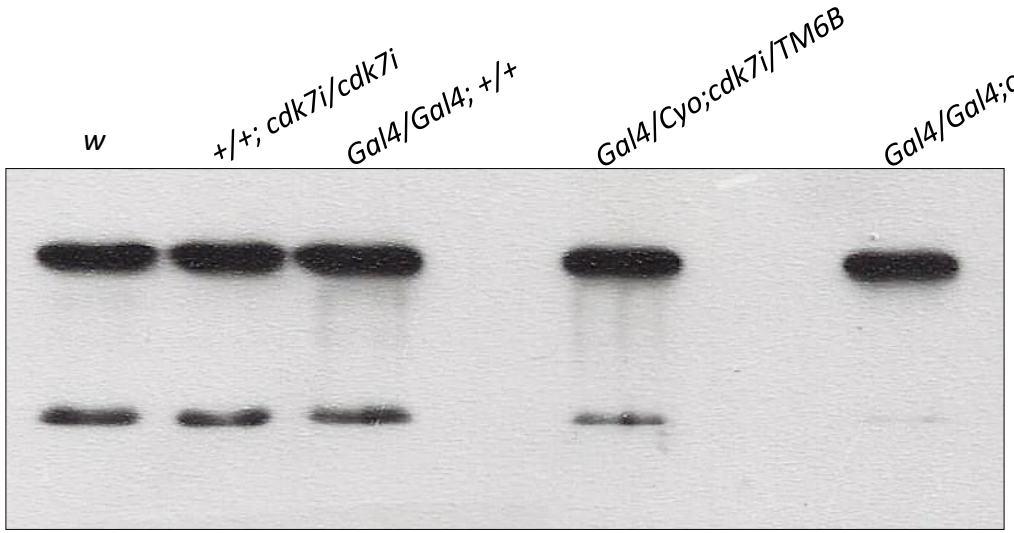
w
+/+; cdk7i/cdk7i
Gal4/Gal4; +/+
Gal4/Cyo;cdk7i/TM6B
Gal4/Gal4;cdk7i/cdk7i
Tubulin
Cdk7

B

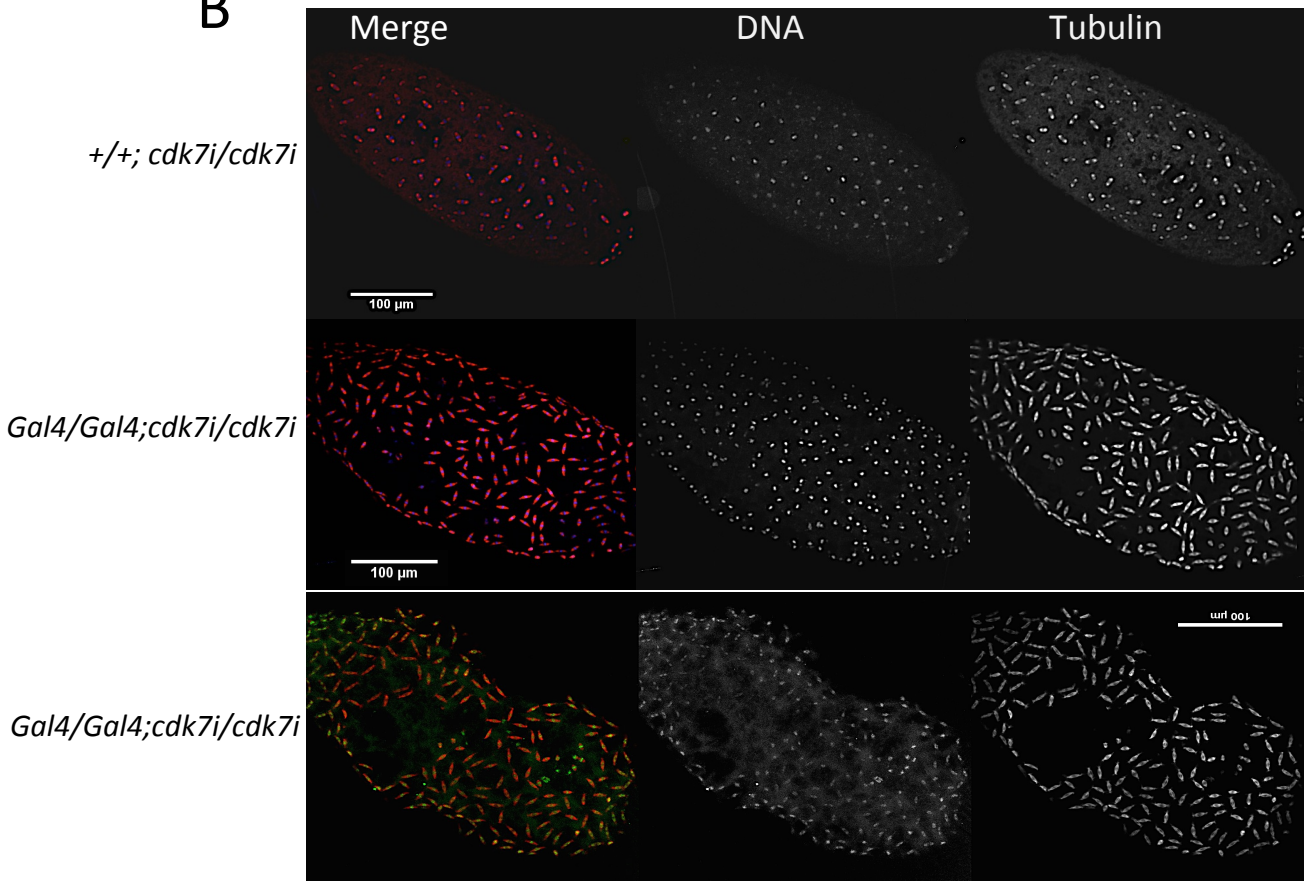
Merge
DNA
Tubulin
+/+; cdk7i/cdk7i
Gal4/Gal4;cdk7i/cdk7i
Gal4/Gal4;cdk7i/cdk7i
100 µm
100 µm

IVYSPRING INTERNATIONAL PUBLISHER

Journal of Cancer

2016; 7(15): 2258-2265. doi: 10.7150/jca.16966

Review

TFIIH: New Discoveries Regarding its Mechanisms and Impact on Cancer Treatment

Mario Zurita✉, Grisel Cruz-Becerra

Departamento de Genética del Desarrollo, Instituto de Biotecnología, Universidad Nacional Autónoma de México. Av. Universidad 2001, Cuernavaca, Morelos 62250, México.

✉ Corresponding author: Mario Zurita, Departamento de Genética del Desarrollo, Instituto de Biotecnología/UNAM. Tel. 52 555 6227657 Email: marioz@ibt.unam.mx.

Received: 2016.07.24; Accepted: 2016.09.30; Published: 2016.11.09

Abstract

The deregulation of gene expression is a characteristic of cancer cells, and malignant cells require very high levels of transcription to maintain their cancerous phenotype and survive. Therefore, components of the basal transcription machinery may be considered as targets to preferentially kill cancerous cells. TFIIH is a multisubunit basal transcription factor that also functions in nucleotide excision repair. The recent discoveries of some small molecules that interfere with TFIIH and that preferentially kill cancer cells have increased researchers' interest to elucidate the complex mechanisms by which TFIIH operates. In this review, we summarize the knowledge generated during the 25 years of TFIIH research, highlighting the recent advances in TFIIH structural and mechanistic analyses that suggest the potential of TFIIH as a target for cancer treatment.

Key words: Anticancer drug, Cell cycle inhibitors, DNA damage, Natural anticancer compounds, Transcription modulators.

Introduction

Since the discovery of TFIIH in the early 1990s by the laboratory of Jean-Marc Egly [54], TFIIH has been the object of extensive research, with studies ranging from structural analyses of the complex to in vitro and in vivo molecular and biochemical evaluations of its functions in transcription and DNA repair. Ten proteins organized in two subcomplexes form the TFIIH complex. Among these proteins, two DNA helicases/ATPases, one of which is also a DNA translocase, a putative E3 ubiquitin ligase and a cyclin-dependent kinase have been identified [2]. However, most of the TFIIH subunits are considered to be regulatory or structural components [3]. The inhibition of some of the TFIIH enzymatic activities has been demonstrated to be effective in cancer treatment [20,41]. Interestingly, recent advances in the solution of the TFIIH complex organization increase the possibility of designing drugs that interfere with the functions of TFIIH. Thus, this review will describe recent discoveries on how TFIIH operates in transcription and DNA repair and how TFIIH is becoming an important target for cancer therapy.

TFIIH's subunits

TFIIH's subunits are organized into two sub-complexes: the CAK and the core, which interact to form the holo-TFIIH complex that is involved in transcription [1]. The CAK contains the cyclin-dependent kinase Cdk7, Cyclin H and MAT1 subunits, which operate in cell cycle control [2,3]. The core is composed of XPB, a 3´-5´ DNA helicase/ATPase, which is also a DNA translocase, XPD, a 5´-3´ DNA helicase/ATPase, p44, a putative E3 ubiquitin ligase, and the structural subunits p62, p52, p34 and p8 [4]. The core of TFIIH plays a determinant role in Nucleotide Excision Repair (NER) [5]. In addition, it has been suggested that XPD modulates the role of the CAK in cell cycle control in an intermediary XPD-CAK complex [6] (Fig. 1). Further, the XPG protein was demonstrated to interact with

XPB, XPD and p62 and copurifies with the holo-TFIIH, suggesting that it could be another component of TFIIH [7–10]. On the other hand, the XPD subunit is also a component of the human MMXD complex, which is required for chromosome segregation and is not related to transcription or DNA repair [11]. However, it is still unknown if the enzymatic activities of XPD helicase/ATPase are necessary for the function of MMXD in chromosome segregation during mitosis. Moreover, the possibility of other subunits of TFIIH, besides XPD, being a part of other protein complexes still is open.

Several protein-protein interactions among the components of TFIIH have been identified by different approaches. Although the crystallographic structure of some subunits and the global architecture of TFIIH has been determined using high-resolution cryo-electron microscopy [10,12,13], determining the atomic structure of this complex is a great challenge. The interaction network in the 10-subunit complex has been recently described using chemical cross-linking combined with mass spectrophotometry and previous high-resolution electron microscopy data. This integrative analysis showed that the p34/p44 heterodimer represents a central "submodule" that connects the other core subunits. The VWA domains of p34 and p44 were shown to contact each other at multiple sites. In addition, these domains interact with p62 and p52. In turn, p62 interacts with XPD. Furthermore, XPD and XPB contact each other and both interact with p44, as well as with MAT1, which anchors Cdk7 and CycH [10]. In addition to the previously reported interactions between XPB and p52 and between p8 and p52, this analysis shows that the p8/p52 heterodimer directly interacts with XPB and p8 does not contact XPD, as was previously suggested [5,10,14]. This detailed model of the TFIIH architecture could be useful to search for drugs that affect the interface between the different subunits through in silico modeling approaches.

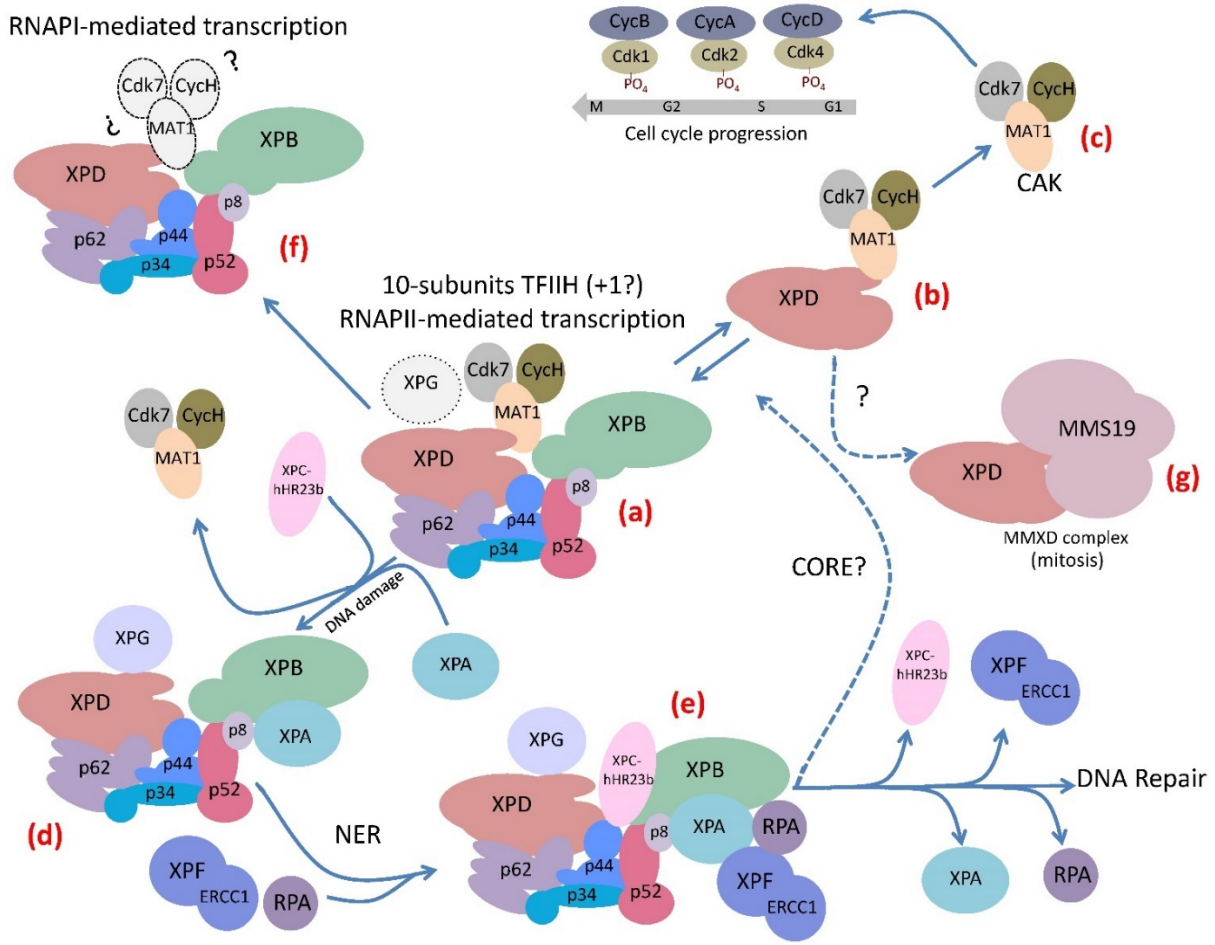

Figure 1. The complex life of TFIIH. (a) The 10-subunit TFIIH participates in transcription by RNA polymerase II. The XPG endonuclease participates in RNAPII transcription by binding to TFIIH. (b) The XPD subunit of TFIIH forms an intermediary complex with the CAK. (c) The CAK subcomplex phosphorylates several cdks that participates in cell cycle regulation. (d) The core subcomplex losses the CAK by the incorporation of XPA to TFIIH when the complex detects a bulky lesion in the DNA. (e) After the recognition of the damaged strand in the DNA the Pre-Incision-Complex is formed by TFIIH and other components of the NER machinery that maintain the reparation bubble in the DNA damaged region, it is stabilized by XPA and RPA and then the XPG and XPF-ERCC1 endonucleases cut the damaged strand. After that a DNA polymerase and a ligase repair the DNA. (f) TFIIH participates in rRNA elongation during RNAPI transcription. However it is unknown whether the CAK subcomplex participates in this mechanism. (g) The XPD subunit is a component of the MMXD complex that is important for the proper segregation of chromosomes during mitosis.

TFIIH-related human diseases

There is a relationship between mutations in some of the TFIIH subunits and three human syndromes associated with DNA repair and transcriptional deficiencies. Most of the TFIIH-affected patients show mutations in the XPB and XPD subunits, which are linked to xeroderma pigmentosum (XP), Cockayne syndrome (CS) and trichothiodystrophy (TTD) [7]. However, the different mutations described in the p8 subunit in humans have only been related to TTD-A [5]. Photosensitivity is a clinical feature among all these diseases, other manifestations are shared in a less extent and some others are syndrome-specific (Fig. 2). For example, XP patients affected in XPD or XPB can develop skin cancer, but TTD patients with different mutations in the same genes are not cancer prone. On the other hand, anomalies in the hair, nails and skin are hallmarks in TTD patients. In agreement, recent studies demonstrated a correlation between skin defects and alterations in the levels of collagen types I and VI in the extracellular matrix (ECM) of primary dermal fibroblast and skin from TTD patients [15,16]. Orioli and colleagues demonstrated the transcript down-regulation of the COL6A1 gene (which encodes for the collagen type VI alpha1 subunit) in skin fibroblasts from XPD-affected TTD patients [16]. On the other hand, transcript overexpression and high protein levels of the active form of the matrix metalloproteinase 1 (which degrades the interstitial collagen from the ECM) and concomitant low levels of collagen type I were detected in primary dermal fibroblast and skin from several different TFIIH-affected TTD patients, when compared with fibroblast from TFIIH-affected XP patients or healthy normal donors [15]. In addition, differential alterations in the TFIIH assembly at the *RARB2* promoter, TFIIH enzymatic activities and chromatin remodeling were revealed by the analysis of the transcriptional role of TFIIH in several cell lines bearing mutations in XPB, XPD or p8. Interestingly the strongest defects were observed in cell lines carrying point mutations in the N-terminal domain of XPB found in TTD or XP/CS patients, while point mutations of the p8 show no effect on any of the steps analyzed [17]. Strikingly, the study of the phenotypes of these patients in relation to the identification of the molecular nature of the mutations that they carry in these genes have been very useful to understand how TFIIH works and reciprocally, to understand these syndromes. An enigmatic question that rises from the analysis of the manifestations in the patients afflicted in XPB, XPD and p8 is why these individuals only present very specific phenotypes even that TFIIH is required for three fundamental cellular functions? Although we still do not have a conclusive answer for this question, we know that the described mutations from these patients are not null and only partially affect the TFIIH functions, making these defects in TFIIH compatible with life [4,18,19].

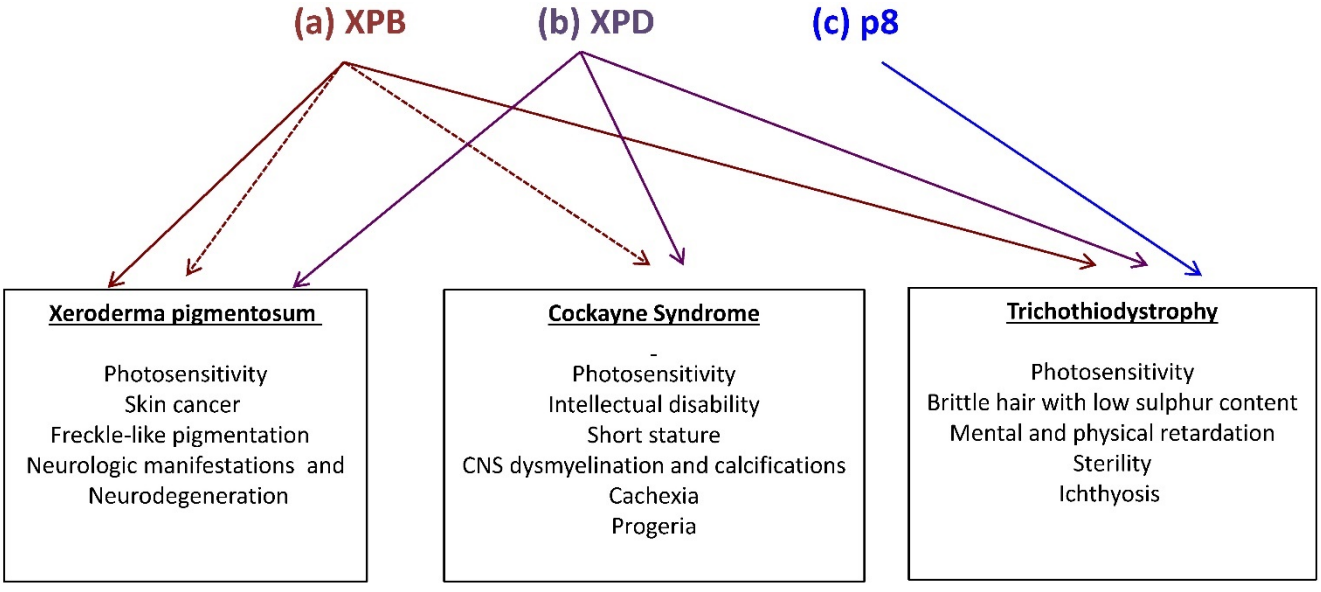

Figure 2. Mutations in the XPB, XPD and p8 subunits of TFIIH are associated with three human syndromes: xeroderma pigmentosum (XP), Cokayne syndrome (CS) and trichothiodystrophy (TTD). (a) Mutations in XPB may generate TTD, XP (brown continuous arrow) or combinations of XP with CS (brown fragmented arrows). (b) Mutations in XPD may generate any of the three syndromes (purple continuous arrow) (c) Mutations in p8 (blue) on the other hand, are only linked to TTD. Syndrome-associated features are enlisted.

TFIIH's functions

Cell Cycle. As mentioned before components of TFIIH participates at least in three functions in the cell. The CAK has a central role in the activities of several Cdks that control cell cycle [2]. Cdk7 phosphorylates Cdk4 controlling the transition G1 to S phase. Also it phosphorylates Cdk2 to promote the entrance for S to G2 phases and Cdk1 to conduct G2 to mitosis [3] (Fig. 1). CAK subunits as the case of the rest of TFIIH are expressed constitutively during G1 in all cells, it is always active and seems to be very promiscuous in the phosphorylation of the Cdks that control the cell cycle which are modulated by specific cyclins. Therefore, the CAK is more like a supported factor for the control of the cell cycle than a regulator. It will be interesting to use the new Cdk7 inhibitor TZH1 [20], which is very specific to see how the cell cycle is affected when the catalytic activity of Cdk7 is inhibited.

Nucleotide excision repair. NER removes helix-distorting DNA lesions that include cyclobutane pyrimidine-pyrimidine dimers and pyrimidine-pyrimidone (6-4) photoproducts. Two pathways recognize this type of DNA damage: transcription coupled-NER (TC-NER) in the actively transcribed DNA strands and global genome-NER (GG-NER) in the non-transcribed DNA sequences. In TC-NER, the RNA polymerase, which is stalled in the presence of a bulky lesion, recognizes the DNA damage. In GG-NER, depending on the DNA-damaging agent, the protein complex RAD23B-Centrin 2 or XPE recognizes the bulky DNA lesion. In any case, the DNA damage recognition step is followed by the recruitment of the NER machinery, including TFIIH, which unwinds the DNA by the ATPase and helicase activities of XPB and XPD, respectively, the XPA and RPA proteins that stabilize the DNA repair bubble, and the endonucleases XPF-ERCC1 and XPG, which remove a segment of 23-27 nucleotides from the damaged DNA strand, which is ultimately refilled by the DNA replication machinery [21–23] (Fig. 1). It was initially proposed that after TFIIH recruitment, the CAK subcomplex dissociates from the core in an XPA-dependent manner [24]. New data suggest that the holo-TFIIH scans the DNA through its XPB and XPD helicase/ATPase activities, which are inhibited by bulky DNA lesions. Then, TFIIH is stalled in the damaged DNA region, followed by the ejection of CAK from the core [25]. However, in vivo experiments are required to confirm this model.

Transcription. TFIIH participates in transcription mediated by RNA polymerases I and II; however, our understanding of the role of TFIIH in RNAPI transcription is still obscure. Since the first report by Grummt and Elgy's groups in 2002, which demonstrated that TFIIH is dispensable for the initiation of RNAPI transcription but required for rRNA elongation [26], only a few studies about the role of TFIIH in RNAPI-mediated transcription have been published. For example, it has recently been reported that TFIIH binds to RNAPI after the initiation of transcription. In agreement, the ATPase activity of XPB is required during rRNA elongation, and CS-related mutations in XPB and XPD disturb the interaction between TFIIH and rDNA, which affects elongation but not transcription initiation [27,28]. In addition, it has been suggested that the NER-related proteins CSB and CSA form a complex with TFIIH in the nucleolus, which is necessary for rDNA transcription [29,30].

However, more extensive studies have been performed to elucidate the role of TFIIH in RNAPII transcription. During the Pre-Initiation Complex (PIC) assembly, TFIIH is recruited by TFIIE and binds to RNAPII [31]. While the enzymatic activities of XPD are dispensable for RNAPII transcription, the ATPase activity of XPB is required for the unwinding of 11 bp in the promoter during the formation of the open complex [32,33]. This configuration is stabilized by the RNAPII cleft and jaw domains [13,34]. Interestingly, XPB does not directly bind at the site of DNA unwinding. Instead, XPB tracks the DNA in a 5´-3´ direction and translocates the downstream DNA into the cleft region of the RNAPII, which generates the DNA unwinding and allows the recognition of the transcription initiation start site in a process that requires the continuous hydrolysis of ATP by XPB [33]. In addition, the current PIC structure model shows that XPB binds downstream of the initiator site and contacts both DNA strands in the promoter [13]. Then, the function of XPB in transcription relies on its translocase activity, and this mechanism is a rate-limiting step in the initiation of transcription. The other major function of TFIIH in RNAPII transcription takes place through its kinase activity. The kinase module phosphorylates serines 5 and 7 (S_5 and S_7) of the heptapeptide repeat (consensus sequence: $Y_1S_2P_3T_4S_5P_6S_7$) in the CTD of the largest subunit of RNAPII. It has been established that S_5 phosphorylation is fundamental for transcription initiation and promoter clearance [35]. However, the in vitro inhibition of the kinase activity of Cdk7 by the Cdk7-specific inhibitor THZ1 (see ahead) had no effect on transcription initiation and promoter realese, but preferentially affected the pausing of the RNAPII after the synthesis of 30-50 nucleotides [36]. Furthermore, the phosphorylation of S_5 by Cdk7 is important for the recruitment of the pausing factors,

the Negative Elongation Factor (NELF) and the DRB-sensitive factor (DSIF), as well as the capping enzyme that guanylates the 5´end of the nascent transcript, a process that requires pausing [37]. However, more recent in vivo experiments in budding yeast show that by using an engineered Kin28 (Cdk7 in yeast) that can be specifically and irreversible inhibited, affect promoter scape as well as RNAPII elongation [38]. Intriguingly, in the absence of S_5 phosphorylation of the CTD, the RNAPII is paused after the transcription initiation site [38]. Then these recent reports, one in vitro [36], and the other in vivo [38] using the budding yeast about the role of the Cdk7 on RNAP II transcription initiation and elongation partially disagree. It will be relevant to perform similar experiments as the reported in yeast, but in human cells. On the other hand, it has been demonstrated that mutations in Kin28 reduce the dissociation of the mediator from the PIC, which affects the escape of the RNAPII to initiate mRNA elongation [39]. Therefore, all of these new data and models on how TFIIH operates in transcription in vitro must be integrated with the in vivo results.

TFIIH as a target for cancer therapy

It is well established that cancer cells require high levels of transcription to survive and to maintain their malignant phenotype [40]. Therefore, the components of the basal transcription machinery could be considered good targets to reduce global transcription, and they might have stronger effects in cancer cells when compared with non-cancerous cells (reviewed in 39).

A very promising drug for the treatment of many cancer types is triptolide (TPL). TPL is a diterpen triepoxide purified from the plant *Tripterygium wilfordii*. Extracts from this plant have been used for centuries in traditional Chinese medicine, and preclinical studies have shown high effectiveness against cancer due to its very strong anti-proliferative effect and apoptosis induction. TPL binds covalently to the ATPase domain of XPB, inhibiting both RNAPII transcription and NER [41]. Although other TPL targets have been proposed, structural and biochemical data show that it is very specific for XPB, and intriguingly, the treatment of *Drosophila* imaginal discs with TPL phenocopies the defects observed in different TFIIH mutant subunits in the fly [41–43]. RNA-seq and DNA microarray analyses from TPL-treated cancerous cells have shown the down-regulation of nearly all the RNAPII-dependent transcripts [44,45]; however, comparative studies at this level between cancer cells and their progenitors are required. TPL is not highly permeable to the cell membrane, and it is hepatotoxic [46]. To overcome these inconveniences in cancer therapy, more permeable and potentially less toxic TPL derivatives have been developed, although it will be important to demonstrate that they are as effective as TPL to kill cancer cells [41].

Based on structural analysis predictions, other drugs have been developed to specifically target the enzymatic functions of TFIIH. For example, the antitumor drug BS-181 is a pyrazolo [1,5-a] pyrimidine-derived compound that inhibits the phosphorylation of Cdk7 targets, inducing cell cycle arrest and apoptosis [45]. More recently, it was shown that THZ1 is a phenylaminopyrimidine with a cysteine reactive acrylamide moiety that covalently binds to the cysteine 312 located outside of the catalytic domain, making THZ1 very specific for Cdk7 [20], although it inhibits Cdk12 at very high concentrations and after long incubation times [36]. Approximately 1000 cancerous cell lines tested were very sensitive to nanomolar concentrations of THZ1, particularly T acute lymphoblastic leukemia cells [20]. Intriguingly, gene-specific effects in transcription were observed in different cell lines after the THZ1 treatment [20,47,48]. For example, the expression of RUNX1, a transcription factor associated with leukemia and whose expression is modulated by a super-enhancer, was highly sensitive to THZ1 [20] (Fig. 3). Similarly, THZ1 affects the expression of genes controlled by super-enhancers, particularly Myc, as well as lineage-specific transcription factors required by the maintenance of the cancerous phenotype in lung cancer cells [47,49] (Fig. 3). However, a new study showed a high potential for THZ1 in the treatment of triple negative breast cancer (TNBC) tumors [50]. TNBC cells were substantially more sensitive to THZ1 when compared to ER/Pr^+ (positive for the estrogen receptor) tumor cells. Interestingly, some sets of genes that encode for signal transduction and transcription factors related to breast cancer, such as TGFβ, STAT, EGFR, and WNT, among other genes, were affected; these genes were named the Achilles cluster of TNBC, and their expression is also regulated by super-enhancers [50]. Therefore, it seems that genes modulated by super-enhancers, which are large regions of DNA that accumulate large quantities of transcription factors [48] and are directly involved in the cancerous phenotype, may be more sensitive to THZ1 [20,47,49] (Fig. 3). A new THZ1 analog named THZ2 is more stable than THZ1 and has an improved effect on Cdk7 inhibition [50].

Another recently identified TFIIH inhibitor is spironolactone (SP), which induces the proteasome-mediated degradation of the XPB subunit and enhances the effect of platinum derivatives in

cancer cells [51]. The SP-induced degradation of XPB clearly affects both NER and transcription. The effect of SP in tumor cells from different origins should be analyzed to determine whether it also preferentially kills malignant cells.

Conclusions and Perspectives

Twenty-five years after the discovery of TFIIH, we have a more comprehensive view of the mechanisms of different functions of TFIIH; however, there are still many questions that must be answered. Although we understand when the enzymatic activities of TFIIH are required and the identities of some of their substrates, it is highly possible that other targets will be discovered. For example, Cdk7 may phosphorylate other transcription factors. TFIIH exhibits crosstalk with the mediator [52] which may be modulated by TFIIH and vice versa; however, this intercommunication is not clear. The role of the other subunits of the core that lack enzymatic activities may be modulators of TFIIH activity, as p52 regulates the ATPase activity of XPB. In addition, p38 and p62 have protein domains that suggest dynamic interactions with the other subunits of the core, and we believe that the complex is not static and exhibits strong internal dynamics. However, important questions remain; for example: Is p44 really a ubiquitin ligase, and if so, what are its targets? Is p8 a real stabilizer of the complex, or does it have a regulatory role in the XPB ATPase activity? Is the CAK subcomplex required for rDNA transcription even if the RNAPI lacks a CTD domain such as the one present in RNAPII? In addition, the fact that two promising drugs for the treatment of cancer exhibit target subunits of TFIIH suggests that new small molecules may be found that inhibit TFIIH but recognize other subunits besides XPB and Cdk7. Furthermore, because we understand in detail the regions of each of the 10 subunits of TFIIH that interact, it is possible to search for small molecules that interrupt the interface of these interactions and affect the assembly of TFIIH and therefore, its functions (Fig. 4). In fact, a new antibiotic that inhibits the interaction between a mediator subunit with a transcriptional activator and that preferentially kills a pathogen fungus has recently been identified [53]. A similar approach may be used to look for new inhibitors of TFIIH. On the other hand, a challenging problem for the development and use of drugs that target nuclear factors is to increase the permeability of these compounds in the nucleus. The treatment with TPL or THZ1 cause an important reduction in transcription in cancer cell lines, showing that an important amount of these molecules permeates the nuclear membrane [4,44,45], however more precise experiments with animal models are needed. In addition, new methods to increase the efficiency to deliver new drugs to the nucleus still have to be developed.

In conclusion, further studies of TFIIH should explore how the complex works at high resolution in transcription and DNA repair, how defects in TFIIH affect development, and why it is an important target for cancer therapy.

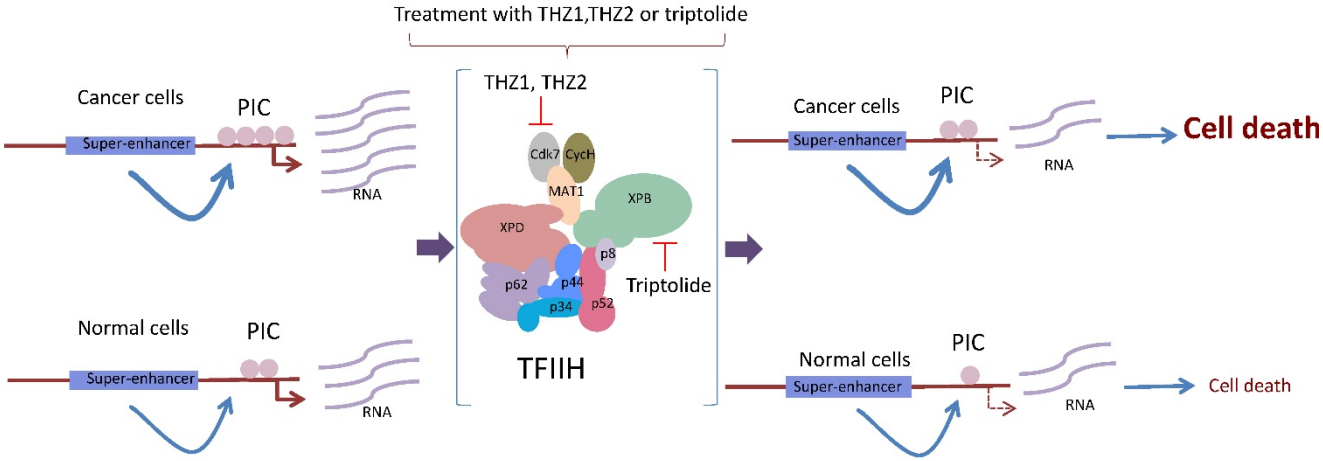

Figure 3. The cancerous cell requires high levels of global transcription to maintain its malignant phenotype. Highly transcribed genes in cancer cells, such as oncogenes, are modulated by super enhancers. These super-enhancers allow the incorporation of the basal transcription machinery at higher frequency in the cancerous cell. The incubation of these cells with either THZ1, THZ2 or triptolide affects the functions of TFIIH by reducing the rate of transcription initiation and elongation, which has a more deleterious effect in malignant than in normal cells.

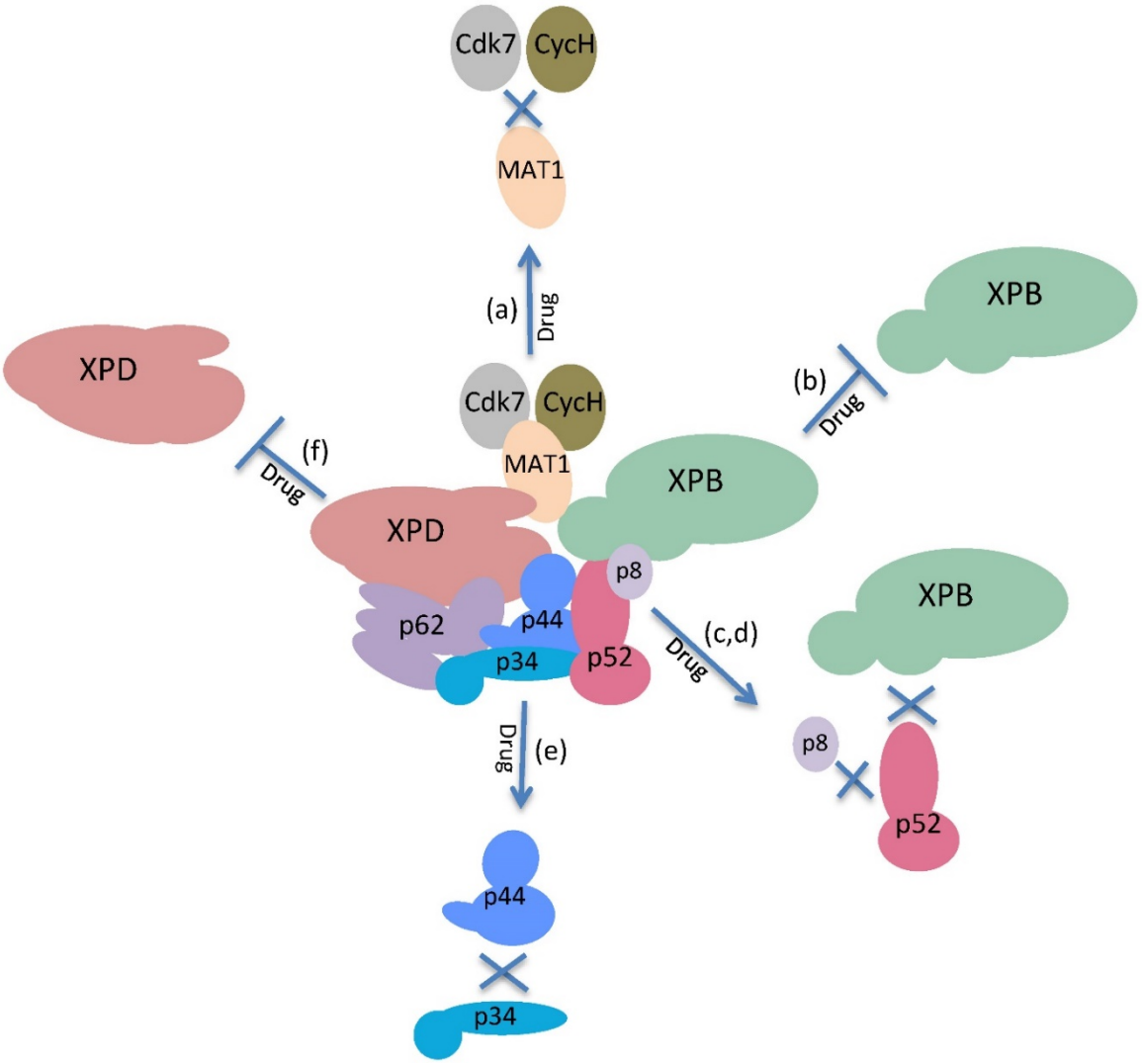

Figure 4. The enzymatic activities and physical interactions of the subunits of TFIIH could be targets for drugs in cancer treatment. Possible targets for the inactivation of the functions of TFIIH: (a) Disruption of the interactions of the MAT1 subunit with cdk7 and Cyc H. (b) Inhibition of the DNA translocase and ATPase activities of XPB. (c,d) Disruption of the interaction of p52 with p8 or XPB. (e) Disruption of the interactions of p34 with p44. (f) Inhibition of the DNA helicase/ATPase activities of XPD.

Abbreviations

RNAPII: RNA polymerase II; RNAPI: RNA polymerase I; NER: nucleotide excision repair; XP: xeroderma pigmentosum; CS: Cockayne syndrome; TTD: trichothiodystropy; TTD-A: trichothiodystropy complementation group A; ECM: extracellular matrix; TC-NER: transcription coupled-NER; GG-NER: global genome-NER; PIC: pre-initiation complex; NELF: negative elongation factor; DSIF: DRB-sensitive factor; TPL: triptolide; TNBC: triple negative breast cancer; SP: spironolactone; CNS: central nervous system.

Acknowledgments.

This work was supported by the grants from CONACyT 219673 and DGAPA UNAM number IN200315.

Competing Interests

The authors have declared that no competing interest exists.

References

1. Zurita M, Merino C. The transcriptional complexity of the TFIIH complex. TRENDS Genet. 2003;19:578–84.
2. Fisher RP. Secrets of a double agent: CDK7 in cell-cycle control and transcription. J. Cell Sci. 2005;118:5171–80.
3. Schachter MM, Merrick KA, Larochelle S, Hirschi A, Zhang C, Shokat KM, et al. A Cdk7-Cdk4 T-Loop Phosphorylation Cascade Promotes G1 Progression. Mol. Cell. 2013;50:250–60.
4. Egly J-M, Coin F. A history of TFIIH: Two decades of molecular biology on a pivotal transcription/repair factor. DNA Repair (Amst). 2011;10:714–21.
5. Compe E, Egly J-M. TFIIH: when transcription met DNA repair. Nat. Rev. Mol. Cell Biol. 2012;13:476–476.
6. Li X, Urwyler O, Suter B. Drosophila Xpd regulates Cdk7 localization, mitotic kinase activity, spindle dynamics, and chromosome segregation. PLoS Genet. 2010;6:10.1371/journal.pgen.1000876.
7. Schärer OD. The molecular basis for different disease states caused by mutations in TFIIH and XPG. DNA Repair (Amst). 2008;7:339–44.
8. Narita T, Narita K, Takedachi A, Saijo M, Tanaka K. Regulation of Transcription Elongation by the XPG-TFIIH Complex Is Implicated in Cockayne Syndrome. Mol. Cell. Biol. 2015;35:3178–88.

9. Ito S, Kuraoka I, Chymkowitch P, Compe E, Takedachi A, Ishigami C, et al. XPG Stabilizes TFIIH, Allowing Transactivation of Nuclear Receptors: Implications for Cockayne Syndrome in XP-G/CS Patients. Mol. Cell. 2007;26:231–43.
10. Luo J, Cimermancic P, Viswanath S, Ebmeier CC, Kim B, Dehecq M, et al. Architecture of the Human and Yeast General Transcription and DNA Repair Factor TFIIH. Mol. Cell. 2015;59:794–806.
11. Ito S, Tan LJ, Andoh D, Narita T, Seki M, Hirano Y, et al. MMXD, a TFIIH-Independent XPD-MMS19 Protein Complex Involved in Chromosome Segregation. Mol. Cell. Elsevier; 2010;39:632–40.
12. Grünberg S, Hahn S. Structural insights into transcription initiation by RNA polymerase II. Trends Biochem. Sci. 2013;38:603–11.
13. Louder R, He Y, Lopez-Blanco J, Fang J, Chacon P, Nogales E. Structure of promoter-bound TFIID and model of human pre-initiation complex assembly. Nature. 2016;531:604–9.
14. Coin F, De Santis LP, Nardo T, Zlobinskaya O, Stefanini M, Egly JM. p8/TTD-A as a repair-specific TFIIH subunit. Mol. Cell. 2006;21:215–26.
15. Arseni L, Lanzafame M, Compe E, Fortugno P, Afonso-Barroso A, Peverali FA, et al. TFIIH-dependent MMP-1 overexpression in trichothiodystrophy leads to extracellular matrix alterations in patient skin. Proc. Natl. Acad. Sci. U. S. A. 2015;112:1499–504.
16. Orioli D, Compe E, Nardo T, Mura M, Giraudon C, Botta E, et al. XPD mutations in trichothiodystrophy hamper collagen VI expression and reveal a role of TFIIH in transcription derepression. Hum. Mol. Genet. 2013;22:1061–73.
17. Singh A, Compe E, Le May N, Egly JM. TFIIH subunit alterations causing xeroderma pigmentosum and trichothiodystrophy specifically disturb several steps during transcription. Am. J. Hum. Genet. 2015;96:194–207.
18. Singh A, et al. TFIIH Subunit Alterations Causing Xeroderma Pigmentosum and Trichothiodystrophy Specifically Disturb Several Steps during Transcription. 2015.
19. Theil AF, Nonnekens J, Steurer B, Mari PO, de Wit J, Lemaitre C, et al. Disruption of TTDA Results in Complete Nucleotide Excision Repair Deficiency and Embryonic Lethality. PLoS Genet. 2013;9:e1003431. doi:10.1371/journal.pgen.1003431.
20. Kwiatkowski N, Zhang T, Rahl PB, Abraham BJ, Reddy J, Ficarro SB, et al. Targeting transcription regulation in cancer with a covalent CDK7 inhibitor. Nature. Nature Publishing Group; 2014;511:616–20.
21. Liu X. In vitro chromatin templates to study nucleotide excision repair. DNA Repair (Amst). 2015;36:68–76.
22. Schärer OD. Nucleotide Excision Repair in Eukaryotes. Cold Spring Harb Perspect Biol. 2013;5:doi: 10.1101/cshperspect.a012609.
23. Oksenych V, Coin F. The long unwinding road: XPB and XPD helicases in damaged DNA opening. Cell Cycle. 2010;9:90–6.
24. Coin F, Oksenych V, Mocquet V, Groh S, Blattner C, Egly JM. Nucleotide Excision Repair Driven by the Dissociation of CAK from TFIIH. Mol. Cell. 2008;31:9–20.
25. Li CL, Golebiowski FM, Onishi Y, Samara NL, Sugasawa K, Yang W. Tripartite DNA Lesion Recognition and Verification by XPC, TFIIH, and XPA in Nucleotide Excision Repair. Mol. Cell. 2015;59:1025–34.
26. Iben S, Tschochner H, Bier M, Hoogstraten D, Hozak P, Egly JM, et al. TFIIH plays an essential role in RNA polymerase I transcription. Cell. 2002;109:297–306.
27. Assfalg R, Lebedev A, Gonzalez OG, Schelling A, Koch S, Iben S. TFIIH is an elongation factor of RNA polymerase I. Nucleic Acids Res. 2012;40:650–9.
28. Nonnekens J, Perez-Fernandez J, Theil AF, Gadal O, Bonnart C, Giglia-Mari G. Mutations in TFIIH causing trichothiodystrophy are responsible for defects in ribosomal RNA production and processing. Hum. Mol. Genet. 2013;22:2881–93.
29. Bradsher J, Auriol J, De Santis LP, Iben S, Vonesch JL, Grummt I, et al. CSB is a component of RNA pol I transcription. Mol. Cell. 2002;10:819–29.
30. Koch S, Gonzalez OG, Assfalg R, Schelling A, Schafer P, Scharffetter-Kochanek K, et al. Cockayne syndrome protein A is a transcription factor of RNA polymerase I and stimulates ribosomal biogenesis and growth. Cell Cycle. 2014;13:2029–37.
31. He Y, Fang J, Taatjes DJ, Nogales E. Structural visualization of key steps in human transcription initiation. Nature. 2013;495:481–6.
32. Kuper J, Braun C, Elias A, Michels G, Sauer F, Schmitt DR, et al. In TFIIH, XPD Helicase Is Exclusively Devoted to DNA Repair. PLoS Biol. 2014;12:doi:10.1371/journal.pbio.1001954.
33. Fishburn J, Tomko E, Galburt E, Hahn S. Double-stranded DNA translocase activity of transcription factor TFIIH and the mechanism of RNA polymerase II open complex formation. Proc. Natl. Acad. Sci. U. S. A. 2015;112:3961–6.
34. Jeronimo C, Collin P, Robert F. The RNA Polymerase II CTD: The Increasing Complexity of a Low-Complexity Protein Domain. J. Mol. Biol. 2015;doi.org/10.1016/j.jmb.2016.02.006.
35. Akhtar MS, Heidemann M, Tietjen JR, Zhang DW, Chapman RD, Eick D, et al. TFIIH Kinase Places Bivalent Marks on the Carboxy-Terminal Domain of RNA Polymerase II. Mol. Cell. 2009;34:387–93.
36. Nilson K a, Guo J, Turek ME, Brogie JE, Delaney E, Luse DS, et al. THZ1 Reveals Roles for Cdk7 in Co-transcriptional Capping and Pausing. Mol. Cell. 2015;59:576–87.
37. Komarnitsky P, Cho EJ, Buratowski S. Different phosphorylated forms of RNA polymerase II and associated mRNA processing factors during transcription. Genes Dev. 2000;14:2452–60.
38. Rodriguez-Molina JB, Tseng SC, Simonett SP, Taunton J, Ansari AZ, Tseng SC, et al. Engineered Covalent Inactivation of TFIIH-Kinase Reveals an Elongation Checkpoint and Results in Widespread mRNA Stabilization. Mol. Cell. 2016;63:433–44.
39. Wong KH, Jin Y, Struhl K. TFIIH Phosphorylation of the Pol II CTD Stimulates Mediator Dissociation from the Preinitiation Complex and Promoter Escape. Mol. Cell. 2014;54:601–12.
40. Villicaña C, Cruz G, Zurita M. The basal transcription machinery as a target for cancer therapy. Cancer Cell Int. 2014;14:18.
41. Titov D V, Gilman B, He Q-L, Bhat S, Low W-K, Dang Y, et al. XPB, a subunit of TFIIH, is a target of the natural product triptolide. Nat. Chem. Biol. 2011;7:182–8.
42. Villicaña C, Cruz G, Zurita M. The genetic depletion or the triptolide inhibition of TFIIH in p53-deficient cells induces a JNK-dependent cell death in Drosophila. J. Cell Sci. 2013;126:2502–15.
43. Yi J-M, Huan X-J, Song S-S, Zhou H, Wang Y-Q, Miao Z-H. Triptolide Induces Cell Killing in Multidrug-Resistant Tumor Cells via CDK7/Rpb1 rather than XPB or p44. Mol. Cancer Ther. 2016;doi:10.1158/1535-7163.MCT-15-0753.
44. Chen F, Gao X, Shilatifard A, Shilatifard A. Stably paused genes revealed through inhibition of transcription initiation by the TFIIH inhibitor triptolide. Genes Dev. 2015;29:39–47.
45. Wang B, Chen J. Selective CDK7 inhibition with BS-181 suppresses cell proliferation and induces cell cycle arrest and apoptosis in gastric cancer. Drug Des Devel Ther. 2016;1181–9.
46. Qu L, Qu F, Jia Z, Wang C, Wu C, Zhang J. Integrated targeted sphingolipidomics and transcriptomics reveal abnormal sphingolipid metabolism as a novel mechanism of the hepatotoxicity and nephrotoxicity of triptolide. J. Ethnopharmacol. 2015;170:28–38.
47. Chipumuro E, Marco E, Christensen CL, Kwiatkowski N, Zhang T, Hatheway CM, et al. CDK7 inhibition suppresses super-enhancer-linked oncogenic transcription in MYCN-driven cancer. Cell. 2014;159:1126–39.
48. Pott S, Lieb JD. What are super-enhancers? Nat. Genet. 2014;47:8–12.
49. Christensen CL, Kwiatkowski N, Abraham BJ, Carretero J, Al-Shahrour F, Zhang T, et al. Targeting Transcriptional Addictions in Small Cell Lung Cancer with a Covalent CDK7 Inhibitor. Cancer Cell. 2014;26:909–22.
50. Wang Y, Zhang T, Kwiatkowski N, Abraham BJ, Lee TI, Xie S, et al. CDK7-Dependent Transcriptional Addiction in Triple-Negative Breast Cancer. Cell. 2015;163:174–86.
51. Alekseev S, Ayadi M, Brino L, Egly JM, Larsen AK, Coin F. A small molecule screen identifies an inhibitor of DNA repair inducing the degradation of TFIIH and the Chemosensitization of tumor cells to platinum. Chem. Biol. 2014;21:398–407.
52. Kumafuji M, Umemura H, Furumoto T, Fukasawa R, Tanaka A, Ohkuma Y. Mediator MED18 subunit plays a negative role in transcription via the CDK/cyclin module. Genes to Cells. 2014;19:582–93.
53. Nishikawa JL, Boeszoermenyi A, Vale-Silva LA, Torelli R, Posteraro B, Sohn Y-J, et al. Inhibiting fungal multidrug resistance by disrupting an activator-Mediator interaction. Nature. 2016;530:485–9.
54. Gerard M, Fischer L, Moncollin V, Chipoulet JM, Chambon P, Egly JM. Purification and interaction properties of the human RNA polymerase B(II) general transcription factor BTF2. J Biol Chem. 1991;266:20940–5.

CANCER CELL INTERNATIONAL

REVIEW Open Access

The basal transcription machinery as a target for cancer therapy

Claudia Villicaña, Grisel Cruz and Mario Zurita*

Abstract

General transcription is required for the growth and survival of all living cells. However, tumor cells require extraordinary levels of transcription, including the transcription of ribosomal RNA genes by RNA polymerase I (RNPI) and mRNA by RNA polymerase II (RNPII). In fact, cancer cells have mutations that directly enhance transcription and are frequently required for cancer transformation. For example, the recent discovery that MYC enhances the transcription of the majority genes in the genome correlates with the fact that several transcription interfering drugs preferentially kill cancer cells. In recent years, advances in the mechanistic studies of the basal transcription machinery and the discovery of drugs that interfere with multiple components of transcription are being used to combat cancer. For example, drugs such as triptolide that targets the general transcription factors TFIIH and JQ1 to inhibit BRD4 are administered to target the high proliferative rate of cancer cells. Given the importance of finding new strategies to preferentially sensitize tumor cells, this review primarily focuses on several transcription inhibitory drugs to demonstrate that the basal transcription machinery constitutes a potential target for the design of novel cancer drugs. We highlight the drugs' mechanisms for interfering with tumor cell survival, their importance in cancer treatment and the challenges of clinical application.

Keywords: Transcription inhibition, Cancer therapy, Gene expression, RNA polymerase

Review

Cells require transcription for basic processes, such as survival, cell growth and differentiation. Transformation highly correlates with enhanced transcription of oncogenes and other transcription factors in cancer cells [1]. For many years, genotoxic drugs have been administered to combat cancer. In fact, several compounds that reduce cancer cell proliferation also directly or indirectly affect global transcription, a characteristic that mechanistically contributes to their cytotoxicity. For example, intercalator compounds, such as cisplatin, induce DNA damage but also disrupt transcription [1,2].

Interestingly, several studies in various models have demonstrated that oncogenically transformed cells are more susceptible to apoptosis in response to transcriptional inhibition, suggesting that transcriptional inhibition has direct cytotoxic effects in malignant cells. In mouse lymphoma models, tumor cells were more sensitive to apoptosis than wild-type cells after treatment with an inhibitor of RNPI (RNA polymerase I) transcription [3], and similar effects were observed using RNPII (RNA polymerase II) inhibitors [4-6]. The reduction of basal transcription may interfere with transcriptional programming directed by key oncogenes, thereby exerting a greater effect in cancer cells versus normal cells. These findings support the link between transcription and transformation, suggesting that the basal transcription machinery is a promising druggable target to block cancer cell proliferation. Thus, the basal transcription machinery is an increasingly important target for cancer therapies.

In this review, we briefly describe transcriptional machinery components and several transcription inhibitory drugs. We discuss how these drugs interfere with survival of tumor cells as well as the challenges and limitations for clinical application.

General transcription machinery: RNPI and RNPII

The basal transcription machinery, a central component of general transcription, consists of several universal components that are required for promoter interaction, thereby achieving efficient and regulated transcription. Several

* Correspondence: marioz@ibt.unam.mx
Departament of Developmental Genetics, Instituto de Biotecnología, Universidad Nacional Autónoma de México, Mexico, Mexico

components of these transcriptional complexes exhibit enzymatic activity, which can potentially be inhibited by newly designed drugs (Figure 1). In addition, other drugs can be designed that disturb the protein-protein or DNA-protein interactions of these complexes.

RNPI-mediated transcription

The rRNA genes are located in the nucleolus and are transcribed by RNPI in eukaryotic cells. rRNA genes are transcribed during the S and G2 phases of the cell cycle; however, transcription is repressed during mitosis and is slowly recovered in G1 [7]. Selectivity factor 1 (SL1 in humans, TIF-1B in mouse) and upstream binding factor (UBF) are required for promoter binding and the recruitment of RNPI as well as various accessory factors, such as TFIIH; protein kinase CK2; nuclear actin; myosin (NM1); the chromatin modifiers G9A, PCAF and SIRT7; proteins involved in replication and repair; oncogenes and tumor suppressors for review, see: [7,8]. Moreover, rRNA gene expression is highly regulated in response to various environment conditions, including growth factors, nutrients and stress. Thus, the modulation of rRNA synthesis involves several signaling pathways that regulate cell growth and proliferation [8].

RNPII-mediated transcription

The main component of the basal transcription machinery is RNPII, which is composed of 12 subunits [9] and requires accessory factors, such as TFIIA, TFIIB, TFIIE, TFIIF, TFIID, TFIIH, SAGA, P-TEFb and Mediator, at various steps of transcription for review, see [9,10].

TFIID and SAGA (Spt–Ada–Gcn5–acetyltransferase) interact with the promoter and participate in the recruitment of the pre-initiation complex (PIC). SAGA specifically activates gene transcription in response to environmental stress [11-13]. After SAGA or TFIID binding to the promoter, several transcription factors are recruited to form the PIC. PIC factors include TFIIA, TFIIB, TFIID, TFIIE, TFIIF, TFIIH, Mediator and RNPII [10]. TFIIH not only participates in transcription but also nucleotide excision repair (NER) and cell cycle regulation. The XPB subunit is important for open complex formation, which is critical for promoter escape. CDK7 phosphorylates Ser 5 and 7 in the carboxy-terminal domain (CTD) heptapeptide repeat sequence of the large subunit of RNPII, which is important for the recruitment of the mRNA processing machinery during transcription [14,15].

Mediator is a multisubunit complex that cooperatively binds with RNPII and a subset of general factors during an intermediate step of PIC formation. Mediator is a transducer of the signals that link the activators with the general transcription machinery, thereby activating transcription [16,17]. However, these signals inhibit RNPII in certain scenarios [18,19]. On the other hand, the positive elongation factor (P-TEFb) complex is fundamental for transcription elongation through RNPII. The CDK9 subunit of P-TEFb phosphorylates the CTD of RNPII at Ser 2 for transcription elongation [20,21]. Interestingly, P-TEFb interacts with the super elongation complex (SEC) [22]. In addition, P-TEFb also interacts with the bromodomain proteins BRD3 and BRD4, which are required for the efficient recruitment of the P-TEFb complex to

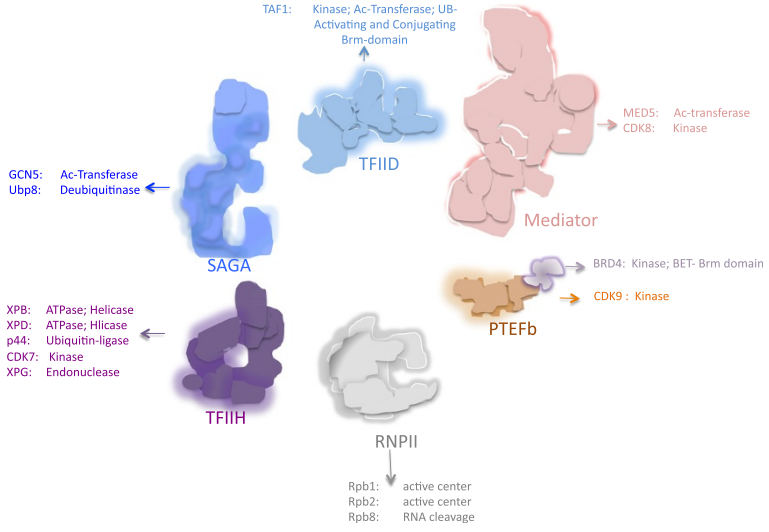

Figure 1 Different subunits of protein complexes involved in basal in basal transcription have different enzymatic activities that are or can be target by drugs inhibiting RNPII transcription. In the case of BRD4, in addition to its kinase activity, the Brm domain is the target of JQ1 and I-BET151, which interferes with the binding to acetylated histones; therefore future drugs that target components of the basal transcription machinery could be designed to interfere the interaction between different subunits into the complex. The different subunits with enzymatic activities of a corresponding complex are indicated in the figure.

the promoter and the activation of transcription elongation through binding to acetylated histones [23,24]. Recently, it was demonstrated that BRD4 is a kinase that phosphorylates Ser 2 of the RNPII CTD domain, suggesting a direct role for BRD4 in transcription elongation [25].

Cancer cells require high levels of transcription

Transformed cells require active transcription for proliferation and survival. Certain oncogenes, ribosomal genes and components of the transcriptional machinery are overexpressed in tumor cells to maintain proliferation [8,26,27]. For RNPI transcription, increased rRNA synthesis is associated with uncontrolled cancer cell proliferation. In fact, enhanced RNPI activity triggers nucleoli enlargement, a marker of aggressive cancer cells associated with a poor prognosis [28]. In addition, RNPII transcription is required to support the high demand of the transcripts, including oncogenes and anti-apoptotic factors, which is necessary for the maintenance of rapid growth and apoptosis resistance (Figure 2). For example, RNPII increases the global transcription of the majority of genes expressed in the cell through P-TEFb, which is important for maintaining the transformed phenotype [29,30]. Likewise, RNPIII activity is increased in tumor cells compared with normal cells, and the overexpression of BRF2, a RNPIII factor, is associated with several cancers [27].

Interestingly, the depletion of Xist RNA, involved in mammalian X-chromosome inactivation, induces hematological cancer in mice due to the increased expression of X-specific transcripts that are potentially associated with carcinogenesis [31]. In this work, Xist RNA depletion induces genome-wide alterations given that X-chromosome reactivation enhances transcription of X-specific transcripts, suggesting that Xist RNA is a cancer suppressor *in vivo*. Additionally, cancer cells can modulate their transcriptome and physiology to enhance survival and proliferation under stress conditions. This notion was demonstrated for heat shock factor 1 (HSF1), which drives a transcriptional program different from the heat shock supporting oncogenic processes, including protein folding, stress response, cell cycle and signaling genes, to maintain highly malignant human cancers [32]. These findings highlight the important role of transcription in maintaining the transcript supply of cancer cells.

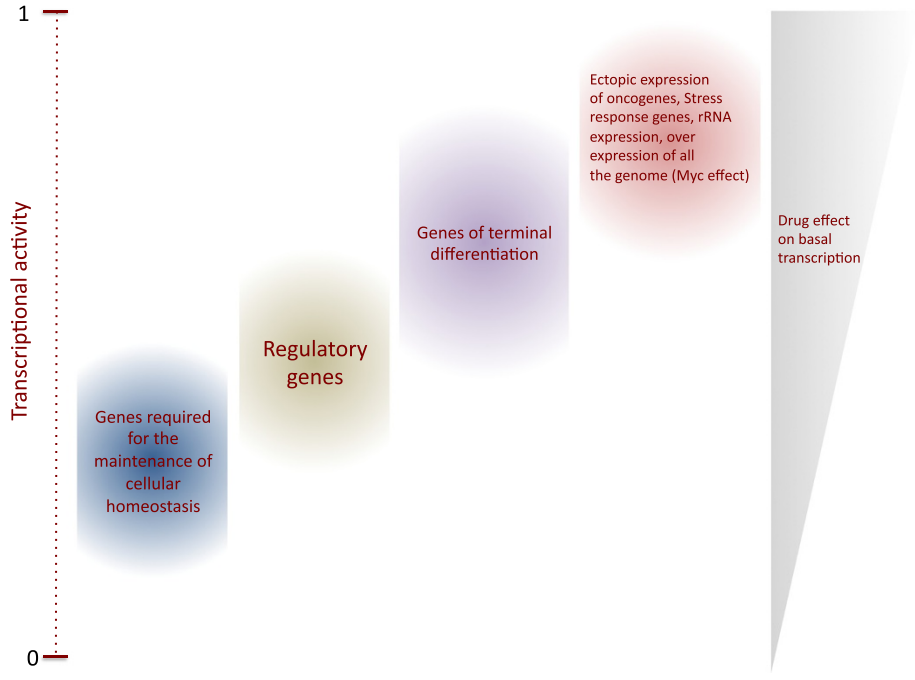

Figure 2 Cancer cells require high levels of basal transcription. To maintain a proliferative state cancer cells need active transcription by the three RNA polymerases. In particular the expression of oncogenes as well genes that suppress apoptosis is enhanced in tumour cells. Also, the enhancement of global transcription by MYC is necessary to maintain the cancerous phenotype. This situation is similar to the requirements of the transcription activity in ectopic expression genes, which is more sensible to the reduction of global transcription than normally expressed genes. Different kind of genes in the genome, require different levels of transcriptional activity. For instance, metabolic and regulatory genes do not require high levels of transcriptional activity. On the other hand, genes that express product of terminal differentiation require higher levels of transcriptional activity. Unregulated and ectopically expressed genes as well as overexpressed genes as response to stress, a situation that occurs in many cancers, require even higher transcriptional activity to maintain a transformed phenotype. Therefore, the reduction of the basal transcription activity preferentially affects these genes.

Transcription inhibitors

Drugs that potentially target the basal transcription machinery components could preferentially affect highly proliferative cells. Various components targeted by drugs include cyclin-dependent kinases (CDKs), RNA polymerases or components of associated transcriptional complexes.

CDK and kinases

Several CDKs that participate in RNPII transcription are targets for global transcription inhibition. CDK7 is a component of the basal transcription factor TFIIH that phosphorylates Ser 5 and 7 in the C-terminal domain (CTD) heptapeptide repeat sequence of the large subunit of RNPII, which is important for promoter escape and the recruitment of the mRNA processing machinery during transcription. CDK7 is a target of global transcription inhibition [14,15]. Additionally, CDK9, a component of P-TEFb, phosphorylates the CTD of RNPII at Ser 2 for transcription elongation [20,21]. Thus, many drugs target CDKs given that CDKs are deregulated in cancer cells. Mechanistically, CDK inhibitors compete with ATP at the enzyme active site. Therefore, CDK inhibition results in RNPII hypophosphorylation [33]. Although CDK inhibitors affect the activity of CDK7, CDK8 and CDK9, most drugs have affinities for several targets, including CDKs not related to transcription and other kinases (see Table 1) [34].

The most commonly used transcription inhibition drugs are flavopiridol and DRB. The flavone flavopiridol is a potent CDK9 inhibitor with a k_i of 3 nM. In addition, flavopiridol inhibits CDK8 with a k_i of 18 nM [35,64]. In chronic lymphocytic leukemia (CLL), flavopiridol cytotoxicity is associated with transcription inhibition mediated by the anti-apoptotic factor Mcl-1 [64]. In addition, flavopiridol is highly toxic, causing severe side effects and acute lysis tumor syndrome [34,65]. In fact, it was recently reported that flavopiridol induces double strand breaks (DSBs), explaining the drug's toxicity [47]. DRB (5,6-dichloro-1-β-D-ribofuranosylbenzimidazole) is an adenosine analog that specifically inhibits CDK9 and moderately inhibits CDK7 and CDK8, disrupting initiation and elongation [33,66]. DRB is widely used as a transcription inhibitor and to measure transcription rates given its rapid uptake; however, it is not used to treat cancer [33].

The isoquinolinesulphonamide derivatives H-7 and H-8 inhibit transcription elongation, inducing RNPII dephosphorylation [36]. However, these compounds belong to a broad spectrum of protein kinase inhibitors that target other kinases, such as PKC, PKA and PKG, with affinities similar those reported for CDK7, CDK8 and CDK9 [35,67]. Isoquinoline compounds are widely used to inhibit signaling pathways to elucidate signal transduction mechanisms; these compounds are typically not employed for cancer treatment [68].

Other CDK inhibitors exhibit cytotoxicity due to the transcriptional inhibition of anti-apoptotic proteins [34]. A number of these drugs are currently approved for cancer treatment, and others are currently being explored in clinical trials for various malignancies (Table 1). Transcription inhibitors can also downregulate genes involved in angiogenesis and metastasis. For example, the anti-angiogenic properties of flavopiridol and SNS-032 are partially attributed to the downregulation of VEGF mRNA and protein, the most potent tumor angiogenic factor [69-71].

Other novel compounds exhibit promising antitumor activity and display lower toxicities compared with traditional inhibitors. CDKI-71 is a novel CDK9 inhibitor that displays a high affinity for CDK9 (k_i = 6 nM), similar to flavopiridol. In fact, CDKI-71 induces apoptosis by downregulating the anti-apoptotic factor Mcl-1 in various cancer cell lines with minimal effects in normal fibroblasts and B and T-cells. Interestingly, CDKI-71 triggers apoptosis in several cancer cell lines with heterogeneous genetic backgrounds, including Rb and p53 mutations, suggesting that cell death is p53-independent [47]. Given that several tumors harbor p53 mutations, the activation of p53-independent cell death pathways represents a promising option to induce apoptosis in these tumors. Ibulocydine is a CDK inhibitor pro-drug that targets CDK7 and CDK9, thereby triggering apoptosis. The apoptotic effects of ibulocydine result in the downregulation of expression of anti-apoptotic factors, including Mcl-1, XIAP and survivin. Ibulocydine is currently under investigation and has exhibited promising results. For example, ibulocydine induces apoptosis without toxic side effects in mouse xenografts of hepatocellular carcinoma (HCC) [72].

Other compounds, such as hypericin, rottlerin and SP600125, are kinase inhibitors that inhibit transcription. The mechanisms of action for each drug have not been described. However, these drugs inhibit TBP phosphorylation during elongation, and SP600125 also inhibits phosphorylation at Ser 2 and 5 of the CTD of RNPII [73]. Similar to other drugs, these compounds also have additional targets. Hypericin inhibits epidermal growth factor, PKC and MAP kinase [74,75], whereas rottlerin inhibits PRAK and MAPKAP-K2 [76]. SP600125 inhibits JNK [77]. These drugs only have been characterized at the biochemical level; thus, research involving *in vivo* models should be explored. Wogonin, a flavone isolated from *Scutellaria baicalensis*, was recently identified as a novel compound. Wogonin inhibits CDK9 and blocks the phosphorylation of the CTD of RNPII. Wogonin induces apoptosis and suppress growth in several cancer cell lines and human cancer xenografts, respectively. The antitumor properties of wogonin reduce RNA synthesis and

Table 1 Drugs targeting proteins involved in transcription

Drug	Target	Mechanism of action	Class gene inhibited	Other targets	Cancer treatment	References
H-7	CDK7, CDK8, CDK9	Reduce levels of phosphorylated RNP III inhibiting elongation	I, II	PKC	Only research	[35-38]
H-8	CDK7, CDK9, CDK8	Reduce levels of phosphorylated RNP II inhibiting elongation	I, II	PKA, PKC, PKG, MLCK	Only research	[29,30]
AT8319	CDK9	Inhibits RNP II phosphorylation on Ser 2 disrupting transcription elongation	II	ND	MM, advanced solid tumors, and refractory non-Hodgkin's lymphoma	[34]
Dinaciclib/ SCH-727965	CDK9	Inhibits RNP II phosphorylation on Ser 2 disrupting transcription elongation. Impaired rRNA processing	I, II	CDK1, CDK2, CDK4, CDK5, CDK7	Solid tumors, hematologicalmalignancies, MM, melanoma, plasma cell neoplasia	[33,34]
RGB-286638	CDK9	Inhibits Ser 2 phosphorylation of RNP II disrupting transcription elongation	II	CDK1, CDK2, CDK4, CDK5, CDK6, CDK7	Hematological malignancies	[34]
R547	CDK9	Inhibits Ser 2 phosphorylation of RNP II disrupting transcription elongation	II	CDK1, CDK2, CDK4, CDK5, CDK7	Solid tumors	[34,39]
P276-00	CDK9	Inhibits transcription elongation	II	CDK1, CDK4	MM, breast, pancreas, melanoma, MCL, HNSCC	[34]
DRB	CDK9	Inhibits RNP II phosphorylation on Ser 2. Impaired rRNA processing	I, II	CDK2, CDK4, CDK7, CDK8, casein kinase I and II	Only Research	[33,34,40]
Roscovitine/ Seliciclib	CDK7 and CDK9	Acts as a competitor for ATP binding inhibiting kinase activity and Ser 5 phosphorylation or RNP II Inhibits rRNA processing	I, II	Cdc2, CDK2, CDK5, Erk1, Erk2, Dyrk, piridoxal kinase	Breast, solid tumors, B-cell malignancies, non-small cell lung cancer, and nasopharyngeal cancer	[33,41-43]
ARC	CDK9	Inhibits phosphorylation Ser 2 and Ser 5 of RNP II inhibiting transcription elongation	II	PKC	CLL, ALL, hairy cell leukaemia	[5,44]
ZK 304709	CDK7, CDK9	Inhibits RNP II phosphorylation on Ser 2.	II	CDK1, CDK2, CDK4, VEGFR1-3, PDGFR-β, Flt-3	Relapsed and/or refractory tumors	[45]
Wogonin	CDK9	Inhibits RNP II phosphorylation on Ser 2.	II	CDK7	Xenografts	[46]
CDKI-71	CDK9	Inhibits RNP II phosphorylation on Ser 2.	II	CDK1, CDK2, CDK7, CDK6	Under evaluation in cancer cell lines	[47]
Flavopiridol	CDK9, CDK8	Inhibits phosphorylation of Ser 2 in CTD of RNPII and interrupts RNA elongation; impaired rRNA processing	I, II	CDK1, CDK2, CDK4, CDK6, CDK7, PKC, Src, EGFR, ERK1	CLL, MM, MCL, indolent B-cell non-Hodgkin's lymphomas, germ line tumor, melanoma, ALM	[33-35,48]
SNS-032	CDK9	Inhibits Ser 2 phosphorylation of RNP II disrupting transcription elongation	II	CDK2, CDK7, GSK3	CLL, ALL, MM	[34,45]
AT7519	CDK9	Inhibit RNP II phosphorylation of Ser 2 and 5	II	CDK2, CDK4, CDK5, GSK-3	MM, solid tumor	[34,45,49]
CX-5461	SL1 complex	Disrupts formation of SL1-rDNA complex	I	ND	Lymphoma and leukemia human cancer xenograft model	[3, 671]
α-amatinin	RNP II and III	Binds to the largest subunit of RNP II and RNP III	II, III	ND	None due to hepatotoxicity	[33,50]
TAS-106	RNA polymerases	Ribonucleoside Inhibits RNA polymerases	I, II and III	ND	Solid tumors	[51,52]

Table 1 Drugs targeting proteins involved in transcription *(Continued)*

Triptolide	XPB subunit of TFIIH	Inhibits RNP I and II by inhibiting XPB ATPase activity. It triggers RNP II degradation	I, II	Polycystin-2 calcium channel, ADAM10.	Leukemia, myeloma, lymphoma, cholangiosarcoma, hepatocelular, cervical, pancreatic, gastric and oral cancer, anaplastic thyroid carcinoma	[33,39,53-55]
BMH-21	RNA polymerase I	Degradation of the RPA194 subunit of the RNA polymerase I	I	Induce p53	Melanoma	[56]
	XPB subunit of TFIIH	Promotes XPB degradation	II	Antagonist of aldosterone	Sensitizes carcinoma cells to cis- platinium	[57]
JQ1 and I-BET151	BRD3 and BRD4	Displace BRD3 and BRD4 from chromatin	II	ND	Multiple myeloma, leukaemia, lymphoma and lung adenocarcinoma in animal models	[57-63]

Abbreviations: ND, non detected; CLL, chronic lymphocytic leukemia; ALL, acute lymphocytic leukemia; AML, acute myeloid leukemia, CML, chronic myelogenousleukemia; HNSCC, head and neck squamous cell carcinoma; MCL, mantle cell lymphoma; MM, multiple myeloma.

downregulate Mcl-1 in a fashion that primarily affects malignant versus normal T-cells [46].

RNP enzymes

Although the expected targets for transcription inhibition are RNP enzymes, only a few drugs that directly affect these enzymes have been described. To date, α-amanitin and TAS-106 are two drugs that directly target RNP enzymes and inhibit transcription. α-amanitin is a cyclic octapeptide isolated from *Amanita* mushrooms that is extremely toxic. α-amanitin inhibits RNPII and III but not RNPI. RNPII is more sensitive to α-amanitin compared with RNPIII, which is a hundred-fold less sensitive than RNPII. The mechanism of action for α-amanitin involves binding to RNA polymerase to prevent DNA and RNA translocation, but α-amanitin does not affect nucleotide entry and RNA synthesis [33]. Although α-amanitin is an effective and specific transcription inhibitor, it is not used in cancer treatment due to high hepatotoxicity [50].

TAS-106 (1-(3-C-ethynyl-b-D-ribo-pentofuranosyl)cytosineECyd) is a cytidine analog that exhibits potent cytotoxic and anti-tumor properties against solid tumors. TAS-106's main mechanism of cytotoxicity is inhibition of RNPI-, II- and III-mediated RNA synthesis, thereby inducing apoptosis [78]. TAS-106 reduces the transcription of several factors required for survival. For example, TAS-106 induces apoptosis in radiation-resistant solid tumor cells through the depletion of hypoxia-inducing factor (HIF-α) [79]. In addition, TAS-106 also triggers apoptosis in cancer cells by reducing DSBs repair via BRCA2 transcript depletion [51].

Recently, a study reported that BMH-21, a compound that is a potent p53 activator and DNA intercalator at GC rich regions, which are abundant in the rRNA genes promoter, induces the degradation of the RPA194 subunit of RNPI, the largest RNPI subunit [56]. As a consequence, reduced rRNA synthesis generates a potent anticancer effect [56]. This effect is independent of p53 and opens the possibility that this drug may be used in cancer treatment. However, it is important to determine the effect of BHM-21 on other GC-rich regions in the genome, such as GpC islands.

Associated transcriptional complexes

Transcription can be disrupted via targeting of associated transcriptional complex components. Triptolide is a diterpene triepoxide that covalently binds to the XPB subunit of TFIIH and inhibits its ATPase activity. This action disrupts the opening of double-stranded DNA for RNPII transcription and repair as well as RNPI transcription [53,80-82]. In fact, triptolide cytotoxicity is associated with the transcriptional inhibition of anti-apoptotic factors and the induction of apoptotic factors [83]. Triptolide has been widely used for the treatment of various cancers with promising outcomes (See Table 1). In *Drosophila*, triptolide phenocopies mutations in TFIIH subunits, inducing apoptosis in the wing discs. Interestingly, apoptosis is enhanced in p53-deficient cells by JNK pathway activation [84]. This finding is interesting as the majority of solid tumors harbor mutations in p53 or components of the p53 pathway, suggesting that triptolide potentially induces apoptosis via JNK in these malignancies. In addition, TFIIH also participates in RNPI-mediated transcription, and triptolide inhibits RNPI elongation [54]. Therefore, triptolide not only affects TFIIH in RNPII transcription but also affects rRNA synthesis. With regard to the XPB subunit of TFIIH, a recent small molecule screen identified spironolactone (SP) as a compound that inhibits nucleotide excision repair (NER) [57]. Intriguingly, SP promotes XPB degradation via ubiquitination and the proteasome. Therefore, SP affects both NER and RNPII-mediated transcription. In this work, the authors focused on the role of SP in potentiating the effect of platinum in the induction of NER in cancer cells; however, SP is also a compound that may be used to treat cancer by inhibiting RNPII transcription, similar to triptolide.

BRD4 inhibition by JQ1 is an emerging and relevant target for the treatment of various cancers. JQ1 is a thieno-triazolo-1,4-diazepine that displaces BET bromodomains from chromatin through competitive binding to the acetyl-lysine recognition pocket, preventing BRD4 reader activity [58]. JQ1 reduces c-MYC or FOSL1 transcription in multiple myeloma, leukemia, lymphoma and lung adenocarcinoma models [59-61]. However, recent evidence indicates that BRD3 and BRD4 exhibit a more generalized effect on gene expression than previously suggested; therefore, the inhibition of these factors has a generalized effect on RNPII transcription [30]. In addition, the GSK12015A (I-BET151) inhibitor developed by GlaxoSmithKline (GSK) displaces BRD3 and BRD4 from chromatin. This action causes the downregulation of BCL-2, MYC and CDK6, thereby inducing cell cycle arrest and apoptosis in leukemia models [62].

CX-5461 is another potent and selective drug that inhibits rRNA transcription by targeting RNPI basal machinery. CX-5461 specifically inhibits rRNA synthesis by directly preventing the interaction between the SL1 complex and rDNA. CX-5461 does not affect RNPII transcription and DNA replication [85]. Interestingly, CX-5461 induces autophagic cell death in solid tumor cancer cells, whereas it induces apoptotic cell death in hematological malignancies [3,85]. Moreover, CX-5461 exhibits potent anti-tumor effects in murine xenografts [3].

Significance of transcription inhibition in cancer treatment

One key of successful therapy is the identification of critical nodes in the oncogenic network that can be inhibited to promote tumor growth cessation by apoptosis, differentiation,

necrosis or senescence. Several findings suggest that cancer cells require high transcription rates and harbor mutations or genetic backgrounds that favor enhanced transcription to sustain growth. Several MLL translocations and components of the SEC complex, including P-TEFb, AF9 and ELL, have been described in various leukemias, suggesting that transcription is misregulated in leukemias [22]. Likewise, CDK8 activity is also associated with the enhanced expression of genes regulated in response to serum and the Wnt/β-catenin pathway. In fact, CDK8 overexpression correlates with β-catenin deregulation in some colon cancers [86]. In addition, the importance of transcription inhibition is underscored by the notion that tumor cells are more sensitive to apoptosis than normal cells. This fact has been demonstrated in several models and tumor cell types [3-6]. Thus, the transcription machinery is an attractive putative target in cancer treatment because its specific tumor cell activity offers the possibility of directly attacking cancer cells and reducing the damage to healthy tissues.

The use of selective inhibitors for the transcriptional machinery offers advantages as these agents are considered less genotoxic to non-tumor cell populations compared with commonly used chemotherapy or radiation. This observation is important because a transcription inhibitor that specifically kills cancer cells may have a reduced incidence of secondary tumors compared with genotoxic agents that also affect normal cells. For example, chronic exposure to cisplatin leads to the development of resistance in patients and mouse models, and it has been demonstrated that enhanced damage repair contributes to tumor progression [87].

Initially, transcription-based therapies were primarily used to inhibit specific oncogenes or key genes required for tumor growth and survival. However, the use of these drugs was limited because the heterogeneity of some tumors allowed for the survival of cancer cell populations. For example, some tumors contain large hypoxic regions, which are generally are resistant to chemotherapy and radiation. Reduced MYC levels have been demonstrated in colon cancer cell lines. Reduced MYC expression is associated with survival because MYC is overexpressed and induces apoptosis in regions with poor energy supply [88]. In contrast, HIF is upregulated and contributes to survival in hypoxic tumors [89]. In these tumor conditions, exclusive MYC targeting is insufficient because each population exhibits different metabolic conditions; however, by targeting general transcription, highly expressed genes, such as MYC and HIF, can be repressed in various cell populations. Inhibitors can also repress transcription through the inhibition of kinases that regulate transcription factors or coactivators in specific tissues. For example, CDK9, which regulates the androgen receptor through direct phosphorylation and downregulation, decreases AR-transcription and proliferation genes in prostate cancer [90].

In addition, transcriptional inhibition also sensitizes stem cell populations that are generally chemoresistant. CDK8 and CDK9 are required for the maintenance of undifferentiated states of tumor embryonic stem cells [91,92]. CDK8 regulates the expression of a subset of genes involved in pluripotency. Moreover, CDK8 activity is partially mediated by MYC, indicating that additional independent mechanisms for the maintenance of undifferentiated states in tumors and stem cells exist. Thus, the loss of CDK8 induces differentiation. Similarly, JQ1-mediated BRD4 inhibition induces apoptosis in leukemic stem cells (LSC), which maintain and propagate the disease and are resistant to conventional chemotherapies [93]. Although JQ1 represents a powerful tool for the elimination of resistant cancer cells, its negative effects on the normal stem cell population must be evaluated to determine toxicity.

On the other hand, the lack of knowledge regarding the regulation of certain genes could generate different outcomes for the same treatment in clinical trials. For example, MYC is overexpressed in several tumors; however, MYC is surprisingly involved in the repression of integrins, which are required for breast cancer cell invasion and motility. This finding suggests that MYC inhibition is contraindicated in certain tumors [47]. A gene can possess oncogene or suppressor functions dependent on the context.

Regardless of the nature of tumorigenic signal, the transcription of certain oncogenic events can be disrupted by transcription inhibition, and therefore the transcriptional consequences cannot be predicted. Several recent findings suggest mechanisms involved in sensitization, which will be described in the following section.

Mechanisms of sensitization

Normal and tumor cells require transcription for survival. So, how does transcription inhibition lead to apoptosis in cancer cells? Transcription inhibition induces apoptosis by four possible mechanisms: altering the balance of apoptotic and anti-apoptotic factors to favor apoptosis, activating p53 and promoting its translocation to mitochondria, inhibiting DNA replication and promoting the accumulation of aberrant proteins in the nucleus [94]. Supporting the first mechanism, the mRNAs of many anti-apoptotic factors have short half-lives. The transcripts of oncogenes and regulators of proliferation also have reduced half-lives. Thus, although transcription inhibitors affect global mRNAs synthesis, oncogene transcripts may be more rapidly downregulated than other transcripts due to the rapid turnover of these mRNAs. Moreover, transcription inhibitors potentially interrupt the transcriptional program directed by these oncogenes, thereby disrupting the tumor's physiological state [95].

In *Drosophila*, the ectopic expression of various genes can be suppressed in a background that is partially deficient in transcription or by the pharmacological inhibition of transcription without affecting the proper expression of host genes [96,97]. Similar to this artificial overexpression system, oncogenes that are frequently overexpressed in cancer cells can be suppressed via transcription inhibition without affecting other genes (Figure 3). For example, various transcriptional inhibitors induce the downregulation of anti-apoptotic proteins, such as Mcl-1, XIAP and survivin [34], or oncogenes, such as MYC, without disrupting the transcription of normal genes in cancer cell lines [53,59]. Additionally, triptolide induces apoptosis by downregulating Bcr-Abl in K562 cells [98] or MYC in non-small lung cancer cells [83]. In addition to oncogenes, the class of genes called non-oncogenes significantly contributes to tumor survival; however, non-oncogenes do not induce cell transformation. Several non-oncogenes have been identified in a variety of tumors, where they are generally overexpressed [99,100]. Transcription inhibition also can disrupt the overexpression of non-oncogenes that are essential for cancer cell survival. For example, Heat shock Factor 1 (HSF1) is involved in survival in several cancer cell lines. Cancer cells are more dependent on HSF1 than normal cells. HSF1 depletion only minimally impacts normal cell viability, whereas cancer cells are strongly

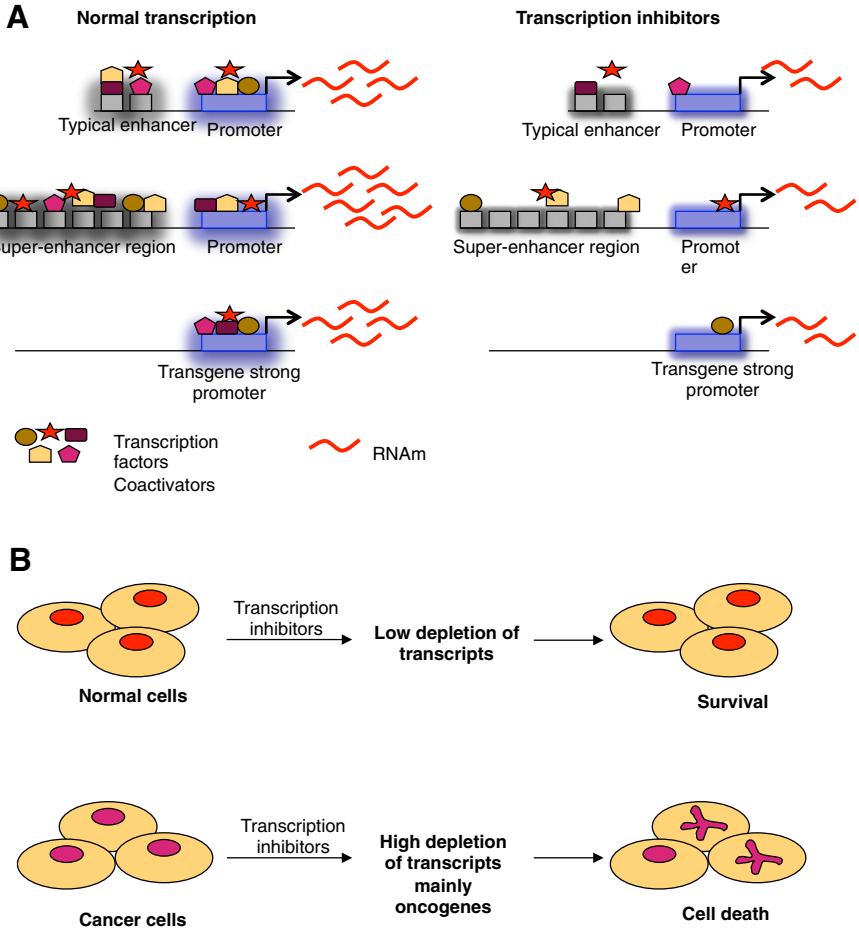

Figure 3 Transcription inhibitors affect differentially regulatory sequences of genes and trigger cell death in cancer cells. A) Transcription inhibitors differentially affect the regulatory sequences of genes and trigger cell death in cancer cells. This fact is related to requirement of transcription factors or coactivators recruited on regulatory sequences such as enhancers and promoters. Typical enhancers recruit several transcription factors and coactivators in order to enhance transcription of downstream gene; however, super-enhancer needs an excess of transcription than a typical enhancer, rendering the gene very sensitive to transcription perturbation. Similarly, transgene overexpression (whose promoter contain specific sequences for transactivators or specific *cis* elements), has been demonstrated to be affected by transcription inhibitors o genetic deficient in transcription [94,95]. In all cases, the final result is the depletion of messenger RNAs mainly genes that showed a high level of expression such as oncogenes. **B)** Cancer cells are more sensitive to suffer cell death after exposition to transcription inhibitors compared with normal cells. As we have seen before, transcription inhibitors cause a depletion of messenger RNAs mainly oncogenes and overexpressed genes; however, because cancer cells are oncogene-dependent for survival, their depletion triggers cell death preferentially in cancer cells, while preserving normal cells. This principle represents a strategic point for designing drug that targets directly cancer cells.

affected by HSF1 depletion [101]. In fact, triptolide induces cell death in pancreatic cancer cells via the inhibition of heat shock proteins [102]. Thus, it is likely that HSF1 depletion in these cells results from the inhibition of general transcription.

How does an inhibitor of general transcription selectively exert its effects on certain genes? Studies suggest that the high levels of expression by transgenes or gain of function mutations are dependent on their promoter, and these proteins are affected when transcription is inhibited or compromised. Moreover, *cis* structures on DNA called super-enhancers have been identified in genes required for cell identity and involved in cancer [63,103,104] (Figure 3). Super-enhancers significantly increase the expression of associated genes compared with typical enhancers. Super-enhancers are large DNA regions primarily occupied by mediator and other coactivators; therefore, super-enhancers are particularly sensitive to transcriptional perturbations that disrupt the transcriptional activity of genes associated with them. Indeed, the expression of Oct 4, a gene that contains a super-enhancer, is reduced in embryonic stem cells (ESC), inducing the downregulation of Mediator subunits [103]. More importantly, super-enhancers also have been identified in oncogenes, such as MYC, in multiple myeloma (MM) cells, and JQ1-mediated BRD4 inhibition causes MYC downregulation [63]. Given that super-enhancers require several-fold more transcription factors than typical enhancers, these structures are exquisitely sensitive to transcription disruption. Thus, it is possible that transcriptional inhibition by several drugs preferentially triggers apoptosis in cancer cells that express more oncogenes than normal cells. Additionally, super-enhancers are not associated with housekeeping genes, and it is plausible that these genes are not downregulated after exposure to transcription inhibitors, such as JQ1, thereby generating a selective effect [103].

In summary, transcription inhibition can interrupt transcriptional programs directed by key oncogenes or disrupt favorable growth conditions associated with the overexpression of non-oncogenes that contribute to survival and tumor progression.

Challenges and limitations

Differential sensitivity of cancer cell lines

Transcription inhibition potentiates apoptosis and other types of cell death in tumor cells. However, studies have demonstrated differential responses to various drugs in a variety of cell lines and tumors. This differential sensitization might be dependent on a variety of factors, such as genetic background, tissue type or tumor heterogeneity. Thus, drugs must be evaluated experimentally to determine clinical efficacy.

Genetic background is a key factor responsible for the variable outcomes of chemotherapy. Triptolide treatment in two prostate cancer cell lines revealed that LNCaP cells (androgen dependent) are more sensitive to triptolide-induced apoptosis than PC-3 cells (androgen independent) [105]. These results indicate that different mechanisms are responsible for triptolide-induced apoptosis and that the genetic background of one cell line is more sensitive than the other. In addition, specific tumor mutations could be responsible for the differential responses. For example, DRB does not induce apoptosis in colon carcinoma cell lines with mutant p53 [106]. In fact, cells with p53 mutations are more chemoresistant [107]. With regard to tumor heterogeneity, this finding importantly indicates that random mutations in different cell populations within a tumor respond differently to the same treatment, thereby generating treatment-resistant populations. It is important to determine which factors are more effective in cancer stem cells to avoid the generation of secondary tumors. Numerous leukemia cell lines show differential sensitivities based on particular aberrations and genetic backgrounds. Exposure to the BRD4 inhibitor JQ1 sensitizes several leukemia cell lines but not the BCR/ABL1-positive chronic myelogenous leukemia cell line K562 [108].

In addition to genetic background, differences in the chemotherapy responses are dependent on the tissue type. For example, CX5461-treated solid tumor cancer cell lines display autophagy and senescence, not apoptosis. In contrast, CX5461 induces p53-dependent apoptotic cell death in hematological malignancies. However, no correlation exists between nucleolar stress and p53 status in solid tumor cell lines, indicating that the stress response is p53-independent [62]. In hematopoietic tissues, such as B-cells, the induction of cell death is highly dependent on p53, and p53 mutations have been associated with poor prognosis in hematological malignancies [109]. In contrast, other tissues, such as keratinocytes, are highly resistant to p53-dependent cell death, demonstrating a clear difference between tissues [110].

Unselective targets

Another interesting point to consider is unselectivity. In this review, we describe the transcription inhibitory activities of many drugs, but only a few drugs exhibit specific effects on transcription given that most drugs target several proteins. For example, most CDK inhibitory drugs exhibit a high affinity for numerous CDKs that are not involved in transcription and proteins that are not cyclins. This unselectivity does not distinguish the target's transcriptional activities from its additional functions. Unselectivity might cause side effects given the association with unspecific partners. Moreover, cytotoxicity may be induced by agents that generate DNA damage, such as flavopiridol [47]. Thus, the design of more specific drugs is a current challenge. However, structural information regarding the enzyme's active site or domains increasingly

aids in the development of small compounds with more specific inhibitory activity that disrupts protein-protein and/or DNA-protein interactions.

Limitations

The targeting of transcriptional machinery represents an interesting mechanism to downregulate the key oncogenes driving tumorigenesis. However, transcription is an essential process that occurs in all living cells. Therefore, this strategy has several limitations. Whole organisms are comprised of several tissues and cell populations with different sensitivities to transcriptional perturbation. Specifically, the BRD4 inhibitor JQ1 disrupts cell specific factors in ESCs involved in pluripotency [103]. Therefore, it is important to determine whether targeting the transcription machinery affects the pluripotency of normal stem cell populations. JQ1 induces cell cycle arrest and apoptosis in AML cells; however, JQ1 only induces cell cycle arrest in normal bone marrow cells even when higher doses are administered [93]. Likewise, JQ1 does not display myelosuppressive effects in several *in vivo* models [59], suggesting that the cytotoxic effects are specific to acute myeloid leukemia (AML) cells. Nonetheless, the evaluation of results from long-term drug exposure is important to determine potential side effects in animal models and clinical trials.

The downregulation of certain proteins involved in transcription results in tumor suppression. For example, the downregulation of the MED-19 subunit of mediator inhibits cell growth and migration in tongue cancer [111], and CDK8 downregulation induces tumor cell differentiation [92]. Thus, mediator represents a putative target for drug inhibition. Recent work has shown that knockdown of the MED-12 subunit confers drug resistance in cancer cell lines by activating transforming growth factor (TGF-βR2) [112]; the activation of TGF-βR2 appears to be a unique function of the MED-12 subunit because other subunits of mediator do not localize outside of the nucleus, suggesting a MED-12-independent function of mediator. In addition to transcription and repair, studies suggest that the XPD and XPB subunits of TFIIH also participate in the regulation of processes, such as chromosome segregation and mitotic spindle dynamic, respectively [113,114]. BRD4 participates in the regulation of Aurora B expression. Reduced Aurora B expression causes severe cytokinesis and abnormal centrosomes in keratinocytes and cancer cells, increasing genomic instability [115]. Thus, the targeted selection of certain components of the transcription machinery should be evaluated if inhibition disrupts essential processes independent of transcription, causing toxicity or side effects.

Combined and personalized therapy

The efficacy of transcription inhibitory drugs can be enhanced when combined with other treatments. Triptolide has been combined with several agents to significantly increase the apoptosis in several tumors using lower doses of the agents without increasing the side effects of chemotherapy [39]. JQ1 combined with Ara-C results in antileukemic effects in several AML malignancies [93]. Various cancers are resistant to certain drugs, but combinations of drugs with varying mechanisms of action can synergize to increase apoptotic induction and sensitize a variety of tumors compared with individually administered drugs.

Gene expression profiling of tumors can aid in the identification of molecular signatures that determine several tumor characteristics, such as proliferation rate, differentiation and metastatic capacity. The technique can also identify a possible spectrum of drugs that are effective for tumor growth inhibition as well as specific drug doses. In addition, possible drug synergies and the effects of genetic variation on clinical outcomes in patients can be predicted. For example, the BCR/ABL1-positive chronic myelogenous leukemia line K562 is resistant to JQ1; however, it may be sensitive to triptolide because triptolide may have a more penetrant effect on global transcription than JQ1 [108].

Conclusions

Cancer cells require increased levels of transcription for growth and survival compared with normal cells. Cancer cells are more susceptible to alterations in gene expression. Various drugs that act as transcription inhibitors have been traditionally used in cancer treatment given that they preferentially reduce the global transcription of tumor cells. Thus, transcription inhibitors can potentially target the proteins that comprise the transcription machinery. As such, the transcription machinery is considered an ideal target for the design and improvement of drugs given that cancer cells are exquisitely sensitive to transcription inhibition and selectively affected by these drugs.

CDKs are one of the most common targets, but additional proteins have been targeted. However, some of these drugs have an affinity for other targets not involved in transcription, thereby generating possible side effects. Although drugs that inhibit transcription have challenges in clinical application, these drugs can be improved based on new discoveries regarding their mechanisms of action and information from clinical trials.

As previously demonstrated, the clinical application of drugs has several parameters that must be considered. However, future investigations on transcription mechanisms in eukaryotic cells will generate more knowledge that will aid in the design of novel drugs targeting new proteins and DNA with enhanced affinities and effects on cancer cells. However, improvements in the pharmacological properties of transcription inhibitors can increase efficacy and potentially reduce toxicity and side effects.

In recent years, it has been established that the genomic information of a tumor will indicate specific treatments for each cancer patient. However, personalized therapy must take into account the fact that tumor cells evolve and genomes are heterogeneous. Therefore, the use of drugs with generalized effects will still be required. However, cancer stem cells are typically chemoresistant. Thus, additional studies on the effects of drugs that alter global transcription must be performed in cancer stem cells to determine which components of the basal transcription machinery preferentially affect cancer stem cells when depleted. It is important to consider whether the cancer type is susceptible to drugs that target the basal transcription machinery.

Although eukaryotic transcription machinery mechanisms still require additional investigation, novel discoveries will offer new targets for the treatment of cancer in the near future.

Abbreviations

RNPI II, III: RNA polymerase I, II, III; TBP: TATA-binding protein; SL1: Selective factor 1; UBF: Upstream binding factor; TFII: Transcription factor II; SAGA: Spt–Ada–Gcn5–acetyltransferase; PIC: Pre-initiation complex; NER: Nucleotide excision repair; CTD: Carboxy-terminal domain; P-TEFb: Positive elongation factor b; CDK: Cyclin depending kinase; BRD4 3: Bromo domain containing protein 4, 3; HSF1: Heat shock factor 1; HCC: Hepatocellular carcinoma; JNK: June kinase; XPB XPD: Xeroderma pigmentosum,B or D; DSBs: Double strand breaks; MM: Multiple myeloma; ESC: Embryonic stem cells; AML: Acute myeloid leukemia; TGF: Transforming growth factor.

Competing interest

The authors of this manuscript declare that they have no competing interests.

Authors' contributions

CV, GC and MZ wrote the manuscript. All authors read and approved the final manuscript.

Acknowledgments

M.Z. is supported by grants from the Programa de Apoyo a Proyectos de Investigación e Inovación Tecnológica (PAPIIT)/Universidad Nacional Autónoma de México (UNAM), the Consejo Nacional de Ciencia y Tecnología (CONACYT) and the Miguel Alemán Foundation.

Received: 19 November 2013 Accepted: 21 February 2014
Published: 28 February 2014

References

1. Bywater MJ, Pearson RB, McArthur GA, Hannan RD: **Dysregulation of the basal RNA polymerase transcription apparatus in cancer.** *Nature Reviews in Cancer* 2013, **13**(5):299–314.
2. Todd RC, Lippard SJ: **Inhibition of transcription by platinum antitumor compounds.** *Metallomics* 2009, **1**(4):280–291.
3. Bywater MJ, Poortinga G, Sanij E, Hein N, Peck A, Cullinane C, Wall M, Cluse L, Drygin D, Anderes K, Huser N, Proffitt C, Bliesath J, Haddach M, Schwaebe MK, Ryckman DM, Rice WG, Schmitt C, Lowe SW, Johnstone RW, Pearson RB, McArthur GA, Hannan RD: **Inhibition of RNA polymerase I as a therapeutic strategy to promote cancer-specific activation of p53.** *Cancer Cell* 2012, **22**(1):51–65.
4. Koumenis C, Giaccia A: **Transformed cells require continuous activity of RNA polymerase II to resist oncogene-induced apoptosis.** *Mol Cell Biol* 1997, **17**(12):7306–7316.
5. Radhakrishnan SK, Gartel AL: **A novel transcriptional inhibitor induces apoptosis in tumor cells and exhibits antiangiogenic activity.** *Cancer Res* 2006, **66**(6):3264–3270.
6. Cho EC, Mitton B, Sakamoto KM: **CREB and leukemogenesis.** *Crit Rev Oncog* 2011, **16**(1–2):37–46.
7. Grummt I: **Life on a planet of its own: regulation of RNA polymerase I transcription in the nucleolus.** *Genes Dev* 2003, **17**(14):1691–1702.
8. Drygin D, Rice WG, Grummt I: **The RNA polymerase I transcription machinery: an emerging target for the treatment of cancer.** *Annu Rev Pharmacol Toxicol* 2010, **50:**131–156.
9. Nikolov DB, Burley SK: **RNA polymerase II transcription initiation: a structural view.** *Proc Natl Acad Sci U S A* 1997, **9**(1):15–22.
10. Thomas MC, Chiang CM: **The general transcription machinery and general cofactors.** *Crit Rev Biochem Mol Bio* 2006, **41**(3):105–178.
11. Huisinga KL, Pugh BF: **A genome-wide housekeeping role for TFIID and a highly regulated stress-related role for SAGA in *Saccharomyces cerevisiae*.** *Mol Cell* 2004, **13**(4):573–585.
12. Rodríguez-Navarro S: **Insights into SAGA function during gene expression.** *EMBO Rep* 2009, **10**(8):843–850.
13. Spedale G, Timmers HT, Pijnappel WW: **ATAC-king the complexity of SAGA during evolution.** *Genes Dev* 2012, **26**(6):527–541.
14. Egly JM, Coin F: **A history of TFIIH: two decades of molecular biology on a pivotal transcription/repair factor.** *DNA Repair* 2011, **10**(7):714–721.
15. Akhtar MS, Heidemann M, Tietjen JR, Zhang DW, Chapman RD, Eick D, Ansari AZ: **TFIIH kinase places bivalent marks on the carboxy-terminal domain of RNA polymerase II.** *Mol Cell* 2009, **34:**387–393.
16. Mittler G, Kremmer E, Timmers HT, Meisterernst M: **Novel critical role of a human Mediator complex for basal RNA polymerase II transcription.** *EMBO Rep* 2001, **2**(9):808–813.
17. Conaway RC, Conaway JW: **Origins and activity of the Mediator complex.** *Semin. Cell Dev Biol* 2011, **22**(7):729–734.
18. Hengartner CJ, Myer VE, Liao SM, Wilson CJ, Koh SS, Young RA: **Temporal regulation of RNA polymerase II by Srb10 and Kin28 cyclin-dependent kinases.** *Mol Cell* 1998, **2**(1):43–53.
19. Akoulitchev S, Chuikov S, Reinberg D: **TFIIH is negatively regulated by CDK8-containing mediator complexes.** *Nature* 2000, **407**(6800):102–106.
20. Peng J, Liu M, Marion J, Zhu Y, Price DH: **RNA polymerase II elongation control.** *Cold Spring Harb Symp Quant Biol* 1998, **63:**365–370.
21. Fu TJ, Peng J, Lee G, Price DH, Flores O: **Cyclin K functions as a CDK9 regulatory subunit and participates in RNA polymerase II transcription.** *J Biol Chem* 1999, **274**(49):34527–34530.
22. Smith E, Lin C, Shilatifard A: **The super elongation complex (SEC) and MLL in development and disease.** *Genes Dev* 2011, **25**(7):661–672.
23. Luo Z, Lin C, Shilatifard A: **The super elongation complex (SEC) family in transcriptional control.** *Nat Rev Mol Cell Biol* 2012, **13**(13):543–547.
24. Wu SY, Chiang CM: **The double bromodomain-containing chromatin adaptor Brd4 and transcriptional regulation.** *J Biol Chem* 2007, **282**(18):13141–13145.
25. Devaiah BN, Lewis BA, Cherman N, Hewitt MC, Albrecht BK, Robey PG, Ozato K, Sims RJ 3rd, Singer DS: **BRD4 is an atypical kinase that phosphorylates serine2 of the RNA polymerase II carboxy-terminal domain.** *Proc Natl Acad Sci U S A* 2012, **109**(18):6927–6932.
26. Adhikary S, Eilers M: **Transcriptional regulation and transformation by Myc proteins.** *Nat Rev Mo Cell Biol* 2005, **6**(8):635–645.
27. Cabarcas S, Schramm L: **RNA polymerase III transcription in cancer: the BRF2 connection.** *Molecular Cancer* 2011, **10:**47. doi: 10.1186/1476-4598-10-47.
28. Derenzini M, Montanaro L, Treré D: **What nucleolus says to a tumor pathologist.** *Histopathology* 2009, **54**(6):753–762.
29. Lin CY, Lovén J, Rahl PB, Paranal RM, Burge CB, Bradner JE, Lee TI, Young RA: **Transcriptional amplification in tumor cells with elevated c-Myc.** *Cell* 2012, **151**(1):56–67.
30. Luo Z, Lin C, Guest E, Garrett AS, Mohaghegh N, Swanson S, Marshall S, Florens L, Washburn MP, Shilatifard A: **The super elongation complex family of RNA polymerase II elongation factors: gene target specificity and transcriptional output.** *Mol Cell Biol* 2012, **32**(13):2608–2617.
31. Yildirim E, Kirby JE, Brown DE, Mercier FE, Sadreyev RI, Scadden DT, Lee JT: **Xist RNA is a potent suppressor of hematologic cancer in mice.** *Cell* 2013, **152**(4):727–742.
32. Mendillo ML, Santagata S, Koeva M, Bell GW, Hu R, Tamimi RM, Fraenkel E, Ince TA, Whitesell L, Lindquist S: **HSF1 drives a transcriptional program distinct from heat shock to support highly malignant human cancers.** *Cell* 2012, **150**(3):549–562.
33. Bensaude O: **Inhibiting eukaryotic transcription: which compound to choose? How to evaluate its activity?** *Transcription* 2011, **2**(3):103–108.
34. Stellrecht CM, Chen LS: **Transcription inhibition as a therapeutic target for cancer.** *Cancers* 2011, **3**(4):4170–4190.

35. Rickert P, Corden JL, Lees E: **Cyclin C/CDK8 and cyclin H/CDK7/p36 are biochemically distinc CTD kinases.** *Oncogene* 1999, **18**(4):1093–1102.
36. Dubois MF, Nguyen VT, Bellier S, Bensaude O: **Inhibitors of transcription such as 5,6-Dichloro-l-β-D-ribofuranosylbenzimidazole and isoquinolinesulfonamide derivatives (H-8 and H-7*) promote dephosphorylation of the carboxyl-terminal domain of RNA polymerase II largest subunit.** *J Biol Chem* 1994, **269**(18):13331–13336.
37. Kumahara E: **Immediate-early genes *zif268* and *c-fos* by a mechanism unrelated to inhibition of protein kinase C but possibly related to inhibition of phosphorylaton of RNA polymerase II.** *J Biol Chem* 1998, **274**(15):10430–10438.
38. DePinto W, Chu XJ, Yin X, Smith M, Packman K, Goelzer P, Lovey A, Chen Y, Qian H, Hamid R, Xiang Q, Tovar C, Blain R, Nevins T, Higgins B, Luistro L, Kolinsky K, Felix B, Hussain S, Heimbrook D: ***In vitro* and *in vivo* activity of R547: a potent and selective cyclin-dependent kinase inhibitor currently in phase I clinical trials.** *Mol Cancer Ther* 2006, **5**(11):2644–2658.
39. Liu Q: **Triptolide and its expanding multiple pharmacological functions.** *Int Immunopharmacol* 2011, **11**(3):377–383.
40. Tuniretto V, Porcedda P, Orlando L, De Marchi M, Amoroso A, Giachino C: **The cyclin-dependent kinase inhibitor 5,6-dichloro-1-beta-D-ribofurano-sylbenzimidazole induces nongenotoxic, DNA replication-independent apoptosis of normal and leukemic cells, regardless of their p53 status.** *BMC Cancer* 2009. doi:10.1186/1471-2407-9-281.
41. Bach S, Knockaert M, Reinhardt J, Lozach O, Schmitt S, Baratte B, Koken M, Coburn SP, Tang L, Jiang T, Liang DC, Galons H, Dierick JF, Pinna LA, Meggio F, Totzke F, Schächtele C, Lerman AS, Carnero A, Wan Y, Gray Meijer N: **Roscovitine targets, protein kinases and pyridoxal kinase.** *J Biol Chem* 2005, **280**(35):31208–31219.
42. Ljungman M, Paulsen MT: **The cyclin-dependent kinase inhibitor roscovitine inhibits RNA synthesis and triggers nuclear accumulation of p53 that is unmodified at Ser15 and Lys382.** *Mol Pharmacol* 2001, **60**(4):785–789.
43. Hsieh WS, Soo R, Peh BK, Loh T, Dong D, Soh D, Wong LS, Green S, Chiao J, Cui CY, Lai YF, Lee SC, Mow B, Soong R, Salto-Tellez M, Goh BC: **Pharmacodynamic effects of seliciclib, an orally administered cell cycle modulator in undifferentiated nasopharyngeal cancer.** *Clin Cancer Res.* 2009, **15**(4):1435–1442.
44. Stockwin LH, Yu SX, Stotler H, Hollingshead MG, Newton DL: **ARS (NSC 188491) has identical activity to sangivamycin (NSC65346) including inhibition of both P-TEFb and PKC.** *BMC Cancer* 2009. doi:10.1186/1471-2407-9-63.
45. Malumbres M, Pevarello P, Barbacid M, Bischoff JR: **CDK inhibitors in cancer therapy: what is the next?** *Trends Pharmacol Sci* 2008, **29**(1):16–21.
46. Polier G, Ding J, Konkimalla BV, Eick D, Ribeiro N, Köhler R, Giaisi M, Efferth T, Desaubry L, Krammer PH, Li-Weber M: **Wogonin and related natural flavones are inhibitors of CDK9 that induce apoptosis in cancer cells by transcriptional suppression of Mcl-1.** *Cell Death Dis* 2011, **2**:e182. doi: 10.1038/cddis.2011.66.
47. Liu X, Shi S, Lam F, Pepper C, Fischer PM, Wang S: **CDKI-71, a novel CDK9 inhibitor, is preferentially cytotoxic to cancer cells compared with flavopiridol.** *Int J Cancer* 2012, **130**(5):1216–1226.
48. Chao SH, Price DH: **Flavopiridol inactivates P-TEFb and blocks most RNA polymerase II transcription *in vivo*.** *J Biol Chem* 2001, **276**:31793–31799.
49. Mahadevan D, Plummer R, Squires MS, Rensvold D, Kurtin S, Pretzinger C, Dragovich T, Adams J, Lock V, Smith DM, Von Hoff D, Calvert H: **A phase I pharmacokinetic and pharmacodynamic study of AT7519, a cyclin-dependent kinase inhibitor in patients with refractory solid tumors.** *Annals of Oncology* 2011, **22**(9):2137–2143.
50. Zheleva A, Tolekova A, Zhelev M, Uzunova V, Platikanova M, Gadzheva V: **Free radical reactions might contribute to severe alpha amanitin hepatotoxicity—A hypothesis.** *Med Hypotheses* 2007, **69**(2):361–367.
51. Meike S, Yamamori T, Yasui H, Eitaki M, Matsuda A, Morimatsu M, Fukushima M, Yamasaki Y, Inanami O: **A nucleoside anticancer drug, 1-(3-C- ethynyl-β-D-ribo-pentofuranosyl)cytosine (TAS-106), sensitizes cells to radiation by suppressing BRCA2 expression.** *Molecular Cancer* 2011. doi:10.1186/1476-4598-10-92.
52. Friday B, Lassere Y, Meyers CA, Mita A, Abbruzzese JL, Thomas MB: **A phase I study to determine the safety and pharmacokinetics of intravenous administration of TAS-106 once per week for three consecutive weeks every 28 days in patients with solid tumors.** *Anticancer Res* 2012, **32**(5):1689–1696.
53. Titov DV, Gilman B, He QL, Bhat S, Low WK, Dang Y, Smeaton M, Demain AL, Miller PS, Kugel JF, Goodrich JA, Liu JO: **XPB, a subunit of TFIIH, is a target of the natural product triptolide.** *Nat Chem Biol* 2011, **7**(3):182–188.
54. Nonnekens J, Perez-Fernandez J, Theil AF, Gadal O, Bonnart C, Giglia-Mari G: **Mutations in TFIIH causing trichothiodystrophy are responsible for defects in ribosomal RNA production and processing.** *Hum Mol Genet* 2013, **22**(14):2881–2893.
55. Soundararajan R, Sayat R, Robertson GS, Marignani PA: **Triptolide: an inhibitor of a disintegrin and metalloproteinase 10 (ADAM10) in cancer cells.** *Cancer Biol Ther* 2009, **8**(21):2054–2062.
56. Peltonen K, Colis L, Liu H, Trivedi R, Moubarek MS, Moore HM, Bai B, Rudek MA, Bieberich CJ, Laiho MA: **Targeting modality for destruction of RNA polymerase I that possesses anticancer activity.** *Cancer Cell* 2014, **13**(1):77–90.
57. Alekseev S, Ayadi M, Brino L, Egly JM, Larsen AK, Coin F: **A small molecule screen identifies an inhibitor of DNA repair inducing the degradation of TFIIH and the chemosensitization of tumor cells to platinum.** *Chem Biol* 2014. doi:10.1016/j.chembiol.2013.12.014. [Epub ahead of print].
58. Filippakopoulos P, Qi J, Picaud S, Shen Y, Smith WB, Fedorov O, Morse EM, Keates T, Hickman TT, Felletar I, Philpott M, Munro S, McKeown MR, Wang Y, Christie AL, West N, Cameron MJ, Schwartz B, Heightman TD, La Thangue N, French CA, Wiest O, Kung AL, Knapp S, Bradner JE: **Selective inhibition of BET bromodomains.** *Nature* 2010, **468**(7327):1067–1073.
59. Delmore JE, Issa GC, Lemieux ME, Rahl PB, Shi J, Jacobs HM, Kastritis E, Gilpatrick T, Paranal RM, Qi J, Chesi M, Schinzel AC, McKeown MR, Heffernan TP, Vakoc CR, Bergsagel PL, Ghobrial IM, Richardson PG, Young RA, Hahn WC, Anderson KC, Kung AL, Bradner JE, Mitsiades CS: **BET bromodomain inhibition as a therapeutic strategy to target c-Myc.** *Cell* 2011, **146**(6):904–917.
60. Zuber J, Shi J, Wang E, Rappaport AR, Herrmann H, Sison EA, Magoon D, Qi J, Blatt K, Wunderlich M, Taylor MJ, Johns C, Chicas A, Mulloy JC, Kogan SC, Brown P, Valent P, Bradner JE, Lowe SW, Vakoc CR: **RNAi screen identifies Brd4 as a therapeutic target in acute myeloid leukaemia.** *Nature* 2011, **478**(7370):524–528.
61. Lockwood WW, Zejnullahu K, Bradner JE, Varmus H: **Sensitivity of human lung adenocarcinoma cell lines to targeted inhibition of BET epigenetic signaling proteins.** *Proc Natl Acad Sci U S A* 2011, **109**(47):19408–19413.
62. Dawson MA, Prinjha RK, Dittmann A, Giotopoulos G, Bantscheff M, Chan WI, Robson SC, Chung CW, Hopf C, Savitski MM, Huthmacher C, Gudgin E, Lugo D, Beinke S, Chapman TD, Roberts EJ, Soden PE, Auger KR, Mirguet O, Doehner K, Delwel R, Burnett AK, Jeffrey P, Drewes G, Lee K, Huntly BJ, Kouzarides T: **Inhibition of BET recruitment to chromatin as an effective treatment for MLL-fusion leukaemia.** *Nature* 2011, **478**(7370):529–533.
63. Lovén J, Hoke HA, Lin CY, Lau A, Orlando DA, Vakoc CR, Bradner JE, Lee TI, Young RA: **Selective inhibition of tumor oncogenes by disruption of super-enhancers.** *Cell* 2013, **153**(2):320–344.
64. Chen R, Keating MJ, Gandhi V, Plunkett W: **Transcription inhibition by flavopiridol: mechanism of chronic lymphocytic leukemia cell death.** *Blood* 2005, **106**(9):2513–2519.
65. Blum KA, Ruppert AS, Woyach JA, Jones JA, Andritsos L, Flynn JM, Rovin B, Villalona-Calero M, Ji J, Phelps M, Johnson AJ, Grever MR, Byrd JC: **Risk factors for tumorlysis syndrome in patients with chronic lymphocytic leukemia treated with the cyclin-dependent kinase inhibitor, flavopiridol.** *Leukemia* 2011, **25**(9):1444–1451.
66. Yankulov K, Yamashita K, Roy R, Egly JM, Bentley DL: **Inhibitor 5,6-dichloro-1-β-D-ribofuranosylbenzimidazole inhibits transcription factor IIH-associated protein kinase.** *J Biol Chem* 1995, **270**(41):23922–23925.
67. Shima D, Yugami M, Tatsuno M, Wada T, Yamaguchi Y, Handa H: **Mechanism of H-8 inhibition of cyclin-dependent kinase 9: study using inhibitor-inmobilized matrices.** *Genes to Cells* 2003, **8**(3):215–223.
68. Engh RA, Girod A, Kinzel V, Huber R, Bossemeyer D: **Crystal structure of catalytic subunit of cAMP-dependent protein kinase in complex with isoquinolinesylfonyl protein kinase inhibitors H7, H8 and H89.** *J Biol Chem* 1996, **271**(42):26157–26164.
69. Khattar V, Thottassery JV: **Cks1: structure, emerging roles and implications in multiple cancers.** *J Cancer Ther* 2013, **4**(8):1341–1354.
70. Ali MA, Choy H, Habib AA, Saha D: **SNS-032 prevents tumor cell-induced angiogenesis by inhibiting vascular endothelial growth factor.** *Neoplasia* 2007, **9**(5):370–381.
71. Melillo G, Sausville EA, Cloud K, Lahusen T, Varesio L, Senderowicz AM: **Flavopiridol, a protein kinase inhibitor, downregulates hypoxic induction of vascular endothelial growth factor expression in human monocytes.** *Cancer Res* 1999, **59**(21):5433–5437.

72. Cho SJ, Kim YJ, Surh YJ, Kim BM, Lee SK: **Ibulocydine is a novel prodrug Cdk inhibitor that effectively induces apoptosis in hepatocellular carcinoma cells.** *J Biol Chem* 2011, **286**(22):19662–19671.
73. Morachis JM, Huang R, Emerson BM: **Identification of kinase inhibitors that target transcription initiation by RNA polymerase II.** *Oncotarget* 2011, **1–2:**18–28.
74. de Witte P, Gostinis P, Van Lint J, Merlevede W, Vandenheede JR: **Inhibition of epidermal growth factor receptor tyrosine kinase activity by hypericin.** *Biochem Pharmacol* 1993, **46**(11):1929–1936.
75. Lavie G, Meruelo D, Aroyo K, Mandel M: **Inhibition of the $CD8^+$ T cell-mediated cytotoxic reaction by hipericin: potential for treatment of T cell-mediated diseases.** *Int Immunol* 2000, **12**(4):479–486.
76. Davies SP, Reddy H, Caivano M, Cohen: **Specificity and mechanism of action of some commonly used protein kinase inhibitors.** *Biochem* 2000, **351**(1):95–105.
77. Bennett BL, Bennett BL, Sasaki DT, Murray BW, O'Leary EC, Sakata ST, Xu W, Leisten JC, Motiwala A, Pierce S, Satoh Y, Bhagwat SS, Manning AM, Anderson DW: **SP600125, an anthrapyrazolone inhibitor of Jun N-terminal kinase.** *Proc Natl Acad Sci* 2001, **98**(4):13682–13686.
78. Shimamoto Y, Fujioka A, Kazuno H, Murakami Y, Ohshimo H, Kato T, Matsuda A, Sasaki T, Fukushima M: **Antitumor activity and pharmacokinetics of TAS-106, 1-(3-C-ethynyl-β-D-ribo-pentofuranosyl) cytosine.** *Cancer Res* 2001, **92**(3):343–351.
79. Yasui H, Ogura A, Asanuma T, Matsuda A, Kashiwakura I, Kuwabara M, Inanami O: **Inhibition of HIF-1α by the anticancer drug TAS106 enhances X-ray-induced apoptosis *in vitro* and *in vivo*.** *Br J Cancer* 2008, **99**(9):1442–1452.
80. Iben S, Tschochner H, Bier M, Hoogstraten D, Hozák P, Egly JM, Grummt I: **TFIIH plays an essential role in RNA polymerase I transcription.** *Cell* 2002, **109**(3):297–306.
81. Assfalg R, Lebedev A, Gonzalez OG, Schelling A, Koch S, Iben S: **TFIIH is an elongation factor of RNA polymerase I.** *Nucleic Acids Res* 2011, **40**(2):1–10.
82. Manzo SG, Zhou ZL, Wang YQ, Marinello J, He JX, Li YC, Ding J, Capranico G, Miao ZH: **Natural product triptolide mediates cancer cell death by triggering CDK7-dependent degradation of RNA polymerase II.** *Cancer Res* 2012, **72**(20):5363–5373.
83. Vispé S, DeVries L, Créancier L, Besse J, Bréand S, Hobson DJ, Svejstrup JQ, Annereau JP, Cussac D, Dumontet C, Guilbaud N, Barret JM, Bailly C: **Triptolide is an inhibitor of RNA polymerase I and II-dependent transcription leading predominantly to down-regulation of short-lived mRNA.** *Mol Cancer Ther* 2009, **8**(10):2780–2790.
84. Villicaña C, Cruz G, Zurita M: **The genetic depletion or the triptolide inhibition of TFIIH in p53 deficient cells induce a JNK-dependent cell death in *Drosophila*.** *J Cell Sci* 2013, **126**(11):2502–2515.
85. Drygin D, Lin A, Bliesath J, Ho CB, O'Brien SE, Proffitt C, Omori M, Haddach M, Schwaebe MK, Siddiqui-Jain A, Streiner N, Quin JE, Sanij E, Bywater MJ, Hannan RD, Ryckman D, Anderes K, Rice WG: **CX-5461 Inhibits ribosomal RNA synthesis and solid tumor growth.** *Cancer Res* 2011, **71**(4):1418–1430.
86. Morris EJ, Ji JY, Yang F, Di Stefano L, Herr A, Moon NS, Kwon EJ, Haigis KM, Näär AM, Dyson NJ: **E2F1 represses beta-catenin transcription and is antagonized by both pRB and CDK8.** *Nature* 2008, **455**(7212):552–556.
87. Oliver TG, Mercer KL, Sayles LC, Burke JR, Mendus D, Lovejoy KS, Cheng MH, Subramanian A, Mu D, Powers S, Crowley D, Bronson RT, Whittaker CA, Bhutkar A, Lippard SJ, Golub T, Thomale J, Jacks T, Sweet-Cordero EA: **Chronic cisplatin treatment promotes enhanced damage repair and tumor progression in a mouse model of lung cancer.** *Genes Dev* 2010, **24**(8):837–852.
88. Okuyama H, Endo H, Akashika T, Kato K, Inoue M: **Downregulation of c-MYC protein levels contributes to cancer cell survival under dual deficiency of oxygen and glucose.** *Cancer Res* 2010, **70**(24):10213–10223.
89. Whitesell L, Lindquist S: **Inhibiting the transcription factor HSF1 as an anticancer strategy.** *Expert Opin Ther Targets* 2009, **13**(4):469–478.
90. Gordon V, Bhadel S, Wunderlich W, Zhang J, Ficarro SB, Mollah SA, Shabanowitz J, Hunt DF, Xenarios I, Hahn WC, Conaway M, Carey MF, Gioeli D: **CDK9 regulates AR promoter selectivity and cell growth through serine 81 phosphorylation.** *Mol Endocrinol* 2010, **24**(12):2267–2280.
91. Kaichi S, Takaya T, Morimoto T, Sunagawa Y, Kawamura T, Ono K, Shimatsu A, Baba S, Heike T, Nakahata T, Hasegawa K: **Cyclin-dependent kinase 9 forms a complex with GATA4 and is involved in the differentiation of mouse ES cells into cardiomyocytes.** *J Cell Physiol* 2011, **226**(12):248–254.
92. Adler AS, McCleland ML, Truong T, Lau S, Modrusan Z, Soukup TM, Roose-Girma M, Blackwood EM, Firestein R: **CDK8 maintains tumor dedifferentiation and embryonic stem cell pluripotency.** *Cancer Res* 2012, **72**(8):2129–2139.
93. Herrmann H, Blatt K, Shi J, Gleixner KV, Cerny-Reiterer S, Müllauer L, Vakoc CR, Sperr WR, Horny HP, Bradner JE, Zuber J, Valent P: **Small-molecule inhibition of BRD4 as a new potent approach to eliminate leukemic stem- and progenitor cells in acute myeloid leukaemia (AML).** *Oncotarget* 2012, **3**(12):1588–1599.
94. Derheimer FA, Chang CW, Ljungman M: **Transcription inhibition: a potential strategy for cancer therapeutics.** *Eur J Cancer* 2005, **41**(16):2569–2576.
95. Lam LT, Pickeral OK, Peng AC, Rosenwald A, Hurt EM, Giltnane JM, Averett LM, Zhao H, Davis RE, Sathyamoorthy M, Wahl LM, Harris ED, Mikovits JA, Monks AP, Hollingshead MG, Sausville EA, Staudt LM: **Genomic-scale measurement of mRNA turnover and the mechanisms of action of the anti-cancer drug flavopiridol.** *Genome Biol* 2001, **2:**research0041.0041-research0041.0011.
96. Gutiérrez L, Merino C, Vázquez M, Reynaud E, Zurita M: **RNA polymerase II 140wimp mutant and mutations in the TFIIH subunit XPB differentially affect homeotic gene expression in *Drosophila*.** *Genesis* 2004, **40**(1):58–66.
97. Merino CE, Reynaud M, Vazquez M, Zurita M: **DNA repair and transcriptional effects on mutations in TFIIH in *Drosophila* development.** *Mol Biol Cell* 2002, **13**(19):3246–3256.
98. Lou YJ, Jin J: **Triptolide down-regulates bcr-abl expression and induces apoptosis in chronic myelogenous leukemia cells.** *Leuk Lymphoma* 2004, **45**(2):373–376.
99. Chen DY, Liu H, Takeda S, Tu HC, Sasagawa S, Van Tine BA, Lu D, Cheng EH, Hsieh JJ: **Taspase 1 function as a non-oncogene addiction protease that coordinates cancer cell proliferation and apoptosis.** *Cancer Res* 2010, **70**(13):15358–15367.
100. Gabai VL, Meng L, Kim G, Mills TA, Benjamin IJ, Sherman MY: **Heat shock transcription factor HSF1 is envolved in tumor progresión via regulation of hypoxia-inducible factor 1 and RNA-binding protein HuR.** *Mol Cell Biol* 2012, **32**(5):929–940.
101. Dai C, Meng L, Kim G, Mills TA, Benjamin IJ, Sherman MY: **Heat shock factor 1 is a powerful multifaceted modifier of carcinogenesis.** *Cell* 2007, **130**(6):1005–1018.
102. Phillips DA, Dudeja V, McCarroll JA, Borja-Cacho D, Dawra RK, Grizzle WE, Vickers SM, Saluja AK: **Triptolide induces pancreatic cancer cell death via inhibition of the heat shock protein 70.** *Cancer Res* 2007, **67**(19):9407–9416.
103. Whyte WA, Orlando DA, Hnisz D, Abraham BJ, Lin CY, Kagey MH, Rahl PB, Lee TI, Young RA: **Master transcription factors and mediator establish super-enhancers at key cell identity genes.** *Cell* 2013, **153**(2):307–319.
104. Kagey MH, Newman JJ, Bilodeau S, Zhan Y, Orlando DA, van Berkum NL, Ebmeier CC, Goossens J, Rahl PB, Levine SS, Taatjes DJ, Dekker J, Young RA: **Mediator and cohesin connect gene expression and chromatin architecture.** *Nature* 2010, **467**(7314):430–435.
105. Huang W, He T, Chai C, Yang Y, Zheng Y, Zhou P, Qiao X, Zhang B, Liu Z, Wang J, Shi C, Lei L, Gao K, Li H, Zhong S, Yao L, Huang ME, Lei M: **Triptolide inhibits the proliferation of prostate cancer cells and down-regulates SUMO-specific protease 1 expression.** *PLoS One* 2012, **7**(5):e37693.
106. Poele RH, Okorokov AL, Joel SP: **RNA synthesis block by 5, 6-dichloro-1-beta-D-ribofuranosylbenzimidazole (DRB) triggers p53-dependent apoptosis in human colon carcinoma cells.** *Oncogene* 1999, **18**(42):5765–5772.
107. Stavrovskaya AA: **Cellular mechanisms of multidrug resistance of tumor cells.** *Biochemistry* 2000, **65**(1):95–106.
108. Ott CJ, Kopp N, Bird L, Paranal RM, Qi J, Bowman T, Rodig SJ, Kung AL, Bradner JE, Weinstock DM: **BET bromodomain inhibition targets both c-Myc and IL7R in high-risk acute lymphoblastic leukemia.** *Blood* 2012, **120**(14):2843–2852.
109. Slatter TL, Ganesan P, Holzhauer C, Mehta R, Rubio C, Williams G, Wilson M, Royds JA, Baird MA, Braithwaite AW: **p53-mediated apoptosis prevents the accumulation of progenitor B cells and B-cell tumors.** *Cell Death and Differentiation* 2010, **17**(3):540–550.
110. Tron VA, Trotter MJ, Tang L, Krajewska M, Reed JC, Ho VC, Li G: **p53-regulated apoptosis is differentiation dependent in ultraviolet B-irradiated mouse keratinocytes.** *Am J Pathol* 1998, **153**(2):579–585.
111. Zhu LJ, Yan WX, Chen ZW, Chen Y, Chen D, Zhang TH, Liao GQ: **Disruption of mediator complex subunit 19 (Med19) inhibits cell growth and migration in tongue cancer.** *World J Surg Oncol* 2013, **11:**116.
112. Huang S, Hölzel M, Knijnenburg T, Schlicker A, Roepman P, McDermott U, Garnett M, Grernrum W, Sun C, Prahallad A, Groenendijk FH, Mittempergher L, Nijkamp W, Neefjes J, Salazar R, Dijke P, Uramoto H, Tanaka F, Beijersbergen RL, Wessels LFA, Bernards R: **MED12 controls the response to**

multiple cancer drugs through regulation of TGF-β receptor signaling. *Cell* 2012, **151**(5):937–950.
113. Ito S, Tan LJ, Andoh D, Narita T, Seki M, Hirano Y, Narita K, Kuraoka I, Hiraoka Y, Tanaka K: **MMXD, a TFIIH-independent XPD-MMS19 protein complex involved in chromosome segregation.** *Mol Cell* 2010, **39**(4):632–640.
114. Weber A, Chung H, Springer E, Heitzmenn D, Warth R: **The TFIIH subunit p89 (XPB) localizes to the centrosome during mitosis.** *Cell Oncol* 2010, **32**(1–2):121–130.
115. You J, Li Q, Wu C, Kim J, Ottinger M, Howley PM: **Regulation of Aurora B expression by the bromodomain protein Brd4.** *Mol Cell Biol* 2009, **29**(18):5094–5103.

doi:10.1186/1475-2867-14-18
Cite this article as: Villicaña *et al.*: The basal transcription machinery as a target for cancer therapy. *Cancer Cell International* 2014 **14**:18.

The genetic depletion or the triptolide inhibition of TFIIH in p53-deficient cells induces a JNK-dependent cell death in *Drosophila*

Claudia Villicaña, Grisel Cruz and Mario Zurita*

Departamento de Genética del Desarrollo, Instituto de Biotecnología, Avenida Universidad 2001, Cuernavaca Morelos, 62250, México

*Author for correspondence (marioz@ibt.unam.mx)

Accepted 7 March 2013
Journal of Cell Science 126, 2502–2515

doi: 10.1242/jcs.122721

Summary

Transcription factor IIH (TFIIH) participates in transcription, nucleotide excision repair and the control of the cell cycle. In the present study, we demonstrate that the Dmp52 subunit of TFIIH in *Drosophila* physically interacts with the fly p53 homologue, Dp53. The depletion of Dmp52 in the wing disc generates chromosome fragility, increases apoptosis and produces wings with a reduced number of cells; cellular proliferation, however, is not affected. Interestingly, instead of suppressing the apoptotic phenotype, the depletion of Dp53 in Dmp52-depleted wing disc cells increases apoptosis and the number of cells that suffer from chromosome fragility. The apoptosis induced by the depletion of Dmp52 alone is partially dependent on the JNK pathway. In contrast, the enhanced apoptosis caused by the simultaneous depletion of Dp53 and Dmp52 is absolutely JNK-dependent. In this study, we also show that the anti-proliferative drug triptolide, which inhibits the ATPase activity of the XPB subunit of TFIIH, phenocopies the JNK-dependent massive apoptotic phenotype of Dp53-depleted wing disc cells; this observation suggests that the mechanism by which triptolide induces apoptosis in p53-deficient cancer cells involves the activation of the JNK death pathway.

Key words: Apoptosis, Drosophila, JNK, TFIIH, Triptolide, p53

Introduction

To carry out their function, several multisubunit complexes involved in transcription and/or DNA repair establish multiple interactions with other factors. This interplay between different components is highly dynamic, and in many cases, the interactions are transitory although fundamental for different cellular processes. A typical example is the 10-subunit complex TFIIH, which participates in RNA pol II- and RNA pol I-mediated transcription, in nucleotide excision repair (NER) and in the control of the cell cycle (Zurita and Merino, 2003). It has been reported that during transcription by RNA pol II, TFIIH must interact with different components of the pre-initiation complex, including TFIIE, subunits of the mediator and RNA pol II (Egly and Coin, 2011). It has also been reported that TFIIH interacts with different transcriptional activators (Esnault et al., 2008; Chymkowitch et al., 2011). These interactions are essential for the primary functions of TFIIH in transcription, including the formation of the DNA bubble at the transcription initiation site that is catalysed by the 3′-to-5′ helicase activity of the XPB subunit and the ATPase activity of XPD. In addition, the phosphorylation of serines 5 and 7 of the CTD domain of the large subunit of RNA pol II, which is necessary to initiate and elongate transcription, is catalysed by the transcription-specific kinase module (CAK) of TFIIH, composed of Cdk7, CycH and MAT1 (Akhtar et al., 2009; Glover-Cutter et al., 2009). In NER, TFIIH is recruited to the damaged site by the DDB and XPC-HR23-β centrin complex in untranscribed regions and by the stalled RNA pol II in transcribed chromatin (Coin et al., 2008). The ATPase activity of XPB is required to anchor TFIIH to the damaged DNA, and the XPD helicase melts the DNA in the 5′ to 3′ direction, thus allowing the incision of damaged strand by XPG and ERCC1-XPF endonucleases. TFIIH maintains a close interaction with XPG and XPA, which stabilise the NER complex (Egly and Coin, 2011). In fact, it has been suggested that XPG forms a complex with TFIIH that participates not only in NER but also in transcription (Ito et al., 2007).

A particularly relevant issue related to TFIIH is its association with human diseases: mutations in its XPB, XPD and p8 subunits are linked to xeroderma pigmentosum, Cockayne syndrome, trichothiodystrophy and cancer (Bergoglio and Magnaldo, 2006). Mutations in other subunits of TFIIH associated with syndromes have not yet been reported in humans. Using *Drosophila melanogaster* as a model to reveal the function of other subunits, it has been demonstrated that *Dmp52* mutations generate phenotypes associated with these three syndromes, indicating that Dmp52 plays an important role in regulating the entire activity of TFIIH during several cellular processes (Coin et al., 2007; Fregoso et al., 2007).

One of the transcriptional activators that have been shown to interact with TFIIH is the tumour suppressor p53 (Léveillard et al., 1996). After genotoxic stress, p53 is activated and can induce either cell cycle arrest, DNA repair or direct the cell toward apoptosis, depending on the severity of the DNA damage (Brady and Attardi, 2010). The transactivation domain (TAD) of p53 can interact with the PH domain of the p62 subunit of TFIIH in human cells; this interaction is correlated with the ability of

Journal of Cell Science

these proteins to activate both the initiation and elongation of transcription (Okuda et al., 2008; Di Lello et al., 2008). In addition, the CAK complex phosphorylates p53 and enhances its DNA-binding activity (Ko et al., 1997). For UV-induced DNA damage, p53 is required for the recruitment of TFIIH to the damaged DNA sites (Wang et al., 1996). Genetically, it has been demonstrated that in human cells derived from patients whose XPD and XPB subunits have been mutated, the apoptotic effect caused by p53 overexpression is suppressed (Wang et al., 1996). In *Drosophila*, a similar result was obtained in XPB (*haywire*) mutant flies (Fuller et al., 1989; Merino et al., 2002). Although these results suggest that p53 requires the presence of intact TFIIH to promote apoptosis, these experiments were conducted in an artificial situation in which p53 was overexpressed. In addition to the established interactions between p62 and the XPB and XPD subunits of TFIIH, a previous report suggested that p53 may also interact with a 52-kDa protein that is present in the TFIIH complex (Léveillard et al., 1996); while this protein was not characterised at the time of the initial publication of its existence, the obvious candidate is the p52 subunit of TFIIH.

The reports of interactions between TFIIH and p53 suggest that these interactions play an important role at some point during the cell cycle and during the processes that occur after DNA damage. However, there is still limited information on the cross talk between p53 and TFIIH during animal development. Here, we present evidence that the fly homologue of p53 (Dp53) directly interacts with the fly p52 (Dmp52) subunit of TFIIH in the absence of genotoxic stress. The depletion of Dmp52 in the wing disc caused growth and differentiation defects during development as well as chromosomal aberrations that can induce apoptosis. Intriguingly, the simultaneous depletion of TFIIH and Dp53 increased the presence of chromosomal aberrations that activate apoptosis in a JNK-dependent manner. Furthermore, the specific inhibition of XPB by the natural product triptolide phenocopies the apoptotic response caused by the absence of p52. This discovery has important implications for the treatment of cell tumours deficient in p53.

Results

Dp53 physically interacts with the Dmp52 subunit of TFIIH

It has been reported that p53 interacts with the p62 subunit of TFIIH through its PH domain (Okuda et al., 2008; Di Lello et al., 2008). Intriguingly, published data also point to the existence of a possible direct contact between p53 and the p52 subunit of TFIIH (Léveillard et al., 1996). To gain insight into the physical interactions between Dp53 and Dmp52 in *Drosophila*, we constructed recombinant Dp53 short (DΔNp53) and large (Dp53) isoform proteins (Bourdon et al., 2005) with FLAG or V5 tags at the C-terminal end and Dmp52 tagged at the N-terminal end (FLAG-Dmp52). These constructions were expressed in S2R$^+$ cells, and the expression of the recombinant Dp53 and Dmp52 proteins were verified by western blots and immunoprecipitation assays using specific antibodies (supplementary material Fig. S1).

Using total protein extracts from cells transfected with the Dp53-tag constructs, we performed co-immunoprecipitation (CoIP) assays. CoIP experiments using whole cell extracts against Dp53-FLAG and the DΔNp53-V5 recombinant proteins enabled the pulldown of the endogenous cellular Dmp52 (Fig. 1A,B, upper panels). In fact, by using a specific Dp53 antibody that recognises both isoforms (supplementary material Fig. S5), CoIP of the endogenous Dmp52 using S2R$^+$ total protein cell extracts was possible (Fig. 1A, lower panel). In the case of the DΔNp53-V5 immunoprecipitation experiments, we also analysed whether Cdk7 and DmXPB (other components of the TFIIH complex) immunoprecipitated with Dp53-V5. Surprisingly, we detected no Cdk7 and only very low levels of DmXPB (Fig. 1B). However, we cannot dismiss the idea that the location of the V5-epitope on the target protein may affect the CoIP results or our experimental conditions, thereby impeding or disaggregating the entire TFIIH complex.

Reciprocal CoIPs using DmXPB, Dp53 or Cdk7 antibodies on non-transfected S2R$^+$ cells showed that the XPB antibody was able to co-immunoprecipitate Dp53 and p62 but not Cdk7 (Fig. 1C; supplementary material Fig. S1C). In addition, we did not detect any CoIP of Cdk7 with either the Dp53 or XPB antibodies. We have observed similar results in the protein extracts of these cells using antibodies against other TFIIH core subunits (unpublished results). Furthermore, CoIPs conducted with Cdk7 antibodies were not able to immunoprecipitate other analysed components of TFIIH (Fig. 1C). It is possible that the conditions used in our CoIP experiments were very strong, which could have resulted in a disrupted interaction between the CAK complex and the core of TFIIH. At this point, we decided to

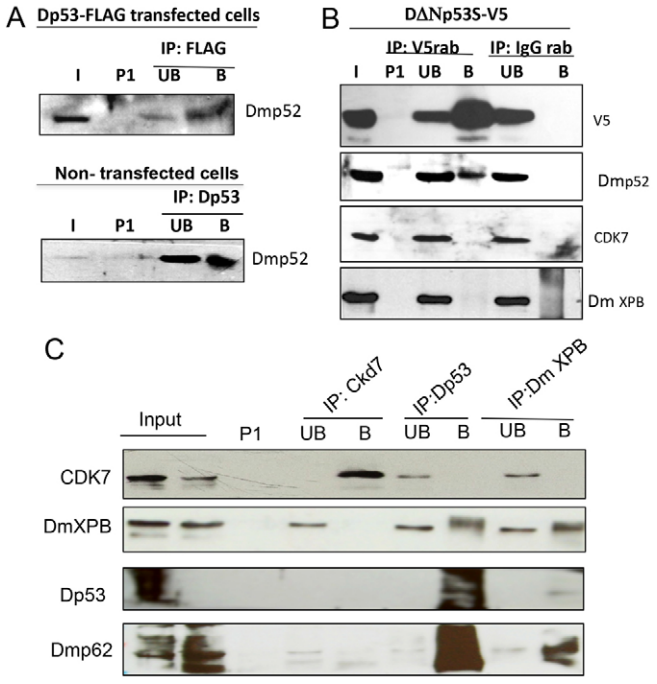

Fig. 1. Dp53 co-immunoprecipitates with TFIIH components. (**A**) Upper panel: endogenous Dmp52 co-immunoprecipitates with Dp53 in whole cell extracts of Dp53-FLAG S2R$^+$ transfected cells. Immunoprecipitation (IP) was performed using FLAG antibody. Lower panel: S2R$^+$ protein cell extracts were immunoprecipitated with the specific Dp53 antibody and the IP material analyzed by western blots using the Dmp52 antibody. (**B**) Endogenous Dmp52 co-immunoprecipitates with DΔNp53. CoIP assays were performed with whole cell extracts of DΔNp53-V5 transfected cells and DΔNp53 was pulled down with an antibody that recognizes V5. CoIP was revealed against other components of TFIIH with Cdk7 and XPB specific antibodies. (**C**) Endogenous Dp53 co-immunoprecipitates with XPB and p62 in wild type cell extracts. CoIP assays were performed with specific antibodies against XPB, Cdk7 and Dp53. I, input; P1, preclearing 1; UB, unbound; B, bound.

examine whether both Dp53 isoforms and Dmp52 interact with each other using extracts of S2R^{+} cells that had been co-transfected with both tagged proteins. We demonstrated that FLAG-Dmp52 can interact with both isoforms of V5-tagged Dp53 in CoIP assays (supplementary material Fig. S1). Together, these experiments strongly suggest that Dmp53 may interact with some TFIIH subunits, even in conditions in which DNA damage has not been induced.

We next analysed whether Dp53 and Dmp52 can interact directly. To achieve this goal, we expressed recombinant proteins containing different regions of Dmp52 fused to GST in *E. coli* (Fig. 2A). These GST-Dmp52 proteins were used in pulldown experiments against the Dp53 and DΔNp53 isoforms and against constructs that cover different regions of Dmp53 expressed *in vitro* in a coupled transcription translation system (Fig. 2A). Fig. 2B shows that DΔNp53 interacts with the complete Dmp52 protein. We next tested the interaction of the two Dp53 isoforms with the complete Dmp52 protein and the C-terminal domain (CTD-Dmp52) of Dmp52, which has been shown to be important for the interaction with the p8 subunit of TFIIH. We also tested a construct with a deletion of the Dmp52 CTD (Dmp52ΔCTD) (Fig. 2A). We found that both polypeptides (Dp53 and DΔNp53) can interact with the complete Dmp52 protein (Fig. 2C). Intriguingly, we also observed that Dp53 contacts the CTD region of Dmp52 as well as the rest of the protein. Multiple contacts in different regions between p52 and XPB have been demonstrated (Jawhari et al., 2002), and, together with our data, these results suggest that Dmp52 can interact with different proteins simultaneously through different regions. We next analysed the two isoforms containing a deletion of the CTD of Dp53 and analysed the CTD alone for its interaction with Dmp52. We again found that both Dp53 isoforms interact with Dmp52 but that Dp53 CTD, which contains the complete oligomerisation domain, does not recognise Dmp52 (Fig. 2D, lower panel). In summary, these results demonstrate that Dp53 most likely interacts with Dmp52 through its DBD even in the absence of genotoxic stress and that Dmp52 can be added to the list of factors that may have direct physical contact with Dmp53.

Depletion of TFIIH in the wing imaginal disc affects growth and cell number in the adult wing

In *Drosophila*, mutant alleles of the *Dmp52* gene are lethal, but heteroallelic combinations of these mutants may generate adult organisms that are smaller than wild-type flies with melanotic

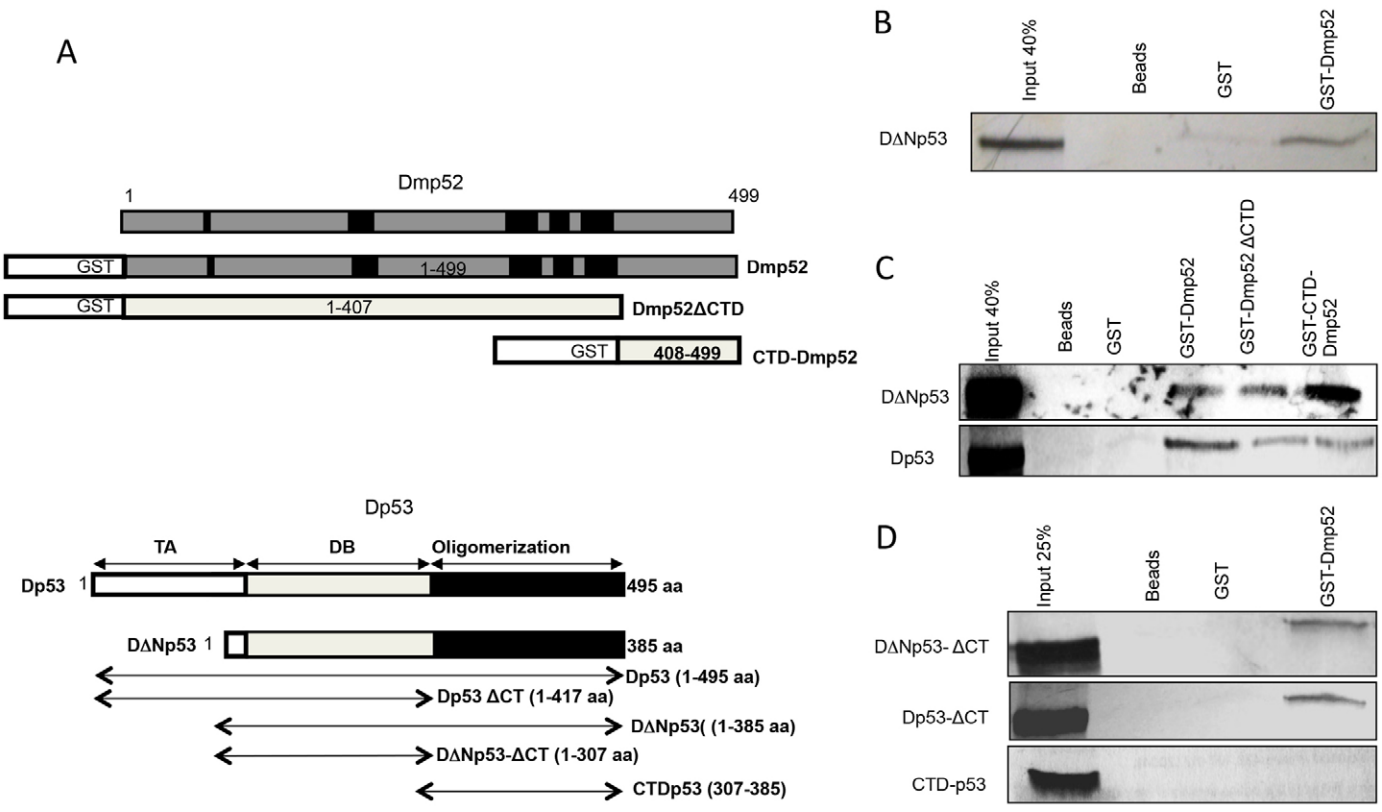

Fig. 2. Dmp52 interacts physically with both isoforms of Dp53. (**A**) Schematic representation of Dmp52 and Dp53 proteins. Upper panel: Dmp52 scheme showing full length protein and fragments of recombinant GST-tagged Dmp52 used to perform pulldown assays. Dmp52 fragments include a CTD domain and protein excluding this domain fused to GST (GST-Dmp52ΔCTD). Lower panel: Dp53 scheme showing full length protein of both isoforms in addition to protein fragments transcribed and translated *in vitro* and marked with radioactive ^{35}S. Fragments of Dp53 consist in CTD-domain of Dp53, which is the same in both isoforms, and their respective fragments with truncated CTD eliminating the oligomerisation domain. (**B**) Pulldown assay demonstrating that recombinant GST-Dmp52 protein interacts physically with DΔNp53 isoform. Although a weak signal is detected for GST-only, DΔNp53 signal is stronger on incubation with GST-Dmp52, indicating an interaction between these proteins. (**C**) Pulldown assay of Dmp52 and its fragments with both isoforms of Dp53. Both Dp53 isoforms interacts physically with full length Dmp52, the CTD domain and GST-Dmp52ΔCTD, indicating at least two binding sites on Dmp52. (**D**) Pulldown assay of Dp53 fragments and full length Dmp52. Dmp52 interacts with Dp53 through a region that excludes its oligomerisation domain.

tumours and chromosomal instabilities (Fregoso et al., 2007). These phenotypes are pleiotropic and may be caused by the accumulation of defects during development; it is therefore difficult to determine the contribution of the genetic interaction of factors such as Dp53. Therefore, we decided to analyse the effect of the depletion of Dmp52 in a particular tissue at a specific time. To achieve this objective, we decided to use dsRNA against Dmp52 specifically directed to the wing disc using the UAS-GAL4 system. The wing disc is a monolayer epithelium that grows several thousand-fold in mass and cell number during larval development and is an excellent model for the study of cell growth, proliferation and differentiation (Martín et al., 2009). Thus, to direct the expression of *Dmp52i*, we first used the *MS1096* driver, which directs the expression of Gal4 in the dorsal domain of the wing pouch; we then crossed these flies with flies carrying dsRNA against Dmp52 (*Dmp52i*) from the Vienna Resource Center. Consistent with results from our previous work using *Dmp52* mutant alleles (Fregoso et al., 2007), we observed a reduction in the size of adult wings in flies expressing *Dmp52i* compared with flies carrying only the driver (Fig. 3). We also observed deformation of the wing shape and the presence of extra veins in the wing (Fig. 3).

To confirm these results and to determine if the expression of *Dmp52i* in a different wing disc domain generates similar phenotypes, we used an *engrailed* driver (*en-Gal4*) that directs the expression of *Dmp52i* to the posterior domain of the wing disc (Fig. 3). A reduction in wing size and the presence of extra veins (indicated by arrows in Fig. 3) were also observed with the *en-Gal4* driver. In addition, the posterior cross vein was so highly reduced that it almost disappeared. Interestingly, in the case of the *en-GAL4* driver, we observed that the proportion of the wing territories was relatively well maintained, even in regions where *Dmp52i* was not expressed, although the reduction in size was stronger in the posterior domain than in the anterior domain (supplementary material Fig. S2). In addition, the presence of extra veins was also detected in territories outside the driver expression. It has been recently reported that stressful conditions that reduce the cell size in a particular territory in the wing disc generate a non-autonomous effect to coordinate cell growth in adjacent cell populations (Mesquita et al., 2010; Wells and Johnston, 2012); it appears that this scenario also applied in the case of the depletion of the Dmp52 subunit of TFIIH in the posterior wing disc.

To confirm that the observed phenotypes are caused by the depletion of Dmp52 in the dorsal wing disc domain, we created flies that contain the *MS1096-Gal4* driver, *Dmp52i* and *Gal80^{ts}*, which is an inhibitor of Gal4. We found that the phenotype of reduced wing size and extra wing veins reverted, confirming that those phenotypes are caused by the expression of *Dmp52i* in the wing disc (supplementary material Fig. S3A). Furthermore, we also showed that the levels of Dmp52 protein were reduced in salivary glands expressing *Dmp52i*, reinforcing the specificity of the dsRNA (supplementary material Fig. S3B). However, different phenotypes were observed in the wing when we previously used the *MS1096-Gal4* driver to express dsRNA against different targets (unpublished results), indicating that the wing phenotypes observed by depleting Dmp52 are specific.

Recently, reports have suggested that subunits of TFIIH could associate with other complexes, independent of TFIIH. This description is true for XPD, which has been shown to interact with the MMS19 complex involved in chromosome segregation (Ito et al., 2010). Thus, we evaluated whether the phenotypes generated by the depletion of Dmp52 were due to an independent TFIIH functional effect on Dmp52 or to a generalised effect on TFIIH. We also decided to evaluate whether these phenotypes are also caused by the depletion of other TFIIH subunits. We directed the expression of a dsRNA against the *Drosophila* p34 subunit of TFIIH (*Dmp34* in the fly) using the *MS1096* driver. The depletion

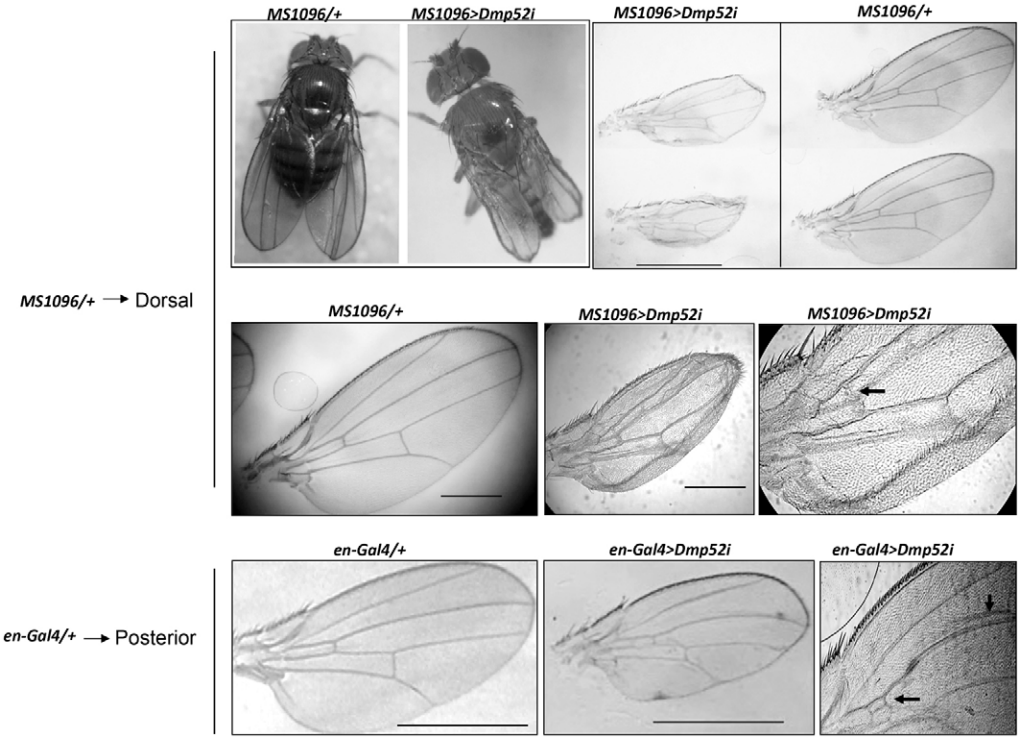

Fig. 3. Expression of dsRNA against Dmp52 (*Dmp52i*) reduces wing size and causes rising of extra veins. Dmp52 depletion in the wing on the dorsal domain causes a 'bent out' phenotype in wings (upper left-hand panel) and a marked wing size reduction compared with controls (upper right-hand panel). Analysis by light microscopy of wings Dmp52 depleted shows extra veins on the wing blade (indicated by an arrow). Expression of *Dmp52i* with *en-Gal4* driver shows similar phenotypes to those observed with *MS1096* driver. Extra veins are also formed in regions outside of Gal4 expression (arrows). The bars in the wing images indicate an equivalent real size.

of Dmp34 shows similar phenotypes to those observed for the depletion of Dmp52, although phenotypes were more severe in the wing when using *MS1096-Gal4* driver and identical when using the *en-GAL4* driver, indicating that the observed defects in the wing are caused by a reduction in the activity of TFIIH (supplementary material Fig. S4). The differences in the severity of phenotypes associated with *Dmp34i* and *Dmp52i* using *MS1096* as the driver could be due to differences in RNAi efficiency, as was observed when the temperature was modulated (supplementary material Fig. S4A). Furthermore, using an *eyeless-Gal4* driver that directs Gal4 expression to the eyes, we found that similar growth defects were also observed in both *Dmp52i* and *Dmp34i* (supplementary material Fig. S4C).

The reduction in the wing size and the appearance of extra veins suggest that the depletion of Dmp52 may be affecting cell proliferation and/or cell growth as well as cell differentiation. To determine if the reduction in the wing size was due to fewer or smaller wing cells, we counted the number of hairs in the wing; these hairs are nonsensory apical projections that form from single cells present in a specific area (Quijano et al., 2011). Fig. 4A shows a comparison of control wings and *Dmp52i* wings. The knockdown wing clearly has more hairs per area, a disorganised hair pattern and deformations in the longitudinal and cross veins (indicated by an arrow in Fig. 4A; Fig. 4B). Likewise, the overall size of the *Dmp52i* wing is approximately half the size of the control wing (Fig. 4C). In addition, the

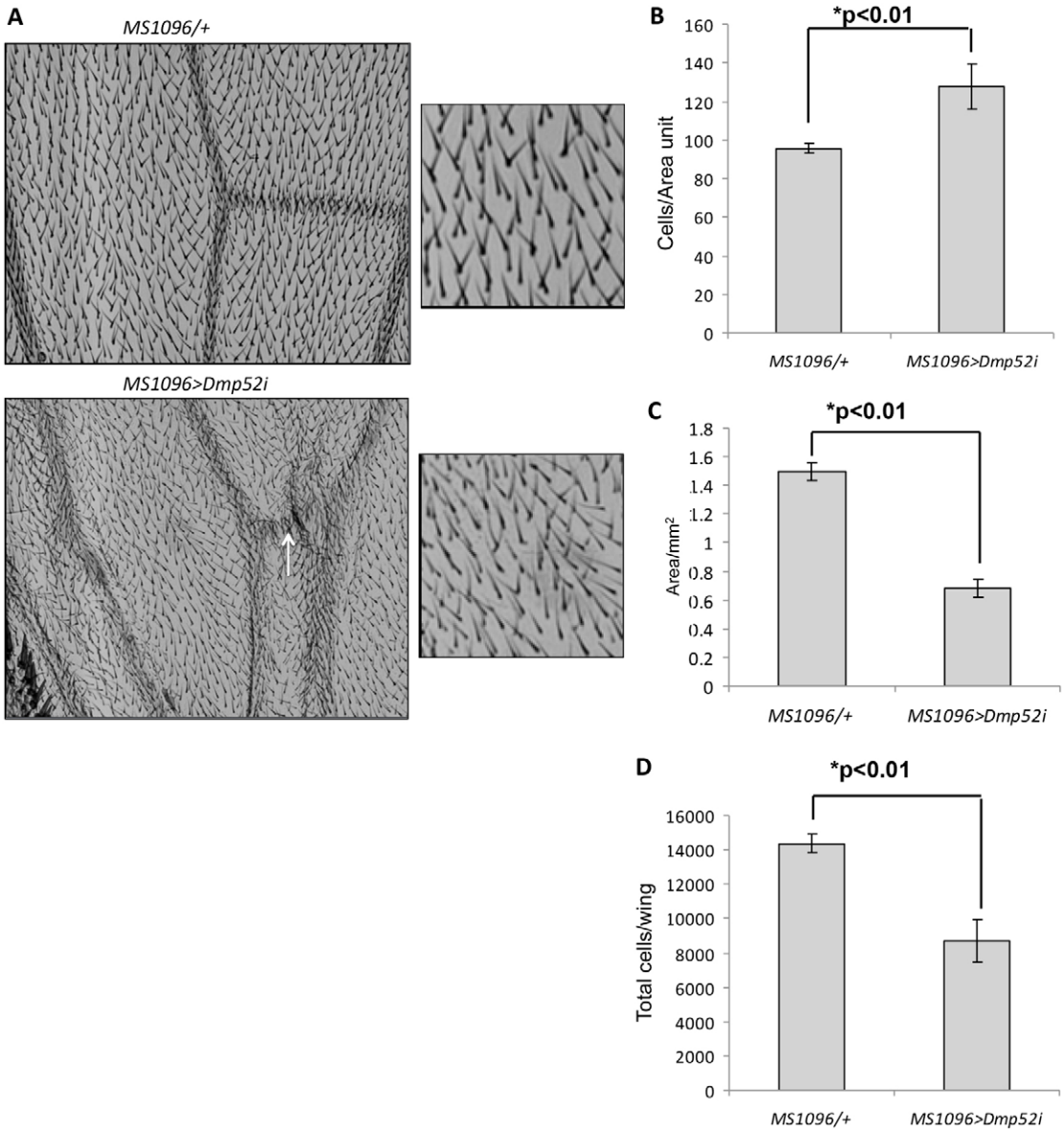

Fig. 4. Dmp52 depletion generates a higher cell density per area and wings that have a lower number of total cells. (**A**) *MS1096 >Dmp52i* wings showed a higher density of brittles per unit area. The arrow indicates a deformation in the wing vein. (**B**) Quantification of cells per unit area in Dmp52 depleted wings reveals a higher cell density, indicating that cell size is smaller compared with controls. (**C**) Quantification of wing area. The blade wing is reduced by approximately 50% in *MS1096 >Dmp52i*. (**D**) Quantification of number of total cells per wing indicates that although *MS1096 >Dmp52i* exhibits a higher cell density, the number of total cells is lower if compared with the *MS1096/+* control. Results in B–D are means±s.e.m.

number of cells per specific area is ~20% greater in the *Dmp52i* wing than in controls, indicating that every cell is smaller and that a defect is present in the growth of each individual cell (Fig. 4B). However, even though the number of cells per unit area is higher in the *Dmp52i* wing than in the control wing, the total number of cells in the whole wing is lower in the *Dmp52i* wing than in the control wing (Fig. 4D). Therefore, the depletion of Dmp52 in the wing disc affects both the cell size and the total number of cells, indicating that both cell growth and total cell number are affected. In addition, the presence of extra veins suggests alterations in the differentiation process that establishes the vein pattern in the wing when TFIIH is not completely functional.

Dmp52 interacts genetically with Dp53, and its simultaneous depletion enhances a JNK-dependent massive cell death

The reduction in the total cell number observed in the wings depleted in Dmp52 may be caused either by a reduction in proliferation or by an increase in cell death during wing development. To determine which of these processes was involved in the generation of this phenotype, wing discs were analysed for apoptosis using TUNEL assays, the incorporation of BrdU to visualise DNA replication and the detection of H3Pser10 to visualise the entry into mitosis. Interestingly, we observed that the incorporation of BrdU in DNA and the distribution and number of nuclei that were positive for H3Pser10 were not affected in wing discs with reduced levels of Dmp52 at any developmental stage (Fig. 5A and data not shown). However, Dmp52-depleted wing discs showed higher rates of apoptotic cell death than discs carrying only the driver (Fig. 5A). This result suggests that the reduction in the cell number is at least in part due to an increase in apoptosis during development of the wing disc.

In a previous analysis of mutant alleles in Dmp52, we discovered the presence of chromosomal aberrations in neuroblast metaphasic chromosomes (Fregoso et al., 2007). This defect may be related to the increase in apoptosis observed in the wing discs that have reduced levels of Dmp52. Therefore, we analysed the presence of aberrant chromosomes in these discs with a loss of heterozygosity assay (LOH) using the mwh^1 marker. Homozygous mwh^1/mwh^1 clones form groups of three

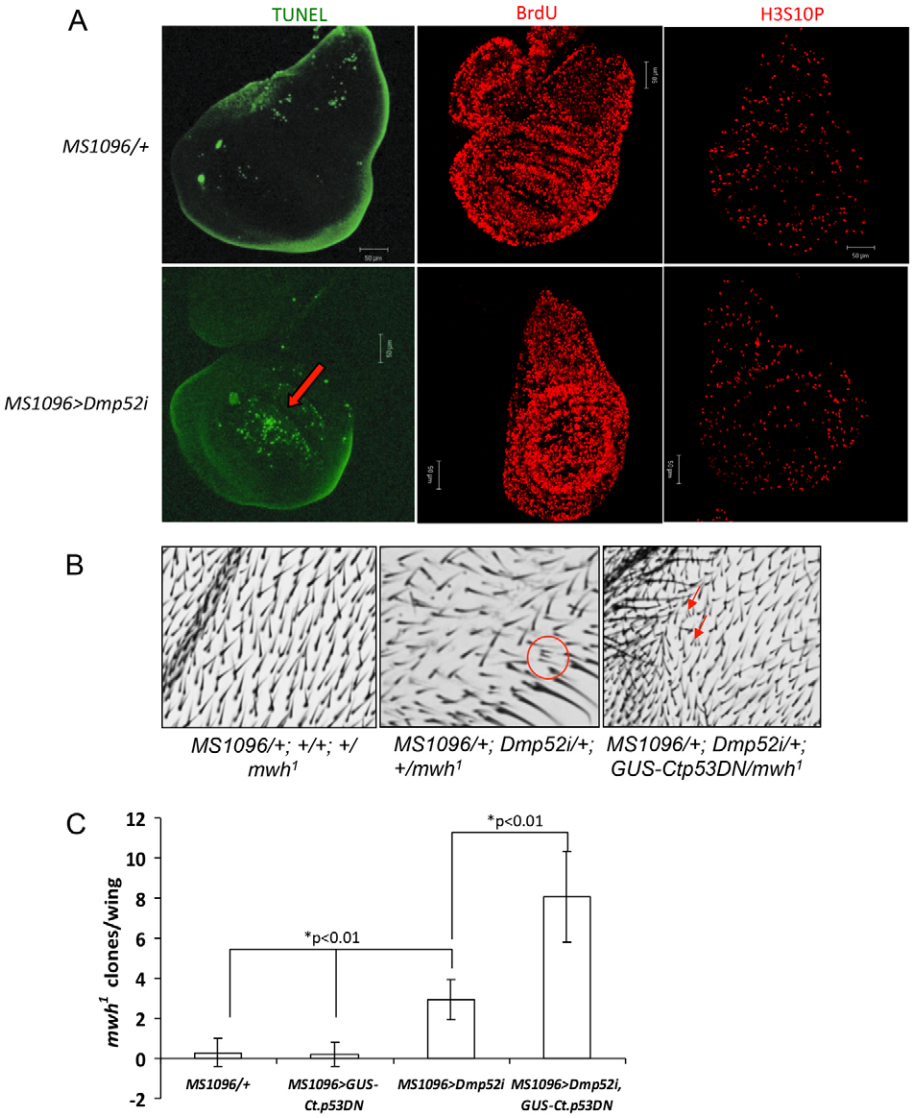

Fig. 5. Reduction of levels of Dmp52 induces apoptosis in wings and generates chromosomal instability. (**A**) BrdU incorporation, H3S10P immunostaining and TUNEL labeling of wing discs. Dmp52 depleted wing discs exhibit more apoptotic bodies than controls; no changes in BrdU or H3S10P were observed, indicating that cell cycle progression is not perturbed. The arrow indicates apoptotic bodies. Scale bars: 50 µm. (**B**) Reducing levels of Dmp52 causes genomic instability in wings. Control and *GUS-Ctp53DN* expressing wings exhibit almost no mwh^1 clones, but *MS1096>Dmp52i* wings showed a higher number of mwh^1 clones; interestingly, the highest number of mwh^1 clones was present in *MS1096>Dmp52i, GUS-Ctp53DN* wings. (**C**) Quantification of mwh^1 clones per wing. The genotypes are indicated in the figure. Results are means±s.e.m.

bristles in the wing, and thus, when heterozygous mwh^1/+ individuals suffer chromosomal rearrangements (loss of the wild-type allele by deletions of segments or the complete loss of the chromosome), they generate this particular phenotype (de Andrade et al., 2004). Using this assay, we found a higher frequency of mwh^1 homozygous clones in wings of Dmp52-depleted flies than in wings of flies heterozygous for the mwh^1 allele carrying only the driver *MS1096* (Fig. 5B,C). These results indicate that when TFIIH is not completely functional, aberrant chromosomes are generated; the increase in apoptosis in the wing disc could therefore be generated by the presence of these chromosomal aberrations.

Because Dp53 and Dmp52 interact directly with each other, we decided to analyse the interaction between these two factors at the genetic level by taking advantage of the specific apoptotic phenotype observed in the wing when the levels of Dmp52 are reduced. Genetic interactions between TFIIH and p53 have been demonstrated in human cells derived from patients afflicted with xeroderma pigmentosum who carry mutations in XPD and XPB as well as in *Drosophila* XPB mutants (Robles et al., 1999; Wang et al., 2003; Merino et al., 2002). These studies were performed by overexpressing p53 to induce apoptosis in backgrounds deficient for XPD or XPB. However, no studies have been performed *in vivo* using mutants or RNAi that affect both TFIIH and p53 functions simultaneously. To determine the developmental effect of depleting both TFIIH and p53 in a particular tissue at the same time, we expressed *Dmp52i* together with a dominant negative mutant form of Dp53 (*GUS-Ctp53DN*) that has been used as a bona fide inhibitor of Dp53 (Brodsky et al., 2000; Shlevkov and Morata, 2012), again using the UAS-GAL4 system and the *MS1096* driver. The expression of the dominant negative form of Dp53 does not have an effect on the development of the wing (Brodsky et al., 2000) (Fig. 6C). Intriguingly, *Dmp52i* in combination with the *GUS-Ctp53DN* mutant enhanced the defects that were produced in the wing by the depletion of Dmp52 (Fig. 6D). Similar results were observed with an inducible dsRNA that covers the two Dp53 isoforms (*Dmp53i*) together with the simultaneous expression of *Dmp52i* (supplementary material Fig. S5A,C). These results suggest that the depletion of Dmp52 generates defects that require a functional Dp53 to reduce the effects caused by a defective TFIIH.

Because the depletion of Dmp52 induces apoptosis, we analysed the wing discs of *MS1096 >Dmp52i,GUS-Ctp53DN*

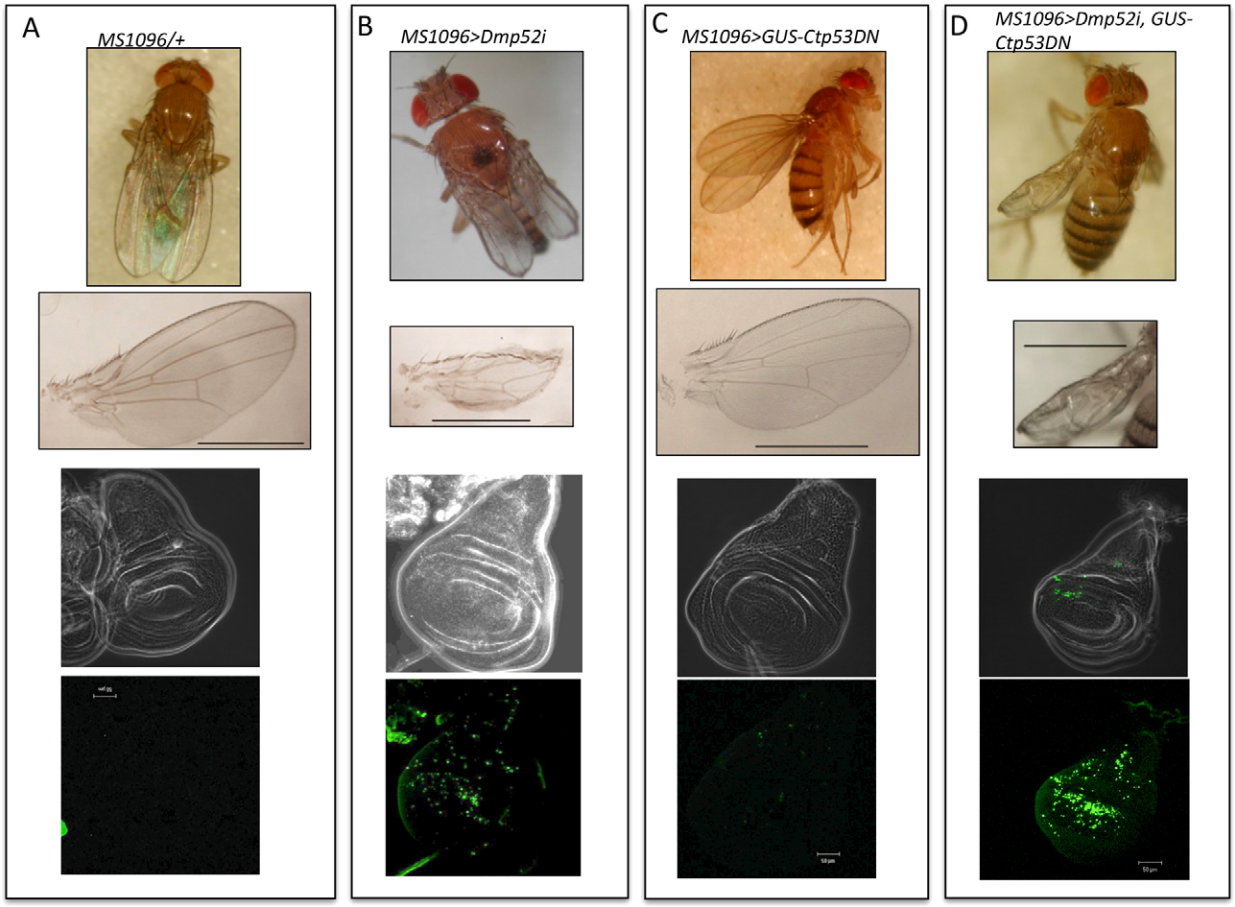

Fig. 6. Loss of function of *Dmp52* and *Dp53* causes a massive cell death in wing discs. (**A**) Control wings show a wild-type phenotype (top two panels) and reduced number of apoptotic bodies on wing discs (bottom panel). (**B**) *MS1096 >Dmp52i* wings show a bent out phenotype and reduction in size as previously described in Fig. 4 and several apoptotic bodies on wing discs. (**C**) *MS1096 >GUS-Ctp53DN* wings show a wild-type phenotype (top two panels) and reduced number of apoptotic bodies in wing discs. (**D**) *MS1096 >Dmp52i,GUS-Ctp53DN* wings showed enhanced morphological defects compared with *MS1096 >Dmp52i* (top two panels) and causes a massive apoptotic cell death in wing discs. The bars in the wing images (second row) indicate an equivalent real size. Scale bar: 50 µm (bottom panels).

flies using TUNEL assays and acridine orange staining. Intriguingly, we observed a dramatic increase in cell death in these discs, explaining the enhancement of the wing defects in the *Dmp52i* adult flies when Dp53 was not functional (Fig. 6; supplementary material Fig. S5B). Furthermore, the same enhancement in apoptosis was observed in flies expressing the *Dmp34 RNAi* in conjunction with the expression of *GUS-Ctp53DN* (supplementary material Fig. S5C). Thus, the inactivation of Dmp53 does not suppress cell death but instead enhances it when Dmp52 or Dmp34 (TFIIH) is depleted. We also evaluated DNA synthesis and the mitotic status in these flies and did not find any difference from the control organisms (supplementary material Fig. S6). Interestingly, when we analysed the wings of *MS1095 >Dmp52i,GUS-Ctp53DN* flies for LOH, we found a higher number of mwh^1 clones than in the wings of *Dmp52i* flies (Fig. 5C). These data suggest that in the absence of Dmp52 and Dp53, there is an increase in chromosome fragility that cannot be repaired, resulting in the generation of a higher rate of chromosomal aberrations. This hypothesis is supported by the fact that UV-induced DNA damage enhances the apoptotic phenotype in flies with depleted Dp53 and Dmp52 (supplementary material Fig. S7A).

The next focus was to corroborate the hypothesis that the enhancement of the *Dmp52i* phenotype by the absence of a functional Dp53 is linked to apoptosis. We therefore first expressed the p35 inhibitor of caspases that inhibit apoptosis, together with *Dmp52i* in the wing and found that the defects in the adult wing were increased, but the appearance of the wing was different than that of the wings of flies in which Dmp52 and Dp53 were simultaneously depleted (Fig. 7A). The adult wings exhibited a large blister in which the dorsal and ventral wing surfaces were separated. Furthermore, the expression of the caspase inhibitor p35 abolished the apoptosis induced by the depletion of Dmp52, indicating that the cell death generated by the reduction of Dmp52 detected by TUNEL is caspase-dependent and confirming that the TUNEL assay was detecting apoptosis (Fig. 7B). We next investigated whether the enhancement of apoptosis in *MS1096 >Dmp52i;GUS-Ctp53DN* discs is also caspase-dependent by co-expressing p35. Fig. 7C shows that blocking the caspase Drice by p35 suppressed the massive apoptosis generated by the co-depletion of Dmp52 and Dp53 in the wing disc. We also determined if the depletion of Dmp52 in combination with the expression of p35 in the wing disc caused alterations in the control of the cell cycle. Again, we

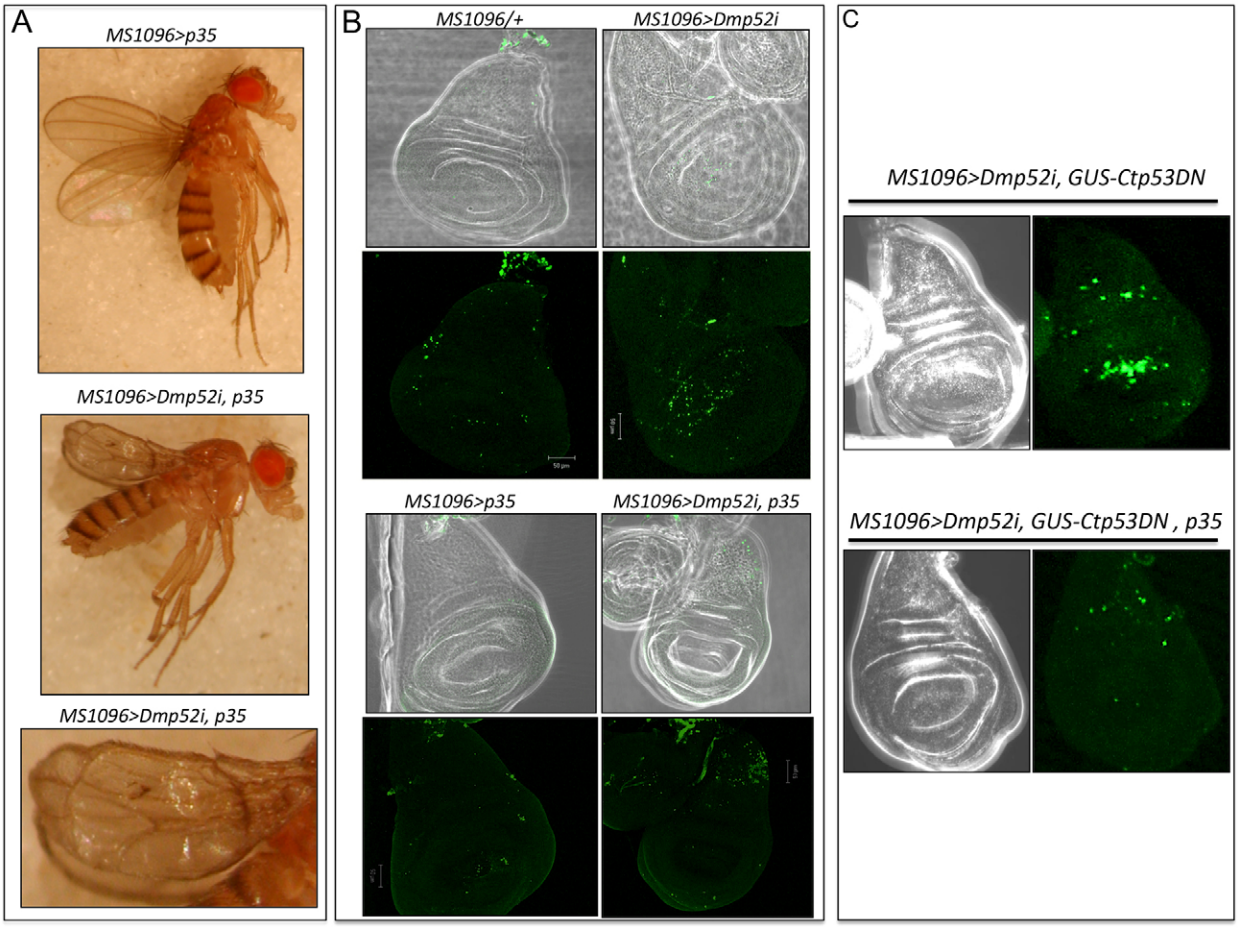

Fig. 7. Coexpression of p35 abolishes cell death, indicating a caspase-dependent pathway. (**A**) Coexpression of p35 in *MS1096 >Dmp52i* background causes blisters and altered wing morphology. (**B**) TUNEL assay demonstrating that apoptosis generated in *MS1096 >Dmp52i* is abolished when p35 is co-expressed on this genetic background. (**C**) The massive cell death detected by TUNEL on *MS1096 >Dmp52i*, *GUS-Ctp53DN* wing discs is also caspase-dependent. Apoptotic bodies are abolished when p35 is co-expressed on *MS1096 >Dmp52i*, *GUS-Ctp53DN* wing discs. The genotypes are indicated in each panel. Scale bars: 50 μm.

analysed the incorporation of BrdU in the S phase and of H3Pser10 for the entry into M phase. Intriguingly, we did not detect any change in the number of cells in the S phase or M phase of the cell cycle (supplementary material Fig. S6). These results suggest that when Dmp52 is not functional in the dorsal region of the wing disc in the absence of Dp53 or when apoptosis is inhibited, the different checkpoints are not responding to the cellular stress present in this condition; these data suggest that TFIIH plays a direct role in the checkpoint response.

It is known that *Drosophila* responds to stress stimuli through the Dp53 and JNK pathways, thereby activating the expression of pro-apoptotic genes (Brodsky et al., 2000; Luo et al., 2007). In fact, it has been recently demonstrated that Dp53 and JNK establish a feedback loop that amplifies the initial apoptotic stimuli (Shlevkov and Morata, 2012). However, it has also been reported in a p53 mutant context that a p53-independent apoptosis mechanism is activated in response to ionising radiation and that this mechanism depends on the JNK pathway (McNamee and Brodsky, 2009). Based on these reports, we decided to analyse the effect of the depletion of JNK (*basket* in *Drosophila*) on apoptosis in wing discs that were also depleted of Dmp52 and Dp53. To achieve this goal, we used the *MS1096* driver to direct the expression of a dsRNA against the JNK transcript. Interestingly, the depletion of Dmp52 increased the levels of phosphorylated JNK (P-JNK), although apoptosis was not completely abolished when JNK was depleted (Fig. 8A,B). These results suggest that the increase in cell death in Dmp52-depleted wing discs, although linked to the activation of JNK, is not completely suppressed by the absence of JNK and does not produce the same response as the depletion of Dp53 when Dmp52 is not present. However, when we analysed Dmp52-, Dp53- and JNK-depleted flies, apoptosis was practically abolished (Fig. 8A,B; supplementary material Fig. S7B). These results correlate with the fact that the levels of P-JNK are dramatically enhanced in discs depleted in Dmp52 and Dmp53 (Fig. 8B). Together, these results indicate that the enhancement of apoptosis observed in Dmp52- and Dp53-depleted wing discs depends on the JNK pathway.

Inhibition of the ATPase activity of XPB using triptolide phenocopies the massive apoptotic phenotype in Dmp52-Dp53- depleted cells

Triptolide is a diterpene triepoxide derived from *Tripterygium wilfordii*, a plant used in traditional medicine in China that has been shown to have a potent antiproliferative effect on different types of cancers in preclinical studies. Recently, it has been demonstrated that triptolide specifically inhibits the ATPase activity of the XPB subunit of TFIIH, accounting for most of the pharmacological effects of this natural product (Titov et al., 2011). Interestingly, most of the studies using triptolide report that apoptosis is the principal cause of death in cancer cells (Liu, 2011). Therefore, we decided to determine if the treatment of third instar larvae wing discs with triptolide in a Dp53-deficient context phenocopies the apoptotic phenotype generated by the simultaneous depletion of functional Dmp52 and Dp53. To determine the effect of triptolide on third instar larvae wing discs,

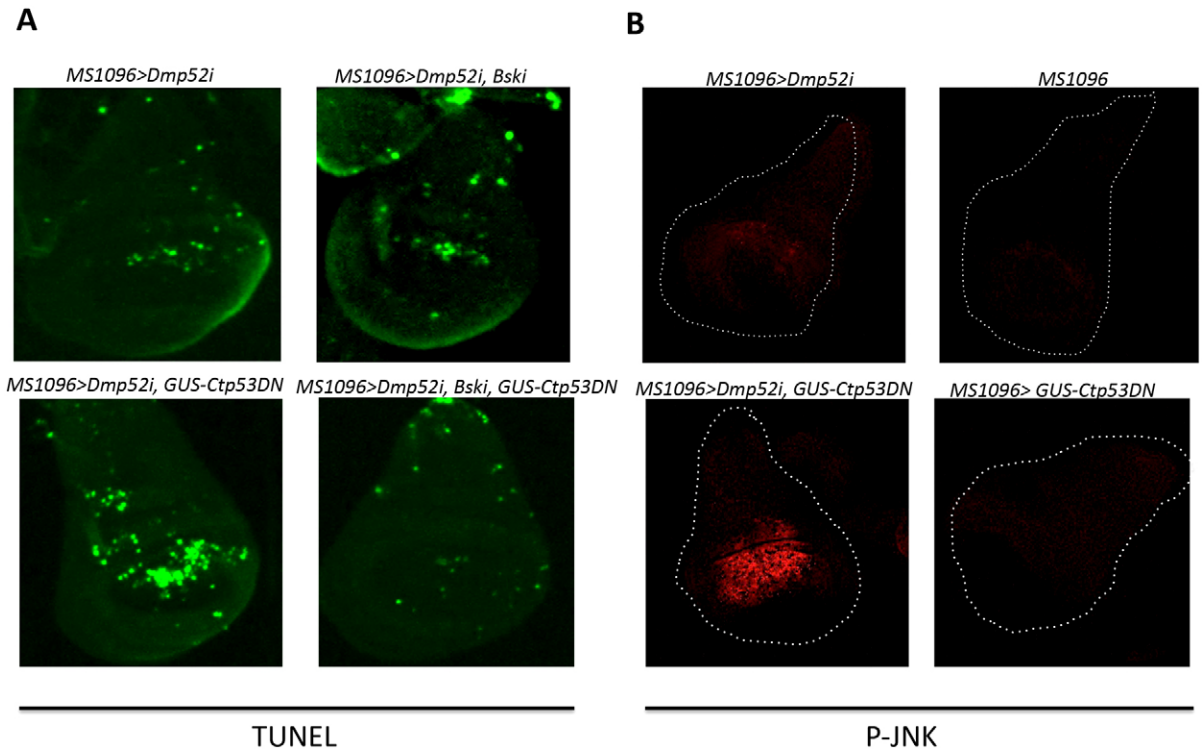

Fig. 8. Massive apoptotic cell death in *MS1096 >Dmp52i, GUS-Ctp53DN* discs is JNK-dependent. (**A**) The expression of dsRNAi against *Basket* (*Bski*) abolishes apoptosis induced in wing discs by loss of function of Dmp52 and Dp53 (lower panels), indicating that apoptosis in this background is JNK-dependent. However, apoptosis induced in Dmp52 depleted wing discs is partially *Bski*-independent, shown by the observation that it is not completely abolished when *Bski* is co-expressed in *MS1096 >Dmp52i* background (upper panels). (**B**) The depletion of Dmp52 activates the JNK pathway. However, the simultaneous depletion of Dmp52 and Dp53 induce an enhancement of JNK phosphorylation. Note that no signal is detected in the control genotypes.

we incubated wing discs *in vitro* with different concentrations of the compound at different times. We found that the incubation of same-age wild-type third instar larvae wing discs generated apoptosis in a dose- and time-dependent manner (supplementary material Fig. S8). From these studies, we decided to incubate the wing discs with 100 μM triptolide for 3 hours. Under these conditions, the rate of apoptosis in all wing discs was similar to that observed in discs expressing the dsRNA against Dmp52 in the dorsal domain of the wing pouch using *MS1096* as a driver. We next incubated wing discs expressing the *GUS-Ctp53DN* dominant-negative form of Dp53 using the *MS1096* driver with triptolide and found that as in the case of the double depletion of Dmp52 and Dp53 in this wing compartment, an increase in apoptosis occurred (Fig. 9). Thus, the inhibition of the ATPase activity of the XPB subunit of TFIIH by triptolide in cells deficient in functional Dmp53 generates the same phenotype as when the TFIIH subunit Dmp52 and Dp53 are simultaneously depleted. We determined if the increase in apoptosis generated by the combined action of triptolide and the depletion of functional Dp53 was also JNK-dependent. We found that the depletion of JNK in wing discs treated with triptolide in a Dp53-deficient context reduced the number of apoptotic cells (Fig. 9). Therefore, treatment with triptolide phenocopies all of the phenotypes produced by depleting Dmp52, Dp53 and JNK and supports the recent report that the target for this natural product is TFIIH (Titov et al., 2011). Reciprocally, these results also confirm that the phenotypes observed by the depletion of Dmp52 and Dmp34 using RNAi are indeed caused by deficiencies in TFIIH activities.

Discussion

TFIIH subunits play a role in at least three mechanisms that are critical for the cell: transcription by RNA pol II, DNA repair by NER and the control of the cell cycle. Therefore, disruption of TFIIH may cause a dramatic and generalised stressful situation for the cell. The depletion of TFIIH in the *Drosophila* wing disc produces wings that contain smaller and fewer cells per wing. The defects in growth may be produced by the global reduction of transcription, making this defect a minute-like phenotype, as we have previously described (Fregoso et al., 2007). However, the reduction in the total cell number is not due to a defect in cell proliferation or in delays in the entry to mitosis. As was documented in this work, the most obvious response to the absence of TFIIH is the induction of apoptosis, which may explain the deformation of the wing shape and the reduction in

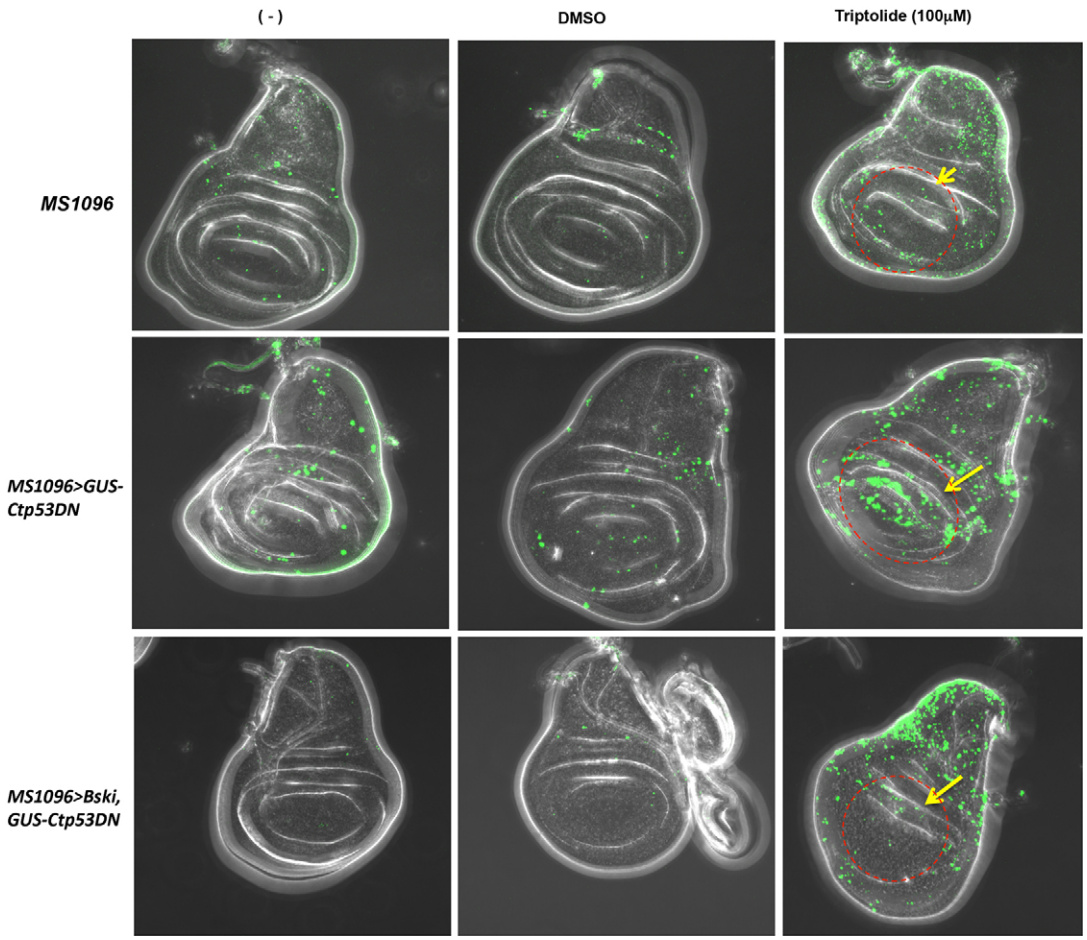

Fig. 9. Triptolide phenocopies the apoptotic induction in Dp53 depleted cells. Third instar imaginal wing discs carrying the *MS1096* driver or in combination with the Dp53 dominant negative (GUS-Ctp53DN) or the GUS-CTp53DN plus the *Bsk* RNAi were incubated for 3 hours in insect medium (see the Materials and Methods and supplementary material Fig. S8), alone or with DMSO (vehicle) or 100 μM of triptolide, and tested for apoptosis by TUNEL assays. An increase in apoptotic bodies in the *MS1096 >GUS-CTP53DN* disc, in the *GAL4* expression domain (indicated by an arrow and a red circle), is observed. This phenotype is suppressed by the presence of the dsRNA that depletes *Bsk* at the same wing domain. Phenotypes are indicated in the figure.

the total number of cells in the wings depleted of Dmp52 or Dmp34.

Stimuli- and signalling-activated apoptosis is complex and context-dependent. In *Drosophila*, factors that induce apoptosis under different stress situations converge to produce an activation of caspases that cause the death of the cell (Shlevkov and Morata, 2012). Recently, it has been reported that E2F plays a dual role in apoptosis, as it is anti-death in Dp53-independent apoptosis and pro-death in Dp53-dependent apoptosis. Moreover, E2F and Dp53 are involved in inducing apoptosis in an independent manner during development, but both are required for apoptosis when DNA is damaged (Moon et al., 2008). However, in previous works, it has been reported that the apoptosis that is generated by the overexpression of p53 requires the presence of a functional TFIIH (Robles et al., 1999; Merino et al., 2002). In this study, we found that when both TFIIH and Dp53 were not functional in the wing imaginal disc, apoptosis was dramatically enhanced. This apoptosis is dependent on JNK, as the simultaneous depletion of Dmp52 and Dp53 induced the activation of JNK (P-JNK) at very high levels and the depletion of JNK abolished apoptosis. However, it is important to take in account that Ctp53DN or the *Dp53i* used in this work affects both Dp53 isoforms, and since both are capable to induce apoptosis (Dichtel-Danjoy et al., 2013), we can not differentiate if the effects that we are observing are due to the depletion of the activity of both Dp53 isoforms or just one.

Although Dp53 is a regulator of several processes (including the apoptotic response), some signals that activate apoptotic programmes are dependent on other proteins. The overexpression of the tumour suppressor LKB1 or the ZBP-89 protein generates an apoptotic cell death that is p53-independent but JNK-dependent, suggesting that this kinase may be an apoptosis instigator (Bai et al., 2004; Lee et al., 2006). Furthermore, it has been demonstrated that sirtuins can induce apoptosis mediated by JNK signalling independent of Dp53 (Griswold et al., 2008). Our results are consistent with previous reports that demonstrate that the response to ionising radiation (IR) in discs deficient in Dp53 and the checkpoint protein Chk1 (GRP in *Drosophila*) generates a strong JNK-dependent apoptotic phenotype (McNamee and Brodsky, 2009). In this situation, IR generates chromosomal aberrations, and the checkpoint controls mediated by Chk1 are not functional; cells that are still able to progress in the cell cycle but that contain chromosomal abnormalities (including aneuploidy) are thereby generated. The activation of JNK subsequently eliminates these cells by activating the apoptotic programme. On the other hand, it has been recently reported that aneuploidy induces a Dp53-independent apoptosis that requires JNK (Dekanty et al., 2012). However, the initial apoptosis that we observed to be caused by the depletion of Dmp52 was partially dependent on JNK, as in the absence of JNK, apoptotic bodies could still be detected in the wing discs. In other words, our results suggest that the initial absence of Dmp52 activates an apoptotic programme that does not completely depend on JNK but that likely depends on Dp53. Therefore, it appears that JNK is not a limiting factor required for the apoptosis that is induced by the depletion of Dmp52 but that when Dp53 function is compromised and TFIIH activities are affected, the JNK pathway is over-activated to induce apoptosis. This pathway is likely similar to the pathway induced by IR in a Dp53- and Chk1-deficient cell. This point is supported by the demonstration that the absence of Dmp52 generates a loss of heterozygosity and chromosomal aberrations (Fig. 5C) (Fregoso et al., 2007). Somehow, this condition may be equivalent to the generation of DNA damage by IR, and because TFIIH also participates in DNA repair and the control of the cell cycle, it is possible that the checkpoint controls may not be completely operational. Other works have also demonstrated that a reduction in the number of repair proteins such as DDB1 generates chromosomal instability (Shimanouchi et al., 2006). Therefore, we propose that in the cells that are deficient in TFIIH and Dp53, more chromosomal aberrations are generated because Dp53 also participates in the activation of DNA repair genes such as XPC and DDB2 (Adimoolam and Ford, 2002) and the response by the organism to avoid the propagation of these defects is to over-activate the JNK pathway and thereby induce apoptosis (Fig. 10). This model is supported by the fact that UV irradiation enhances the apoptosis observed in Dmp52- and Dp53-depleted cells. Furthermore, the reported evidence that defects in DNA repair and/or the reduction in transcription increases the levels of activated JNK, thus inducing a sustained apoptotic phenotype, supports this hypothesis (Roos and Kaina, 2006). Thus, the induction of massive cell death in the Dmp52 and Dp53 double-depleted cells may be a response to the accumulation of chromosomal aberrations, as we demonstrated in the LOH assay and by the reduction in transcription caused by the depletion of TFIIH activities (Fig. 10). In addition the regulation of the active JNK (P-JNK) is mediated by the phosphatase Puckered (Puc); the expression of Puc is Dp53-dependent and therefore deficient in Dp53-depleted cells (McEwen and Peifer, 2005). All of these findings support the hypothesis of an induction of a JNK-dependent massive apoptosis in cells depleted of TFIIH and Dp53.

In human p53-deficient cells undergoing DNA damage, treatment with caffeine for ATR inhibition sensitises cells to lethal Premature Chromatin Condensation, which is a process that has been shown to be independent of p53 function (Nghiem et at., 2001; Chanoux et al., 2009). Indeed, the elimination of apoptosis

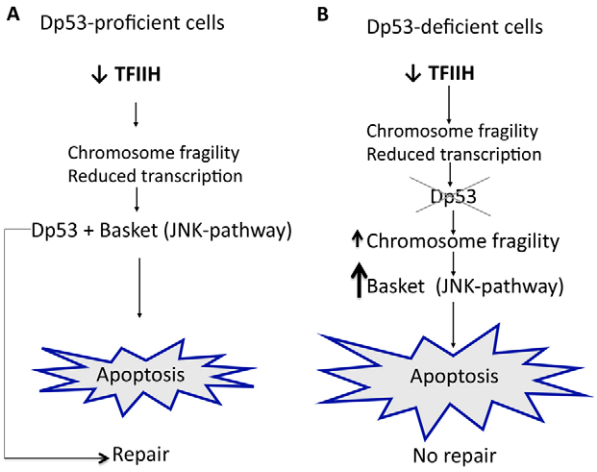

Fig. 10. Model of TFIIH and Dmp53 interactions. (**A**) In a background of Dp53-proficient cells, reducing levels of TFIIH relay a signal activating Dp53 and JNK. Activation of Dp53 could be involved in repair and to induce apoptosis. (**B**) However, in a background of Dp53-deficient cells, reducing levels of Dmp52 causes massive apoptosis on wing discs caused by an enhancement of P-JNK. The increment in apoptotic cell death could be due to an increment on DNA damage by the loss of function of Dmp52 and Dp53.

in wing cells depleted of Dmp52 by the expression of p35 generates a different phenotype than that observed in the wings of flies that were only Dmp52-depleted (Fig. 7). Because the depletion of Dmp52 causes chromosomal instability, it is possible that the absence of apoptosis allows for the proliferation of cells with chromosomal aberrations that generate this particular phenotype. Pérez-Garijo et al. (Pérez-Garijo et al., 2004) have demonstrated that the suppression of apoptosis by the caspase inhibitor p35 in irradiated wing discs generates developmental aberrations due to abnormal growth induced by the invasion and persistent misexpression of *wingless* (*wg*) and *decapentaplegic* (*dpp*) signalling. It is possible that the remaining damaged cells that were Dmp52-depleted and that expressed the caspase inhibitor p35 continued dividing and constantly emitted Wg and Dpp signals, thus contributing to the developmental abnormalities.

As mentioned above, our results suggest that the first response to the stress caused by the absence of a functional TFIIH is the induction of apoptosis by Dp53 and partially by the JNK pathway, in agreement with the feedback loop between Dmp53 and JNK that has been suggested to be essential for the apoptotic response to stress. However, when both TFIIH and Dp53 activities are depleted, this feedback loop may not be operating because Dp53 is not present (Shlevkov and Morata, 2012); this possibility suggests that if the feedback loop is affected by the absence of Dp53, the JNK pathway is over activated by the DNA repair and transcriptional stress generated by the absence of TFIIH and Dp53.

The results presented in this study have important implications for the understanding of the diseases associated with TFIIH mutations in humans, including cancer. Furthermore, the fact that the wing disc cells deficient in Dmp52 and Dp53 suffer massive cell death may have implications for the treatment of cancer cells. This observation is particularly relevant because of the recent discovery that the drug triptolide, which has potent antiproliferative and immunosuppressive activities and has been tested to be effective against cancer in preclinical trails, specifically targets the XPB subunit of TFIIH (Titov et al., 2011). In fact, we demonstrated that triptolide treatment of wing imaginal discs that are deficient in functional Dp53 phenocopied the JNK-dependent apoptotic phenotype observed in Dmp52-depleted discs. Most of the solid tumours in humans are deficient in p53 or in some of the modulators involved in p53-related functions; thus, it is possible that the treatment of different types of cancer cells with triptolide induces apoptosis through the JNK pathway, thus explaining the mechanism of the killing of cancer cells that has been demonstrated for this natural product. Similarly, drugs such as PRIMA have been shown to induce cell death in p53-mutated cancer cell lines through a JNK pathway (Li et al., 2005). Therefore, to search for possible targets for future cancer therapies, it will be important to determine if p53-deficient cancer cells are more susceptible to apoptosis than normal cells when TFIIH is affected.

The manner in which the phenotypes caused by the genetic interaction between Dmp52 and Dp53 are related to the physical interactions between the two molecules is not clear at this point. However, it is interesting that we can detect these physical interactions in fly cells without causing DNA damage, suggesting a dynamic behaviour between TFIIH and Dp53, two factors that establish interactions with other factors involved in DNA damage and transcription. Also relevant is the report that human cells deficient in the TFIIH subunits XPD and XPB are deficient in the induction of apoptosis by the overexpression of p53 (Robles et al., 1999). Our own research has shown that the same condition occurs when Dp53 is overexpressed in flies with a mutated version of the *Drosophila* homologue of XPB (Merino et al., 2002). Interestingly, we found that the depletion of Dmp52 induced apoptosis, and that, in the absence of Dp53, this apoptosis is not suppressed but rather enhanced in a JNK-dependent manner. Thus, the data concerning p53 overexpression and the lack of function of Dp53 in a TFIIH-deficient context are not easy to reconcile. The analysis of the overexpression experiments can generate many different interpretations. In this particular case, because TFIIH is essential for the expression of most of the RNA pol II-transcribed genes and because p53 is a transcription factor that activates the expression of pro-apoptotic genes and physically interacts with TFIIH, the reduction in the activity of TFIIH may affect the expression of these pro-apoptotic genes directly. An explanation may be that the expression of genes induced by the ectopic expression of a transcription factor such as p53 is more sensitive to the general reduction in transcription. Indeed, the incubation of fly embryos with low doses of α-amanitin suppresses the homeotic transformations caused by the overexpression of homeotic genes without affecting other genes (Gutiérrez et al., 2004). However, we cannot rule out the possibility that the enhancement in apoptosis by the simultaneous depletion of TFIIH and Dp53 may be related to the direct interaction between these two factors. Nevertheless, there is a clear functional link between TFIIH and p53 in human and *Drosophila* cells, and these interactions are relevant not only for understanding the manifestations present in humans with affected TFIIH but also for the understanding of cancer and the possible targeting of these interactions in future therapies.

Materials and Methods

Drosophila stocks

Flies were grown in standard meal to 25℃, unless another temperature was indicated. The *Drosophila* strains include: *en-gal4*, *MS1096*^{bx}, *eyeless-Gal4*, Sgs3-Gal4, *UAS-DicerIII*, *UAS-p35*, *TubP-Gal80*^{ts}, *GUS-Ctp53DN/TM6B*, *UASp53i*, *UAS-p53* and *mwh*^{1} were obtained from Bloomington *Drosophila* Stock Center. Stock generating RNAi against *Dmp52* (v39069), *Dmp34* (v101309) and *Basket* (v34138) was provided by Vienna *Drosophila* RNAi Center.

Pulldown assay

For interaction assays, overexpression of Dmp52 fused to GST in bacteria was induced with 0.4 mM IPTG during 4 h. GST-Dmp52 was purified using Glutathione-Sepharose (Amersham). Pulldown assays were performed as reported in Valadez-Graham et al. (Valadez-Graham et al., 2012).

Cell culture, transfection and co-immunoprecipitation

Dmp52, DΔNp53 and Dp53 were cloned into *Eco*RI/*Xho*I sites of pAc5.1/V5-HisA vector (Invitrogen). 3×-FLAG was cloned in pAc5.1/HisA generating a carboxy- and amino-termini 3×-FLAG where Dmp52, Dp53 and DΔNp53 were cloned.

Drosophila S2R^{+} cells were maintained in Schneider medium with 10% fetal bovine serum and 100 µg streptomycin/0.25 µg amphotericin. Cells were cotransfected with 10 µg of each construction by calcium method. Forty-eight hours after transfection, the cells were collected and lysed. Lysates were clarified to 13,000 rpm at 4℃. CoIPs were performed as indicated in Herrera-Cruz et al. (Herrera-Cruz et al., 2012)

Antibodies

Antibodies used were Dp53: D-200 and H3 (both antibodies recognize the two Dp53 isoforms), p62 Q-19, p89 S-19 and Cdk7 ds-17 (Santa Cruz); Dp53-H3 and Anti-BrdU G3G4 (Hybridoma Bank). Dmp52 antibody was raised using a carboxy-terminal peptide (-CDVKRYWKKYSKSGV-) by New England Peptides.

TUNEL assay in wing discs

Third instar imaginal discs wing were dissected in PBS and fixed in 4% formaldehyde during 20 min. Terminal deoxynucleotidyl transferase dUTP nick-end labeling (TUNEL) assay was performed using the In-Situ-Cell-Death-Detection-kit (Roche). For the quantitative analysis all discs were treated in the

same conditions. The region of interest was then selected and then the number particles at the highest intensity (255 arbitrary units) were quantified using the Image-J software (NIH): In each image analysed a high-density threshold corresponding with the labeling of the TUNEL reaction was adjusted. Standard Deviations were calculated using Microsoft Excel.

Wing disc immunostaining

For BrdU immunostaining, imaginal wing disc was incubated in 75 µg/ml BrdU in complete Schneider medium for 30 min at room temperature. Tissue was fixed with 4% formaldehyde, permeabilised 30 min in PBS with 0.6% Triton X-100 and DNA was denatured for 30 min with 2N HCl. BrdU was detected by mouse anti-BrdU at dilution 1:5,000. For other immunostaining, wing disc was dissected in PBS, fixed in 4% formaldehyde in PBS during 30 min and permeabilised 30 min in PBS with 0.6% Triton X-100. Rabbit anti-H3Pser10 was used at 1:1,000. Secondary antibodies Alexa Fluor 568 goat anti-mouse and goat anti-rabbit (Invitrogen) were used at 1:250 dilutions. Rabbit a-PJNK (Abcam) was used 1:100.

Phenotypic analyses of wings and bristle counting

Female wings were collected in ethanol and fixated with lactic acid:ethanol 6:5 and mounted. Cell density and total number cells was calculated as described by Moon et al. considering the number of hairs per defined area of 0.01 mm^2 (Moon et al., 2008). Wing area was measured using ImageJ 1.28u. For determining anterior and posterior areas with *en-GAL4*, we considered veinL4 as the boundary between both compartments. A minimum of 10 wings were analyzed per genotype. Two-sided *t*-tests were performed to determine significant differences.

Loss of heterozygosity assay

Larvae heterozygous for mwh^1 were obtained by crossing MS1096;+/+; mwh^1 females with *Dmp52i* males. All surviving flies were collected and wings were dissected and mounted. Only cells with three or more hairs were scored as the $mwh^{-/-}$ phenotype (de Andrade et al., 2004).

Total extracts and western blot

Total extracts from salivary glands was performed as described previously (Palomera-Sanchez et al., 2010). Gels were transferred into nitrocellulose membranes and were revealed for western blot using an ECL chemiluminescence detection kit (Amersham).

Triptolide treatment

Third instar larval wing imaginal discs from *Ore R*, *MS1096*, *MS1096*; *Bski*, *MS1096;+/+;GUS-ctp53DN* or *MS1096;Bski;GUS-ctp53DN* dissected in PBS were incubated in Shields and Sang M3 insect medium (Sigma) supplemented with 2% fetal bovine serum and 1% penicillin-streptomycin (Gibco) in presence or absence of 100 µM TPL (Biovision) or DMSO at 25˚C for different times periods. Discs were washed once with the same medium without drug, fixed in 4% formaldehyde in PBS for 20 minutes and washed three times for 10 minutes with PBST (PBS with 0.3% Triton X-100). Then apoptosis was determined by TUNEL assay as described.

Acknowledgements

We thank Andrés Saralegui for his advice in microscopy. We also thank Dr Martha Vazquez and Dr Viviana Valadez-Graham for discussions about this work.

Author contributions

C.V. and G.C. performed experimental work, C.V., G.C. and M.Z. designed the project and analyzed the results and wrote the paper.

Funding

This study was supported by the Programa de Apoyo a Proyectos de Investigación e Innovación Tecnológica (PAPIIT)/Universidad Nacional Autónoma de México (UNAM) [grant number IN 20109-3]; the Consejo Nacional de Ciencia y Tecnología (CONACyT) [grant number 127440]; Ixtli/UNAM; and the Fundación Miguel Alemán.

Supplementary material available online at
http://jcs.biologists.org/lookup/suppl/doi:10.1242/jcs.122721/-/DC1

References

Adimoolam, S. and Ford, J. M. (2002). p53 and DNA damage-inducible expression of the xeroderma pigmentosum group C gene. *Proc. Natl. Acad. Sci. USA* **99**, 12985-12990.

Akhtar, M. S., Heidemann, M., Tietjen, J. R., Zhang, D. W., Chapman, R. D., Eick, D. and Ansari, A. Z. (2009). TFIIH kinase places bivalent marks on the carboxy-terminal domain of RNA polymerase II. *Mol. Cell* **34**, 387-393.

Bai, L., Yoon, S. O., King, P. D. and Merchant, J. L. (2004). ZBP-89-induced apoptosis is p53-independent and requires JNK. *Cell Death Differ.* **11**, 663-673.

Bergoglio, V. and Magnaldo, T. (2006). Nucleotide excision repair and related human diseases. *Genome Dyn.* **1**, 35-52.

Bourdon, J. C., Fernandes, K., Murray-Zmijewski, F., Liu, G., Diot, A., Xirodimas, D. P., Saville, M. K. and Lane, D. P. (2005). p53 isoforms can regulate p53 transcriptional activity. *Genes Dev.* **19**, 2122-2137.

Brady, C. A. and Attardi, L. D. (2010). p53 at a glance. *J. Cell Sci.* **123**, 2527-2532.

Brodsky, M. H., Nordstrom, W., Tsang, G., Kwan, E., Rubin, G. M. and Abrams, J. M. (2000). Drosophila p53 binds a damage response element at the reaper locus. *Cell* **101**, 103-113.

Chanoux, R. A., Yin, B., Urtishak, K. A., Asare, A., Bassing, C. H. and Brown, E. J. (2009). ATR and H2AX cooperate in maintaining genome stability under replication stress. *J. Biol. Chem.* **284**, 5994-6003.

Chymkowitch, P., Le May, N., Charneau, P., Compe, E. and Egly, J. M. (2011). The phosphorylation of the androgen receptor by TFIIH directs the ubiquitin/proteasome process. *EMBO J.* **30**, 468-479.

Coin, F., Oksenych, V. and Egly, J. M. (2007). Distinct roles for the XPB/p52 and XPD/p44 subcomplexes of TFIIH in damaged DNA opening during nucleotide excision repair. *Mol. Cell* **26**, 245-256.

Coin, F., Oksenych, V., Mocquet, V., Groh, S., Blattner, C. and Egly, J. M. (2008). Nucleotide excision repair driven by the dissociation of CAK from TFIIH. *Mol. Cell* **31**, 9-20.

de Andrade, H. H., Reguly, M. L. and Lehmann, M. (2004). Wing somatic mutation and recombination test. *Methods Mol. Biol.* **247**, 389-412.

Dekanty, A., Barrio, L., Muzzopappa, M., Auer, H. and Milán, M. (2012). Aneuploidy-induced delaminating cells drive tumorigenesis in Drosophila epithelia. *Proc. Natl. Acad. Sci. USA* **109**, 20549-20554.

Di Lello, P., Miller Jenkins, L. M., Mas, C., Langlois, C., Malitskaya, E., Fradet-Turcotte, A., Archambault, J., Legault, P. and Omichinski, J. G. (2008). p53 and TFIIE alpha share a common binding site on the Tfb1/p62 subunit of TFIIH. *Proc. Natl. Acad. Sci. USA* **105**, 106-111.

Dichtel-Danjoy, M.-L., Ma, D., Dourlen, P., Chatelain, G., Napoletano, F., Robin, M., Corbet, M., Levet, C., Hafsi, H., Hainaut, P. et al. (2013). Drosophila p53 isoforms differentially regulate apoptosis and apoptosis-induced proliferation. *Cell Death Differ.* **20**, 108-116.

Egly, J. M. and Coin, F. (2011). A history of TFIIH: two decades of molecular biology on a pivotal transcription/repair factor. *DNA Repair (Amst.)* **10**, 714-721.

Esnault, C., Ghavi-Helm, Y., Brun, S., Soutourina, J., Van Berkum, N., Boschiero, C., Holstege, F. and Werner, M. (2008). Mediator-dependent recruitment of TFIIH modules in preinitiation complex. *Mol. Cell* **31**, 337-346.

Fregoso, M., Lainé, J. P., Aguilar-Fuentes, J., Mocquet, V., Reynaud, E., Coin, F., Egly, J. M. and Zurita, M. (2007). DNA repair and transcriptional deficiencies caused by mutations in the Drosophila p52 subunit of TFIIH generate developmental defects and chromosome fragility. *Mol. Cell. Biol.* **27**, 3640-3650.

Fuller, M. T., Regan, C. L., Green, L. L., Robertson, B., Deuring, R. and Hays, T. S. (1989). Interacting genes identify interacting proteins involved in microtubule function in Drosophila. *Cell Motil. Cytoskeleton* **14**, 128-135.

Glover-Cutter, K., Larochelle, S., Erickson, B., Zhang, C., Shokat, K., Fisher, R. P. and Bentley, D. L. (2009). TFIIH-associated Cdk7 kinase functions in phosphorylation of C-terminal domain Ser7 residues, promoter-proximal pausing, and termination by RNA polymerase II. *Mol. Cell. Biol.* **29**, 5455-5464.

Griswold, A. J., Chang, K. T., Runko, A. P., Knight, M. A. and Min, K. T. (2008). Sir2 mediates apoptosis through JNK-dependent pathways in Drosophila. *Proc. Natl. Acad. Sci. USA* **105**, 8673-8678.

Gutiérrez, L., Merino, C., Vázquez, M., Reynaud, E. and Zurita, M. (2004). RNA polymerase II 140wimp mutant and mutations in the TFIIH subunit XPB differentially affect homeotic gene expression in Drosophila. *Genesis.* **40,** 58-66.

Herrera-Cruz, M., Cruz, G., Valadez-Graham, V., Fregoso-Lomas, M., Villicaña, C., Vázquez, M., Reynaud, E. and Zurita, M. (2012). Physical and functional interactions between Drosophila homologue of Swc6/p18Hamlet subunit of the SWR1/SRCAP chromatin-remodeling complex with the DNA repair/transcription factor TFIIH. *J. Biol. Chem.* **287**, 33567-33580.

Ito, S., Kuraoka, I., Chymkowitch, P., Compe, E., Takedachi, A., Ishigami, C., Coin, F., Egly, J. M. and Tanaka, K. (2007). XPG stabilizes TFIIH, allowing transactivation of nuclear receptors: implications for Cockayne syndrome in XP-G/CS patients. *Mol. Cell* **26**, 231-243.

Ito, S., Tan, L. J., Andoh, D., Narita, T., Seki, M., Hirano, Y., Narita, K., Kuraoka, I., Hiraoka, Y. and Tanaka, K. (2010). MMXD, a TFIIH-independent XPD-MMS19 protein complex involved in chromosome segregation. *Mol. Cell* **39**, 632-640.

Jawhari, A., Lainé, J. P., Dubaele, S., Lamour, V., Poterszman, A., Coin, F., Moras, D. and Egly, J. M. (2002). p52 Mediates XPB function within the transcription/repair factor TFIIH. *J. Biol. Chem.* **277**, 31761-31767.

Ko, L. J., Shieh, S. Y., Chen, X., Jayaraman, L., Tamai, K., Taya, Y., Prives, C. and Pan, Z. Q. (1997). p53 is phosphorylated by CDK7-cyclin H in a p36MAT1-dependent manner. *Mol. Cell. Biol.* **17**, 7220-7229.

Lee, J. H., Koh, H., Kim, M., Park, J., Lee, S. Y., Lee, S. and Chung, J. (2006). JNK pathway mediates apoptotic cell death induced by tumor suppressor LKB1 in Drosophila. *Cell Death Differ.* **13**, 1110-1122.

Léveillard, T., Andera, L., Bissonnette, N., Schaeffer, L., Bracco, L., Egly, J. M. and Wasylyk, B. (1996). Functional interactions between p53 and the TFIIH complex are affected by tumour-associated mutations. *EMBO J.* **15**, 1615-1624.

Li, Y., Mao, Y., Brandt-Rauf, P. W., Williams, A. C. and Fine, R. L. (2005). Selective induction of apoptosis in mutant p53 premalignant and malignant cancer cells by PRIMA-1 through the c-Jun-NH2-kinase pathway. *Mol. Cancer Ther.* **4**, 901-909.

Liu, Q. (2011). Triptolide and its expanding multiple pharmacological functions. *Int. Immunopharmacol.* **11**, 377-383.

Luo, X., Puig, O., Hyun, J., Bohmann, D. and Jasper, H. (2007). Foxo and Fos regulate the decision between cell death and survival in response to UV irradiation. *EMBO J.* **26**, 380-390.

Martín, F. A., Peréz-Garijo, A. and Morata, G. (2009). Apoptosis in Drosophila: compensatory proliferation and undead cells. *Int. J. Dev. Biol.* **53**, 1341-1347.

McEwen, D. G. and Peifer, M. (2005). Puckered, a Drosophila MAPK phosphatase, ensures cell viability by antagonizing JNK-induced apoptosis. *Development* **132**, 3935-3946.

McNamee, L. M. and Brodsky, M. H. (2009). p53-independent apoptosis limits DNA damage-induced aneuploidy. *Genetics* **182**, 423-435.

Merino, C., Reynaud, E., Vázquez, M. and Zurita, M. (2002). DNA repair and transcriptional effects of mutations in TFIIH in Drosophila development. *Mol. Biol. Cell* **13**, 3246-3256.

Mesquita, D., Dekanty, A. and Milán, M. (2010). A dp53-dependent mechanism involved in coordinating tissue growth in Drosophila. *PLoS Biol.* **8**, e1000566.

Moon, N. S., Di Stefano, L., Morris, E. J., Patel, R., White, K. and Dyson, N. J. (2008). E2F and p53 induce apoptosis independently during Drosophila development but intersect in the context of DNA damage. *PLoS Genet.* **4**, e1000153.

Nghiem, P., Park, P. K., Kim, Y., Vaziri, C. and Schreiber, S. L. (2001). ATR inhibition selectively sensitizes G1 checkpoint-deficient cells to lethal premature chromatin condensation. *Proc. Natl. Acad. Sci. USA* **98**, 9092-9097.

Okuda, M., Tanaka, A., Satoh, M., Mizuta, S., Takazawa, M., Ohkuma, Y. and Nishimura, Y. (2008). Structural insight into the TFIIE-TFIIH interaction: TFIIE and p53 share the binding region on TFIIH. *EMBO J.* **27**, 1161-1171.

Palomera-Sanchez, Z., Bucio-Mendez, A., Valadez-Graham, V., Reynaud, E. and Zurita, M. (2010). Drosophila p53 is required to increase the levels of the dKDM4B demethylase after UV-induced DNA damage to demethylate histone H3 lysine 9. *J. Biol. Chem.* **285**, 31370-31379.

Pérez-Garijo, A. F., Martín, F. A. and Morata, G. (2004). Caspase inhibition during apoptosis causes abnormal signalling and developmental aberrations in Drosophila. *Development* **131**, 5591-5598.

Quijano, J. C., Stinchfield, M. J. and Newfeld, S. J. (2011). Wg signaling via Zw3 and mad restricts self-renewal of sensory organ precursor cells in Drosophila. *Genetics* **189**, 809-824.

Robles, A. I., Wang, X. W. and Harris, C. C. (1999). Drug-induced apoptosis is delayed and reduced in XPD lymphoblastoid cell lines: possible role of TFIIH in p53-mediated apoptotic cell death. *Oncogene* **18**, 4681-4688.

Roos, W. P. and Kaina, B. (2006). DNA damage-induced cell death by apoptosis. *Trends Mol. Med.* **12**, 440-450.

Shimanouchi, K., Takata, K., Yamaguchi, M., Murakami, S., Ishikawa, G., Takeuchi, R., Kanai, Y., Ruike, T., Nakamura, R., Abe, Y. et al. (2006). Drosophila damaged DNA binding protein 1 contributes to genome stability in somatic cells. *J. Biochem.* **139**, 51-58.

Shlevkov, E. and Morata, G. (2012). A dp53/JNK-dependant feedback amplification loop is essential for the apoptotic response to stress in Drosophila. *Cell Death Differ.* **19**, 451-460.

Titov, D. V., Gilman, B., He, Q. L., Bhat, S., Low, W. K., Dang, Y., Smeaton, M., Demain, A. L., Miller, P. S., Kugel, J. F. et al. (2011). XPB, a subunit of TFIIH, is a target of the natural product triptolide. *Nat. Chem. Biol.* **7**, 182-188.

Valadez-Graham, V., Yoshioka, Y., Velazquez, O., Kawamori, A., Vázquez, M., Neumann, A., Yamaguchi, M. and Zurita, M. (2012). XNP/dATRX interacts with DREF in the chromatin to regulate gene expression. *Nucleic Acids Res.* **40**, 1460-1474.

Wang, X. W., Vermeulen, W., Coursen, J. D., Gibson, M., Lupold, S. E., Forrester, K., Xu, G., Elmore, L., Yeh, H., Hoeijmakers, J. H. et al. (1996). The XPB and XPD DNA helicases are components of the p53-mediated apoptosis pathway. *Genes Dev.* **10**, 1219-1232.

Wang, Q. E., Zhu, Q., Wani, M. A., Wani, G., Chen, J. and Wani, A. A. (2003). Tumor suppressor p53 dependent recruitment of nucleotide excision repair factors XPC and TFIIH to DNA damage. *DNA Repair (Amst.)* **2**, 483-499.

Wells, B. S. and Johnston, L. A. (2012). Maintenance of imaginal disc plasticity and regenerative potential in Drosophila by p53. *Dev. Biol.* **361**, 263-276.

Zurita, M. and Merino, C. (2003). The transcriptional complexity of the TFIIH complex. *Trends Genet.* **19**, 578-584.

Journal of Cell Science

THE JOURNAL OF BIOLOGICAL CHEMISTRY VOL. 287, NO. 40, pp. 33567–33580, September 28, 2012

Physical and Functional Interactions between *Drosophila* Homologue of Swc6/p18^{Hamlet} Subunit of the SWR1/SRCAP Chromatin-remodeling Complex with the DNA Repair/Transcription Factor TFIIH*[S]

Received for publication, May 24, 2012, and in revised form, August 2, 2012 Published, JBC Papers in Press, August 3, 2012, DOI 10.1074/jbc.M112.383505

Mariana Herrera-Cruz[1], Grisel Cruz[1], Viviana Valadez-Graham, Mariana Fregoso-Lomas, Claudia Villicaña, Martha Vázquez, Enrique Reynaud, and Mario Zurita[2]

From the Department of Developmental Genetics, Instituto de Biotecnología, Universidad Nacional Autónoma de México, Av. Universidad 2001, Cuernavaca Morelos 62250, México

Background: TFIIH interacts with multiple factors.
Results: The fly p8 subunit of TFIIH is encoded in a bicistronic transcript with the homolog of the Swc6/p18^{Hamlet} subunit of the SWR1/SRCAP complex and physically and genetically interacts with TFIIH.
Conclusion: There is a functional link between Swc6/p18^{Hamlet} and TFIIH.
Significance: This functional interaction opens new avenues to study how TFIIH modulates transcription and DNA repair.

The multisubunit DNA repair and transcription factor TFIIH maintains an intricate cross-talk with different factors to achieve its functions. The p8 subunit of TFIIH maintains the basal levels of the complex by interacting with the p52 subunit. Here, we report that in *Drosophila*, the homolog of the p8 subunit (*Dmp8*) is encoded in a bicistronic transcript with the homolog of the Swc6/p18^{Hamlet} subunit (*Dmp18*) of the SWR1/SRCAP chromatin remodeling complex. The SWR1 and SRCAP complexes catalyze the exchange of the canonical histone H2A with the H2AZ histone variant. In eukaryotic cells, bicistronic transcripts are not common, and in some cases, the two encoded proteins are functionally related. We found that Dmp18 physically interacts with the Dmp52 subunit of TFIIH and co-localizes with TFIIH in the chromatin. We also demonstrated that *Dmp18* genetically interacts with *Dmp8*, suggesting that a cross-talk might exist between TFIIH and a component of a chromatin remodeler complex involved in histone exchange. Interestingly, our results also show that when the level of one of the two proteins is decreased and the other maintained, a specific defect in the fly is observed, suggesting that the organization of these two genes in a bicistronic locus has been selected during evolution to allow co-regulation of both genes.

Several multisubunit complexes participate in transcription in eukaryotic cells. TFIIH is an intriguing complex because it participates not only in transcription but also in nucleotide excision repair (NER)[3] and cell cycle regulation (1, 2). TFIIH was discovered 20 years ago, and since then, the 10 subunits that form this complex have been characterized by biochemical, molecular, and genetic studies (2). In the cell, TFIIH subunits are found in a seven-subunit core complex composed of the XPD and XPB ATPases/DNA helicases together with p62, p52, p44, p34, and p8, which participate in NER. The cyclin-dependent kinase CDK7 along with cyclin H and MAT1 form the CAK complex, which, by itself, may also participate in cell cycle regulation. The core and the CAK complexes form the 10-subunit TFIIH complex, which participates in transcription mediated by RNA polymerases I and II (1–4). In addition, it has been suggested that the XPG endonuclease that participates in NER may interact with the 10 subunits of TFIIH and participate in transcription (5). Recently, a new putative subunit of TFIIH has been reported in yeast (6). This new subunit, called Tfb6, appears to be important for the dissociation of Ssl2 (XPB) from the rest of TFIIH after transcription initiation (6). Another important aspect of the study of TFIIH is that mutations in the XPB and XPD subunits are linked to three human syndromes: xeroderma pigmentosum (XP), Cockayne syndrome combined with xeroderma pigmentosum (CS/XP), and trichothiodystrophy (TTD). Whereas XP is caused by defects in NER, CS has been associated with defects in the mechanism of transcription-coupled repair, and TTD may be associated with deficiencies in transcription and DNA repair (1, 7). XP patients are hypersensitive to sunlight and have a high predisposition for skin cancer (7). Individuals suffering from CS have slow growth, cachexia, and defects in the nervous system. Patients with TTD have the characteristic manifestations of brittle hair, ichthyosis, and fragile nails (7). A particular form of TTD, termed TTD-A, is linked to mutations in the p8 subunit of TFIIH. Cells derived from patients with TTD-A have reduced levels of all of the

* This study was supported by funds from Programa de Apoyo a Proyectos de Investigación e Innovación Tecnológica/Universidad Nacional Autónoma de México IN 20109-3, Consejo Nacional de Ciencia y Tecnologia Grant 127440, IXTLI/Universidad Nacional Autónoma de México, Fundación Miguel Alemán, and the Howard Hughes Medical Institute (to M. Z.).
[S] This article contains supplemental Fig. S1.
[1] Both authors contributed equally to this work.
[2] To whom correspondence should be addressed: Dept. of Developmental Genetics, Instituto de Biotecnología, Universidad Nacional Autónoma de México, Av. Universidad 2001, Cuernavaca Morelos 62250, México. Tel.: 52-555-6227659; E-mail: marioz@ibt.unam.mx.

[3] The abbreviations used are: NER, nucleotide excision repair; XP, xeroderma pigmentosum; CS, Cockayne syndrome; TTD, trichothiodystrophy; IP, immunoprecipitation; CTD, C-terminal domain.

other TFIIH subunits, suggesting that p8 is important for maintaining the stability of the complex (8). The p8 subunit is a small, 71-amino acid protein that is highly conserved in all eukaryotes (8). The function of p8 has been linked to DNA repair *in vitro* (9). Tracking experiments in cultured human cells suggest that p8 is located in two different kinetic pools, one associated with TFIIH inside the nucleus and the other free of TFIIH in the cytoplasm (10). However, upon UV irradiation, the free pool is translocated into the nucleus, where it associates with TFIIH (10).

We have previously reported that in *Drosophila*, the overexpression of the p8 homolog (*Dmp8*) suppresses the phenotypes generated by mutations in other components of TFIIH, such as p52 (named *Dmp52* in the fly) and XPB (named *haywire* in the fly) (11, 12). In addition, overexpression of *Dmp8* generates flies that are more resistant to UV irradiation (12). In this study, we report that the *Dmp8* gene is encoded in a bicistronic transcript along with the fly homolog of the Swc6/p18^{Hamlet} (referred to here as *Dmp18*) subunit present in yeast SWR1 and in human SRCAP chromatin remodeling complexes. In addition, p18^{Hamlet} has been linked to the genotoxic stress response mediated by p38 and p53 (13–15). Here, we demonstrate that Dmp18 physically and functionally interacts with two components of TFIIH. Defects due to the depletion of Dmp8 and Dmp18 are synergistic and suggest a functional link between TFIIH and Dmp18, a subunit present in chromatin remodeling complexes.

EXPERIMENTAL PROCEDURES

Fly Strains—Fly stocks were maintained at 25 °C on standard food. *Oregon-R* and w^{1118} were used as the wild-type strains. The following alleles were obtained from the Bloomington stock center: *Df(2L)Exel7022*, *Df(2L)BSC172*, *Df(2L)BSC110*, and *P{GawB}Bx*^{MS1096}. RNA interference (RNAi) flies for *Dmp18* (*P{GD10407}v25909*) were obtained from the Vienna *Drosophila* RNAi Center (39), and *P{lacW}l(2)SH1279*^{SH1279} strain was obtained from the Szeged *Drosophila* stock center. *In(2LR)Gla, wg*$^{Gla-1}$ *Bc*^{1} *Egfr*^{E1} was used as a balancer for deficiencies or insertions on the second chromosome to enable identification of homozygous adults.

Antibodies—Two different polyclonal rabbit antibodies against Dmp8 were generated by New England Peptides, Inc., using synthetic peptides containing amino acids 45–59 and 62–73, respectively. Rabbit anti-Dmp18 antibodies were raised against a synthetic peptide corresponding to amino acids 92–108 (Sigma). Rat polyclonal antibodies against Dmp52 were generated using a peptide that corresponds to the last 15 amino acids of the protein as antigen (New England Peptides, Inc.). Polyclonal antibodies against TFIIH subunits (anti-XPB (15), CDK7 (ds-17), and XPD (S-19)) were purchased from Santa Cruz Biotechnology, Inc. (Santa Cruz, CA). Monoclonal antibodies against β-tubulin (E7) were obtained from the Developmental Studies Hybridoma Bank. Mouse monoclonal anti-FLAG M2 (Sigma) and mouse monoclonal anti-V5 (ab27671, Abcam) were used in COIP experiments.

Cell Transfection and Co-IP Assays—The complete wild-type *Dmp8* and *Dmp18* cDNA sequences were obtained by reverse transcription-PCR and cloned in the pGEX4T-1 vector. The PCR product of the complete open reading frame of *Dmp8* was sequenced and subcloned into the EcoRI-NotI sites of a modified pAc5.1/V5-His A vector to generate a Dmp8 protein with three repeats of the FLAG epitope at the C terminus (Dmp8-FLAG). The Dmp18 expression plasmid was constructed in a modified pAc5.1/V5-His A vector to produce the protein with the FLAG sequences at the N terminus (FLAG-Dmp18). *Drosophila* S2R+ cells were independently transfected with each of the recombinant expression vectors for transient expression of the Dmp8 or Dmp18 proteins by means of calcium phosphate. After 2 days, the transfected cells were harvested and lysed in 50 μl of lysis buffer (25 mM Tris-HCl, 150 mM NaCl, 1% Nonidet P-40, 1% Triton X-100, 0.2 mM PMSF, pH 7.8) containing protease inhibitors. The protein concentration was determined with Bradford reagent and tested for expression by Western blotting. A fraction of the extract was saved as input. The remaining extract was precleared by incubating with 40 μl of protein G-Sepharose (Invitrogen) for 1 h at 4 °C. The first half of the precleared extract was incubated overnight in a cold room on a rotator with 2 μg of mouse monoclonal anti-FLAG antibody M2 (Sigma)/mg of protein lysate. The remaining extract was incubated with an irrelevant antibody (anti-mouse IgG or anti-rabbit IgG) in the same conditions. 20 μl of protein G-Sepharose were added to each sample and incubated 2 h at 4 °C on a rotator. The samples were centrifuged, and the supernatant was saved as the unbound fraction. The immunoprecipitated fraction was washed four times in 1 ml of lysis buffer. Samples were separated by SDS-PAGE and blotted onto nitrocellulose membrane.

Protein Detection—Proteins were analyzed by immunoblotting using standard procedures. Immunodetection of co-IP complexes was performed using anti-FLAG M2 (1:10,000), rabbit polyclonal anti-Dmp8 (1:1000), affinity-purified rabbit-polyclonal anti-Dmp18 (1:1000), rat polyclonal anti-Dmp52 (1:500), anti-XPB (1:1000), anti-CDK7 (1:1000).

Immunostaining of Polytene Chromosomes—Fixation and spreading of the chromosomes was made following the protocol reported (17). Co-staining of polytene chromosomes using a rat polyclonal anti-XPD (16) and rabbit polyclonal anti-Dmp18 was performed simultaneously.

Expression Analysis—Total RNA was isolated using TRIzol (Invitrogen). cDNA was prepared by reverse transcription of total RNA from adult flies or salivary glands. *Dmp8* and *Dmp18* transcript levels were assayed by reverse transcription (RT)-PCR, with specific primers: for *Dmp8*, 5′-GGCAACATGGTAAATGTTATGAAAGGA-3′ (forward) and 5′-CTAAGCGTCCTTGTCGTGCAGCGGAAA-3′ (reverse); for *Dmp18*, 5′-ACAACCATGACGGGTCGCGAATCCAAC-3′ (forward) and 5′-TCAGGCCGTCCACTTGAGGCAGCGCGT-3′ (reverse). The expression of the bicistronic mRNA was analyzed with the forward *Dmp8* and reverse *Dmp18* primers. *rp49* was used as the control in these experiments. Transgene expression was verified by PCR from genomic DNA using a primer that specifically hybridizes with a sequence of pCasper-hsp83 vector (forward, 5′CGATACCGTCGACCTCGAG3′) and a reverse primer specific for *Dmp8* or *Dmp18*.

Transgenic Flies and Genetic Crosses—Constructs encoding six histidines at the N or C terminus of Dmp8 (12) and a Myc

epitope at the N or C terminus of Dmp18 were cloned into the pCaSpeR-hsp83 and pUAST vectors. The constructions were sequenced to confirm their integrity. Transgenic flies were made by Genetic Services Inc. (18). All stocks were crossed with w^{1118} stock, and independent lines were established and balanced using *CyO* for the second chromosome and *TM2* or *MKRS* for the third chromosome.

Rescue of viability, fertility, and held-out wing phenotype of homozygous *P{lacW}l(2)SH1279*^{SH1279} flies was performed by crossing these mutants with the different pCaSper-hsp83 transgenic lines. Briefly, transgenic flies expressing *Dmp8* or *Dmp18* in the third chromosome and *CyO* balanced in the second chromosome were crossed with heterozygous *P{lacW}l(2) SH1279*^{SH1279} flies with third chromosome balanced with *TM2* and *MKRS*; the F1 progeny was intercrossed to generate homozygous containing one or two copies of the *Dmp8* or *Dmp18* transgene.

Crosses to overexpress the RNAi for Dmp18 (dsDmp18) in the adult wing were performed by crossing the Vienna *Drosophila* RNAi Center transgenic line with the w^{1118}, *P{GawB}Bx*^{MS1096} driver. To enhance the RNAi expression, a copy of Dicer-2 was added. The genetic interaction between Dmp8 and Dmp18 was evaluated in flies expressing the dsDmp18 induced by *MS1096* driver plus one or two copies of the *P{lacW}* insertion.

The rescue of the genetic interaction was analyzed in RNAi-expressing flies where Dmp8-H6 or Myc-Dmp18 expression was also induced by the *MS1096* driver. *P{GawB}Bx*^{MS1096}; *Dmp8-H6* or *myc-Dmp18/+*; *dsDmp18/dsDmp18* males were compared with *P{GawB}Bx*^{MS1096}; *+/+*; *dsDmp18/dsDmp18*.

Yeast Two-hybrid Interaction Assay—Yeast two-hybrid interaction analyses were made with the MATCHMAKER GAL4 Two-Hybrid System 3 (Clontech). pGBKT7 or pGADT7 vectors were used for GAL4 DNA binding domain or GAL4 DNA activation domain fusion constructs, respectively. The full-length coding sequences of *Dmp8*, *Dmp18*, and *Dmp52* were cloned into these vectors, and yeast strains AH109 and Y187 were transformed. Yeast mating was conducted, and colony selection was performed on minimal standard medium without His, Leu, and Trp (Clontech), supplemented with 2.5 mM 3-amino-1,2,4-triazole after 7 days. Finally, positive colonies were considered after α- and β-galactosidase enzymatic assays as reported previously (19, 20).

Northern Blotting—For Northern hybridization, 20 μg of total RNA per sample was separated on a 1% agarose gel. The RNA was transferred by capillarity onto a Hybond N^+ membrane (Amersham Biosciences) using 20× SSPE (3 M NaCl, 0.25 M NaH_2PO_4, 0.02 M EDTA, pH 7.4) as transfer buffer. UV cross-linking of the RNA to the membrane was performed by using the Auto cross-link mode of a UV Stratalinker 2400 (Stratagene). The membrane was prehybridized for 6 h at 42 °C with prehybridization buffer (0.25 M Tris, pH 7.5, 0.5% sodium pyrophosphate, 1% polyvinylpyrrolidone, 1% BSA, 1% Ficoll, 5% SDS, 1 M NaCl, 50% (v/v) formamide, 100 μg/ml denatured salmon sperm DNA). Hybridization was carried out overnight at the same temperature and with the same buffer as the prehybridization. DNA fragments for rp49 or the bicistronic transcript obtained by PCR with specific primers were used as probes after random prime labeling (Prime it II, Stratagene) with [α-^{32}P]dCTP. Then the membrane was washed at high stringency with wash buffer (0.1% 20× SSPE, 1% SDS), and the signal was detected by autoradiography.

GST Pull-down Assays and GST Pull-down Competition Assays—Pull-down assays were carried out as described previously (19). GST fusion proteins for full-length Dmp8 (GST-Dmp8), Dmp52 (GST-Dmp52), and Dmp18 (GST-Dmp18) or its fragments (GST-Dmp52(1–400), GST-Dmp52(401–500), GST-Dmp18(1–76), and GST-Dmp18(49–152)) were produced by cloning each sequence onto the pGEX4T-1 vector (Stratagene) and expressed in BL-21-competent bacterial cells. The same quantity of affinity-purified GST or GST fusion protein was used as bait in each assay. For generation of *in vitro* translated ^{35}S-labeled proteins, the full-length sequences of *Dmp8*, *Dmp52*, and *Dmp18* cloned into the pGADT7 vector were subjected to a one-step *in vitro* transcription and translation system (TNT System, Promega) in the presence of [^{35}S]cysteine. Binding assays were carried out at 4 °C for 4 h in 500 μl of pull-down buffer (20 mM Hepes, pH 7.9, 200 mM NaCl, 1 mM EDTA, 4 mM $MgCl_2$, 1 mM DTT, 10% glycerol, 0.1% nonidet-P40 and protease inhibitors) containing 5 μl of the ^{35}S-labeled *in vitro* translated protein and Sepharose beads loaded with GST or GST fusion proteins. The beads were washed six times with pull-down buffer containing 1% Nonidet P-40. The bound proteins were eluted by boiling the beads in the presence of Laemmli buffer (21), separated by SDS-PAGE, and visualized by autoradiography. For competition assays, all three proteins were incubated at the same time in each assay. The amount of GST or GST fusion protein as well as one of the ^{35}S-labeled interacting proteins was maintained constant in all assays while the other ^{35}S-labeled protein was increased as indicated in Fig. 3 for each assay.

RESULTS

The Dmp8 Subunit of TFIIH Is Encoded as a Bicistronic Transcript along with the Drosophila Homolog of the Swc6/p18^{Hamlet} *Subunit of the SWR1/SRCAP Complex*—During the characterization of the *Drosophila melanogaster Dmp8* gene, we noticed that it is encoded in a bicistronic locus (Fig. 1*A*). This bicistronic locus maps to chromosome 2L, and its transcript encodes two open reading frames (NM_135051 and NM_001144319; Fig. 1*A*). The bicistronic transcript has a small 58-bp intron located 35 bp downstream of the translation initiation codon of *Dmp8* (Fig. 1*A*). As expected, the *Dmp8* product is highly conserved, with the highest similarity in the N terminus of the protein (Fig. 1*B*) (8). The second ORF (named *Dmp18* in this study) is highly similar to the human p18^{Hamlet}/ZNHIT1 protein (Swc6 in yeast) that has been reported to be part of the chromatin remodeling complexes SWR1 in yeast and SRCAP in humans (Fig. 1*B*) (22–25). The SWR1 and SRCAP complexes catalyze the exchange of the canonical histone H2A with the H2AZ variant, which appears to be relevant for promoter activation and removal of phosphorylated H2AX after DNA damage (25–27). In addition, p18^{Hamlet} has also been associated with genotoxic stress response as a substrate of p38α and p38β MAPKs and as a coactivator of p53-dependent transcriptional responses (22, 23). The particular gene organization

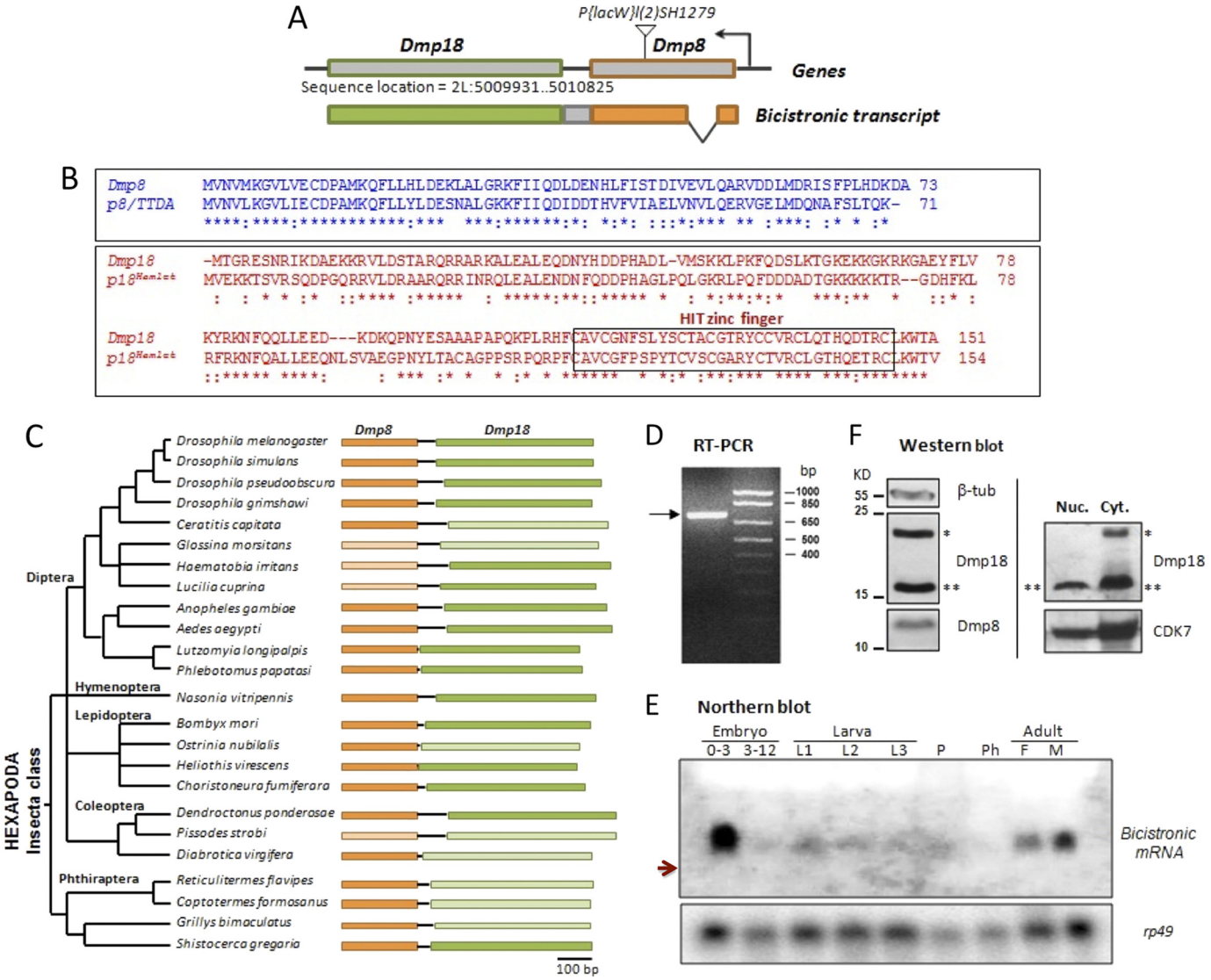

FIGURE 1. **The Dmp8 subunit of TFIIH and the Swc6/p18^{Hamlet} homologue of *Drosophila* (Dmp18) are encoded in the same mRNA.** *A*, molecular organization of the *Dmp8-Dmp18* locus. The chromosomal position in the second chromosome is based in BDGP annotation deposited in FlyBase. Note that full-length transcripts encoding for both proteins have been documented (shown as *orange boxes* for *Dmp8* and *green boxes* for *Dmp18* as the translated exons; the *small gray box* represents the intergenic sequence). The position of the *P[lacW] l(2)SH1279* insertion in exon 2 of the *Dmp8* gene, which disrupts its coding sequence and is used in this work, is indicated as a *white triangle*. The *angled arrow* represents the direction of transcription. *B*, alignment of the Dmp8 (*blue*) and Dmp18 (*red*) proteins with their human homologues p8/TTDA and p18^{Hamlet}, respectively. Note that the identity between the fly and human proteins is very high (*asterisks* represent conserved identical amino acids). The HIT-zinc finger motif of Dmp18 is indicated in a *box*. *C*, *Dmp8-Dmp18* bicistronic transcript is expressed in different insect species. The transcript sequences were obtained from cDNAs reported in GenBank™. The p8 ORF is indicated in *green*, and p18 ORF is shown in *orange*. *Light green* and *light orange* represent incomplete cDNAs either at the 5′ end (p8) or the 3′ end (p18). Note that the intergenic sequence between the two ORFs is not longer than 90 nucleotides and in some cases is very short, as in *Heliothis virescens*, which includes only 2 nucleotides. *D*, Dmp8 and Dmp18 are only expressed in the fly from a bicistronic transcript. The RT-PCR product of the bicistronic transcript is amplified by specific primers that flank the *Dmp8-Dmp18* mRNA. This fragment was sequenced, confirming the presence of the two ORFs. *E*, the developmental Northern blot, using the Dmp8-Dmp18 full-length cDNA as probe, shows that the bicistronic transcript is presented in embryos (0–3 and 3–12 h); first, second, and third instar larvae (*L1*, *L2*, and *L3*); pupas (*P*); pharates (*Ph*); and adults (*F* and *M*). Any other transcript of different size was not identified. The *arrow* indicates the rp49 mRNA migration position that is about 650 nucleotides. *F*, the Western blot experiments from soluble proteins from adults using specific antibodies for Dmp8 and Dmp18 show that both proteins exist in the fly. Note that the Dmp18 antibody recognizes two bands, one corresponding to the expected Dmp18 size (**) and other of higher molecular weight (*). The low molecular weight band is preferentially nuclear (*Nuc.*), and the high molecular weight is preferentially located in the cytoplasm (*Cyt.*). β-Tubulin is used as loading control.

of Dmp8 and Dmp18 is intriguing because there are examples of bicistronic transcripts in eukaryotic cells where the two protein products are functionally related (28–33); in this case, the two factors are components of two different complexes involved in transcription and DNA repair.

Next, we determined whether this particular gene organization is also present in other *Drosophila* species. We found that these two genes are organized as a bicistronic locus not only in *D. melanogaster* but also in all other *Drosophila* species sequenced thus far (Fig. 1*C*). Although information is available only from some *Drosophila* species expressed sequence tags, the same configuration of genes is found in all of the species, including the short intergenic sequence between the two ORFs (supplemental Fig. S1). Furthermore, this form of gene organization is also present in mosquitoes and other arthropods for which genome sequence and/or expressed sequence tags have

been reported (Fig. 1*C* and supplemental Fig. S1), suggesting that this configuration of gene organization has been evolutionarily conserved by more than 350 million years of evolution to ensure coordinated gene expression of the factors encoded by the bicistronic mRNA. Interestingly, the intergenic sequences between the two genes are of different lengths but are always very short (no more than 90 bp) and, in some cases, consist of no more than a dozen nucleotides (Fig. 1*C* and supplemental Fig. S1).

To confirm that in the fly, the two genes are transcribed into a single mRNA, we performed an RT-PCR experiment using oligonucleotide primers that flank the bicistronic loci (see "Experimental Procedures"). Fig. 1*D* shows that an RT-PCR product was obtained by this approach. The identity of the RT-PCR product was confirmed by DNA sequencing (data not shown). Using Northern blot analysis, we found that the bicistronic transcript is present in all developmental stages analyzed, and no other transcripts encoding *Dmp8* and/or *Dmp18* were detected (Fig. 1*E*). These data and the fact that all of the reported expressed sequence tags in Flybase (including organisms other than flies) encode for the two proteins in the same mRNA confirm that *Dmp8* and *Dmp18* are encoded in the same transcript. Moreover, there are no other copies of these two ORFs in the *Drosophila* genome (data not shown), suggesting that the two genes are functional.

The fact that both *Dmp8* and *Dmp18* are encoded in the same transcript does not necessarily indicate that both proteins are expressed in the fly. To verify the expression of both proteins, we generated antibodies specific for each protein (see "Experimental Procedures") and analyzed the presence of both products by Western blot. A product of the expected molecular weight was identified for Dmp8 (Fig. 1*F*). In the case of Dmp18, two bands were recognized by the antibody, one corresponding to the expected size and the other of slower mobility in the gel (Fig. 1*F*). By biochemical cell fractionation experiments, we found that the protein corresponding to the expected molecular weight was preferentially localized in the nucleus, whereas the higher molecular weight protein was localized in the cytoplasm (Fig. 1*F*). We are confident that the antibodies recognize the expected proteins because these antibodies are capable of recognizing the GST fusion proteins, and, in competition experiments, antigenic peptides abolish the recognition of the specific bands (data not shown). Taken together, our results show that *Dmp8* and *Dmp18* are encoded in a bicistronic transcript and that both ORFs are expressed in the fly. The highly conserved configuration of the gene organization of *Dmp8* and *Dmp18* indicates that the co-transcription of these two genes may be related to their functions.

Dmp18 Physically Interacts with the Dmp52 Subunit of TFIIH and Co-localizes with TFIIH in the Chromatin—As mentioned previously, there are examples of functionally related eukaryotic proteins encoded in the same bicistronic transcript. Interestingly, in a yeast two-hybrid-based *Drosophila* protein interactome analysis, it was reported that the Dmp52 subunit of TFIIH interacts with the ORF that corresponds to Dmp18 (34). This information suggests that Dmp18 may interact with TFIIH. However, because Dmp8 is present in the same transcript with Dmp18 and because p52 has clearly been demonstrated to physically interact with p8 in humans and yeast (35, 36), there is a possibility that in the interactome assays, a part of Dmp8 was present in the same construct as Dmp18, which was later identified as interacting with Dmp52. To determine if Dmp18 can interact with Dmp52 or Dmp8, we performed a yeast two-hybrid analysis. Using stringent conditions for mutant complementation and β-gal activity, we found that Dmp18 interacts with both Dmp52 and Dmp8 and may have the ability to form a dimer (Fig. 2*A*). As expected, Dmp8 interacted with Dmp52 in this assay but only when Dmp8 was fused to the Gal4 activation domain (*AD*) and Dmp52 was fused to the Gal4 DNA-binding domain (*BD*) (Fig. 2*A*), indicating that the configuration of the fused proteins may affect their specific interactions.

To confirm the interaction between Dmp18 with Dmp52 and/or Dmp8, we made plasmid constructs for expression in *Drosophila* S2R+ cells that express either Dmp8 with a C-terminal FLAG tag or Dmp18 with a N-terminal FLAG tag (see "Experimental Procedures"). The constructs were transiently transfected into cells, and recombinant protein expression was analyzed by Western blot (data not shown). Co-IP experiments were performed using the FLAG antibody, and the co-immunoprecipitated proteins were analyzed by Western blot using antibodies against specific TFIIH subunits. Our results clearly show that Dmp8-FLAG co-immunoprecipitates with endogenous Dmp52, whereas endogenous Dmp18, DmXPB, and CDK7 do not (Fig. 2*B*). In cells transfected with FLAG-Dmp18, the FLAG antibody co-immunoprecipitates Dmp18 with endogenous Dmp52 but not with Dmp8, CDK7, or DmXPB. The fact that both FLAG-Dmp18 and Dmp8-FLAG proteins co-immunoprecipitate with endogenous Dmp52, but not with each other, suggests that only one protein may interact with Dmp52 at a time, although we cannot exclude the possibility that the presence of the FLAG tag on Dmp8 and Dmp18 may interfere with other potential protein-protein interactions. This result is important especially because Dmp8-FLAG does not co-immunoprecipitate with DmXPB, which is known to directly interact with Dmp52 in the context of TFIIH (37).

To support these results, we evaluated the co-localization of Dmp18 and TFIIH in chromatin. Immunostaining was performed in polytene chromosomes using Dmp18- and DmXPD-specific antibodies. Our results show that Dmp18 co-localizes with the TFIIH DmXPD subunit (Fig. 2*D*), which we have previously reported as co-localizing with other TFIIH components (16, 17), thereby supporting the idea that Dmp18 interacts with the TFIIH complex in the fly.

The results of the yeast two-hybrid assay-based fly protein interactome analysis (34) and the co-IP results presented here suggest that Dmp18 and TFIIH may interact via physical contacts with Dmp52 and/or Dmp8. To analyze this possibility, we performed *in vitro* pull-down assays using Dmp8, Dmp18, and Dmp52 proteins fused to GST (see "Experimental Procedures" and Fig. 3*A*). We also made GST fusion constructs that contained deletions in specific domains of Dmp52 and Dmp18 (Fig. 3*A*). These recombinant proteins were analyzed for specific interactions with *in vitro*-translated products of the full-length Dmp8, Dmp18, and Dmp52 cDNAs. We observed that Dmp18 directly interacts with Dmp52 through its C-terminal region

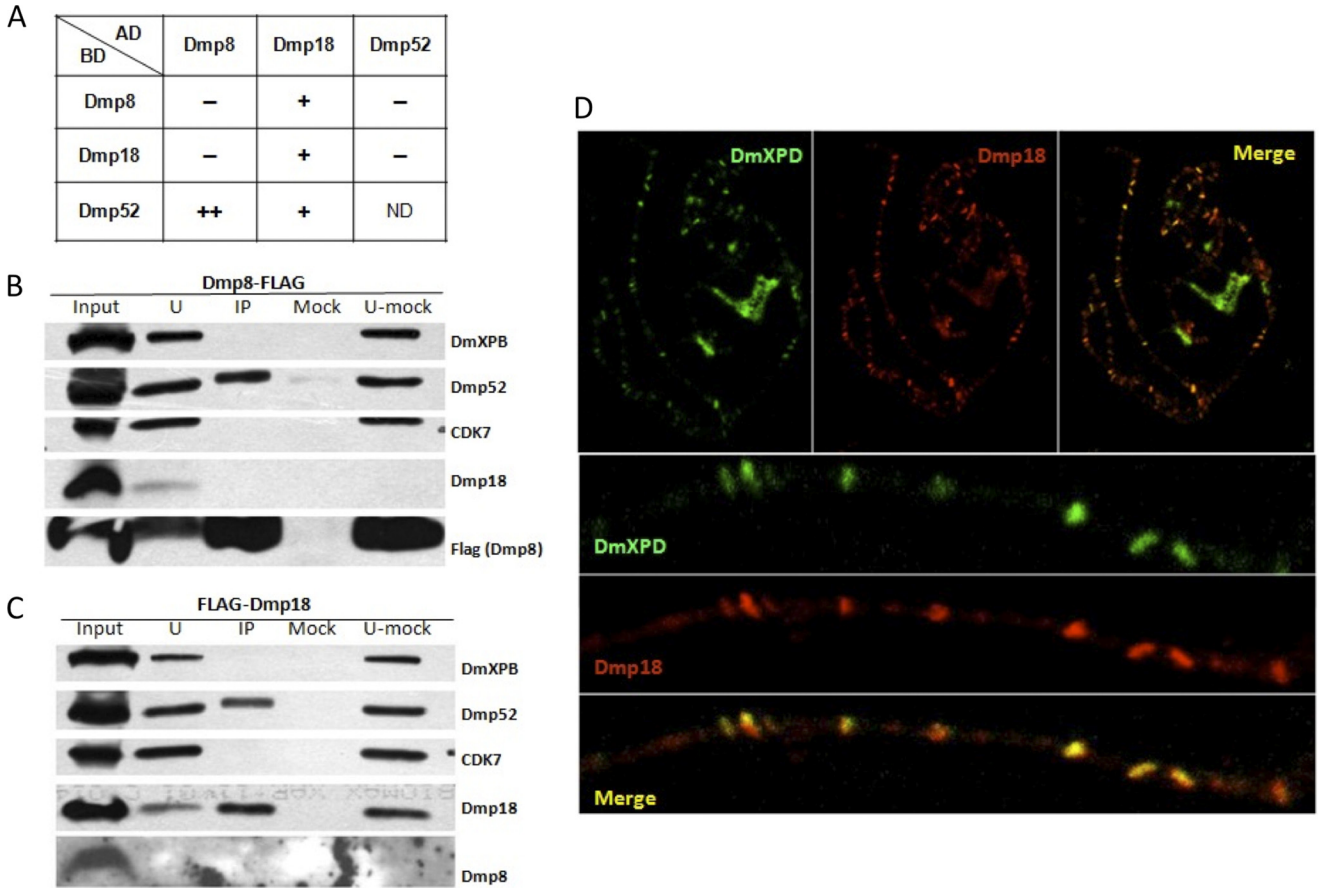

FIGURE 2. **Protein-protein interactions between Dmp18 and TFIIH.** *A*, Dmp18 interacts with Dmp8 and Dmp52 in yeast two-hybrid assays. Proteins of interest were fused either with the DNA binding domain (*BD*) or the activation domain (*AD*) of Gal4 as shown in the *table*. *Crosses*, interaction between proteins, which was tested under restricted conditions; *hyphen*, no interaction; *ND*, non-determined interaction. Note that Dmp18 can interact with Dmp52 and Dmp8 when it is fused with the activation domain, but interaction is not detected when it is fused with the binding domain. As a positive control, we analyzed the interaction between Dmp52 and Dmp8, but these factors only interact when Dmp8 is fused to the activation domain. Dmp18 was not able to interact with the human p53 or the SV40 antigen in any configuration (data not shown). *B* and *C*, Dmp8-FLAG and FLAG-Dmp18 co-immunoprecipitate with Dmp52 in S2R+ cells. Soluble proteins from S2R+ cells expressing a Dmp8 (*B*) or Dmp18 (*C*) fused with FLAG were immunoprecipitated with anti-FLAG antibody and analyzed by Western blot using antibodies against Dmp18 and components of the TFIIH complex. The antibodies used are indicated at the *right* of each *panel*. Only endogenous Dmp52 co-immunoprecipitates with FLAG-fused proteins independently, and Dmp8 and Dmp18 do not co-immunoprecipitate together. *D*, DmXPD and Dmp18 co-localize in chromatin. Shown is immunostaining of polytene chromosomes of wild-type larvae with DmXPD (*green*) and Dmp18 (*red*) antibodies. Note that both proteins co-localize in most of the chromosomal sites.

(Dmp18(49–152)), which contains an HIT-zinc finger domain (Fig. 3*B*). The HIT-zinc finger is a sequence motif found in many proteins with important roles in gene regulation and chromatin remodeling and may mediate protein-protein interactions (the Dmp18 HIT-zinc finger is indicated in Fig. 1*B*). Interestingly, Dmp8 also interacts with the Dmp18 HIT-zinc finger domain (Fig. 3*B*). Next, we analyzed the regions of Dmp52 protein that interact with Dmp18. We found that Dmp18 specifically interacts with the C-terminal region of Dmp52 (amino acids 408–500) and also with the part of the protein that does not contain the C-terminal region (Fig. 3*C*), suggesting that Dmp52 may have two distinct Dmp18-binding sites.

Our pull-down results suggest that Dmp18 can interact with Dmp52 in two different regions of the protein, one of which includes the C-terminal domain. The C-terminal domain of p52 has previously been demonstrated to interact with p8 (35, 36). In fact, the C-terminal domains of p52 and p8 adopt a similar fold, forming a compact heterodimer that appears to stabilize p52 (35). Because we observed that Dmp18 also interacts with the Dmp52 C-terminal domain, we hypothesized that either these three proteins form a complex or Dmp8 and Dmp18 are unable to interact with Dmp52 simultaneously. To evaluate this hypothesis, we performed competition experiments using similar pull-down assays. The different GST constructs (GST-Dmp52 and GST-Dmp18) were co-incubated, keeping one of the *in vitro*-translated products constant and varying the concentration of the other *in vitro*-translated protein. We found that when the GST-HIT (GST-Dmp18(49–152)) domain of Dmp18 was incubated with Dmp52, both peptides interacted (Fig. 3*D*). However, when similar pull-downs were performed in the presence of increasing amounts of Dmp8, the amount of Dmp52 bound to the Dmp18-HIT motif decreased. A portion of Dmp52 was still bound to Dmp18, most likely due to the interaction of the Dmp18-HIT motif outside the C-terminal region of Dmp52 (Fig. 3*D*). Interestingly, under these conditions, we did not observe an interaction between Dmp18 and Dmp8, suggesting that Dmp8 preferentially interacts with Dmp52 (Fig. 3*D*). In contrast, when we performed the co-IP using the GST-fused C-terminal motif of Dmp52 (GST-

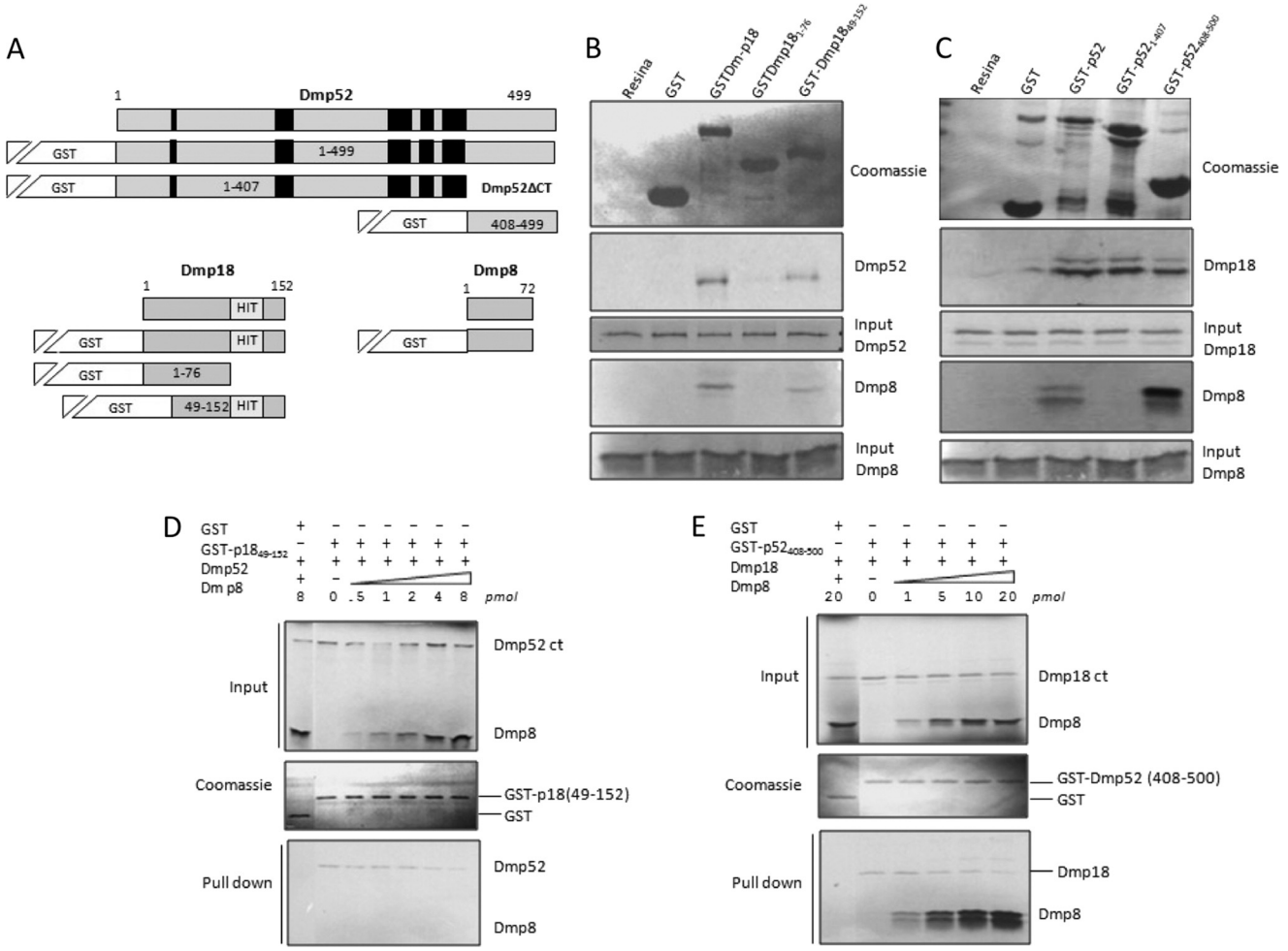

FIGURE 3. **Dmp8 preferentially interacts with Dmp52 than with Dmp18 *in vitro*.** *A*, diagram of the different constructions used to map the physical interactions between Dmp52, Dmp18, and Dmp8. Full-length cDNAs were used for *in vitro* transcription-translation in all cases, and the products used in the pull-down assays with the different recombinant proteins were fused to GST. The *black boxes* in Dmp52 correspond to the highly conserved domains present in different species. The HIT motif present in Dmp18 is indicated. For details, see "Experimental Procedures." *B*, *in vitro* pull-down analysis of GST-Dmp18 constructions with Dmp52 and Dmp8. The *first panel* shows the Coomassie staining of the GST-fused Dmp18 polypeptides. The rest of the *panels* show radiograms of the retention of Dmp52 and Dmp8. The input material used in each experiment is indicated in the figure. Dmp18 interacts with Dmp52 and Dmp8 through the HIT-zinc finger motif. *C*, *in vitro* pull-down analysis of GST-Dmp52 constructions with Dmp8 and Dmp18. The *first panel* shows the Coomassie staining of the different GST-fused Dmp52 polypeptides. The rest of the *panels* show radiograms of the retention of Dmp18 and Dmp8. Note that Dmp18 interacts with the C-terminal domain (CTD) of Dmp52 and another part of Dmp52 that does not contain the CTD. As expected, Dmp8 interacts with the Dmp52 CTD. *D*, competition pull-down assays between the HIT-zinc finger domain of Dmp18 with Dmp52 and Dmp8. The GST-Dmp18 (amino acids 49–152) bound to a glutathione-agarose column was incubated with a constant concentration of Dmp52 and with increasing concentrations of Dmp8. Dmp52 bound to the GST-Dmp18 HIT-zinc finger motif is removed in a concentration-dependent manner by Dmp8. Also note that in the presence of Dmp52, Dmp8 is not retained with GST-Dmp18, showing that Dmp8 preferentially interacts with Dmp52 than Dmp18. However, at high concentrations of Dmp8, some Dmp52 is still bound to Dmp18. *E*, competition experiment between the Dmp52 CTD with Dmp8 and Dmp18. The GST-Dmp52 CTD (amino acids 408–500) fixed in an agarose column was incubated with a constant concentration of Dmp18 and with increased amounts of Dmp8. Note that Dmp8 displaces the interaction of the Dmp52 CTD with Dmp18.

Dmp52(408–500)) while keeping the Dmp18 amount constant and increasing Dmp8 amounts, we found that the Dmp18-Dmp52 interaction was lost. Taken together, these results indicate that although both Dmp18 and Dmp8 can bind to the C-terminal domain of Dmp52, this interaction is not simultaneously possible, at least *in vitro*. However, because Dmp18 also can interact with other regions of Dmp52, we cannot exclude the possibility that Dmp52 and Dmp18 might interact even in the presence of Dmp8. In summary, the results presented in this section strongly suggest that Dmp18 physically interacts with Dmp52, leading to its interaction with the TFIIH holocomplex.

Genetic and Functional Interactions between Dmp18 and Dmp8—The physical interaction between Dmp18 and TFIIH suggests that a functional relationship may exist between these factors. To address this question, we took advantage of the existence of a P element insertion (*P* [*lacW*] *l(2)SH1279*; Fig. 1*A*) in the middle of the Dmp8 ORF, that disrupts the second exon of the *Dmp8* gene. This insertion was confirmed by genomic PCR using primers that flank the insertion site and adjacent DNA sequences (data not shown). It was reported that this insertion is homozygous lethal (FlyBase). In our experience, however, this line is semilethal, and ~25% of the homozygous flies survive (Fig. 4, *A* and *C*). Interestingly, among the homozygous survivors, the males are sterile, the females have reduced fertility (lay very few fertilized eggs of which only very few develop), and all of the adults present a held-out wing phenotype as well as a slight reduction in the wing size (Fig. 4*A*). The held-out wing phenotype has been described for different

A

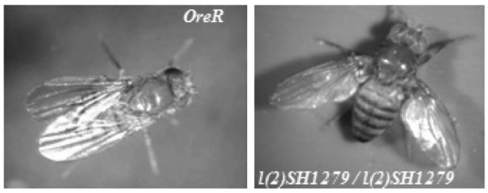

Genotype	Viability Obs./Exp. (%)
l(2)SH1279/+	484/484 (100)
l(2)SH1279/l(2)SH1279	64/242 (26.4)

B

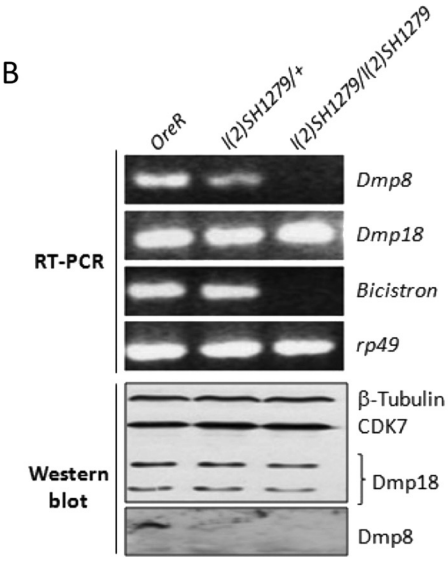

C

TABLE 1

Survival to eclosion of flies with *P{lacW}l(2)SH1279* insertion

Genotype	Viability (%)	Fertility		Flies with held-out wings (%)
		Female	Male	
l(2)SH1279/+	100	F	F	0
l(2)SH1279/ Df(2L)BSC110	100	F	F	0
l(2)SH1279/ Df(2L)Exel7022	50	rF	S	100 [b]
l(2)SH1279/ Df(2L)BSC172	45	rF	S	100 [b]
l(2)SH1279/ l(2)SH1279	26	rF	S	100 [a]

F: fertile, S: sterile, rF:reduced fertility (lay very few fertilized eggs)
[a] held-out wings are at a 45° angle from the body
[b] held-out wings are at ≤45° angle from the body

D

TABLE 2

Homozygous *P{lacW}l(2)SH1279* lethality suppression by *Dmp8* and *Dmp18* expression

Genotype	Survival and phenotypes of *l(2)SH1279/l(2)SH1279*			
	Viability (%)	Fertility		Flies with held-out wings (%)
		Female	Male	
Dmp8-H6(12)/MKRS	99	F	F	0
Dmp8-H6(12)/Dmp8-H6(12)	89	F	F	0
Dmp8-H6(9)/MKRS	73	F	F	0
Dmp8-H6(9)/Dmp8-H6(9)	74	F	F	0
myc-Dmp18(6)/MKRS	50	rF	S	100 [a]
myc-Dmp18(6)/ myc-Dmp18(6)	50	rF	S	100 [a]

F: fertile, S: sterile, rF: reduced fertile (lay very few fertilized eggs)
[a] held-out wings are at a 45° angle from the body
Number in parenthesis indicates the identification number or each strain.

FIGURE 4. **Characterization and rescue of a mutant *Dmp8* allele in the *Dmp8-Dmp18* bicistronic locus that only affects Dmp8.** *A*, the *l(2)SH1279* allele is an insertion of a *P*[*lacW*] in the second exon of the *Dmp8-Dmp18* locus (Fig. *1A*). It is semilethal because about 25% of the homozygous flies survive, as is indicated in the *table* (*C*). All of the adult *l(2)SH1279* homozygous flies have the held-out wing phenotype. *B*, RT-PCR experiment from total adult RNA to identify the presence of transcripts encoding for *Dmp8* and/or *Dmp18* in *l(2)SH1279* homozygous flies shows that the *Dmp8* mRNA encoding region as well as the bicistronic mRNA are not detected, whereas a *Dmp18* transcript can be detected. Specific oligonucleotide primer sets to amplify the complete *Dmp8-Dmp18* bicistronic mRNA, only the *Dmp8* mRNA coding region, or only the *Dmp18* mRNA coding region were utilized. As controls, total RNA from wild type and heterozygous *l(2)SH1279/+* flies was used. The Western blot supports the existence of Dmp18 protein in *l(2)SH1279* homozygous survivors, and Dmp8 protein was not detected. CDK7 and β-tubulin were used as loading controls. *C*, the reduced viability, disrupted fertility, and held-out wing phenotype observed in homozygous *l(2)SH1279* flies are due to the insertion of the P element in the *Dmp8-Dmp18* locus. The combination of *l(2)SH1279* insertion with two different deficiencies that uncover the *Dmp8-Dmp18* bicistronic locus generates the same phenotypes observed in the *l(2)SH1279* homozygous flies. *D*, *Dmp8*, but not *Dmp18*, transgenic constructs are enough to rescue all of the phenotypes observed in *l(2)SH1279/l(2)SH1279* flies. The survival increase and the phenotypic rescue of *l(2)SH1279* homozygous were evaluated by the expression of one or two copies of *Dmp8*-H6 or Myc-*Dmp18* together with the *l(2)SH1279* insertion. One copy of the *Dmp8*-H6 transgene was sufficient to increase the survival, abolish the held-out wing phenotype, and recover the fertility.

mutations in *Drosophila*, such as mutations in transcription regulators to genes that encode proteins involved in muscle formation and can be used to follow the interactions between functionally related genes (38).

Next, we analyzed the presence of the bicistronic transcript in adult homozygous *l(2)SH1279* flies by RT-PCR. Using specific primer sets, we found that a transcript encompassing the *Dmp8* gene or the bicistronic mRNA is not present in these flies (Fig. 4*B*). Interestingly, in the homozygous *l(2)SH1279* organisms, a transcript encompassing the coding region of *Dmp18* is still present (Fig. 4*B*), which may initiate transcription within the P element, suggesting that Dmp18 may be expressed in this homozygous survivor. Western blot analysis for Dmp8 and Dmp18 in this mutant fly indicates that Dmp18 is present in the homozygous organisms (Fig. 4*B*).

To confirm that the phenotypes observed in the flies containing the *l(2)SH1279* mutation are due to the insertion in the *Dmp8-Dmp18* bicistronic gene, we analyzed two deficiencies (deletions) that lack the *Dmp8-Dmp18* gene. *Df(2L)Exel7022* spans nucleotides 5,000,838–5,058,522 in chromosome 2L and deletes 17 genes, including the *Dmp8-Dmp18* locus. *Df(2L)BSC172* spans position 5,000,838–5,037,253 in chromosome 2L and deletes six genes. These two deficiencies were crossed with flies carrying the *l(2)SH1279* mutant to verify if trans-heterozygous flies carrying the corresponding deficiency and the insertion generate the same phenotypes observed in the homozygous *l(2)SH1279* flies. In both cases, flies with the genotypes *Df(2L)Exel7022/l(2)SH1279* and *Df(2L)BSC172/l(2)SH1279* were semilethal, the males were sterile, the females had reduced fertility, and all of the adult flies presented the held-out wing phenotype (Fig. 4*C*), indicating that these phenotypes are due to the *l(2)SH1279* insertion. Interestingly, these heteroallelic organisms have a higher rate of survival than the homozygous *l(2)SH1279* that express Dmp18. This result sug-

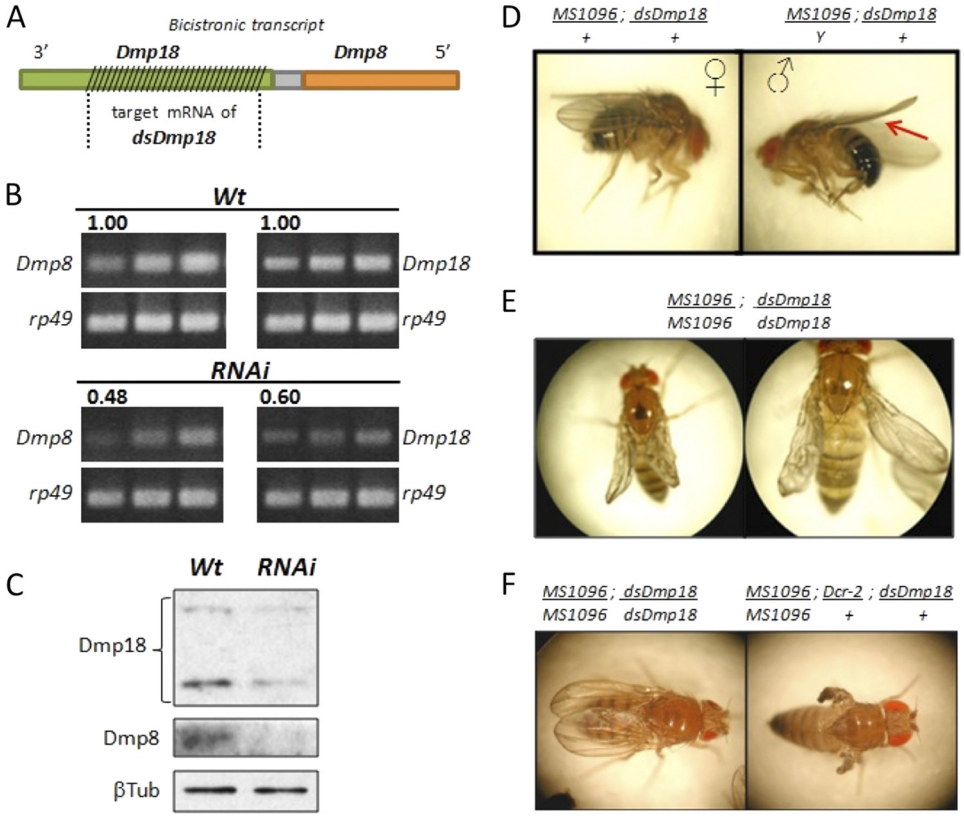

FIGURE 5. **The knockdown of Dmp8 and Dmp18 in the wing of the fly produces deformed and small wings.** *A*, the RNAi transgenic line *dsDmp18* produces a dsRNA directed against a region of the *Dmp18* mRNA. The *dsDmp18* affects the complete bicistronic transcript, causing a decrease in Dmp8 and Dmp18 expression. *B*, total RNAs from third instar larvae with a salivary gland-specific driver (*sgs3*-GAL4; *wt*) or from larvae expressing the *dsDmp18* RNA with this driver (*RNAi*) were analyzed by semiquantitative RT-PCR using specific oligonucleotide primers to amplify the *Dmp8 or Dmp18* coding sequences. *rp49* amplification was used as an internal control. The bands were quantified using the ImageJ program, and the *numbers* indicate the relative band intensity in the RNAi samples when compared with the WT RNA (value of 1). *C*, Western blot analysis of Dmp8 and Dmp18 protein levels in third instar larvae salivary glands expressing the *dsDmp18* RNA as well as in wild type salivary glands. The expression of *dsDmp18* RNA generates a notable reduction of the Dmp8 and Dmp18 protein levels when compared with the wild type tissue. β-Tubulin was used as loading control. *D*, wing phenotype associated with the reduction of Dmp8 and Dmp18 by RNAi when the MS1096 driver is used is enhanced in a dose-dependent manner. Females with one copy of the driver and one copy of *dsDmp18* show negligible wing defects, but the males with the same dose of RNAi but a major expression of the driver (which is located in the X chromosome, where dose compensation occurs) show a curly-like wing (indicated by the *arrow*). *E*, in females and males carrying the major possible doses of both the *MS1096* driver and RNAi, the defects in the wing are enhanced, and a wing size reduction is observed. *F*, Dicer (*Dcr-2*) overexpression enhances the wing phenotype generated by the expression of the *dsDmp18* RNA using the MS1096 driver. Note that the wings are practically absent in these organisms. This phenotype is very similar to the one observed in flies expressing RNAi against other TFIIH subunits.[5]

gests that the ratio between Dmp8 and Dmp18 levels is important for maintenance of homeostasis during fly development (see below). Additionally, we crossed the *l(2)SH1279* flies with a third deficiency *Df(2L)BSC110*, which contains the *Dmp8-Dmp18* locus but lacks the genes that the other two deficiencies have lost, and the *Df(2L)BSC110*/*l(2)SH1279* organisms were 100% viable and fertile (Fig. 4*C*).

The fact that the bicistronic transcript and mRNA encoding *Dmp8* are not present in the homozygous *l(2)SH1279* flies whereas a transcript encoding *Dmp18* is still produced (Fig. 4*B*) suggests that the phenotypes observed in these flies are primarily due to the absence of Dmp8. To confirm this, we constructed transgenic flies that expressed either *Dmp8* fused to a six-histidine tag (12) or *Dmp18* containing the Myc epitope (see "Experimental Procedures"). These flies were crossed with the *l(2)SH1279* flies to generate organisms that were homozygous for the *l(2)SH1279* insertion with one or two copies of the transgene. We found that the presence of one copy of the transgene expressing *Dmp8* with a six-histidine tag at the C terminus (*Dmp8*-H6) was sufficient to rescue viability and all of the other defects (sterility and held-out wing phenotype) observed in the homozygous *l(2)SH1279* flies (Fig. 4*D*). Conversely, the transgenes expressing *Dmp18* with a Myc epitope at the N terminus (Myc-*Dmp18*) were unable to rescue any of the phenotypes observed in the *l(2)SH1279* homozygous flies (Fig. 4*D*). These results confirm that all of the phenotypes observed in the *l(2)SH1279* mutant are due to the absence of Dmp8.

The next question was whether Dmp18 genetically interacts with TFIIH. To answer this question, we decided to use the *l(2)SH1279* mutant because in these flies *Dmp8* is affected, but *Dmp18* is still produced. We also carried out an RNAi approach using a transgenic line from the Vienna collection (39) that expresses a dsRNA directed against the *Dmp18* segment of the bicistronic transcript (*dsDmp18*; Fig. 5*A*) and is regulated by the UAS-GAL4 system (39, 40). The efficiency of *dsDmp18* to reduce Dmp8 and Dmp18 levels was confirmed by semiquantitative RT-PCR and Western blot analysis (Fig. 5, *B* and *C*). The ubiquitous ectopic expression of *dsDmp18* using actin or tubulin drivers was lethal for the fly (the flies die after the third instar larvae stage; data not shown). Therefore, we took advantage of

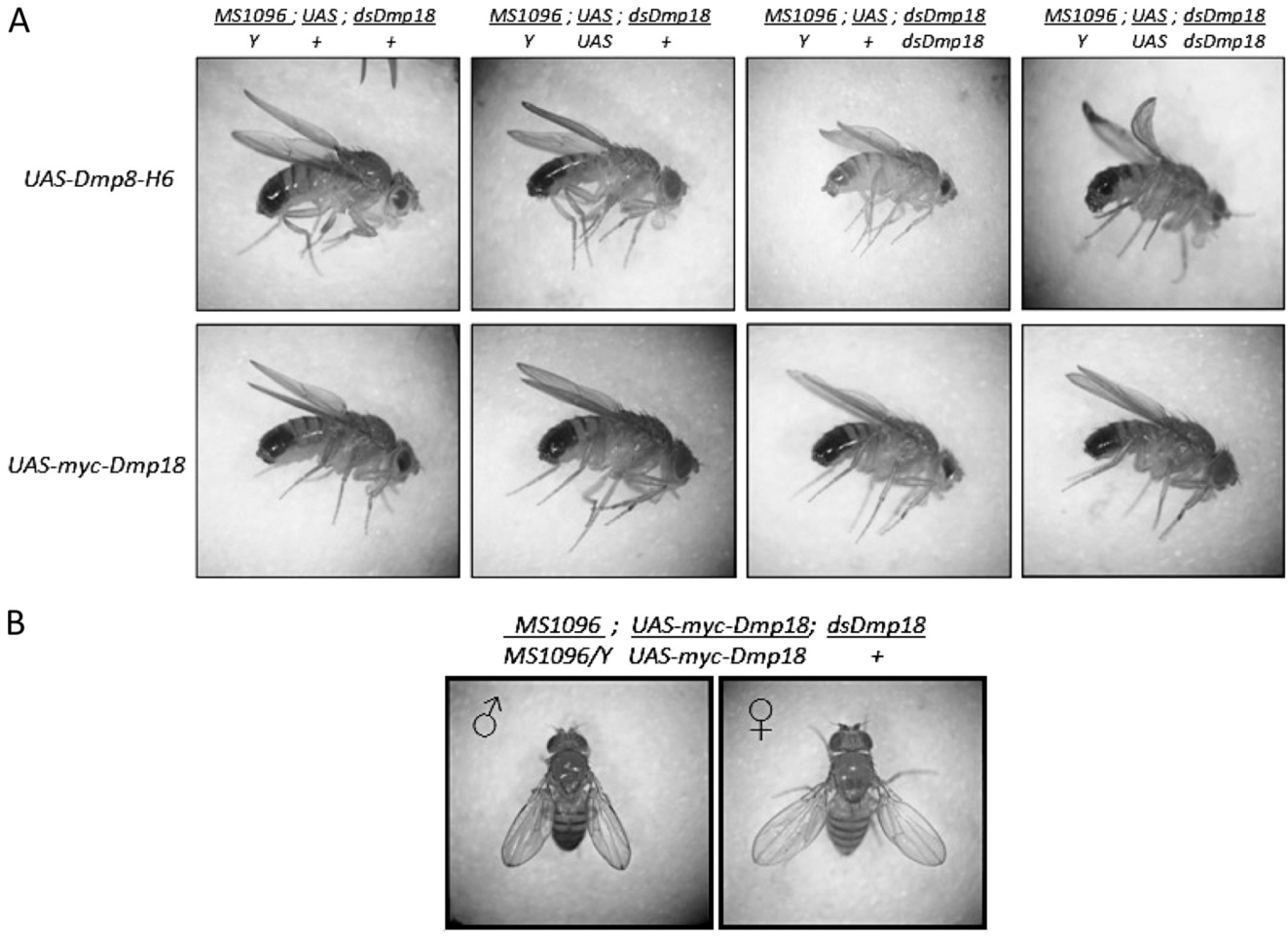

FIGURE 6. **The overexpression of Myc-Dmp18 in the wing disc suppresses the phenotypes generated by the *dsDmp18* RNA and generates the held-out wing phenotype.** *A*, flies expressing the *dsDmp18* RNA together with either Dmp8-H6 or Myc-Dmp18 (indicated in the genotype as UAS) in the wing by the MS1096 driver. In this context, the overexpression of Myc-Dmp18 results in significant suppression of wing defects caused by *dsDmp18* RNA. On the other hand, when Dmp8-H6 is overexpressed, the rescue is not observed. The genotypes are indicated in the figure. *B*, flies overexpressing Myc-Dmp18 in the same domain of the wing disc where *dsDmp18* is expressed present a variable expressivity of the held-out wing phenotype. A similar but slighter phenotype is observed in *dsDmp18* flies that overexpress Dmp8-H6 (data not shown).

the wing phenotypes observed in the *l(2)SH1279* homozygous flies as markers to analyze a possible genetic interaction between *Dmp8* and *Dmp18*, and therefore we directed the *dsDmp18* expression only to the dorsal compartment of the wing discs using the *MS1096* driver (see "Experimental Procedures"). Heterozygous adult male organisms with one copy of the driver and one copy of the *dsDmp18* transgene have a semi-curly-like phenotype in the wings (Fig. 5*D*). When the genetic dose of both the driver and *dsDmp18* are increased, the wings developed blisters and were deformed and small (Fig. 5*E*). Increasing Dicer activity in these flies dramatically enhanced the wing defects (Fig. 5*F*), whereas expressing Gal80, which inhibits Gal4, prevented the appearance of the phenotypes (data not shown). These results indicate that the expression of the *dsDmp18* RNA generates a detectable phenotype in the wing. Furthermore, the expression of two other dsRNA against Dmp52 and Dmp34 subunits of TFIIH, using the same wing driver, showed the generation of very similar wing phenotypes, as deformed and smaller wings.[4] However, we did not detect the held-out wing phenotype in any RNAi flies. The fact that *Dmp8* and *Dmp18* are encoded in a bicistronic transcript and that *dsDmp18* RNA knockdown affects the expression of both genes (Fig. 5, *B* and *C*) may suggest that the held-out wing phenotype observed in homozygous *l(2)SH1279* flies may be due to a change in the ratio of Dmp8 and Dmp18 levels.

When *Dmp8*-H6 was overexpressed in the wing disc of organisms homozygous for the wing driver and *dsDmp18*, a rescue of the wing defects was not observed (Fig. 6*A*). This finding indicates that the phenotype observed in flies expressing *dsDmp18* in the wing is partially caused by depletion of *Dmp18.* Consistent with this hypothesis, overexpression of Myc-*Dmp18* in flies homozygous for the wing driver and *dsDmp18* resulted in significant rescue of wing size and shape defects (Fig. 6*A*). Interestingly, some of the flies that overexpress either *Dmp8*-H6 or Myc-*Dmp18* together with the *dsDmp18* RNA in the wing disc show different expressivity of the held-out wing phenotype (Fig. 6*B*). This may be due to a gradient expression of the RNAi and the transgenes, which deregulates the ratio of Dmp8 and Dmp18 levels.

[4] M. Herrera-Cruz, G. Cruz, V. Valadez-Graham, M. Fregoso-Lomas, C. Villicaña, M. Vázquez, E. Reynaud, and M. Zurita, unpublished data.

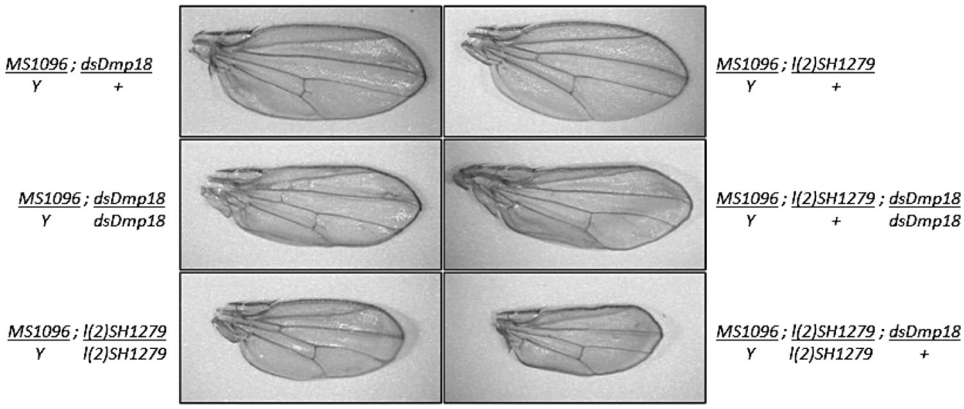

FIGURE 7. **Genetic interaction between Dmp8 and Dmp18.** The combination of *dsDmp18* expression in the wing by *MS1096* driver with the presence of the *l(2)SH1279* insertion enhances the wing deformation and the reduction of the wing size. Representative wings for different dose combinations of RNAi and *l(2)SH1279* insertion are shown in the figure. Homozygous flies for both the RNAi and the insertion do not develop until adults.

To determine if *Dmp18* and *Dmp8* genetically interact, we performed crosses to obtain flies of the *l(2)SH1279* background expressing the *dsDmp18* RNA in the wing. Because RNAi only partially depleted the mRNA (Fig. 5*B*), the combination of *dsDmp18* with the *l(2)SH1279* mutant most likely abolished the expression of *Dmp8* and partially down-regulated the expression of *Dmp18*. Interestingly, in homozygous flies for *l(2)SH1279* and expressing *dsDmp18*, an observable reduction in overall wing size occurred (Fig. 7). In addition, wing deformation was enhanced, and the penetrance of the phenotypes was 100%. Even more, the homozygous flies for both the insertion and the RNAi were not born. These results strongly suggest that simultaneous reduction of Dmp18 and Dmp8 activity in the wing results in an additive effect on the wing growth and development, which indicates a genetic interaction between Dmp18 and Dmp8, which are encoded within the same transcript, and suggests a functional link between them.

DISCUSSION

In this study, we show that the Dmp8 subunit of TFIIH is encoded in a bicistronic transcript that also encodes another protein. This configuration of gene organization is conserved in other arthropods, indicating that the coordinated expression of these two genes has been conserved during evolution (Fig. 1*C*). Intriguingly, in some species, the intergenic sequence between the two ORFs is very short, and if both ORFs are translated from the same mRNA, it suggests the existence of an unknown, unique mechanism of translation. At some point, we must consider the possibility that Dmp8 and Dmp18 may be produced after proteolytic cleavage from a larger polypeptide. However, the detection of only one polypeptide using two independent antibodies against Dmp8 and the lack of polarity of the *l(2)SH1279* insertion on Dmp18 discard this possibility.

The second gene (*Dmp18*) present in this bicistronic transcript appears to be the orthologue of SWC6/p18^{Hamlet}/ZNHIT1, which has been described as a component of the SWR1 complex in yeast and the SRCAP complex in humans (22–25). Both complexes are composed of multiple subunits and catalyze the exchange of histone H2A with the histone variant H2AZ, which is predominantly located in nucleosomes around the transcription initiation site in yeast and in higher animals (41). In addition, SRCAP also catalyzes the removal of phosphorylated histone H2AX from sites of double-stranded breaks after DNA repair (42). Therefore, both TFIIH and SWR1/SRCAP participate in transcription and DNA repair. This observation, along with the evidence that, in some cases, the bicistronic transcripts encode for two proteins with related functions, suggests a link between TFIIH and Dmp18 and probably with a putative fly SWR1/SRCAP complex. In fact, using multiple approaches, we have shown that Dmp18 physically interacts with TFIIH mainly through a direct interaction with the Dmp52 subunit. However, it is intriguing that in the pull-down and yeast two-hybrid analysis, Dmp18 and Dmp8 interact, but this is not observed in the co-IP experiments or in the different conditions inherent to each type of assay. The discrepancy of these data can be explained by the presence of the FLAG tag epitope in the co-IP experiments, which could have interfered with the direct interaction between the proteins.

The interaction of Dmp18 with Dmp52 is intriguing for several reasons. There are no reports indicating the existence of functional p52 free of TFIIH or associated with other proteins besides the ones forming this complex. In humans and yeast, p52 has been demonstrated to directly interact with p8 through the C-terminal domain of p52. This interaction is relevant for the stability of the complete TFIIH complex (36). Moreover, p52 is important for the assembly of XPB into the core of TFIIH and modulates XPB ATPase activity. This interaction occurs through two separate domains, one near the N terminus and the other near the C-terminal domain of p52 (43). Based on our results, Dmp18 may interact with Dmp52 at two different regions: at the C-terminal domain, which is also the Dmp8-interacting region, and outside the C-terminal domain. At least *in vitro*, it appears that Dmp8 has a higher affinity for the C-terminal domain of Dmp52 than Dmp18 does, suggesting that both proteins may not be simultaneously interacting with the C-terminal domain of Dmp52. However, because Dmp18 interacts with Dmp52 also in another region, it is possible that even when all 10 subunits of TFIIH are assembled, Dmp18 may still be interacting with Dmp52. This hypothesis is supported by the fact that Dmp18 co-localizes with TFIIH (DmXPD) in the majority of the immunostained sites within polytene chromo-

somes. Furthermore, these results are reinforced by a recent report showing that TFIIH (yeast RAD3/XPD) and SWR1 (Swr1) co-occupy the +1 nucleosome immediately downstream of the transcriptional start site where H2AZ resides (44).

In addition to the physical interactions described in this study, we found genetic evidence that supports a functional link between Dmp8 and Dmp18. A P element insertion that disrupts the *Dmp8* coding sequence is semilethal because only a few organisms can develop to adulthood. This is interesting because some patients with TTD-A survive without functional p8/TTDA, although several TTD manifestations are present (8). Thus, in flies, a similar situation is found to occur. However, in these flies, the males are sterile, the females have reduced fertility, and all of the homozygous organisms that develop to adulthood have a held-out wing phenotype and a slight reduction in wing size. Sterility and reduction in the size of various structures in the adult flies are phenotypes that we have previously described for Dmp52 (*marionette*) and DmXPB (*haywire*) mutants (11, 45). However, it appears that the held-out wing phenotype is specific for this mutant, and interestingly, our data suggest that this phenotype may be due to an imbalance of *Dmp8* and *Dmp18* expression levels. Furthermore, the dsRNA-mediated depletion of Dmp18 in the wings combined with the presence of the *l(2)SH1279* insertion, which only affects Dmp8, results in wing deformations and wing size reduction compared with flies that are homozygous for the disruption of Dmp8 or flies that only express the dsRNA against Dmp18. However, the held-out wing phenotype observed in *l(2)SH1279* homozygous flies is not augmented in the flies that are homozygous for the *l(2)SH1279* insertion and also express the *dsDmp18* RNA. Thus, it appears that the held-out wing phenotype is only observed when a reduction or depletion of Dmp8 occurs together with an increase of Dmp18 level, suggesting that Dmp8 and Dmp18 levels need to be co-regulated for the adequate wing development. Therefore, the organization of these two genes in a bicistronic locus could be one way to ensure this co-regulation. This hypothesis is supported by evidence that the organization of *Dmp8* and *Dmp18* genes to allow the generation of a bicistronic transcript has been conserved in many insects and probably in several arthropoda (Fig. 1*C* and supplemental Fig. S1) along 350 million years of evolution. Moreover, results from our genetic analysis and the evidence of physical interaction between Dmp52 and Dmp18 suggest a functional link between Dmp18 and TFIIH in *Drosophila*.

The results presented here raise the following question. What is the level of functional interaction between TFIIH and Dmp18? TFIIH participates in transcription and DNA repair. As mentioned previously, the yeast and human homologs of Dmp18 (SWC6 and p18^{Hamlet}/ZNHIT1) have been described as being components of the SWR1 and SRCAP complexes, respectively, that play a role in both transcription and DNA repair and catalyze the exchange of histone H2A with H2AZ (46). In human cells and in *Drosophila*, protein subunits homologous to SWR1 together with subunits identified in the acetyltransferase complex NuA4 form the TIP60 complex (47, 48). In addition to its histone acetyltransferase activity, TIP60 also catalyzes the exchange of H2A for H2AZ (49, 50). The TIP60 complex has been characterized, and its subunits have been identified. However, neither fly Dmp18 nor human p18^{Hamlet}/ZNHIT1 has been found in this complex. Interestingly, a complex similar to SRCAP has not been described in the fly. Thus, it is unknown whether Dmp18 in *Drosophila* is part of a complex involved in the H2A/H2AZ exchange or whether it has other functions independent of TIP60. On the other hand, although neither fly Dmp18 nor the human p18^{Hamlet}/ZNHIT1 are found in this complex, sometimes proteins that behave as integral subunits of a complex in one organism are only interactors in another or are lost during the purification procedure. Therefore, it is still possible that Dmp18 may interact with TIP60 in the fly (49). However, consistent with our genetic interaction analysis, it has been reported that yeast SWC6 (the yeast Dmp18) genetically interacts with RAD3 and SSL1, the homologs of XPD and p44 subunits of TFIIH (51, 52), indicating that also in yeast there is putative functional interaction between p18 and TFIIH. Furthermore, because SWC6 is a *bona* fide component of SWR1, the fly and yeast genetic interactions between SWC6/Dmp18 and TFIIH subunits suggest that phenotypes observed may be the consequence of interactions between SWR1 and TFIIH.

Based on previously published data and the results presented here, the future identification of the complex that contains Dmp18 and the demonstration that this complex directly interacts with TFIIH may explain the incorporation of the histone variant H2AZ in promoters of genes where TFIIH is recruited for transcription initiation. In contrast, Dmp18 alone may directly establish this interaction with TFIIH, resulting in a direct effect on transcription activation or repression. Consistent with this notion, p18^{Hamlet} is phosphorylated by p38 MAPK in response to genotoxic stress in human cells and has been proposed to directly modulate the transcriptional activity of p53 (13–15). p18^{Hamlet} has also been reported to function as a cofactor regulating the activity of nuclear receptors (53). Moreover, TFIIH also interacts with p53 in multiple ways in human cells (54) and in *Drosophila* (45).[5] Therefore, a possible connection between these three factors should be taken into account in future analyses. In conclusion, we have demonstrated that the *Drosophila* homolog of SWC6/p18^{Hamlet}/ZNHIT1 physically and functionally interacts with two components of *Drosophila* TFIIH, thereby opening up new avenues to study how TFIIH modulates transcription and DNA repair.

Acknowledgments—We thank Andrés Saralegui for advice on confocal microscopy. We also thank Dr. Dvorak Montiel-Condado for advice.

REFERENCES

1. Zurita, M., and Merino, C. (2003) The transcriptional complexity of the TFIIH complex. *Trends Genet.* **19,** 578–584
2. Egly, J. M., and Coin, F. (2011) A history of TFIIH. Two decades of molecular biology on a pivotal transcription/repair factor. *DNA Repair* **10,** 714–721
3. Coin, F., Oksenych, V., Mocquet, V., Groh, S., Blattner, C., and Egly, J. M. (2008) Nucleotide excision repair driven by the dissociation of CAK from

[5] M. Herrera-Cruz, G. Cruz, V. Valadez-Graham, M. Fregoso-Lomas, C. Villicaña, M. Vázquez, E. Reynaud, and M. Zurita, unpublished results.

TFIIH. *Mol. Cell* **31,** 9–20
4. Li, X., Urwyler, O., and Suter, B. (2010) *Drosophila* XPD regulates Cdk7 localization, mitotic kinase activity, spindle dynamics, and chromosome segregation. *PLoS Genet.* **6,** e1000876
5. Ito, S., Kuraoka, I., Chymkowitch, P., Compe, E., Takedachi, A., Ishigami, C., Coin, F., Egly, J. M., and Tanaka, K. (2007) XPG stabilizes TFIIH, allowing transactivation of nuclear receptors. Implications for Cockayne syndrome in XP-G/CS patients. *Mol. Cell* **26,** 231–243
6. Murakami, K., Gibbons, B. J., Davis, R. E., Nagai, S., Liu, X., Robinson, P. J., Wu, T., Kaplan, C. D., and Kornberg, R. D. (2012) Tfb6, a previously unidentified subunit of the general transcription factor TFIIH, facilitates dissociation of Ssl2 helicase after transcription initiation. *Proc. Natl. Acad. Sci. U.S.A.* **109,** 4816–4821
7. Schärer, O. D. (2008) Hot topics in DNA repair. The molecular basis for different disease states caused by mutations in TFIIH and XPG. *DNA Repair* **7,** 339–344
8. Giglia-Mari, G., Coin, F., Ranish, J. A., Hoogstraten, D., Theil, A., Wijgers, N., Jaspers, N. G., Raams, A., Argentini, M., van der Spek, P. J., Botta, E., Stefanini, M., Egly, J. M., Aebersold, R., Hoeijmakers, J. H., and Vermeulen, W. (2004) A new, tenth subunit of TFIIH is responsible for the DNA repair syndrome trichothiodystrophy group A. *Nat. Genet.* **36,** 714–719
9. Coin, F., Proietti De Santis, L. P., Nardo, T., Zlobinskaya, O., Stefanini, M., and Egly, J. M. (2006) p8/TTD-A as a repair-specific TFIIH subunit. *Mol. Cell* **21,** 215–226
10. Giglia-Mari, G., Miquel, C., Theil, A. F., Mari, P. O., Hoogstraten, D., Ng, J. M., Dinant, C., Hoeijmakers, J. H., and Vermeulen, W. (2006) Dynamic interaction of TTDA with TFIIH is stabilized by nucleotide excision repair in living cells. *PLoS Biol.* **4,** e156
11. Fregoso, M., Lainé, J. P., Aguilar-Fuentes, J., Mocquet, V., Reynaud, E., Coin, F., Egly, J. M., and Zurita, M. (2007) DNA repair and transcriptional deficiencies caused by mutations in the *Drosophila* p52 subunit of TFIIH generate developmental defects and chromosome fragility. *Mol. Cell Biol.* **27,** 3640–3650
12. Aguilar-Fuentes, J., Fregoso, M., Herrera, M., Reynaud, E., Braun, C., Egly, J. M., and Zurita, M. (2008) p8/TTDA overexpression enhances UV-irradiation resistance and suppresses TFIIH mutations in a *Drosophila* trichothiodystrophy model. *PLoS Genet.* **4,** e1000253
13. Wu, W. H., Alami, S., Luk, E., Wu, C. H., Sen, S., Mizuguchi, G., Wei, D., and Wu, C. (2005) Swc2 is a widely conserved H2AZ-binding module essential for ATP-dependent histone exchange. *Nat. Struct. Mol. Biol.* **12,** 1064–1071
14. Luk, E., Ranjan, A., Fitzgerald, P. C., Mizuguchi, G., Huang, Y., Wei, D., and Wu, C. (2010) Stepwise histone replacement by SWR1 requires dual activation with histone H2A.Z and canonical nucleosome. *Cell* **143,** 725–736
15. Cuadrado, A., Lafarga, V., Cheung, P. C., Dolado, I., Llanos, S., Cohen, P., and Nebreda, A. R. (2007) A new p38 MAP kinase-regulated transcriptional coactivator that stimulates p53-dependent apoptosis. *EMBO J.* **26,** 2115–2126
16. Aguilar-Fuentes, J., Valadez-Graham, V., Reynaud, E., and Zurita, M. (2006) TFIIH trafficking and its nuclear assembly during early *Drosophila* embryo development. *J. Cell Sci.* **119,** 3866–3875
17. Reynaud, E., Lomelí, H., Vázquez, M., and Zurita, M. (1999) The *Drosophila melanogaster* homologue of the xeroderma pigmentosum D gene product is located in euchromatic regions and has a dynamic response to UV light-induced lesions in polytene chromosomes. *Mol. Biol. Cell* **10,** 1191–1203
18. Rubin, G. M., and Spradling, A. C. (1982) Genetic transformation of *Drosophila* with transposable element vectors. *Science* **218,** 348–353
19. Valadez-Graham, V., Yoshioka, Y., Velazquez, O., Kawamori, A., Vázquez, M., Neumann, A., Yamaguchi, M., Zurita, M. (2012) XNP/dATRX interacts with DREF in the chromatin to regulate gene expression. *Nucleic Acids Res.* **40,** 1460–1474
20. Palomera-Sanchez, Z., Bucio-Mendez, A., Valadez-Graham, V., Reynaud, E., and Zurita, M. (2010) *Drosophila* p53 is required to increase the levels of the dKDM4B demethylase after UV-induced DNA damage to demethylate histone H3 lysine 9. *J. Biol. Chem.* **285,** 31370–31379
21. Laemmli, U. K. (1970) Cleavage of structural proteins during the assembly of the head of bacteriophage T4. *Nature* **227,** 680–685
22. Lafarga, V., Cuadrado, A., and Nebreda, A. R. (2007) $p18^{Hamlet}$ mediates different p53-dependent responses to DNA damage-inducing agents. *Cell Cycle* **6,** 2319–2322
23. Cuadrado, A., Corrado, N., Perdiguero, E., Lafarga, V., Muñoz-Canoves, P., and Nebreda, A. R. (2010) Essential role of $p18^{Hamlet}$/SRCAP-mediated histone H2A.Z chromatin incorporation in muscle differentiation. *EMBO J.* **29,** 2014–2025
24. Bao, Y., and Shen, X. (2011) SnapShot. Chromatin remodeling. INO80 and SWR1. *Cell* **144,** 158–158.e2
25. Lu, P. Y., Lévesque, N., and Kobor, M. S. (2009) NuA4 and SWR1-C. Two chromatin-modifying complexes with overlapping functions and components. *Biochem. Cell Biol.* **87,** 799–815
26. van Attikum, H., and Gasser, S. M. (2009) Cross-talk between histone modifications during the DNA damage response. *Trends Cell Biol.* **19,** 207–217
27. Morillo-Huesca, M., Clemente-Ruiz, M., Andújar, E., and Prado, F. (2010) The SWR1 histone replacement complex causes genetic instability and genome-wide transcription misregulation in the absence of H2A.Z. *PLoS One* **5,** e12143
28. Lekven, A. C., Thorpe, C. J., Waxman, J. S., and Moon, R. T. (2001) Zebrafish wnt8 encodes two wnt8 proteins on a bicistronic transcript and is required for mesoderm and neurectoderm patterning. *Dev. Cell* **1,** 103–114
29. Gray, T. A., Saitoh, S., and Nicholls, R. D. (1999) An imprinted, mammalian bicistronic transcript encodes two independent proteins. *Proc. Natl. Acad. Sci. U.S.A.* **96,** 5616–5621
30. Sloan, J., Kinghorn, J. R., and Unkles, S. E. (1999) The two subunits of human molybdopterin synthase. Evidence for a bicistronic messenger RNA with overlapping reading frames. *Nucleic Acids Res.* **27,** 854–858
31. Pavlik, P., Konduri, V., Massa, E., Simonette, R., and Beckingham, K. M. (2006) A dicistronic gene pair within a cluster of "EF-hand" protein genes in the genomes of *Drosophila* species. *Genomics* **88,** 347–359
32. Blumenthal T. (2004) Operons in eukaryotes. *Brief. Funct. Genomic. Proteomic.* **3,** 199–211
33. Betrán, E., and Ashburner, M. (2000) Duplication, dicistronic transcription, and subsequent evolution of the alcohol dehydrogenase and alcohol dehydrogenase-related genes in *Drosophila*. *Mol. Biol. Evol.* **17,** 1344–1352
34. Giot, L., Bader, J. S., Brouwer, C., Chaudhuri, A., Kuang, B., Li, Y., Hao, Y. L., Ooi, C. E., Godwin, B., Vitols, E., Vijayadamodar, G., Pochart, P., Machineni, H., Welsh, M., Kong, Y., Zerhusen, B., Malcolm, R., Varrone, Z., Collis, A., Minto, M., Burgess, S., McDaniel, L., Stimpson, E., Spriggs, F., Williams, J., Neurath, K., Ioime, N., Agee, M., Voss, E., Furtak, K., Renzulli, R., Aanensen, N., Carrolla, S., Bickelhaupt, E., Lazovatsky, Y., DaSilva, A., Zhong, J., Stanyon, C. A., Finley, R. L., Jr., White, K. P., Braverman, M., Jarvie, T., Gold, S., Leach, M., Knight, J., Shimkets, R. A., McKenna, M. P., Chant, J., and Rothberg, J. M. (2003) A protein interaction map of *Drosophila melanogaster*. *Science* **302,** 1727–1736
35. Kainov, D. E., Vitorino, M., Cavarelli, J., Poterszman, A., and Egly, J. M. (2008) Structural basis for group A trichothiodystrophy. *Nat. Struct. Mol. Biol.* **15,** 980–984
36. Zhou, Y., Kou, H., and Wang, Z. (2007) Tfb5 interacts with Tfb2 and facilitates nucleotide excision repair in yeast. *Nucleic Acids Res.* **35,** 861–871
37. Coin, F., Oksenych, V., and Egly, J. M. (2007) Distinct roles for the XPB/p52 and XPD/p44 subcomplexes of TFIIH in damaged DNA opening during nucleotide excision repair. *Mol. Cell* **26,** 245–256
38. Gutiérrez, L., Zurita, M., Kennison, J. A., Vázquez, M. (2003) The *Drosophila* trithorax group gene tonalli (*tna*) interacts genetically with the Brahma remodeling complex and encodes an SP-RING finger protein. *Development* **130,** 343–354
39. Dietzl, G., Chen, D., Schnorrer, F., Su, K. C., Barinova, Y., Fellner, M., Gasser, B., Kinsey, K., Oppel, S., Scheiblauer, S., Couto, A., Marra, V., Keleman, K., and Dickson, B. J. (2007) A genome-wide transgenic RNAi library for conditional gene inactivation in *Drosophila*. *Nature* **448,** 151–156
40. Piccin, A., Salameh, A., Benna, C., Sandrelli, F., Mazzotta, G., Zordan, M.,

Rosato, E., Kyriacou, C. P., and Costa, R. (2001) Efficient and heritable functional knock-out of an adult phenotype in *Drosophila* using a GAL4-driven hairpin RNA incorporating a heterologous spacer. *Nucleic Acids Res.* **29,** 55–65

41. Li, B., Pattenden, S. G., Lee, D., Gutiérrez, J., Chen, J., Seidel, C., Gerton, J., and Workman J. L. (2005) Preferential occupancy of histone variant H2AZ at inactive promoters influences local histone modifications and chromatin remodeling. *Proc. Natl. Acad. Sci. U.S.A.* **102,** 18385–18390
42. Jha, S., Shibata, E., and Dutta, A. (2008) Human Rvb1/Tip49 is required for the histone acetyltransferase activity of Tip60/NuA4 and for the down-regulation of phosphorylation on H2AX after DNA damage. *Mol. Cell Biol.* **28,** 2690–2700
43. Jawhari, A., Lainé, J. P., Dubaele, S., Lamour, V., Poterszman, A., Coin, F., Moras, D., and Egly, J. M. (2002) p52 Mediates XPB function within the transcription/repair factor TFIIH. *J. Biol. Chem.* **277,** 31761–31767
44. Venters, B. J and Pugh, B. F. (2009) A canonical promoter organization of the transcription machinery and its regulators in the *Saccharomyces* genome. *Genome Res.* **19,** 360–371
45. Merino, C., Reynaud, E., Vázquez, M., and Zurita M. (2002) DNA repair and transcriptional effects of mutations in TFIIH in *Drosophila* development. *Mol. Biol. Cell* **13,** 3246–3256
46. Ruhl, D. D., Jin, J., Cai, Y., Swanson, S., Florens, L., Washburn, M. P., Conaway, R. C., Conaway, J. W., and Chrivia, J. C. (2006) Purification of a human SRCAP complex that remodels chromatin by incorporating the histone variant H2A.Z into nucleosomes. *Biochemistry* **45,** 5671–5677
47. Kobor, M. S., Venkatasubrahmanyam, S., Meneghini, M. D., Gin, J. W., Jennings, J. L., Link, A. J., Madhani, H. D., and Rine, J. (2004) A protein complex containing the conserved Swi2/Snf2-related ATPase Swr1p deposits histone variant H2A.Z into euchromatin. *PLoS Biol.* **2,** E131
48. Eissenberg, J. C., Wong, M., and Chrivia, J. C. (2005) Human SRCAP and *Drosophila melanogaster* DOM are homologs that function in the notch signaling pathway. *Mol. Cell Biol.* **25,** 6559–6569
49. Kusch, T., Florens, L., Macdonald, W. H., Swanson, S. K., Glaser, R. L., Yates, J. R., 3rd, Abmayr, S. M., Washburn, M. P., and Workman, J. L. (2004) Acetylation by Tip60 is required for selective histone variant exchange at DNA lesions. *Science* **306,** 2084–2087
50. Squatrito, M., Gorrini, C., and Amati, B. (2006) Tip60 in DNA damage response and growth control. Many tricks in one HAT. *Trends Cell Biol.* **16,** 433–442
51. Collins, S. R., Miller, K. M., Maas, N. L., Roguev, A., Fillingham, J., Chu, C. S., Schuldiner, M., Gebbia, M., Recht, J., Shales, M., Ding, H., Xu, H., Han, J., Ingvarsdottir, K., Cheng, B., Andrews, B., Boone, C., Berger, S. L., Hieter, P., Zhang, Z., Brown, G. W., Ingles, C. J., Emili, A., Allis, C. D., Toczyski, D. P., Weissman, J. S., Greenblatt, J. F., and Krogan, N. J. (2007) Functional dissection of protein complexes involved in yeast chromosome biology using a genetic interaction map. *Nature* **446,** 806–810
52. Costanzo, M., Baryshnikova, A., Bellay, J., Kim Y., Spear, E. D., Sevier, C. S., Ding, H., Koh, J. L., Toufighi, K., Mostafavi, S., Prinz, J., St Onge, R. P., VanderSluis, B., Makhnevych, T., Vizeacoumar, F. J., Alizadeh, S., Bahr, S., Brost, R. L., Chen, Y., Cokol, M., Deshpande, R., Li, Z., Lin, Z. Y., Liang, W., Marback, M., Paw, J., San Luis, B. J., Shuteriqi, E., Tong, A. H., van Dyk, N., Wallace, I. M., Whitney, J. A., Weirauch, M. T., Zhong, G., Zhu, H., Houry, W. A., Brudno, M., Ragibizadeh, S., Papp, B., Pál, C., Roth, F. P., Giaever, G., Nislow, C., Troyanskaya, O. G., Bussey, H., Bader, G. D., Gingras, A. C., Morris, Q. D., Kim, P. M., Kaiser, C. A., Myers, C. L., Andrews, B. J., and Boone, C. (2010) The genetic landscape of a cell. *Science* **327,** 425–431
53. Wang, J., Li, Y., Zhang, M., Liu, Z., Wu, C., Yuan, H., Li, Y. Y., Zhao, X., and Lu, H. (2007) A zinc finger HIT domain-containing protein, ZNHIT-1, interacts with orphan nuclear hormone receptor Rev-erbβ and removes Rev-erbβ-induced inhibition of apoCIII transcription. *FEBS J.* **274,** 5370–5381
54. Okuda, M., Tanaka, A., Satoh, M., Mizuta, S., Takazawa M., Ohkuma, Y., and Nishimura, Y. (2008) Structural insight into the TFIIE-TFIIH interaction. TFIIE and p53 share the binding region on TFIIH. *EMBO J.* **27,** 1161–1171

Supplemental Fig. S1

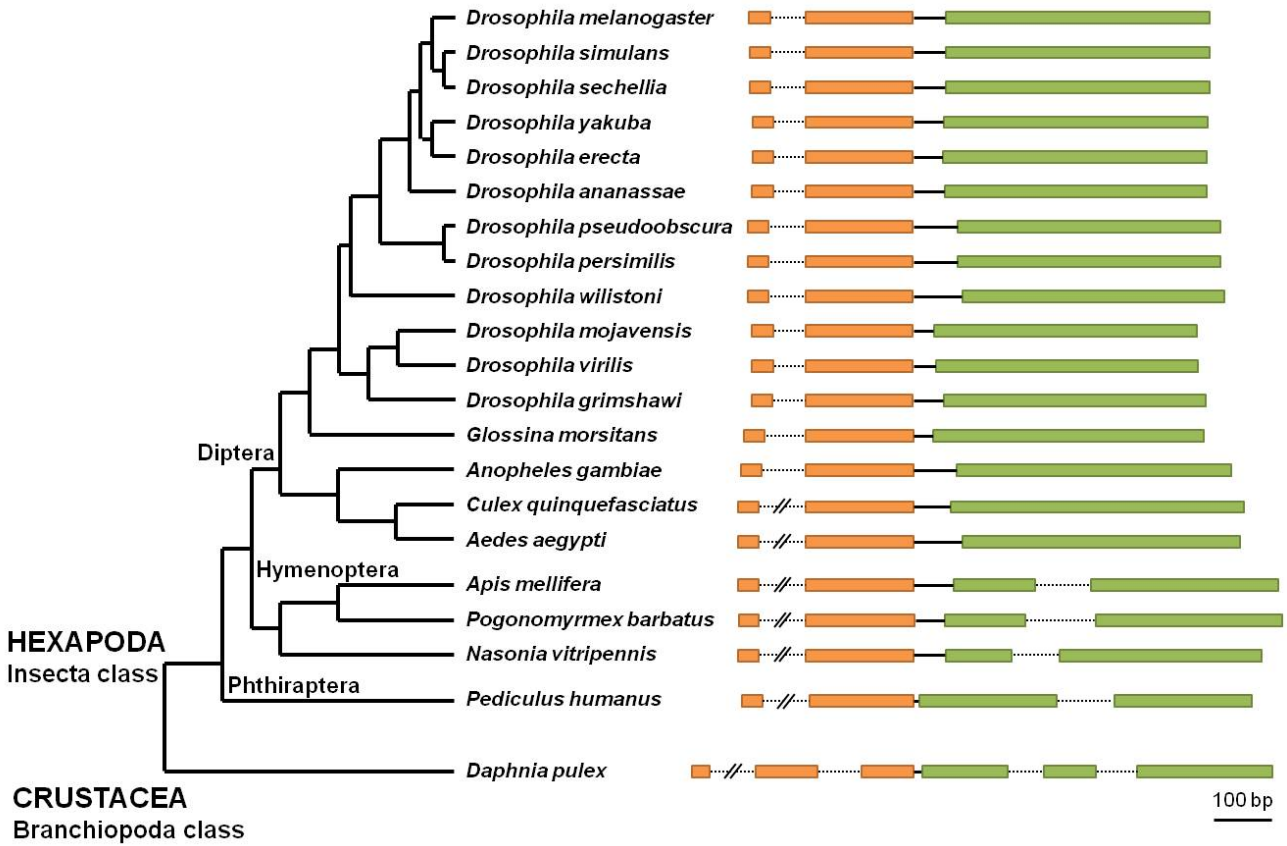

Supplemental Fig. S1. **Gene organization of the *p8-p18* bicistronic loci in different arthropoda species.**
The *p8* gene configuration containing a small exon followed of an intron is present in all the genomes of analyzed organisms. The intergenic sequence between *p8* and *p18* differs in size between the different species, however is always short (no more than 90 bp). The *p18* gene lacks introns in most of the dipteran species, however in other arthropoda one or two introns are present in the *p18* gene. Exons are shown as orange boxes for *p8* and green for *p18*, introns as dot lines and the intergenic sequence as solid line.